APPENDIX C: PHOTOCHEMICAL MODELING FOR THE DFW ATTAINMENT DEMONSTRATION SIP REVISION FOR THE 1997 EIGHT-HOUR OZONE STANDARD

1 Overview

2 Photochemical Model Configuration

3 Base Case Modeling

4 CAMx Model Performance Evaluation

4.1 Operational Evaluations

4.1.1 Statistical Measures

4.1.2 Graphical Measures

4.2 Diagnostic Evaluations

4.2.1 Sensitivity Analyses

4.2.2 Diagnostic Analyses

4.3 Episodic Model Performance Assessment for Ozone

4.3.1 Assessments Based on all Hourly Modeled-Observed Pairs

4.3.2 Assessments Based on Daily Peak Modeled-Observed Pairs at Monitor Sites

4.3.3 Assessments Based on Daily Peak Modeled-Observed Concentrations Unpaired in Space and Time

4.3.4 Episodic Model Performance Assessment

5 May 31 – July 2, 2006 Episode

5.1 Statistical Measures

5.2 Graphical Measures

5.2.1 Time Series

5.2.2 Cumulative Distributions

5.2.3 Peak Ozone Tile Plot

5.2.4 Summary

5.3 Rural Monitor Model Performance Evaluation

5.4 Ozone Sonde Model Performance Evaluation

5.4.1 Summary and Conclusions

5.5 Diagnostic Evaluations

5.5.1 Sensitivity Analyses

5.5.1.1 Alternative Meteorological Configuration

5.5.1.2 Alternative Initial and Boundary Conditions

5.5.1.3 Alternative Modeling Emissions: Louisiana Haynesville Shale Drill Rig Emissions

5.5.1.4 Alternative Modeling Emissions: MOBILE6.2 On-road Emissions

5.5.1.5 Alternative Modeling Emissions: Cross State Air Pollution Rule Point Source (CSAPR) Emissions

5.5.2 Diagnostic Analyses

5.5.2.1 Retrospective Modeling – 1999 Backcast

5.5.2.2 Observational Modeling – Weekday/Weekend

5.5.2.3 Anthropogenic Precursor Culpability Assessment (APCA)

5.5.2.4 Chemical Process Analysis

6 Baseline (2006) And Future Case (2012) Modeling

6.1 Baseline Modeling

6.2 Future Baseline Modeling

6.2.1 Alternative Future Design Value Calculations

6.2.1.1 Minimum Threshold Analysis:

6.2.1.2 Daily RRF Analysis:

6.2.1.3 Grid Cell Array Size Analysis:

6.2.2 Unmonitored Area Analysis

6.2.3 Ozone Metrics

7 Modeling Archive and References

7.1 Modeling Archive

7.2 Modeling References

1 OVERVIEW

Photochemical modeling involves two major phases, the base case modeling and the future year modeling. The purpose of the base case modeling phase is to evaluate the model's ability to adequately replicate measured ozone and ozone precursor concentrations during recent periods with high observed ozone concentrations (the base case episode). The purpose of the future year modeling phase is to predict attainment year ozone design values, as well as evaluate the effectiveness of controls in reaching attainment. The TCEQ developed a Modeling/Analysis protocol describing the process to be followed to model base case and future ozone formation in the DFW area, and submitted the plan to the EPA for review and approval.

The performance evaluation of the base case modeling provides a measure of the adequacy of the model in correctly replicating the relationship between ozone and the emissions of ozone precursors (e.g., NO_X and VOC). The performance evaluations of the base case modeling are composed of two types, operational (e.g., statistical and graphical evaluations) and diagnostic (e.g., sensitivity and probing tools evaluations). As recommended in the EPA guidance (EPA-454/B-07-002, April 2007), these evaluations are considered as a whole in a "weight-of-evidence" approach, rather than individually, in deciding the adequacy of the model in replicating the relationship between ozone and the emissions of ozone precursors and thereby the level of confidence that can be placed in the response of ozone to various control measures.

Future year modeling involves several steps. The first is creating a modeling baseline, which is similar to the base case except that it removes non-systematic emissions variability (e.g. emission events). The future year emissions are developed by applying growth and control factors to the baseline year emissions. Future year ozone design values (attainment test) are then determined using the ratio of the future year to the baseline year modeled ozone concentrations. This ratio is called the relative response factor (RRF).

Both the baseline and future years are modeled using the base case episode meteorological data as inputs. The same meteorological data are used for modeling both the baseline and future years, and thus, the ratio of future year modeled ozone concentrations to the baseline year concentrations provides a measure of the response of ozone to the change in emissions.

The future year ozone design value is calculated by multiplying the RRF by a baseline year ozone design value (DV_B). The DV_B is the average of the regulatory design values for the three consecutive years containing the baseline year (see Figure 1-1: *Baseline Design Value Calculation Illustration*). When the calculated future year ozone design value is less than or equal to 0.08 ppm (84 ppb), this signifies modeled attainment. When the calculated future year ozone design value is greater than 84 ppb, the model can be used to test the effectiveness of various control measures that may be needed.

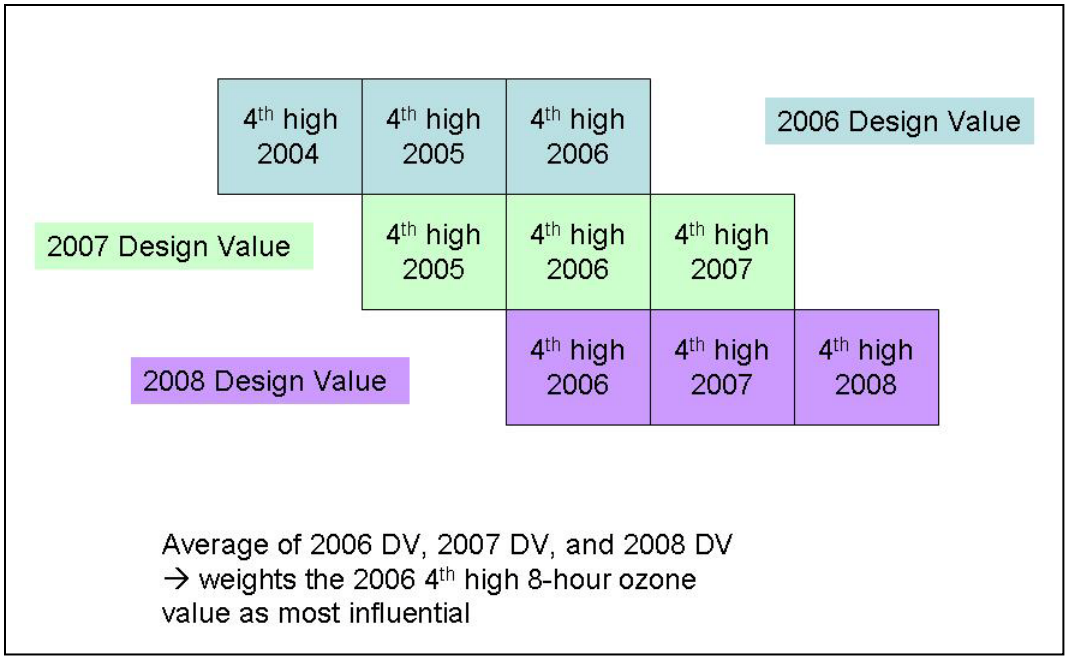

Figure 1-1: Baseline Design Value Calculation Illustration

2 PHOTOCHEMICAL MODEL CONFIGURATION

The TCEQ used the Comprehensive Air quality Model with extensions (CAMx) version 5.20.1pr (Environ, 2010). The model is based on well-established treatments of advection, diffusion, deposition, and chemistry. Another important feature is that NO_X emissions from large point sources can be treated with the plume-in-grid (PiG) submodel, which helps avoid the artificial diffusion that occurs when point source emissions are introduced into a grid volume. In addition, the TCEQ has many years of experience with CAMx. CAMx was used for the modeling conducted in the HGB and BPA nonattainment areas, as well as for modeling being conducted in other areas of Texas (e.g., San Antonio). The model software and the CAMx user's guide are publicly available at http://www.camx.com (Environ, 2010).

CAMx version 5.20.1pr includes a number of upgrades and features from previous versions. The following CAMx 5.20.1pr options were used:

- Parallel processing of the chemistry and transport algorithms;
- CB05 chemical mechanism with EBI chemistry solver;
- Piecewise Parabolic Method (PPM) advection solver;
- Improved vertical transport solvers; and
- Updated Plume-in-Grid (PiG) treatment of larger point sources of NO_X using the Greatly Reduced Execution and Simplified Dynamics (GREASD) Lagrangian module.

In addition to the CAMx inputs developed from the meteorological and emissions modeling, inputs are needed for initial and boundary conditions, spatially resolved surface characteristic parameters, spatially resolved albedo/haze/ozone (i.e., opacity) and photolysis rates, and a chemistry parameters file.

The TCEQ contracted with Environ (Environ, 2008b) who worked with NASA and the Jet Propulsion Laboratory (JPL) to derive episode-specific boundary conditions from the Model for Ozone and Related chemical Tracers (MOZART) global air quality model. Boundary conditions were developed for each grid cell along all four edges of the 36 km domain at each vertical layer for each episode hour. This work also produced initial conditions for each of the episodes. The TCEQ used these episode-specific initial and boundary conditions for this modeling study. The top boundary condition is no longer set as of CAMx version 5.0.

Surface characteristic parameters, including roughness, vegetative distribution, and water/land boundaries, are input to CAMx via a land-use file. The land-use file provides the fractional contribution (0 to 1) of eleven land-use categories, as defined by the UAM-IV conventions (EPA, 1990). For the 36 km and 12 km domains, the TCEQ used the land-use files developed by Environ for the approved 2007 DFW SIP, which were derived from the most recent USGS LULC database. For the 4 km domain, in the vicinity of DFW, the TCEQ used updated land-use files developed by Texas A&M University (Popescu et al., 2008), which were derived from more highly resolved LULC data collected by the Texas Forest Service and the UT-CSR.

Spatially-resolved opacity and photolysis rates are input to CAMx via a photolysis rates file and an opacity file. These rates, which are specific to the chemistry parameters file for the CB05 mechanism, are also input to CAMx. The TCEQ used episode-specific satellite data from the Total Ozone Mapping Spectrometer (TOMS) to prepare the photolysis rates and opacity files.

Figure 2-1: *DFW Photochemical Modeling Domains* depicts the modeling domains used in CAMx. All domains are projected in a Lambert Conformal Projection (LCP) with origin at 100 degrees west and 40 degrees north. The horizontal configuration of the CAMx modeling domains consists of a grid of 4 km x 4 km cells (4 km) encompassing the DFW nonattainment counties (blue box), nested within a grid of 12 km cells covering most of Texas and Louisiana (green box), nested within a grid of 36 km cells covering the eastern part of the United States (black box). The size of the 36 km outer domain was selected to minimize the effect of boundary conditions on predicted ozone concentrations at the finer grid resolutions. The domain specifications are detailed in Table 2-1: *CAMx Modeling Domain Dimensions*.

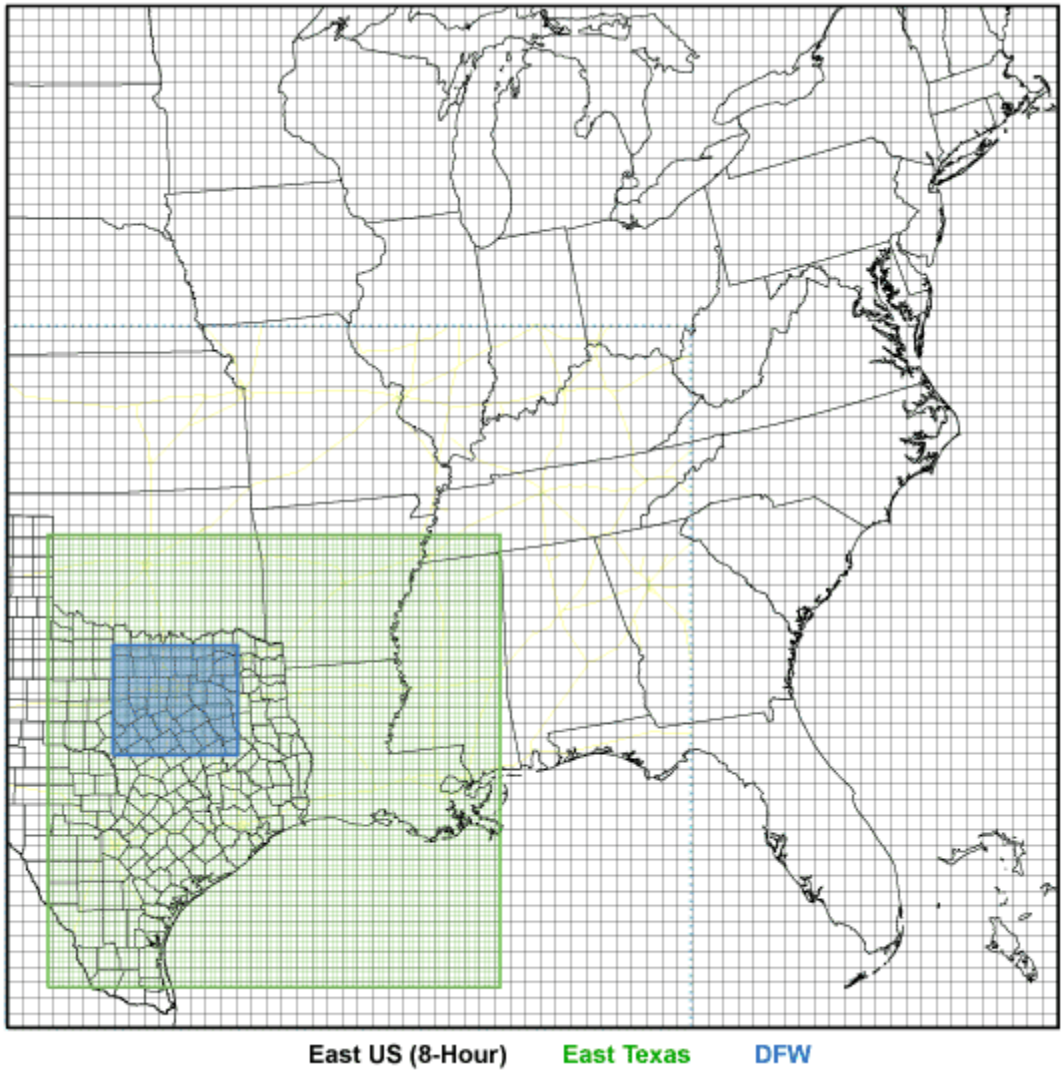

Figure 2-1: DFW Photochemical Modeling Domains

Table 2-1: CAMx Modeling Domain Dimensions

Domain	Easting Range (km)	Northing Range (km)	East/West Grid Points	North/South Grid Points
36 km	(-108, 1512)	(-1584, 828)	69	67
12 km	(-12, 1056)	(-1488, -420)	89	89
4 km	(140, 436)	(-940, -680)	74	65

The vertical configuration of the CAMx modeling domains consists of 28 layers of varying depths as shown in Table 2-2: *CAMx Vertical Layer Structure*.

Table 2-2: CAMx Vertical Layer Structure

CAMx Layer	MM5 Layer	Top (m AGL)	Center (m AGL)	Thickness (m)
28	38	15179.1	13637.9	3082.5
27	36	12096.6	10631.6	2930.0
26	32	9166.6	8063.8	2205.7
25	29	6960.9	6398.4	1125.0
24	27	5835.9	5367.0	937.0
23	25	4898.0	4502.2	791.6
22	23	4106.4	3739.9	733.0
21	21	3373.5	3199.9	347.2
20	20	3026.3	2858.3	335.9
19	19	2690.4	2528.3	324.3
18	18	2366.1	2234.7	262.8
17	17	2103.3	1975.2	256.2
16	16	1847.2	1722.2	256.3
15	15	1597.3	1475.3	249.9
14	14	1353.4	1281.6	243.9
13	13	1209.8	1139.0	143.6
12	12	1068.2	998.3	141.6
11	11	928.5	859.5	137.8
10	10	790.6	745.2	90.9
9	9	699.7	654.7	90.1
8	8	609.5	564.9	89.3
7	7	520.2	476.0	88.5
6	6	431.7	387.8	87.8
5	5	343.9	300.4	87.0
4	4	256.9	213.7	86.3
3	3	170.5	127.7	85.6
2	2	84.9	59.4	51.0
1	1	33.9	16.9	33.9

Note: AGL - Above ground level.

3 BASE CASE MODELING

This CAMx model configuration was applied to the June 2006 base case using the episode-specific meteorological parameters and emissions. The month of June is a time period when elevated ozone concentrations have been historically observed, as shown in Figure 3-1: *Eight-Hour Ozone Exceedance Days in DFW and Other Areas of Texas*. During this 33-day ozone episode, 17 days were eight-hour ozone exceedance days and were meteorologically similar to typical ozone conducive conditions (see Chapter 5).

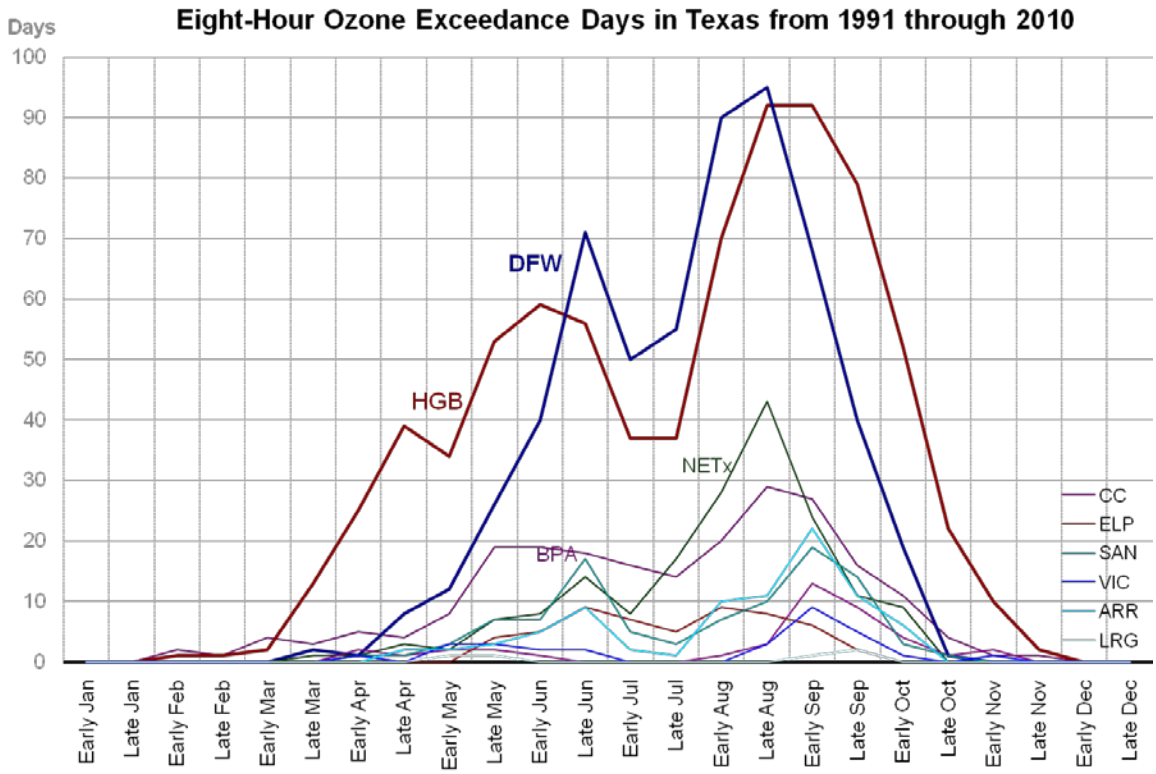

Figure 3-1: Eight-Hour Ozone Exceedance Days in DFW and Other Areas of Texas

Figure 3-2: *June 2006 Episode Eight-Hour Ozone by Monitor* shows the daily maximum eight-hour ozone concentrations observed over the episode. As noted, many days experienced eight-hour ozone concentrations above 90 ppb, which were similar in magnitude to the monitor-specific baseline design values. Also of note are the periods with lower ozone values that occurred after frontal passages and times of strong southerly flow.

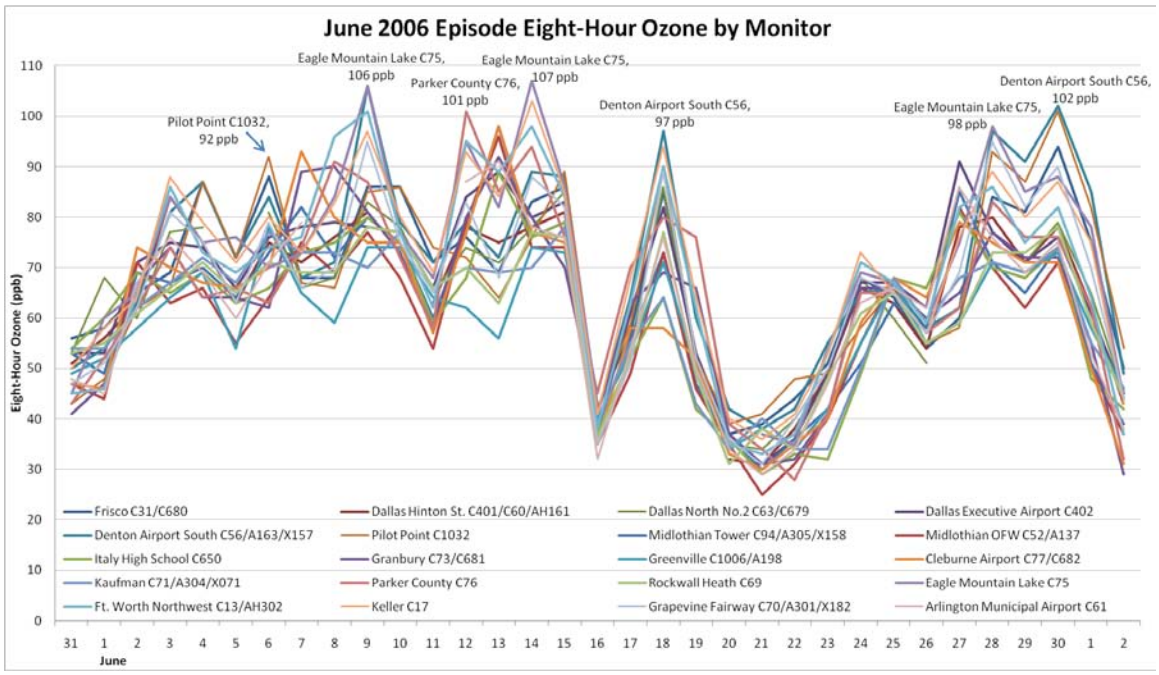

Figure 3-2: June 2006 Episode Eight-Hour Ozone by Monitor

Figure 3-3: *DFW Area Monitors* exhibits the locations of the monitors in and around the DFW nonattainment area. The nine county DFW nonattainment area is outlined in blue.

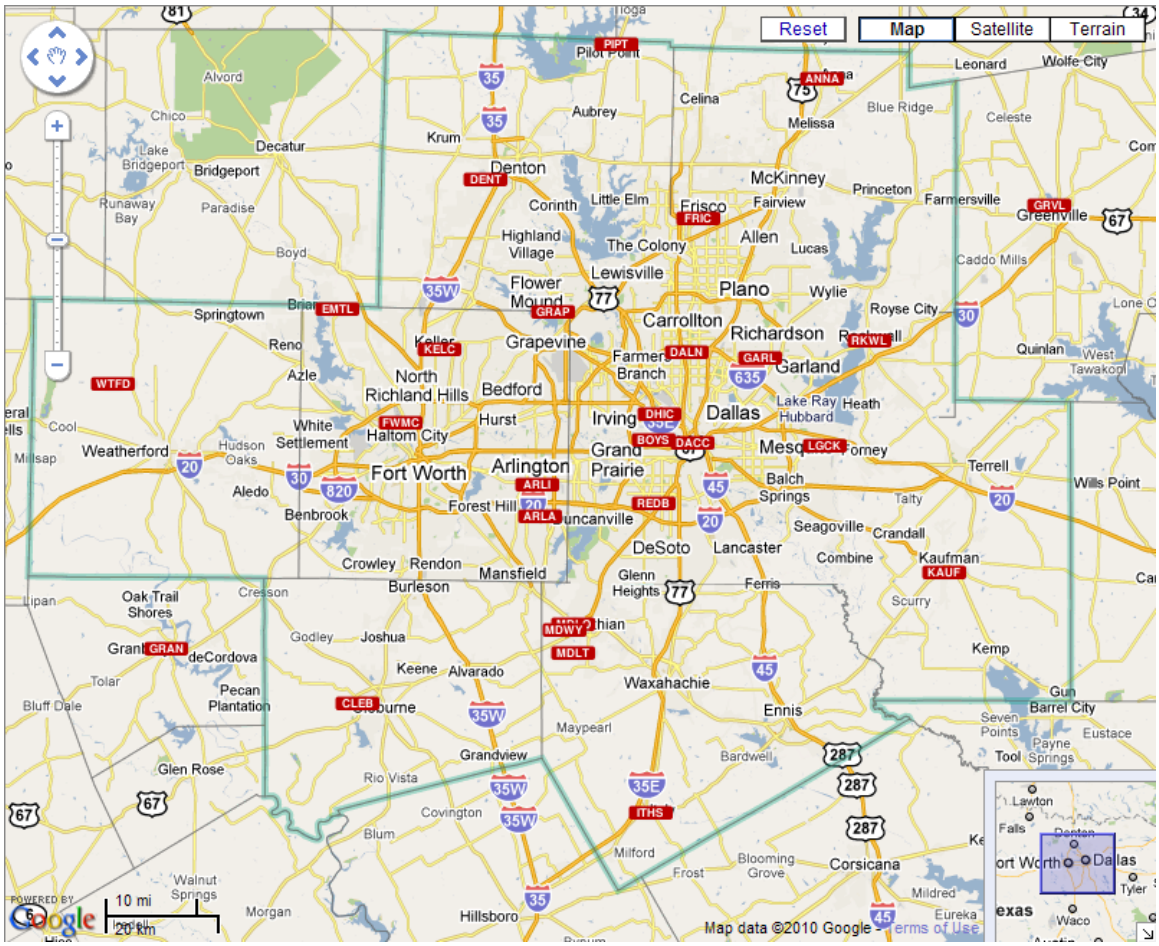

Figure 3-3: DFW Area Monitors

Table 3-1: *DFW Monitor-specific Eight-Hour Ozone Data during the Extended June 2006 Episode* summarizes the observed concentrations at the DFW monitors during the June 2006 episode. The monitors that recorded the highest design values since 2005 (Eagle Mountain Lake C75, Denton Airport South C56, Keller C17, and Ft. Worth Northwest C13), also observed the most exceedance days (eight or nine) and highest peak eight-hour concentrations. While these key monitors did not observe ten days with ozone measured in excess of 85 ppb, they did measure almost twenty days of eight-hour concentrations 70 ppb or greater, which can be used for the RRF calculation. All but the Greenville C1006 monitor had at least ten days 70 ppb or above, although its northeast location is not in the typical path of high ozone. The Greenville monitor is also outside the nine county nonattainment area.

Table 3-1: DFW Monitor-specific Eight-Hour Ozone Data during the Extended June 2006 Episode

Monitor	Max 8-hour Ozone (ppb)	Days ≥ 90 ppb	Days ≥ 85 ppb	Days ≥ 70 ppb	Site-specific Baseline Design Value (ppb)
Eagle Mountain Lake C75	**107**	**5**	8	18	**93.3**
Denton Airport South C56	106	**5**	**9**	17	**93.3**
Keller C17	103	4	8	**19**	91.0
Grapevine Fairway C70	95	3	5	14	90.7

Monitor	Max 8-hour Ozone (ppb)	Days ≥ 90 ppb	Days ≥ 85 ppb	Days ≥ 70 ppb	Site-specific Baseline Design Value (ppb)
Ft. Worth Northwest C13	101	**5**	8	17	89.3
Parker County C76	101	3	5	15	87.7
Frisco C31	94	1	7	14	87.7
Cleburne Airport C77	98	2	2	15	85.0
Dallas Exec. Airport C402	91	1	2	17	85.0
Dallas North No.2 C63	86	0	2	12	85.0
Arlington Municipal Airport C61	91	1	3	11	83.3
Granbury C73	92	2	3	12	83.0
Dallas Hinton St. C401	84	0	0	14	81.7
Rockwall Heath C69	78	0	0	11	77.7
Greenville C1006	78	0	0	8	75.0
Kaufman C71	78	0	0	11	74.7
Pilot Point C1032*	101	4	**9**	14	81.0*
Midlothian Tower C94*	98	1	2	14	80.5*
Midlothian OFW C52*	96	1	1	11	77.7*

* PIPT, MDLT, and MDLO did not measure enough data from 2004 through 2008 to calculate a complete baseline design value ($DV_{B)}$. The DV_B shown uses all available data.

The development of the base case modeling proceeded through a number of iterations, which involved updates from improvements in the meteorological and emissions modeling, as well as improvements to the initial and boundary conditions. Not all iterations (i.e., composite of meteorology, emissions and initial and boundary conditions) were modeled. Three emissions iterations of the base case are presented below. The setup and performance of the meteorological model is described in Appendix A.

Table 3-2: *CAMx Configuration* provides a description of the modeling iterations, as well as the CAMx modeling run designations. Because the various modeling components for the current base case, Reg2_MVS, are described in detail in Chapter 3 and in Appendices A and B, the table only lists explicitly those items which changed between iterations.

Table 3-2: CAMx Configurations

Base Case Model Designation	CAMx Version	Meteorology	Oil & Gas Emissions	On-Road Mobile
Reg2_MVS	5.20.1pr	ETA Planetary Boundary Layer (PBL) Scheme; 4 km TKE Vertical Diffusivity	2006 Railroad Commission Production by county; 2008 TexAER-based drilling emissions	MOVES2010a
Reg2	5.20.1pr	ETA Planetary Boundary Layer (PBL) Scheme; 4 km TKE Vertical Diffusivity	2006 Railroad Commission Production by county; 2008 TexAER-based drilling emissions	MOBILE6.2

Base Case Model Designation	CAMx Version	Meteorology	Oil & Gas Emissions	On-Road Mobile
Reg1b	5.20.1pr	ETA PBL Scheme; 4 km TKE Vertical Diffusivity	2008 TexAER-based production and drilling emissions projected to 2006	MOBILE6.2

In general the modeling iterations designated in Table 3-2 differ only by the on-road mobile emissions model and oil and gas emissions updates.

4 CAMX MODEL PERFORMANCE EVALUATION

The CAMx modeling results were compared to the measured ozone and ozone precursor concentrations at all regulatory monitoring sites, which resulted in a number of modeling iterations to implement improvements to the meteorological and emissions modeling and subsequent CAMx modeling. A complete set of model performance evaluations for the final modeling iteration for the base case episode can be found at http://www.tceq.texas.gov/airquality/airmod/data/dfw8h2.

The performance evaluation of the base case modeling demonstrates the adequacy of the model to correctly replicate the relationship between levels of ozone and the emissions of NO_X and VOC. The model's ability to suitably replicate this relationship is necessary to have confidence in the model's prediction of the response of ozone to various control measures. As recommended in the EPA modeling guidance (EPA, 2007), the TCEQ has incorporated the recommended eight-hour performance measures into its evaluations but focuses primarily on one-hour performance analyses, especially in the DFW area. The localized small-scale (i.e., high resolution) meteorological and emissions features characteristic of the DFW area require model evaluations to be performed at the highest resolution possible to determine whether or not the model is getting the right answer for the right reasons. Although the primary focus of the model performance evaluation is on the nine-county DFW nonattainment area (Figure 3-3), the TCEQ evaluated the model performance at some of the more rural monitors within Texas. Since the modeling resolution is more coarse in the rural areas (e.g., 12 km grid), the performance evaluations are based on graphical measures.

Also in accordance with the EPA modeling guidance, the TCEQ conducted two types of performance evaluations, operational and diagnostic. Operational evaluations include statistical and graphical measures, which compared the modeled ozone and ozone precursors to measured concentrations. Diagnostic evaluations compare the response of the model to changes in the inputs (sensitivity analyses), such as emissions, and the predictive capability of the model (diagnostic analyses), such as retrospective modeling.

4.1 Operational Evaluations

4.1.1 Statistical Measures

Statistical measures provide a quantitative evaluation of model performance. The TCEQ used EPA recommended statistics (EPA, 2007) in evaluating performance of the base case modeling, including the Unpaired Peak Accuracy (UPA), the Mean Normalized Bias (MNB) and the Mean Normalized Gross Error (MNGE). For each of these statistical measures, which use measured and modeled pairs in their calculation, the TCEQ used a modeled value based on a bi-linear interpolation of the ozone concentrations in the four grid cells around and including the

monitor. A comprehensive set of modeled statistical performance measures is available at: http://www.tceq.texas.gov/airquality/airmod/data/dfw8h2.

The UPA statistic compares the difference between the maximum modeled ozone concentration and the highest monitored ozone concentration found over all hours and over all monitoring stations for each day simulated. This comparison was made for both one- and eight-hour peak ozone concentrations. EPA has recommended a range of ± 15-20% for one-hour ozone UPA comparisons, however, no range has been recommended for the eight-hour UPA comparisons. This statistic is more suited to assessing model under-prediction than over-prediction, because the model simulates ozone concentrations across the entire domain, while only a relatively few locations are actually monitored. Even if the model predicted the observations perfectly, its maximum predicted concentration would exceed the maximum observed concentration unless the modeled maximum happened to occur at precisely the location of a monitor.

The MNB statistic compares the relative difference between modeled and monitored ozone concentrations, paired in time and space, averaged over all hours and over all monitoring stations. The MNB was calculated for individual episode days (i.e., average over all monitoring stations) and individual sites (averaged over all days). The MNB provides a measure of the model's tendency to over- or under-predict monitored ozone concentrations. A positive bias indicates that the model's ozone concentrations are higher than measured, and a negative bias indicates the converse. A bias near zero is desirable, although this does not necessarily mean the model is replicating ozone concentrations well, since combining large positive and negative relative differences can result in a near zero MNB. Since the MNB is a relative measure, it involves dividing the difference between modeled and observed concentrations by the observed concentration. For this reason, a cutoff value is always used to prevent division by zero or by very small numbers.

For one-hour ozone, EPA has recommended a range of ± 5-15% for the MNB, for monitored ozone concentration of 60 ppb or greater. For eight-hour ozone, EPA also recommends limiting the calculation of the MNB to monitored ozone concentrations over a minimum threshold of 40 ppb or 60 ppb, but no range is given for consideration of suitable performance. The TCEQ computes the MNB for both the one- and eight-hour ozone concentrations using a minimum threshold of 60 ppb for the one-hour and 40 ppb for the eight-hour. The MNB can be either positive or negative, the former indicating the model is predominantly over-predicting ozone concentrations, the latter indicating a predominant under-prediction (an MNB of zero would mean the model equally over- and under-predicted).

The MNGE statistic is similar to the MNB, except that the absolute value of the relative differences between modeled and monitored ozone concentrations, paired in time and space, averaged over all hours and over all monitoring stations is used. The MNGE was calculated for individual episode days (i.e., average over all monitoring stations) and individual sites (averaged over all days). This statistic is representative of the overall deviation between the modeled and monitored concentrations and is always greater than or equal to zero.

Also similar to the MNB, EPA recommends only calculating the MNGE for measured and modeled pairs where the monitored ozone concentration is greater than a minimum threshold. The TCEQ computes the MNGE for both the one- and eight-hour ozone concentrations using a minimum threshold of 60 ppb for the one-hour and 40 ppb for the eight-hour. For one-hour, the EPA-recommended range for MNGE is ≤ 30-35%, but for eight-hour no range is specified.

4.1.2 Graphical Measures

Graphical measures provide a qualitative evaluation of model performance. The TCEQ used time series plots, scatter plots and peak ozone tile plots as recommended in the EPA guidance. A comprehensive set of modeled statistical performance measures is available at: http://www.tceq.texas.gov/airquality/airmod/data/dfw8h2.

Time series plots are used to compare the hourly modeled concentrations with those measured at a monitor for each hour of an episode. This comparison is used to assess how well the model predicts diurnal and/or daily variation in the ozone and ozone precursor concentrations at specific locations. Comparing the time series of modeled versus measured concentrations of ozone and ozone precursors can indicate whether the model is correctly replicating the physico-chemical processes by which ozone was actually generated. Because of the large number of monitors used in the model performance evaluation and number of pollutants provided by CAMx (30, including some combined species like NO_X and NO_Y), it is not feasible to provide a comprehensive set of time series graphics for every pollutant and monitor. Time series of hourly ozone and key precursors are provided for specific monitors selected because of their measured ozone concentrations.

Scatter plots of hourly measured and modeled ozone and precursor concentrations show overall patterns of under- and/or over-prediction for the episode. Since the typical ambient concentration for some precursors species (e.g., isoprene) is close to their analytical minimum detection limits (MDL), the scatter plots also include the measurement MDL for pertinent precursor species. In addition, on the scatter plots are the measured versus modeled Quantile-Quantile (QQ) plots, which plot the same measured and modeled concentrations as shown in the normal scatter plot, but the respective values are independently sorted from smallest to largest. The QQ plots indicate the comparability of the distributions of the measured versus modeled concentrations. If the QQ plot lies near the 1-1 line (also depicted on the plots), then it indicates that the model produces about the same number of low, medium, and high values as the monitor. The scatter plots also show the coefficient of determination, R^2, which measures the correlation between modeled and measured concentrations. However, this statistic is not emphasized, since R^2 is a measure of correlation, not predictive accuracy, and since photochemical grid models such as CAMx and CMAQ are not designed to simulate precursor species to the same degree of accuracy as ozone. There is often notable scatter for precursor species due to a variety of reasons, including the incommensurability of modeled and measured concentrations of primarily-emitted species at small spatial scales, and the limitations of the model at the sub-grid scale. Thus for many chemical species, the QQ plot is more useful than R^2 for evaluating model performance.

Peak (daily maximum) eight-hour ozone tile plots (overlaid with monitored maximum values) were developed to provide a visual means of assessing where the model predicts daily maximum eight-hour ozone concentrations compared to observations.

4.2 Diagnostic Evaluations

4.2.1 Sensitivity Analyses

Sensitivity analyses were conducted to check the response of the modeled ozone to changes in model inputs including meteorological parameters and precursor emissions. The results of these analyses were also used in quality assuring the input. The TCEQ conducted several sensitivity analyses, including an alternative meteorological configuration, an alternative set of initial and boundary conditions, and alternative modeling emissions.

The alternative meteorological configuration sensitivity analysis compared the use of the Medium Range Forecast (MRF) boundary layer scheme to the use of the ETA boundary layer scheme on the 4 km domain. MRF was used on the outer domains.

The alternative set of initial and boundary conditions compared the MOZART global atmospheric model conditions developed by Environ in 2008 to those using the updated MOZART version 3 model.

One sensitivity of alternative modeling emissions compared oil and gas inventories with and without Louisiana Haynesville Shale drill rig emissions. Another alternative modeling emissions sensitivity compares results using MOBILE6.2 versus MOVES2010a on-road mobile emissions. One other modeling emissions sensitivity discusses the differences between modeling the EPA's Cross State Air Pollution Rule (CSAPR) and the EPA's Clean Air Interstate Rule.

The episodic model performance (Section 4.3.4) discusses model performance for three different base case configurations that differ due to implementations of the Texas oil and gas emissions and the choice of the on-road mobile emissions model.

4.2.2 Diagnostic Analyses

Diagnostic analyses were conducted to focus on the model's change in predicted ozone to changes in the ozone precursor emissions. The TCEQ conducted several diagnostic analyses, including retrospective modeling, observational modeling and source apportionment analysis.

The retrospective modeling was conducted by using the attainment test methodology to predict eight-hour ozone design values for 1999 (i.e., projecting back in time rather than forward). The model-projected eight-hour zone design values at the various monitors for the year 1999 were compared to the year 1999 design values calculated from the eight-hour ozone concentration measurements.

The observational modeling was conducted for weekdays and weekends. Weekend emissions in urban areas tend to be lower than weekday emissions primarily due to lower traffic volumes (i.e., fewer miles driven). The effect is most pronounced on weekend mornings, especially Sundays, since commuting is much lower than weekdays.

The source apportionment analysis was conducted on the future (2012) year modeling. This analysis provides an estimate of the contribution to the 2012 modeled ozone concentration from the various emission source categories in selected regions.

The chemical process analysis was conducted on the base case modeling. This analysis was used to evaluate the relative roles of local ozone production and regional background ozone, and to examine the sensitivity of ozone formation in DFW to VOC and NO_X concentrations

Additional information on these analyses is presented in subsequent sections of this appendix.

4.3 Episodic Model Performance Assessment for Ozone

This section presents a set of episode-wide performance assessments for one- and eight -hour ozone for the base case episode. These episodic assessments are similar to the usual one- and eight-hour statistical and graphical performance measures, but are calculated across all days in the episode to provide overall model performance assessments. It would be inappropriate to rely on these summary metrics instead of performing a detailed day-by-day performance assessment; nevertheless, episode-wide statistics can provide a first-order basis for comparing

model performance across iterations of the base case, which is shown below for three DFW base cases, Reg1a, Reg1b and Reg2. For these assessments, five low-ozone days (June 16, 20, 21, 22 and July 2) were excluded because of very low eight-hour observed ozone (< 50 ppb).

4.3.1 Assessments Based on all Hourly Modeled-Observed Pairs

The first assessment (Episode Mean Relative Bias) is an extension of the usual mean normalized bias (MNB) statistic, but instead of being calculated across monitors and hours within each day, Assessment 1 is calculated across all monitors and all hours of all days in the episode. Therefore, Assessment 1 quantifies the model's tendency to over-predict or under-predict measured (observed) ozone concentrations for the overall episode. Assessment 1 is calculated as:

where i represents one of I episode days, j represents one of J monitors, and k represents one of K hours included in the calculation ($K \leq 24$). O_{ijk} is observed ozone concentration on day i at monitor j for hour k. M_{ijk} similarly represents the modeled value at monitor j for the indicated day and hour. Model values at the monitor locations are calculated through bilinear interpolation from the four grid cell centers nearest the monitor. As is the case with the usual MNB statistic, data points with observed one-hour ozone concentrations less than 60 ppb are not included in this case, and consequently five days with monitored ozone concentrations less than 60 ppb were excluded from the calculations (even though other statistics can be calculated including these days, they were excluded because they are of no interest). Note that this performance metric, along with the three that follow, is not calculated for eight-hour ozone concentrations. Because the eight-hour concentration for an hour only differs from that of the previous hour by a single hourly concentration, both the observed and modeled values in Assessment 1 are highly inter-correlated and interpretation of the result would be very difficult.

A related statistic (Episode Mean Bias) uses the non-normalized differences to calculate the model bias in the original units of measurement (ppb) instead of percent like Assessment 1. It is shown below:

The third assessment (Episode Mean Relative Error) presented is similar to Assessment 1, but the (M – O) differences are replaced by their absolute values as shown below:

This statistic measures the overall difference between modeled and observed values, and as such includes both the bias and the spread of the differences. The lower bound for this statistic is the absolute value of the bias calculated in Equation 1, but can be considerably larger in cases where the model under-predicts on some days and over-predicts on others.

The fourth assessment (Episode Mean Error) is similar to Assessment 1_A, but uses the absolute differences instead of the relative differences as shown:

Again, this metric is represented in the original units of measurement (ppb) instead of percent.

4.3.2 Assessments Based on Daily Peak Modeled-Observed Pairs at Monitor Sites

Assessments 3-4_A are based on the daily peaks observed and modeled at each monitor location. While these assessments are particularly suited to eight-hour ozone concentrations, it is still informative to calculate these assessments for one-hour peaks. In this (and the following) section, modeled and observed daily peak concentrations represent either one- or eight-hour values.

Assessment 3 (Episode Mean Site Peak Relative Bias) is akin to Assessment 1, except the sum is taken over only two indices (site and day):

Assessment 3_A (Episode Mean Site Peak Bias) used non-normalized Modeled - Observed values, and is in units of ppb (the formula is omitted for brevity).

Assessment 4 (Episode Mean Site Peak Error) is similar to Assessment 3, but with the parentheses replaced by absolute value symbols (see Equations 1 and 2). Assessment 4_A (Episode Mean Site Peak Error) is similar to Assessment 2_A, but with one fewer summation indices. These two formulae are also omitted.

4.3.3 Assessments Based on Daily Peak Modeled-Observed Concentrations Unpaired in Space and Time

This assessment compares two values per day, domain-wide peak modeled ozone concentration and the domain-wide observed concentration. This assessment is primarily useful for ensuring that the model is simulating peak concentrations that are reasonably close to the highest observed values. Because the model simulates ozone concentrations across the domain while the observed concentrations are limited to the monitor locations, it is reasonable to expect the modeled peak to exceed the observed peak.

Assessment 5 (Episode Relative Mean Domain-wide Peak-Peak Comparison) is similar to Assessment3, but this time the sum is taken only over days:

Similarly, Assessment 5_A (Episode Mean Domain Wide Peak-Peak Comparison) provides the mean modeled-observed non-normalized difference (equation not shown).

4.3.4 Episodic Model Performance Assessment

Using these ten model performance assessments, comparisons across three iterations of the base case (Reg1b, Reg2, and Reg2_MVS) are performed below. A brief description of the three modeling configurations is presented in Table 3-2.

Figure 4-1: *DFW One-Hour Episodic Ozone Performance Statistics (normalized), Three Base Cases* compares the one-hour relative assessments across model configurations, and Figure 4-2: *DFW One-Hour Episodic Ozone Performance Statistics (non-normalized), Three Base Cases* compares the one-hour assessments (non-normalized) across configurations. Because the figures are very similar to one another, only the latter figure is discussed since its units are in ppb and not percent. Note that days with observed peak one hour ozone < 60 ppb are not included in any of the statistics presented in this section.

Overall, episode mean bias shows that for all three model runs there is a general under-prediction in the 6-10 ppb range. The episode mean error is in the 9-11 ppb range, which is only a little larger than the absolute value of the bias, indicating that only a small amount of error is caused through over-prediction and the remainder is attributable to under-prediction. The episode mean site peak bias and error are on the order of 1-3 ppb smaller (closer to zero) than the values calculated using all pairs, indicating that the model simulates the monitored daily peaks better than it simulates the overall set of observed data. In the case of Reg2_MVS, the error is about twice the absolute bias, meaning the model over-predicts the site daily one-hour peaks relatively more often than it does the hourly observations. Finally, the episode mean domain-wide peak-peak comparison shows that, on average, Reg2_MVS predicts the domain-wide peaks well while the other two base cases tend to under-predict by a few ppb. Overall, the Reg2_MVS base case shows a reduced tendency towards under-prediction of both the hourly concentrations and the daily one-hour peaks compared with the earlier base cases.

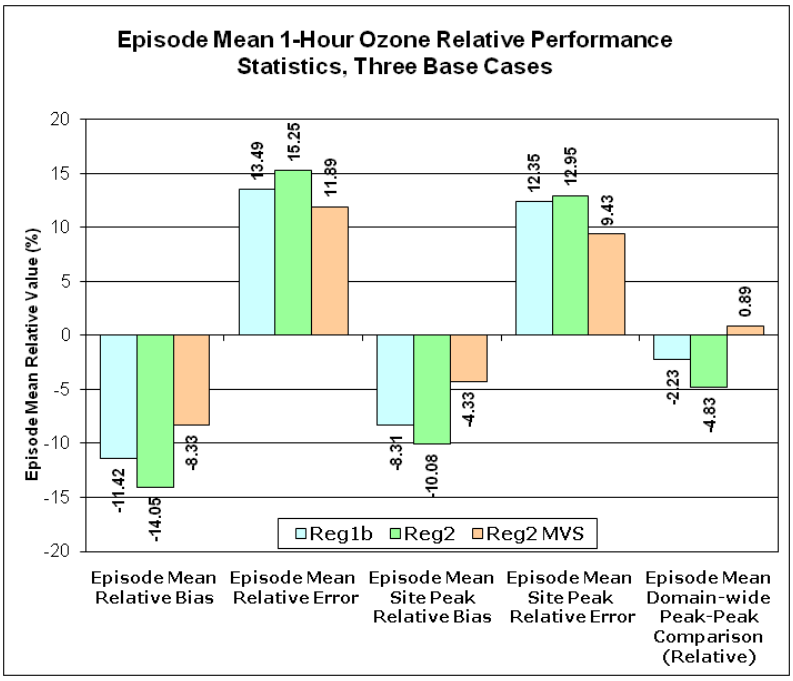

Figure 4-1: DFW One-Hour Episodic Ozone Performance Statistics (normalized), Three Base Cases

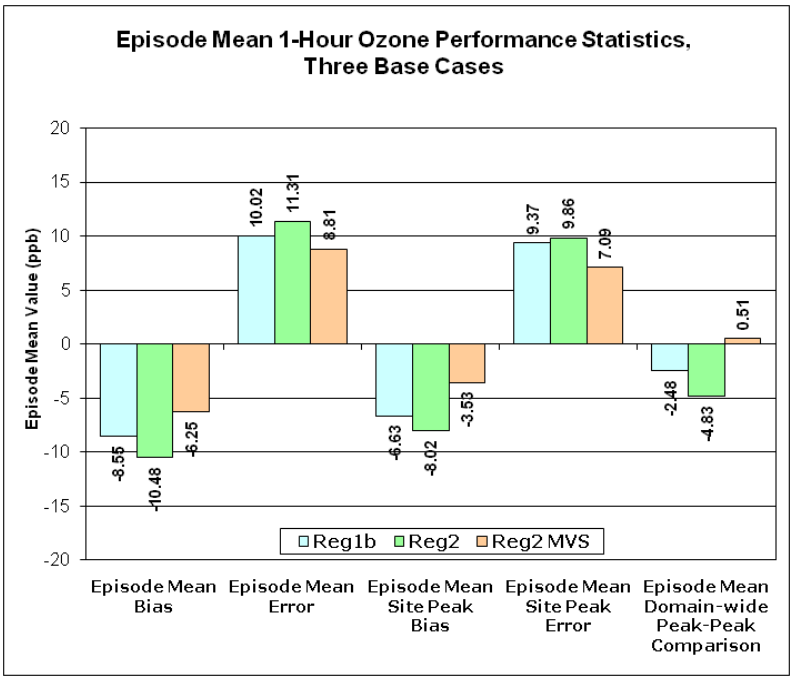

Figure 4-2: DFW One-Hour Episodic Ozone Performance Statistics (non-normalized), Three Base Cases

Figure 4-3: *DFW Eight-Hour Episodic Model Performance Statistics (normalized), Three Base Cases* and Figure 4-4: *DFW Eight-Hour Episodic Model Performance Statistics (non-normalized), Three Base Cases* compare the eight-hour daily peak ozone statistics among model configurations. Because the data values are daily maxima, all model-observation pairs are included (except as noted above). Focusing on Figure 4-4, the bias and error for the eight-hour concentrations are 2 or 3 ppb better than their one-hour analogues, but the peak-peak comparison is slightly worse. As was the case with one-hour ozone concentrations, the Reg2_MVS base case 8-hour underprediction bias is smaller than those of its predecessor base cases. Based on the episodic model performance evaluation, Reg2_MVS represents a notable improvement in model performance over both the Reg1b and Reg2 base cases.

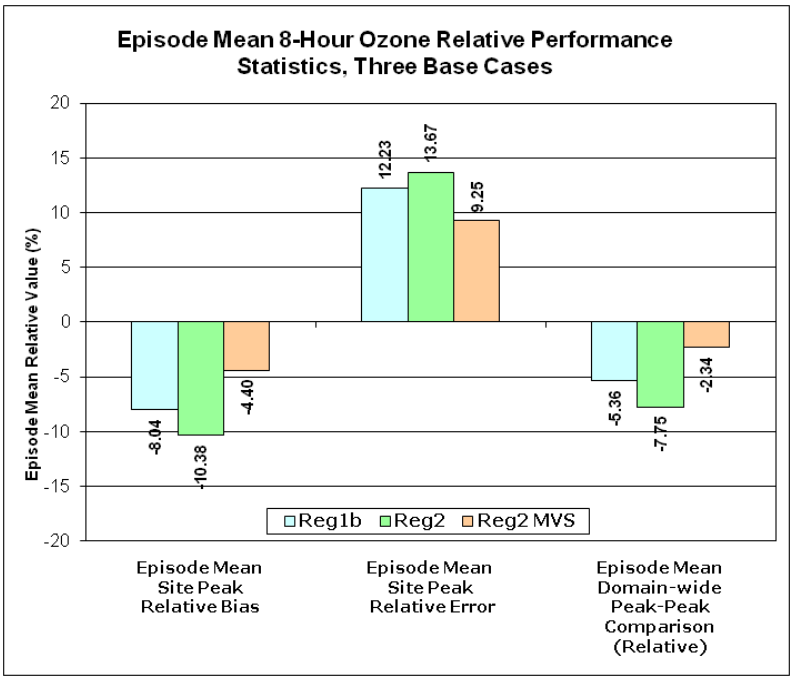

Figure 4-3: DFW Eight-Hour Episodic Model Performance Statistics (normalized), Three Base Cases

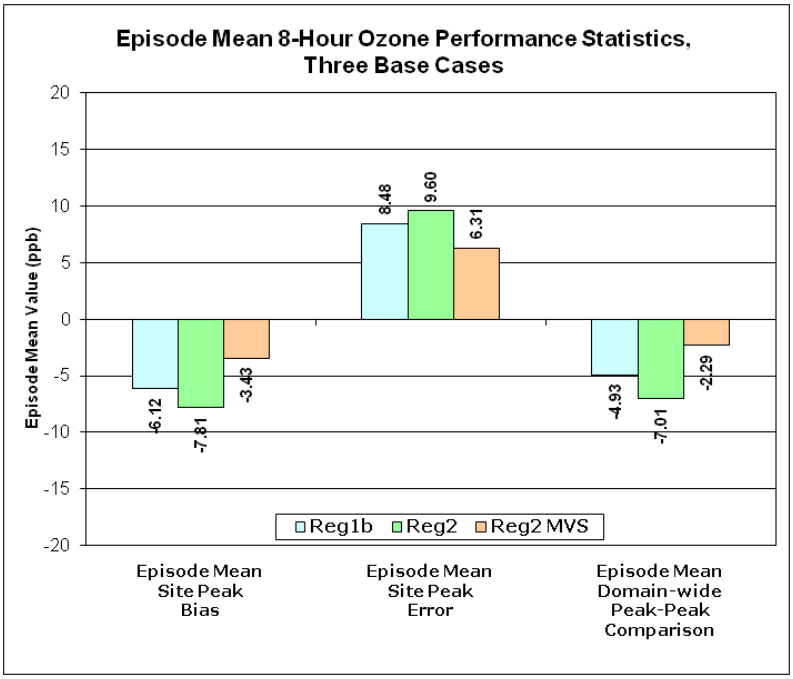

Figure 4-4: DFW Eight-Hour Episodic Model Performance Statistics (non-normalized), Three Base Cases

5 MAY 31 – JULY 2, 2006 EPISODE

5.1 Statistical Measures

The statistical measures UPA, MNB and MNGE were calculated comparing measured and bi-linearly interpolated modeled ozone concentrations for all episode days and regulatory monitors. Graphical measures comprised of time series and scatter plots of hourly measured and bi-linearly interpolated modeled ozone and some ozone precursors (e.g., NO, NO_2, ETH, CO) concentrations, where applicable for each regulatory monitoring site, and tile plots of daily maximum eight-hour ozone concentrations are shown.

Figure 5-1: *Monitored versus Modeled Peak Hourly Ozone Concentrations* compares the monitored and modeled peak hourly ozone concentrations for each day for the sequence of base case modeling iterations for the episode. The differences between the observed and modeled bars show the UPA for monitored hourly ozone concentrations for the sequence of base case modeling iterations. The model predicts the peak monitored one-hour ozone concentrations very well, with all days with observed concentrations above 60 ppb within the recommended limit of $\pm$ 20%. While the iterations of modeling configurations from Reg1b and Reg2 show similar responses through the episode, Reg2_MVS shows a more favorable comparison for most days with higher monitored peak hourly ozone concentrations.

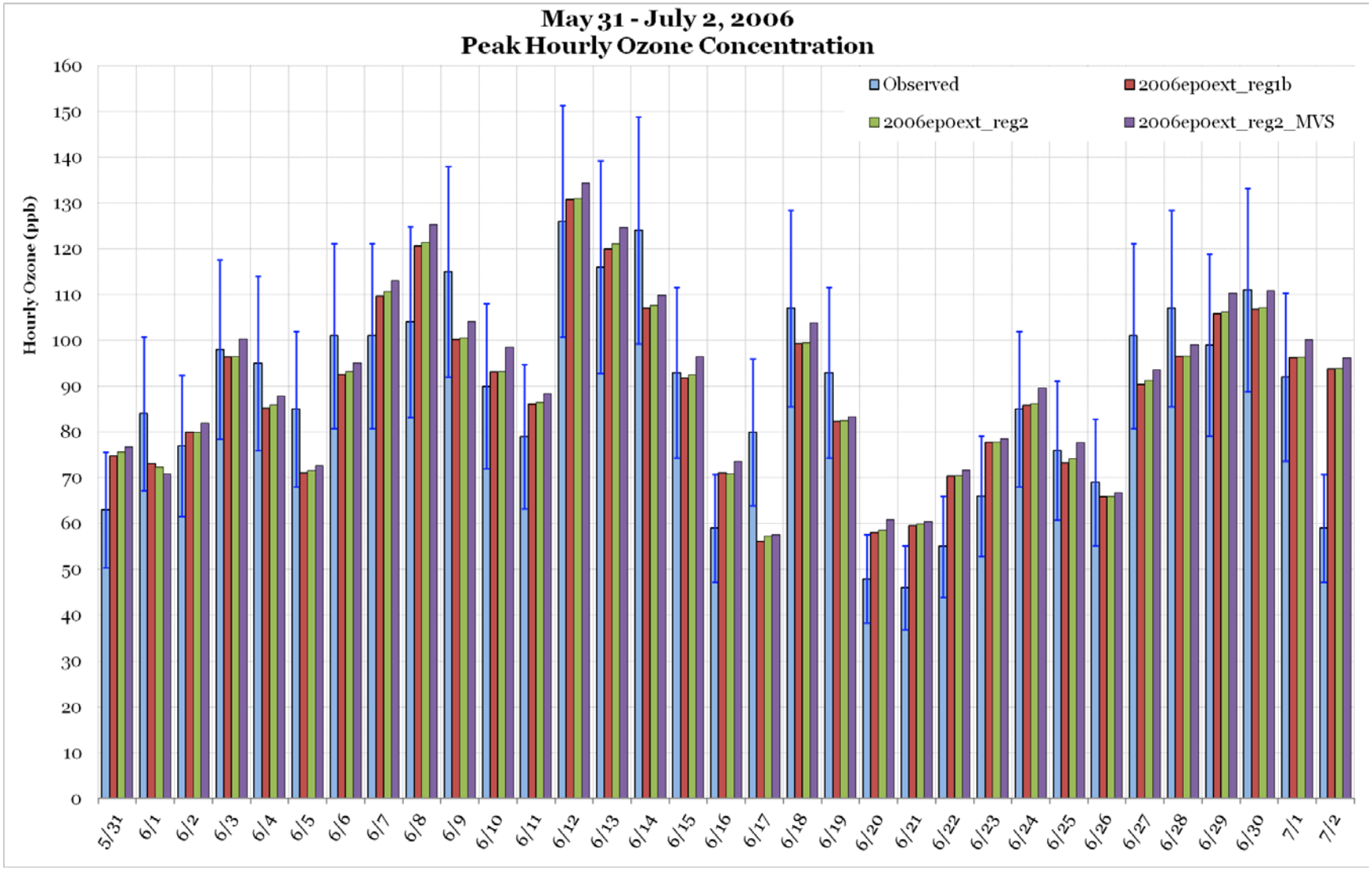

Figure 5-1: Monitored versus Modeled Peak Hourly Ozone Concentrations

Figure 5-2: *Soccer-style Plot of Hourly MNGE and MNB by Day* shows the MNGE and MNB statistics for paired modeled and measured hourly ozone concentrations for each modeling iteration, when the measured hourly ozone concentration was greater than 60 ppb. The plot derives its name from its resemblance to a soccer goal box, indicating the area in which both MNB and MNGE meet the EPA performance goals established in the 1990 Guidance (EPA, 1990). Note that it is mathematically impossible for the MNGE to be smaller than the MNB, hence all the points plotted lie within a 90 degree wedge whose vertex lies at the origin (0,0).

The MNB show that the model tends to under-predict the hourly ozone concentrations on most days. The Reg2_MVS run under-predicts less on almost every day.

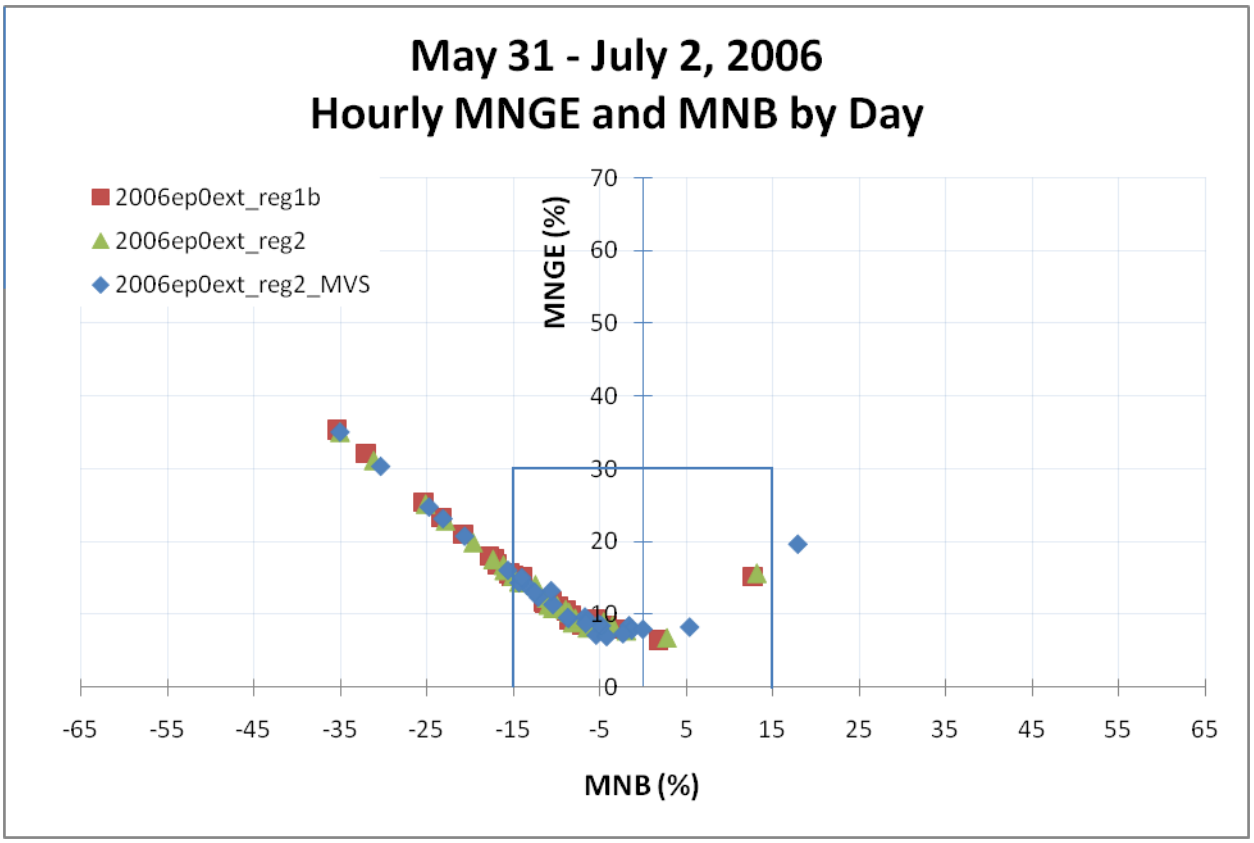

Figure 5-2: Soccer-style Plot of Hourly MNGE and MNB by Day

Figure 5-3: *Soccer-style Plot of Hourly MNGE and MNB by Monitor* shows the MNGE and MNB statistics for paired modeled and measured hourly ozone concentrations for each modeling iteration, when the measured hourly ozone concentration was greater than 60 ppb. The MNGE was less than the recommended maximum measure of 30% for all iterations. The MNB show that the model tends to under-predict the hourly ozone concentrations at most sites, with zero sites less than the recommended measure of -15% using the Reg2_MVS run.

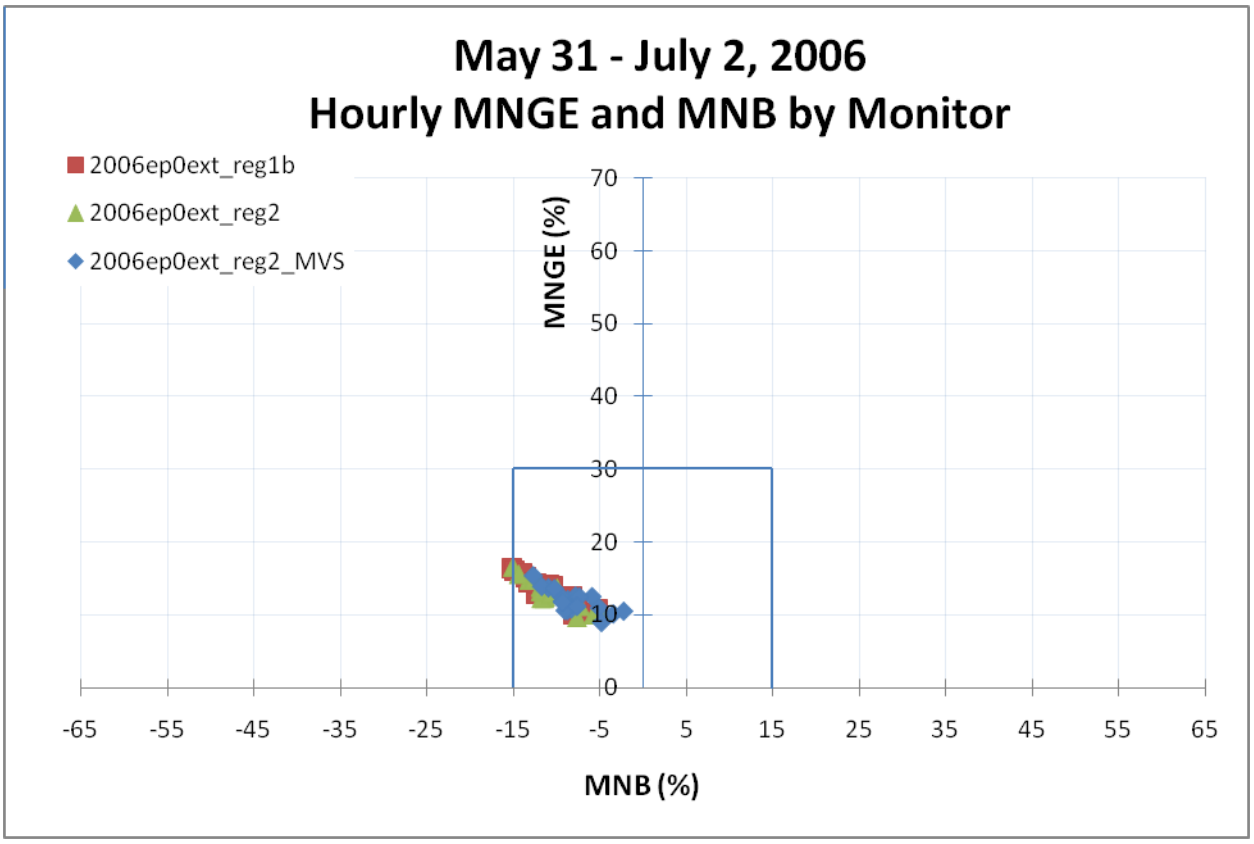

Figure 5-3: Soccer-style Plot of Hourly MNGE and MNB by Monitor

Figure 5-4: *Measured versus Modeled Peak Eight-Hour Ozone Concentrations* compares the monitored and modeled peak eight-hour ozone concentrations for each episode day for the sequence of base case modeling iterations. The Reg1b and Reg2 runs tend to under-predict the eight-hour ozone peaks. The Reg2_MVS run matches the observed peaks much better.

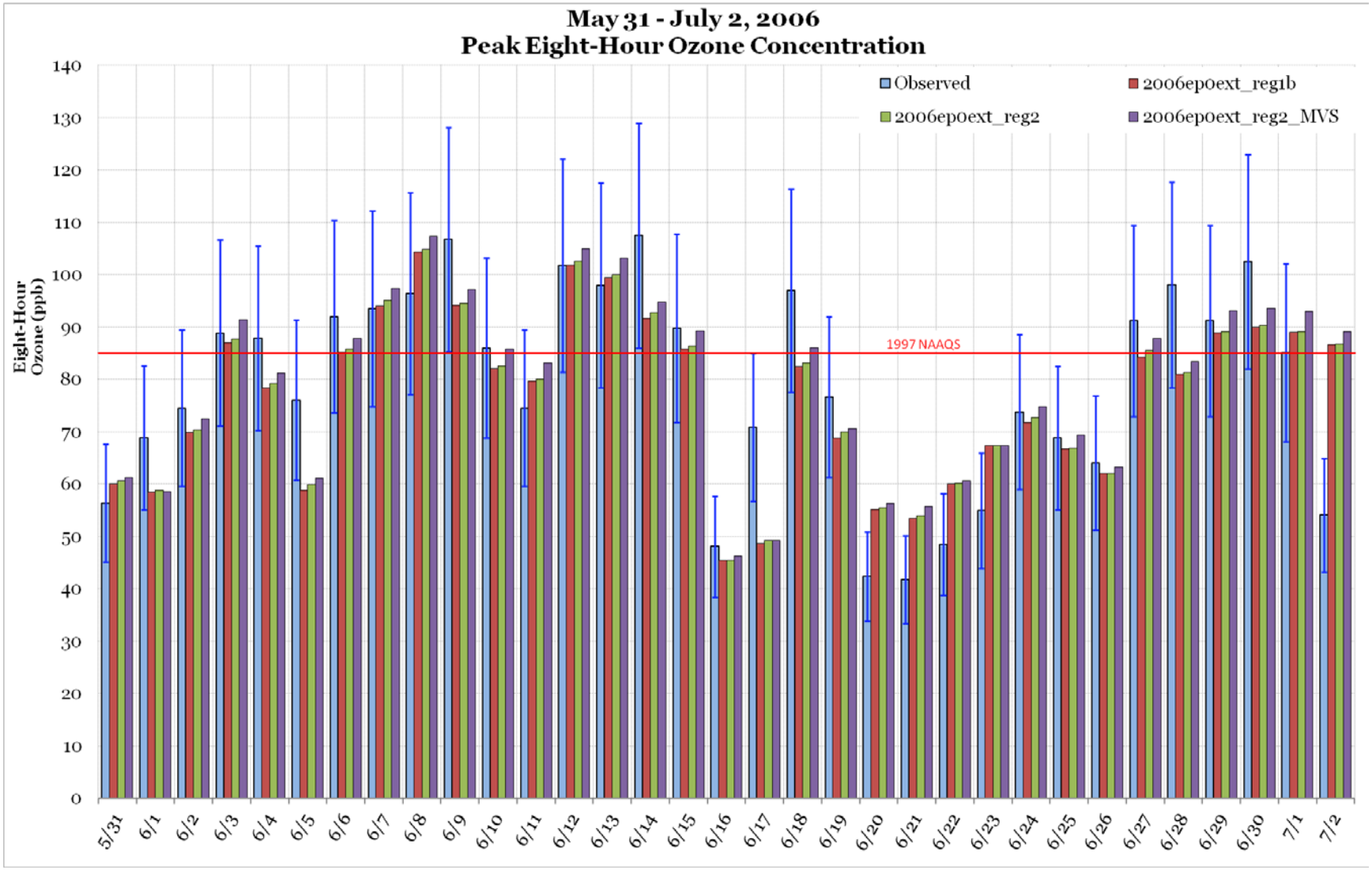

Figure 5-4: Measured versus Modeled Peak Eight-Hour Ozone Concentrations

Figure 5-5: *Soccer-style Plot of Eight-Hour MNGE and MNB by Day* shows the MNGE and MNB statistics for paired modeled and measured daily maximum eight-hour ozone concentrations for each modeling iteration. Although there are no recommended limits for the eight-hour MNGE and MNB, it is reasonable to expect that the criteria for eight-hour MNGE and MNB should not be more than the recommended 30% and ± 15%, respectively. Using these criteria as a guide, the MNB and MNGE compare quite favorably for all iterations. Only two ozone exceedance days fall outside of the benchmarks, June 18 and July 1. On both days the meteorological conditions proved difficult to replicate. The reversing winds with a slow-moving front were not captured well on June 18. The cloudy conditions were not simulated on July 1 resulting in an over-prediction of ozone.

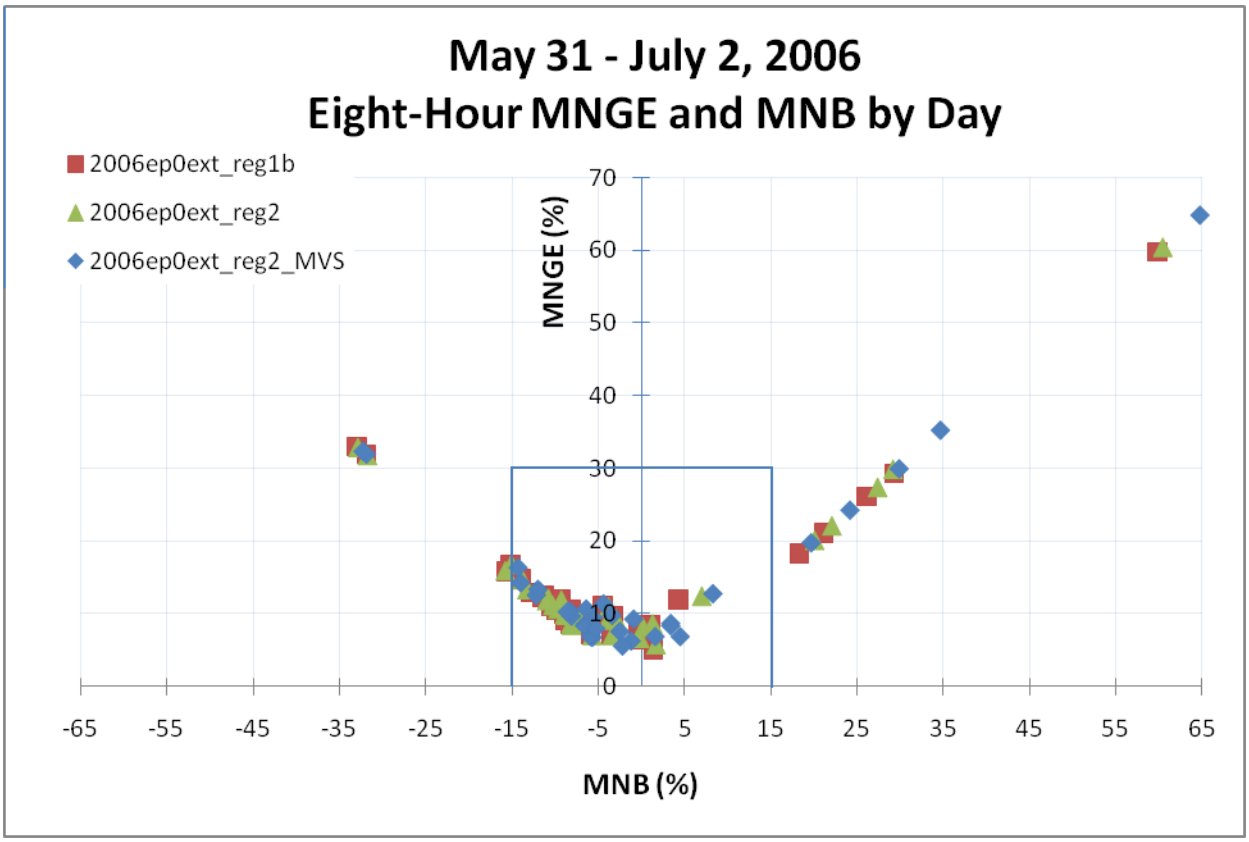

Figure 5-5: Soccer-style Plot of Eight-Hour MNGE and MNB by Day

Figure 5-6: *Soccer-style Plot of Eight-Hour MNGE and MNB by Monitor* shows the MNGE and MNB statistics for paired modeled and measured eight-hour ozone concentrations for each modeling iteration, when the measured eight-hour ozone concentration was greater than 80 ppb. While all monitors meet the MNGE benchmark, the model has a consistent negative bias at each of the monitors except Arlington (ARLA). In the reg1b and reg2 runs Eagle Mountain Lake and Pilot Point both have biases just outside of the -15% goal. With MOVES (reg2_MVS), all monitors meet the bias and gross error goals.

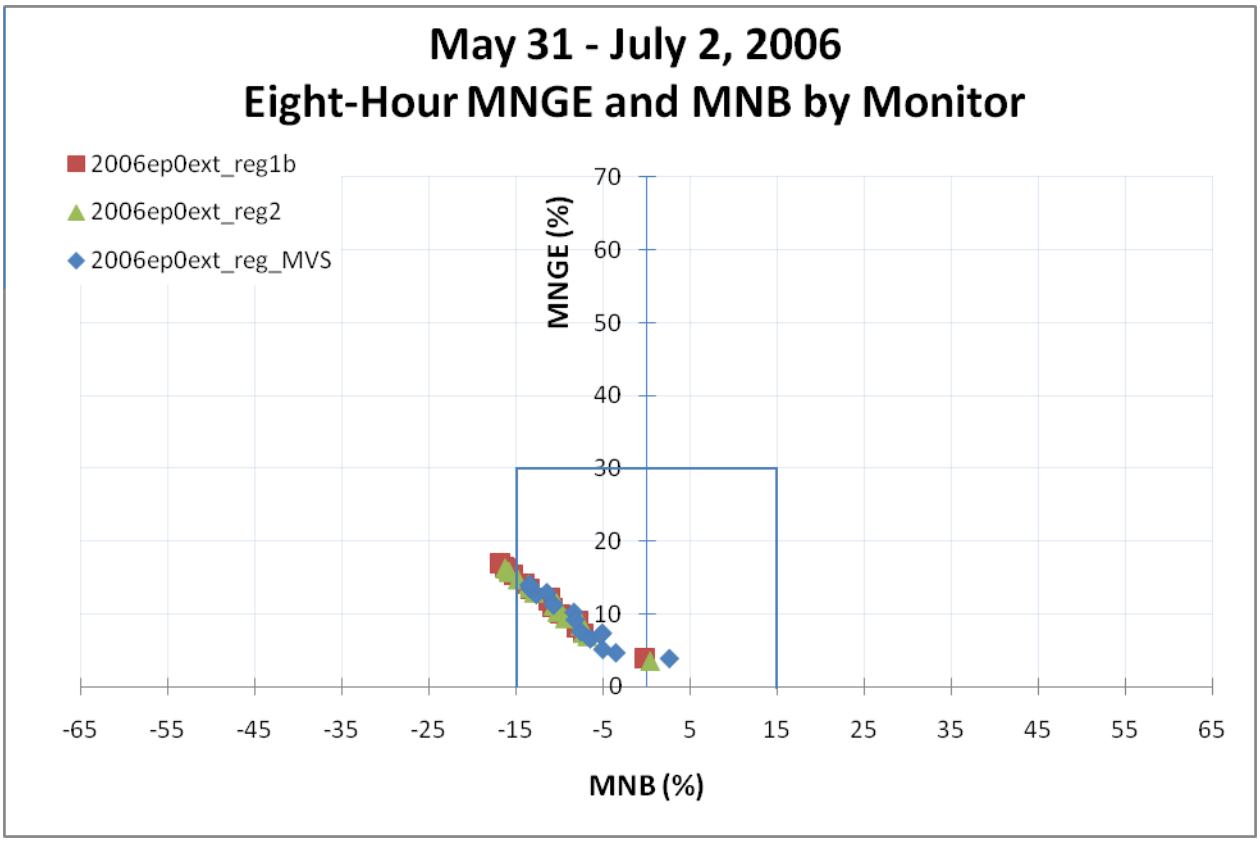

Figure 5-6: Soccer-style Plot of Eight-Hour MNGE and MNB by Monitor

Table 5-1: *Episode Daily Maximum Eight-Hour Ozone Statistical Measures for the Reg2_MVS Modeling Iteration* summarizes the daily maximum eight-hour statistics (i.e., MNB, MNGE, UPA) by episode day evaluated for all monitors for the Reg2_MVS modeling iteration. The MNB and MNGE values are those plotted in Figure 5-5, and the UPA values correspond to the percent difference between the modeled and measured peak daily maximum eight-hour ozone concentrations plotted in Figure 5-4.

Table 5-1: Episode Daily Maximum Eight-Hour Ozone Statistical Measures for the Reg2_MVS Modeling Iteration

Episode Day	MNB (%)	MNGE (%)	UPA (%)	Modeled Eight-Hour Peak Ozone (ppb)	Measured Eight-Hour Peak Ozone (ppb)
5/31/2006	-3.4	9.7	8.6	61.3	56.4
6/1/2006	-4.4	11.3	-15.0	58.6	68.9
6/2/2006	-5.7	6.7	-2.6	72.5	74.5
6/3/2006	3.4	8.6	2.9	91.4	88.9
6/4/2006	-5.9	6.8	-7.5	81.3	87.9
6/5/2006	-14.3	16.3	-19.7	61.1	76.1
6/6/2006	-8.1	9.6	-4.6	87.8	92.0
6/7/2006	-1.2	6.2	4.2	97.4	93.5
6/8/2006	3.4	8.3	11.4	107.3	96.4

Episode Day	MNB (%)	MNGE (%)	UPA (%)	Modeled Eight-Hour Peak Ozone (ppb)	Measured Eight-Hour Peak Ozone (ppb)
6/9/2006	-8.3	10.3	-8.9	97.2	106.8
6/10/2006	-2.2	5.5	-0.2	85.8	86.0
6/11/2006	4.5	6.8	11.7	83.2	74.5
6/12/2006	1.6	6.8	3.2	105.0	101.8
6/13/2006	-0.9	9.2	5.3	103.2	98.0
6/14/2006	-6.3	8.4	-11.9	94.8	107.5
6/15/2006	-6.5	8.5	-0.5	89.3	89.8
6/16/2006	-12.2	12.5	-3.8	46.3	48.1
6/17/2006	-31.9	31.9	-30.4	49.3	70.9
6/18/2006	-32.3	32.3	-11.2	86.1	97.0
6/19/2006	-6.6	8.3	-7.8	70.6	76.6
6/20/2006	24.2	24.2	32.9	56.3	42.4
6/21/2006	29.9	29.9	33.6	55.8	41.8
6/22/2006	19.7	19.7	25.0	60.6	48.5
6/23/2006	8.3	12.7	22.5	67.4	55.0
6/24/2006	-5.6	9.4	1.4	74.8	73.8
6/25/2006	-6.4	10.6	0.9	69.4	68.8
6/26/2006	-14.0	14.2	-1.2	63.3	64.1
6/27/2006	-8.6	10.2	-3.8	87.8	91.2
6/28/2006	-12.0	13.3	-15.0	83.4	98.1
6/29/2006	-5.3	7.9	2.1	93.1	91.2
6/30/2006	-2.5	7.5	-8.6	93.6	102.5
7/1/2006	34.7	35.2	9.2	93.0	85.1
7/2/2006	64.8	64.8	64.8	89.2	54.1

Table 5-2: *Monitor Specific Eight-Hour Ozone Statistical Measures for the Reg2_MVS Modeling Iteration* summarizes the eight-hour statistics (i.e., MNB, MNGE) by monitor. The MNB and MNGE are evaluated using paired measured and modeled eight-hour ozone concentrations, for which the measured eight-hour ozone concentration was greater than 80 ppb. MNB and MNGE values that are blank indicate that there were no measured eight-hour ozone concentrations greater than 80 ppb during this episode at the specific site. The MNB and MNGE values are those plotted in Figure 5-6, for the Reg2_MVS modeling iteration.

Table 5-2: Monitor Specific Eight-Hour Ozone Statistical Measures for the Reg2_MVS Modeling Iteration

Monitor	Monitor	MNB (%)	MNGE (%)
ARLA	Arlington C61	2.6	3.9
CLEB	Cleburne C77	-5.1	5.2
DALN	Dallas North C63	-12.7	12.7
DENT	Denton C56	-10.8	11.4

Monitor	Monitor	MNB (%)	MNGE (%)
DHIC	Dallas Hinton C401	-7.6	7.6
EMTL	Eagle Mountain Lake C75	-13.6	14.1
FRIC	Frisco C31	-13.5	13.6
FWMC	Fort Worth Northwest C13	-8.4	10.3
GRAP	Grapevine Fairway C70	-5.1	7.4
KAUF	Kaufman C71		
KELC	Keller C17	-8.3	9.3
MDLO	Midlothian OFW C52	-3.6	4.7
MDLT	Midlothian Tower C94	-6.5	6.7
PIPT	Pilot Point C1032	-13.5	14.0
REDB	Dallas Exec Airport C402	-10.8	11.3
RKWL	Rockwall Heath C69		
WTFD	Weatherford Parker County C76	-11.5	13.0
GRAN	Granbury C73	-5.4	7.2
GRVL	Greenville C1006		

5.2 Graphical Measures

5.2.1 Time Series

Time series plots are used to compare modeled hourly concentrations of pollutants against measurements at a site throughout a period of time, in this case throughout an episode. Because of the large number of monitors used in the model performance evaluation (29) and number of pollutants provided by CAMx (30, including some combined species like NO_X and NO_Y) it is not feasible to provide a comprehensive set of time series graphics for every monitor. This section instead focuses on four specific monitors; two (Hinton Street – DHIC and Meacham Field – FWMC) were selected because they have speciated hourly hydrocarbon measurements from the automated gas-chromatograph instruments located at the sites, and two (Denton – DENT and Eagle Mountain Lake – EMTL) because of their high ozone concentrations in the episode. Along with the final base case (Reg2_MVS), an earlier base case, Reg2, is also shown to illustrate the effects on modeled atmospheric concentrations of replacing the original on-road mobile source emissions (MOBILE6.2) with MOVES2010a-based emissions.

Figure 5-7: *Time Series of Hourly Modeled and Observed Ozone Concentrations at* (Top to Bottom) *Hinton Street* (DHIC), *Meacham Field* (FWMC), *Denton (DENT*) and *Eagle Mountain Lake (EMTL*) shows that at Hinton Street, model performance is overall quite good through most of the episode, but the model did under-predict observed peaks by over 5 ppb on June 3 and 27. Overnight model performance is fairly good, with only a small positive bias seen on most nights. This is in contrast to Houston modeling, where the model tended to over-predict overnight concentrations often by 20-30 ppb or more. The increased on-road mobile source emissions in the Reg2_MVS base case noticeably increased peak ozone concentrations over the Reg2 base on several days, most notably June 3 and 30, improving model performance in most cases.

At Meacham field, the model predicted very well the high peaks recorded on June 8 and 12, but under-predicted peaks on June 9, 13, 14, 18, and 27 by 5 to 10 ppb or more. A slight increase

between Reg2 and Reg2_MVS can be seen in the daytime peaks of several days due to additional on-road mobile source emissions, but the effect is smaller than at Hinton Street likely due to lower local traffic volume. Overnight performance is similar to that seen at Hinton Street, with only marginal differences between base cases.

At Denton, the model under-predicted most of the higher peak concentrations by between 5 and 20 ppb, but did predict some 80+ ppb peaks well, including June 10-12, 15, and July 1. The Reg2_MVS case is seen to enhance afternoon peak ozone concentrations, especially on June 3, 9, 10, 14, 15, and June 29- July 1, leading to improved performance in most cases.

At Eagle Mountain Lake, the model reproduced the observed peaks on June 3, 8, and 12 and on July 1 well, but under-predicted the remaining 80+ ppb peaks by 5-20 ppb. At this site, the difference between the Reg2 and Reg2_MVS base cases is fairly small, but Reg2_MVS increases afternoon peak concentrations by a few ppb, especially later in the episode.

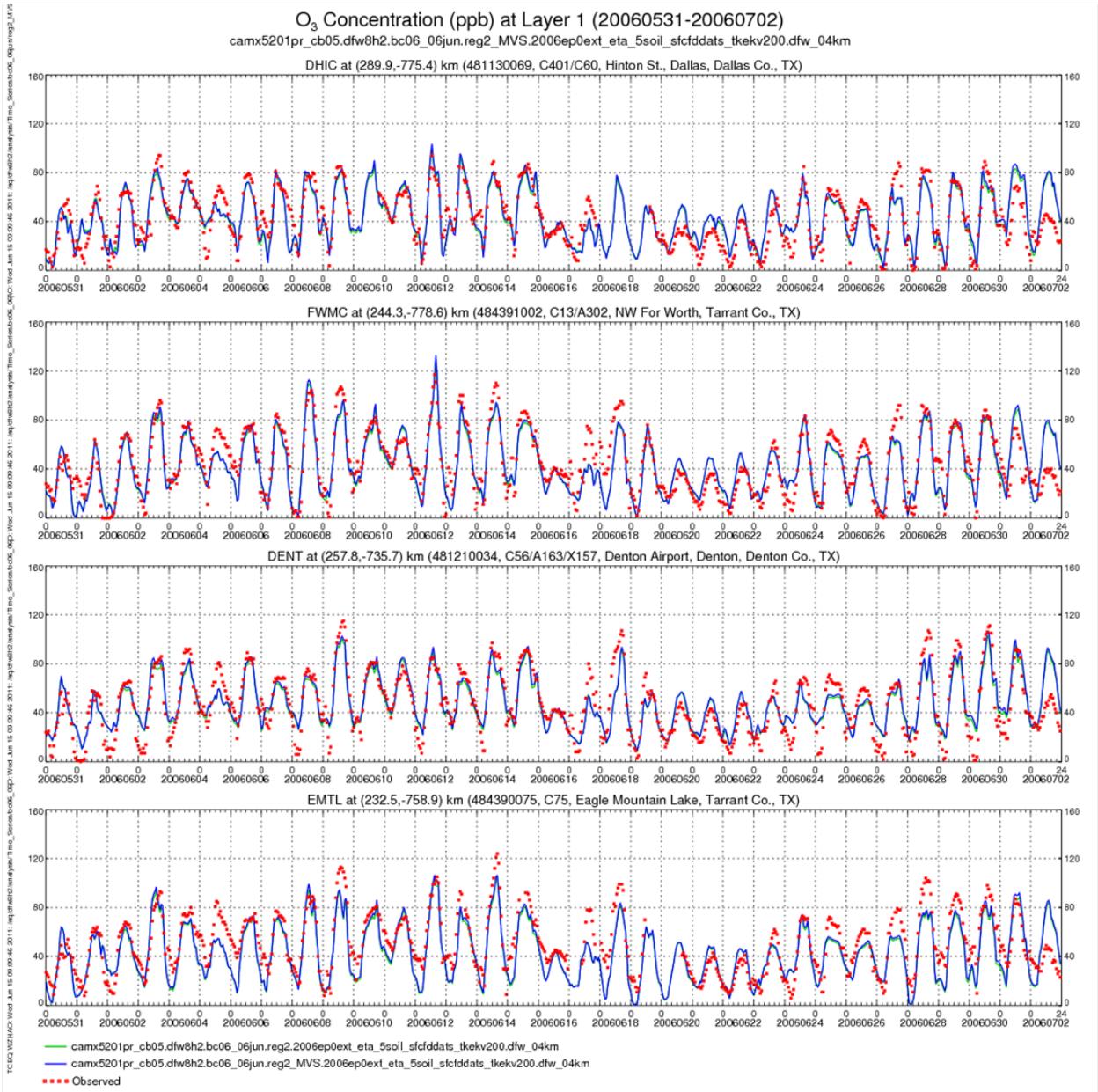

Figure 5-7: Time Series of Hourly Modeled and Observed Ozone Concentrations at (Top to Bottom) Hinton Street (DHIC), Meacham Field (FWMC), Denton (DENT) and Eagle Mountain Lake (EMTL)

Figure 5-8: *Time Series of Hourly Modeled and Observed* NOX *Concentrations at* (Top to Bottom) *Hinton Street* (DHIC), *Meacham Field* (FWMC), *Denton (DENT*) and *Eagle Mountain Lake (*EMTL) shows that at Hinton Street the model does a good job of reproducing the overall temporal patterns seen in the observations, and in fact reproduces the observations quite well on several days. The model under-predicts the morning (rush hour) peaks on June 7 and 14, and does not capture the very high concentrations seen on the mornings of June 27 and 28, but otherwise simulates well this important period. The morning peaks on several days show the effects of the increased on-road emissions in Reg2_MVS.

At both Meacham Field and Denton, the model also reproduced well the temporal patterns seen in the observed NO_X concentrations, but in both cases under-predicted high morning concentrations on most days. At these sites and at Eagle Mountain Lake (which did not have a NO_X monitor during the episode) little difference between base cases can be seen.

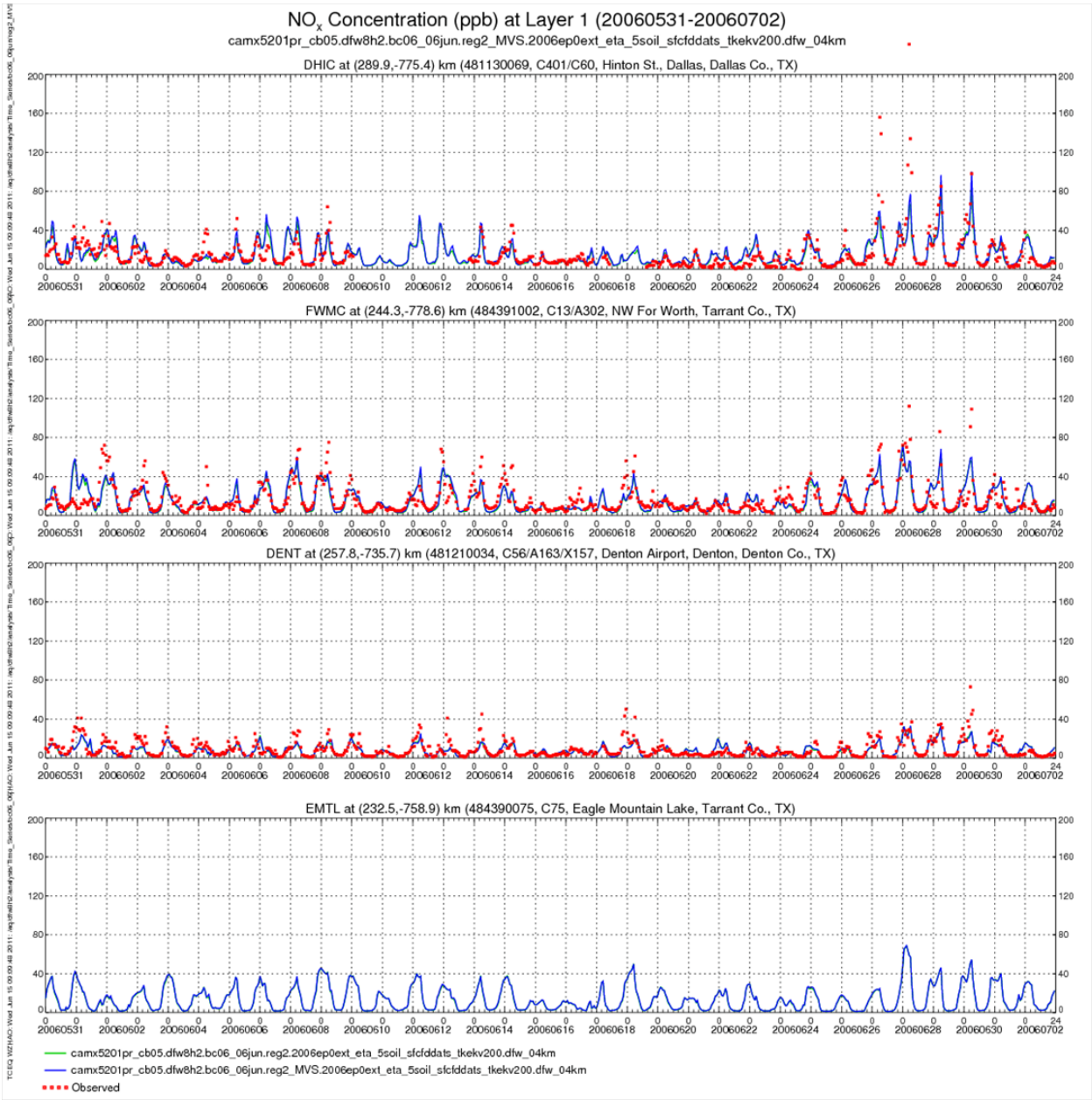

Figure 5-8: Time Series of Hourly Modeled and Observed NO_X Concentrations at (Top to Bottom) Hinton Street (DHIC), Meacham Field (FWMC), Denton (DENT) and Eagle Mountain Lake (EMTL)

PAR is a composite hydrocarbon species used by the model's Carbon Bond 05 mechanism to represent a variety of molecular fragments characterized by single carbon-carbon bonds. For comparison with modeled concentrations, observed hydrocarbon concentrations were

transformed into CB05 species using a process similar to that used to transform reported hydrocarbon emissions into CB05 species required for CAMx modeling.

Figure 5-9*: Time Series of Hourly Modeled and Observed PAR Concentrations at (Top to Bottom) Hinton Street (DHIC), Meacham* Field (FWMC), Denton (DENT) and Eagle Mountain Lake (EMTL) shows modeled and observed hourly PAR at these sites. Only Hinton Street and Meacham Field had continuous hydrocarbon sampling during the 2006 episode, so no observational data is shown for Denton and Eagle Mountain Lake.

PAR is not highly reactive, meaning it is slow to form ozone, but is a good indicator of overall hydrocarbon concentrations because it is emitted by a large number of processes including internal and external combustion processes and oil and gas production. At Hinton Street, the model is seen to replicate the temporal pattern of PAR observations well, but the model over-predicts the PAR concentrations by a factor of 2 to 3. At Meacham Field, the modeled concentrations also match the observed temporal distribution, but the modeled concentrations match the observations reasonably well on most days.

At all four sites little difference is seen between Reg2 and Reg2_MVS. Late in the episode, overnight PAR concentrations at Hinton Street from Reg2_MVS are slightly lower than those produced from Reg2. Even though PAR emissions across the 4 km modeling domain changed only slightly because of MOVES2010a, localized changes can be relatively large because the more detailed breakdown of emissions by operating mode afforded by MOVES2010a allowed starting and evaporative emissions to be spatially distributed to trip start/end locations. Because MOBILE6.2 did not provide this breakdown, all modeling prior to Reg2_MVS had allocated these emissions along roadways. Since the Hinton Drive monitor is located near the intersection of several major highways, re-allocating the start and evaporative emissions caused a net decrease in that location.

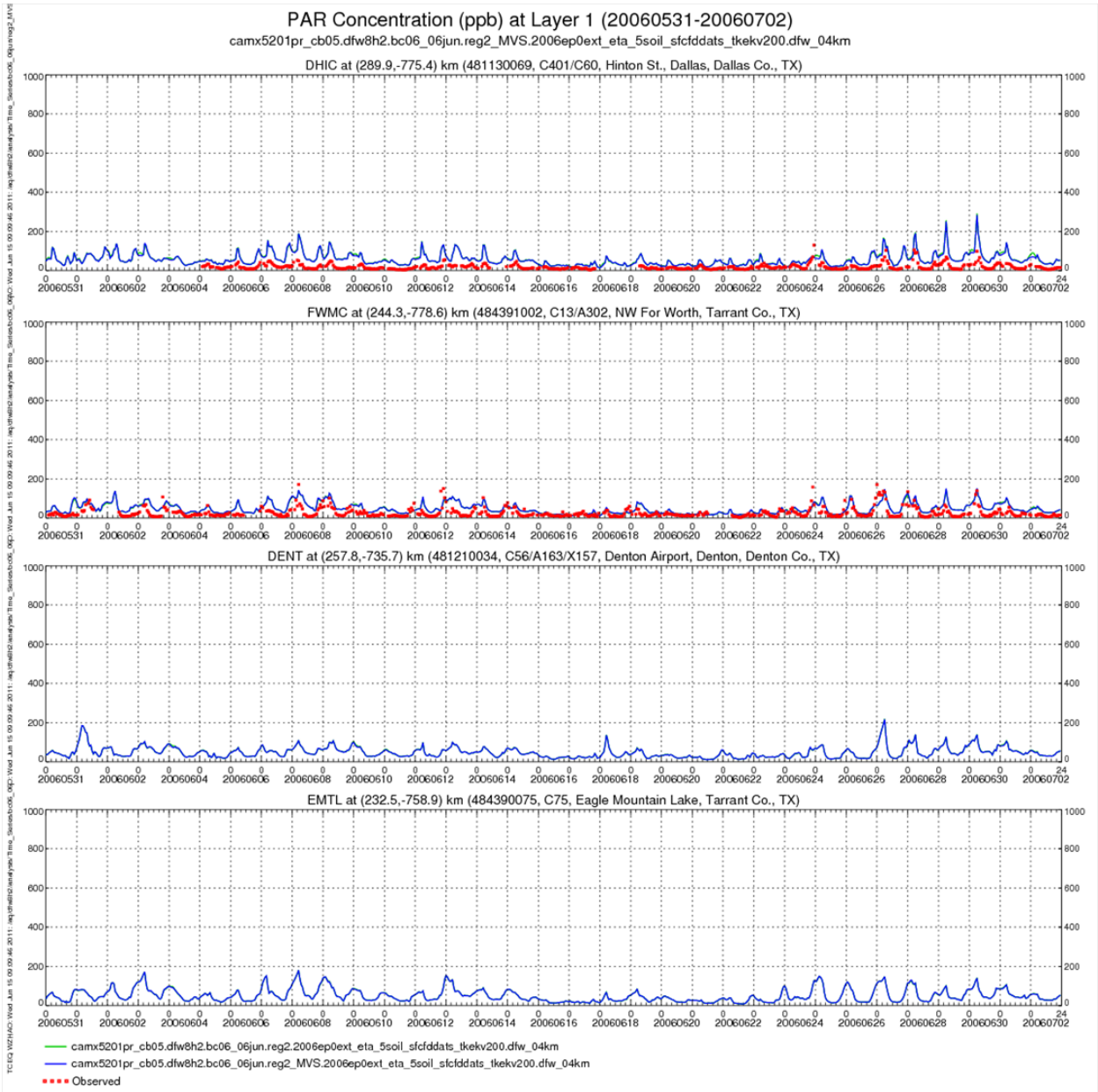

Figure 5-9: Time Series of Hourly Modeled and Observed PAR Concentrations at (Top to Bottom) Hinton Street (DHIC), Meacham Field (FWMC), Denton (DENT) and Eagle Mountain Lake (EMTL)

Figure 5-10: *Time Series of Hourly Modeled and Observed Ethylene Concentrations at* (Top to Bottom) *Hinton Street* (DHIC), *Meacham Field* (FWMC), *Denton (DENT*) and *Eagle Mountain Lake (*EMTL) shows modeled and observed hourly ethylene (also called ethene, and labeled ETH in CB05) concentrations at these sites. ETH is highly-reactive (it forms ozone quickly) and has been shown to be very important to ozone production in the Houston-Galveston-Brazoria (HGB) airshed. Both modeled and observed concentrations of ethylene in the DFW area are much lower than those seen in the HGB area, but are still sufficient to contribute to the airshed's total reactivity. Figure 5-10 shows that the model has a tendency to over-predict ethylene concentrations at Hinton Street, but predicts ethylene quite well at Meacham Field.

Overnight and early morning modeled ethylene concentrations at Hinton Street, show relatively large decreases due to the spatial re-allocation of MOVES2010a emissions described above. These decreases moderate, but do not eliminate, the over-prediction bias at this site. Smaller decreases are seen at the remaining three sites shown.

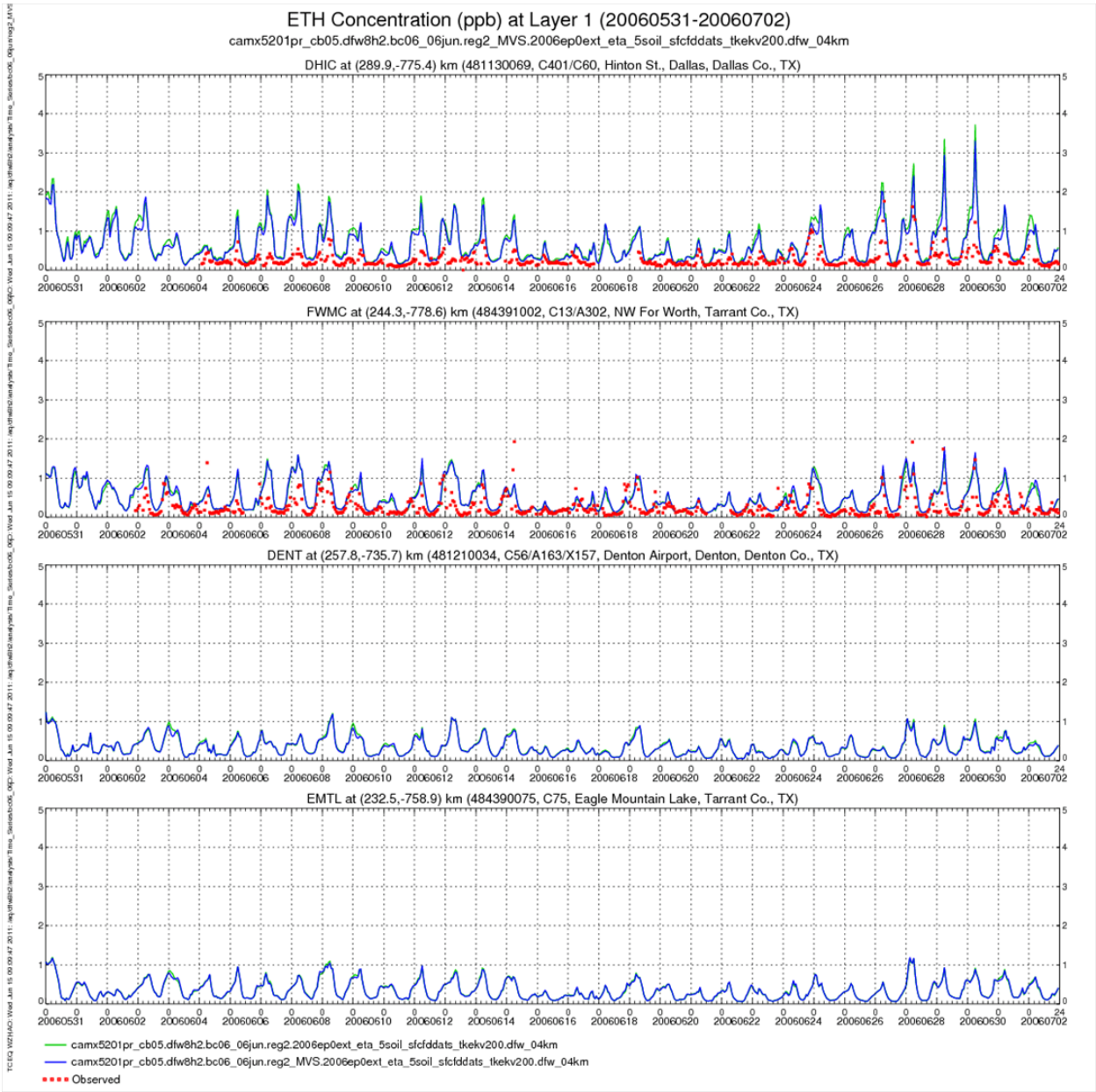

Figure 5-10: Time Series of Hourly Modeled and Observed Ethylene Concentrations at (Top to Bottom) Hinton Street (DHIC), Meacham Field (FWMC), Denton (DENT) and Eagle Mountain Lake (EMTL)

Figure 5-11: *Time Series of Hourly Modeled and Observed OLE Concentrations at* (Top to Bottom) *Hinton Street* (DHIC), *Meacham Field* (FWMC), *Denton (DENT*) and *Eagle Mountain Lake (*EMTL) shows modeled and observed hourly OLE concentrations at these sites. Like PAR, OLE is a composite CB05 species representing double carbon-carbon bonds in certain olefins

with higher molecular weight than ethylene. In practice, OLE is usually mostly composed of propylene (also known as propene). OLE is somewhat more reactive than ethylene, and, like ethylene, is found in low quantities, but still sufficient to contribute to the DFW airshed's total reactivity.

Figure 5-11 shows that OLE is predicted fairly well at Hinton Street, with only a few periods over-predicted, and OLE is slightly under-predicted at Meacham Field during several periods. Similar to ethylene, overnight and early morning OLE concentrations decreased as a result of adopting MOVES2010a emissions.

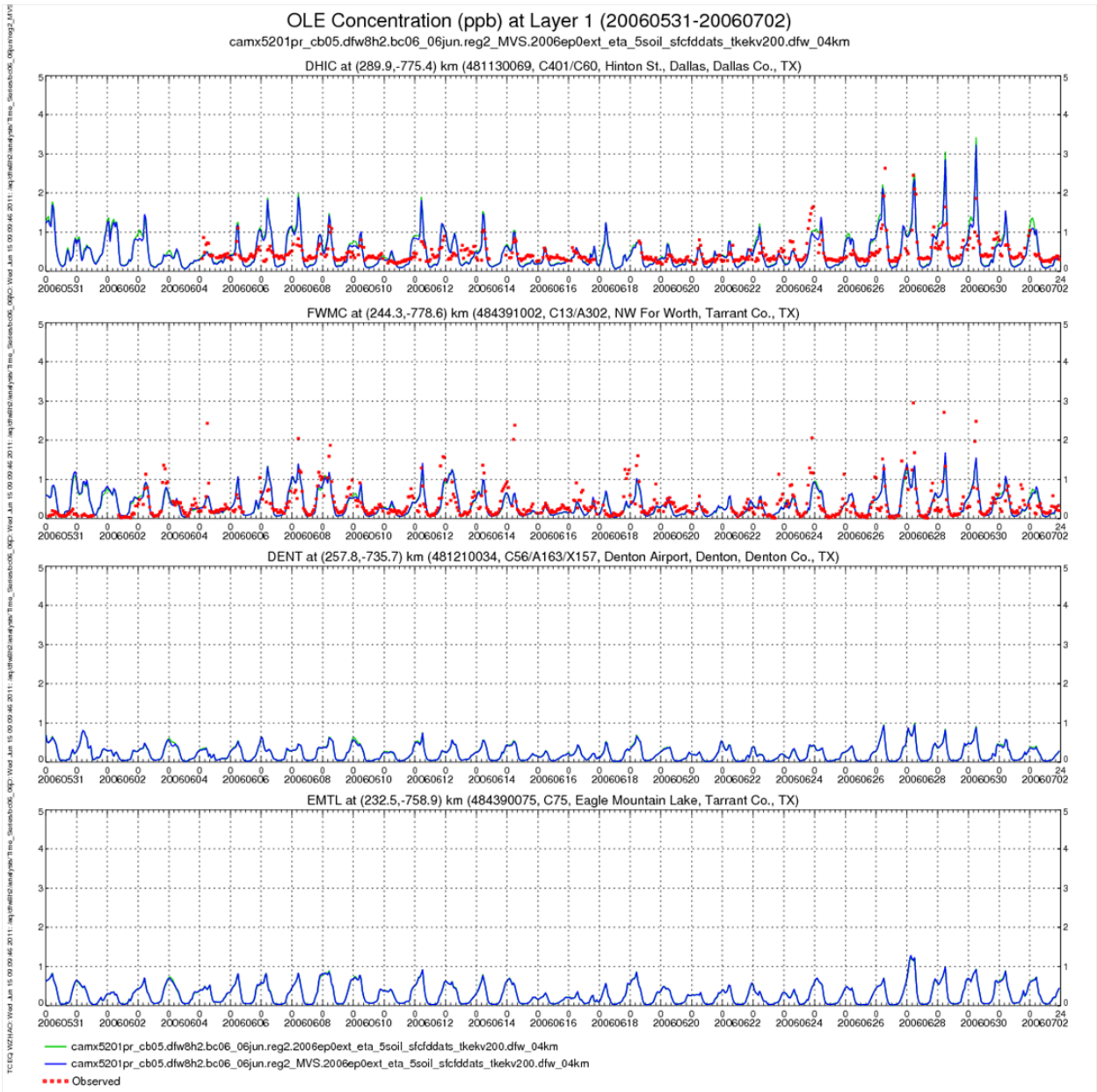

Figure 5-11: Time Series of Hourly Modeled and Observed OLE Concentrations at (Top to Bottom) Hinton Street (DHIC), Meacham Field (FWMC), Denton (DENT) and Eagle Mountain Lake (EMTL)

Like ethylene and propylene, isoprene is an olefin and is also highly-reactive. Most isoprene is produced by trees, but some is emitted from anthropogenic sources. Figure 5-12: *Time Series of Hourly Modeled and Observed Isoprene Concentrations at (Top to Bottom) Hinton Street (DHIC), Meacham Field (FWMC), Denton (DENT) and Eagle Mountain Lake (EMTL)* shows isoprene (ISOP in CB-05) concentrations are under-predicted at Hinton Street, and are over-predicted at Meacham Field, although both modeled and observed concentrations are low. More highly-resolved, up-to-date land cover/vegetation classification data should improve the modeling at both sites. No noticeable difference between isoprene concentrations between Reg2 and Reg2_MVS is evident in any of the four time series shown.

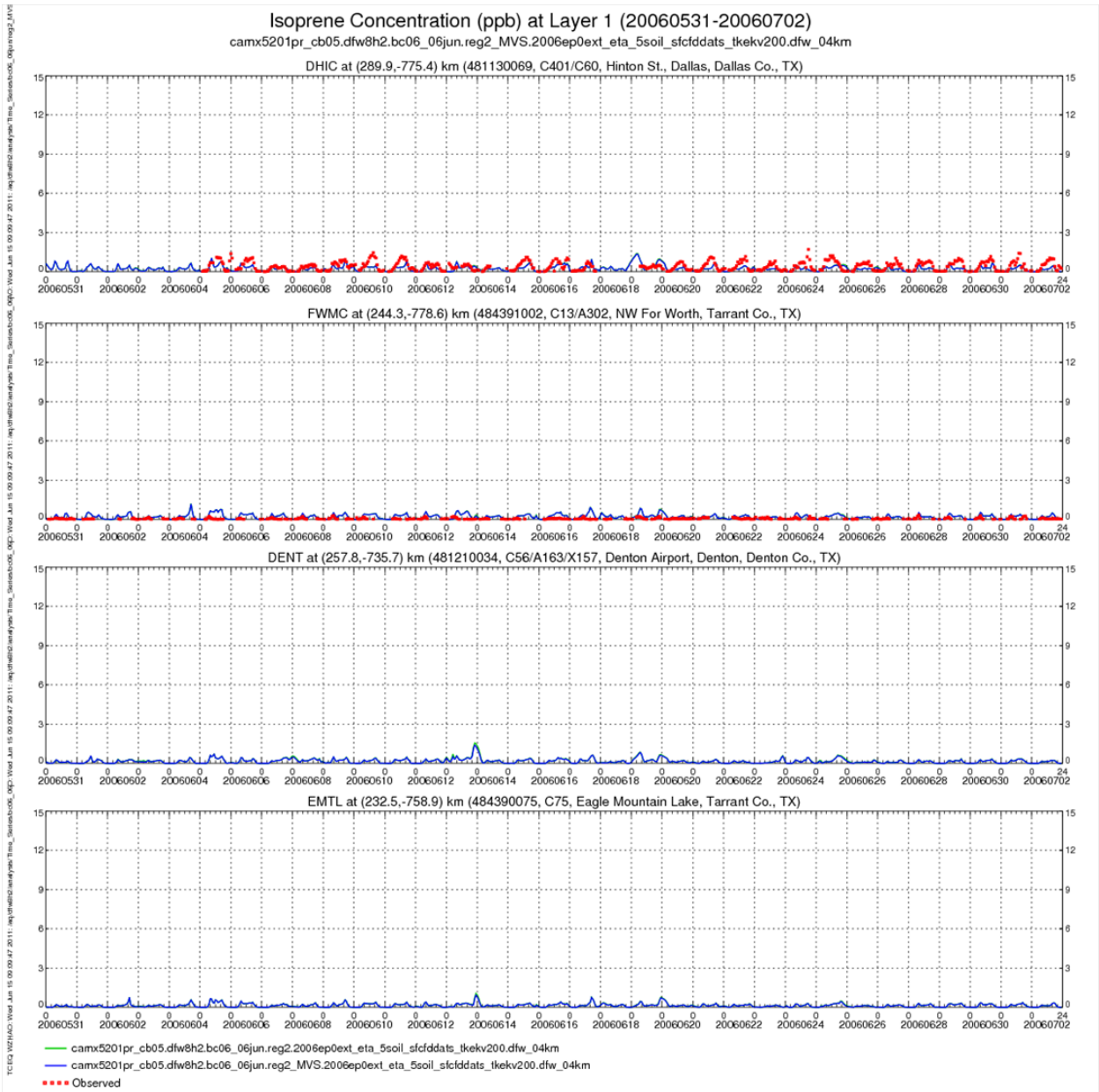

Figure 5-12: Time Series of Hourly Modeled and Observed Isoprene Concentrations at (Top to Bottom) Hinton Street (DHIC), Meacham Field (FWMC), Denton (DENT) and Eagle Mountain Lake (EMTL)

5.2.2 Cumulative Distributions

While time-series plots provide a detailed hour-by-hour comparison of modeled and observed pollutant concentrations at a site, it is often useful to examine data which has been summarized in one or more ways. The following plots show the cumulative distribution (CD) of several pollutants. To read a CD plot, look at the vertical (Y) axis to find a value between zero and one. The X value corresponding to zero is the smallest (modeled or measured) concentration value for the pollutant of interest, and the X value corresponding to one is the largest concentration. The value corresponding to 0.5 is the median concentration (the number of values above the median is equal to the number of values below). Where the curve rises slowly there are few values, but where it rises steeply there is a high density of values. An example is the upper left-hand panel of Figure 5-13: *Cumulative Distribution Plots of Modeled and Observed Ozone Concentrations at Hinton Street* (DHIC) (upper left), *Meacham Field* (FWMC) (upper right), *Denton (DENT*) (lower left) and *Eagle Mountain Lake (*EMTL) (lower right). The red line represents the set of ozone concentrations measured at Hinton Street throughout the episode. The smallest observed ozone concentration is near zero, and the largest is around 100 ppb, with the median value around 40 ppb. The blue and green lines represent the Reg2_MVS and Reg2 base cases, respectively. The distribution of modeled values is very close to the observed distribution, except at the two ends of the distribution. At the lower end, the model did not produce values as small as measured. At the top end, the Reg2 modeling did not produce values quite as high as measured but the Reg2_MVS distribution matched the observed distribution very well. Note that both the green and blue lines extend farther right than the red line, indicating a small number of modeled values exceeded the largest value observed at Hinton Street by up to about 10 ppb. The value of the CD plots is that model tendencies towards producing values too high or low relative to the observations can be seen immediately.

In the upper right-hand panel of Figure 5-13, at Meacham Field the model does a fairly good job of predicting the correct proportion of concentrations up to about 50 ppb, but falls short for higher concentrations excepting a few extreme modeled values which are up to 20 ppb larger than the maximum observed concentration. The Reg2_MVS base case shows a slight performance improvement over Reg2 for values between about 60 and 90 ppb.

At Denton (lower left-hand panel) the model does not produce either enough low or high concentrations; the modeled values are clustered more tightly around the center of the distribution than the observations. The steep slope of the blue and green lines shows that the modeled values mostly lie between 20 and 80 ppb, while the observations are spread more evenly between 0 and 100+ ppb. At Eagle Mountain Lake (lower right-hand panel) the modeled concentrations are mostly distributed between around 10 and 90 ppb, while the observations range from 10 to over 100 ppb. At both sites, Reg2_MVS produced ozone concentrations slightly higher than Reg2.

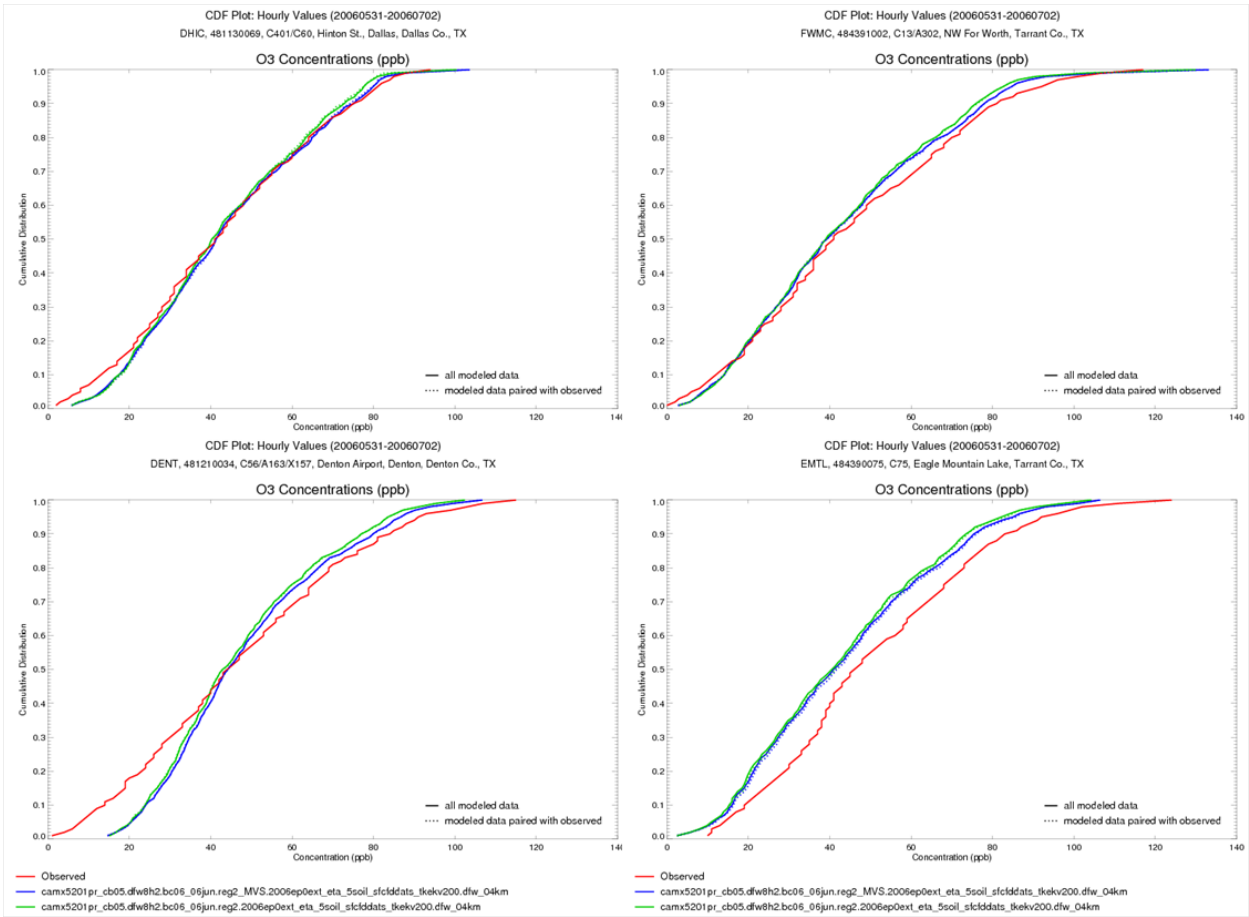

Figure 5-13: Cumulative Distribution Plots of Modeled and Observed Ozone Concentrations at Hinton Street (DHIC) (upper left), Meacham Field (FWMC) (upper right), Denton (DENT) (lower left) and Eagle Mountain Lake (EMTL) (lower right)

Figure 5-14: *Cumulative Distribution Plots of Modeled and Observed NOX Concentrations at Hinton Street* (DHIC) (upper left), *Meacham Field* (FWMC) (upper right), *Denton (DENT*) (lower left) and *Eagle Mountain Lake (*EMTL) (lower right) shows cumulative distributions of modeled and observed NO_X at these sites. The upper left-hand panel shows very good agreement between the modeled and observed distributions of NO_X concentrations at Hinton Street. At Meacham Field, the model similarly does a good job of matching the distribution of observed concentrations, except it does not capture the distribution of the very highest concentrations (> 30 ppb). At Denton, however, the model diverges from the observed distribution above around 10 ppb and clearly does not produce enough concentrations above that point. The Reg2 and Reg2_MVS distributions only differ slightly at all four sites, and are virtually indistinguishable at Eagle Mountain Lake (which did not measure NO_X).

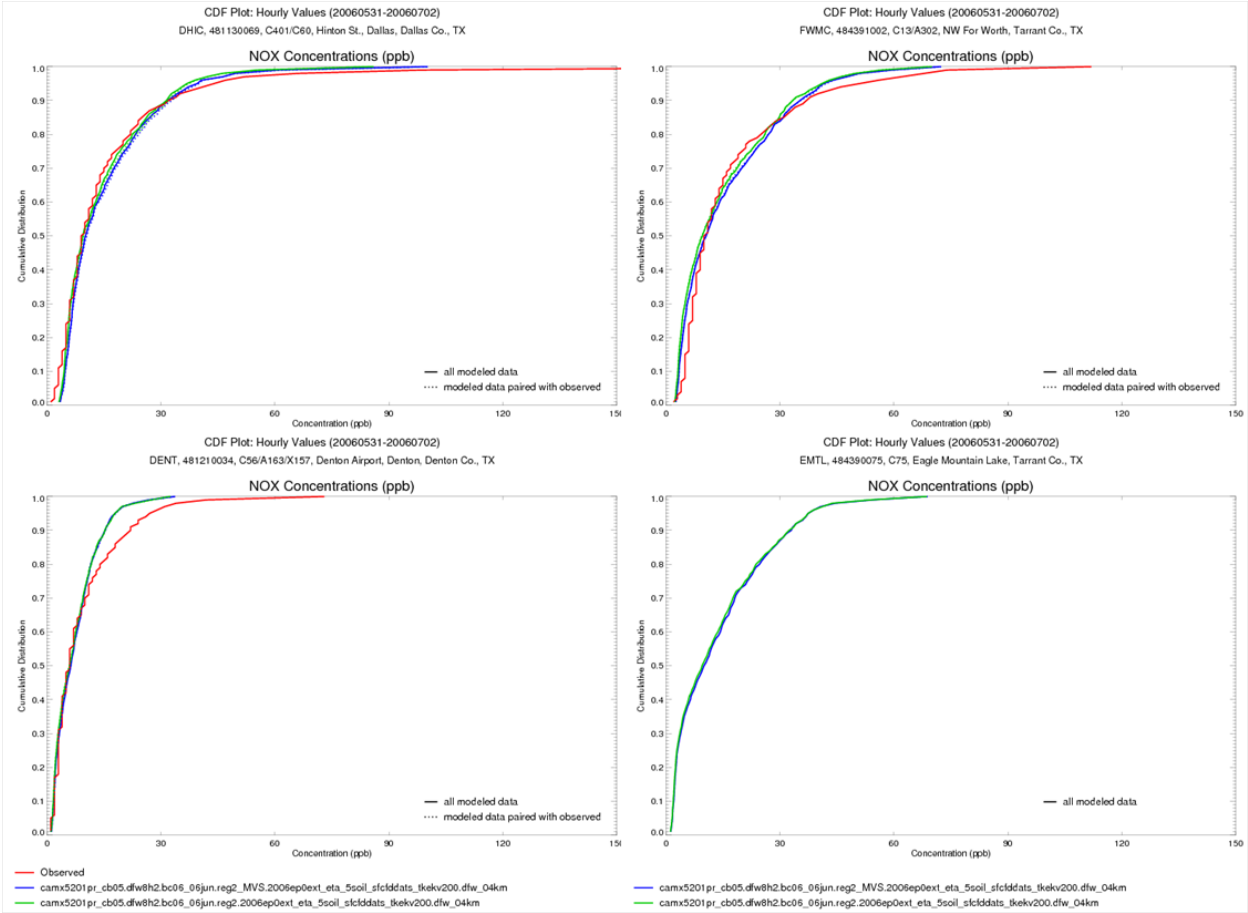

Figure 5-14: Cumulative Distribution Plots of Modeled and Observed NO_X Concentrations at Hinton Street (DHIC) (upper left), Meacham Field (FWMC) (upper right), Denton (DENT) (lower left) and Eagle Mountain Lake (EMTL) (lower right)

Figure 5-15: *Cumulative Distribution Plots of Modeled and Observed PAR Concentrations at Hinton Street* (DHIC) (upper left), *Meacham Field* (FWMC) (upper right), *Denton (DENT*) (lower left) and *Eagle Mountain Lake (*EMTL) (lower right) shows cumulative distributions of the CB05 PAR species at these sites. The upper left-hand panel shows that PAR is substantially over-predicted at Hinton Street, with modeled values spread mostly between about 20 and 150 ppb, but the observations lie mostly between 5 and 50 ppb. At Meacham Field, the disparity is not as great, but the modeled PAR is still almost twice the observed distribution. Denton and Eagle Mountain Lake lack observational data, but the cumulative distribution plots show the distributions of the two base cases are almost identical to one another.

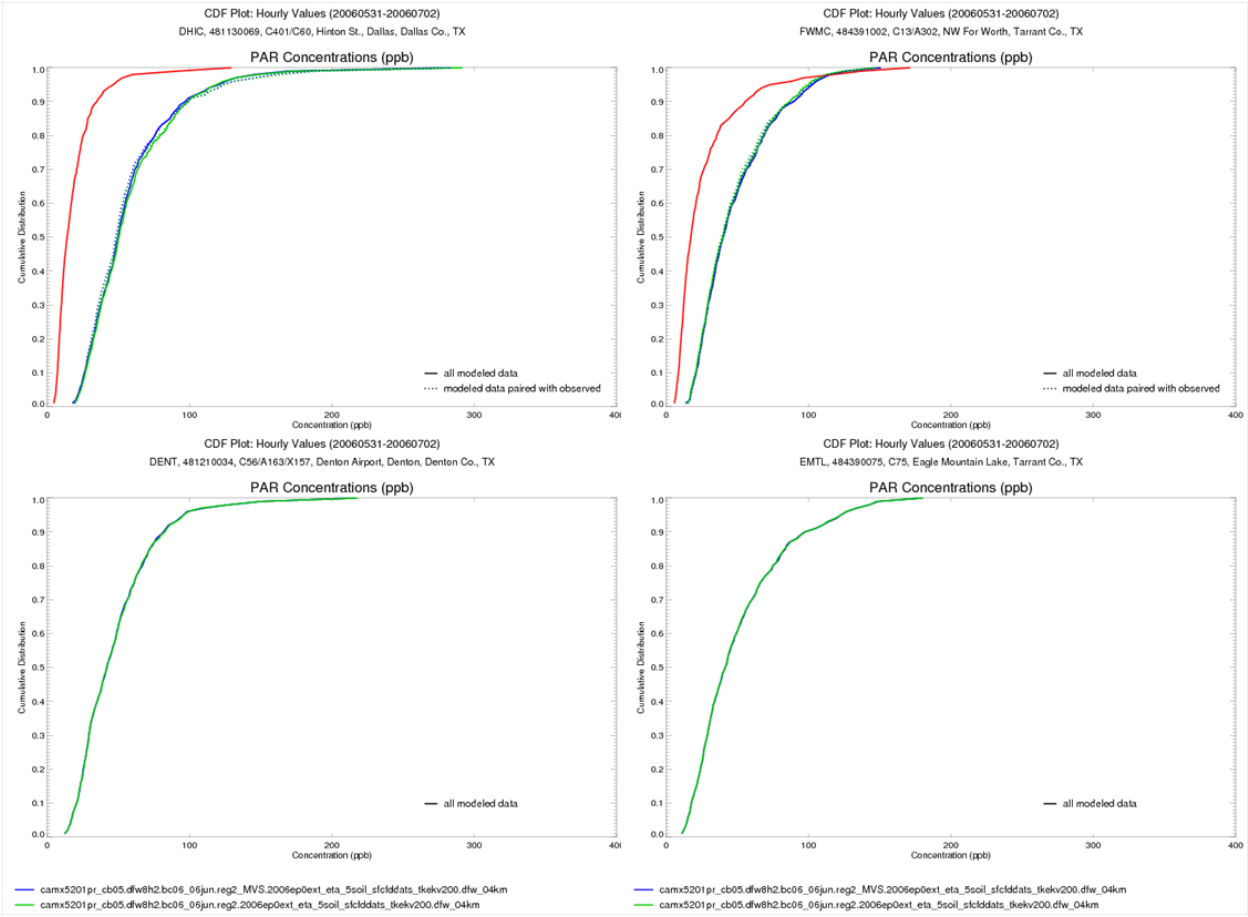

Figure 5-15: Cumulative Distribution Plots of Modeled and Observed PAR Concentrations at Hinton Street (DHIC) (upper left), Meacham Field (FWMC) (upper right), Denton (DENT) (lower left) and Eagle Mountain Lake (EMTL) (lower right)

The upper left-hand panel of Figure 5-16: *Cumulative Distribution Plots of Modeled and Observed Ethylene Concentrations at Hinton Street* (DHIC) (upper left), *Meacham Field* (FWMC) (upper right), *Denton (DENT*) (lower left) and *Eagle Mountain Lake (*EMTL) (lower right) shows that ethylene is substantially over-predicted at Hinton Street, with modeled values spread mostly between about 0.2 and 2 ppb while the observations lie mostly between 0.05 and 0.5 ppb. The Reg2_MVS case does show some improvement over Reg2 (see the discussion of the corresponding time series for why this is so). At Meacham Field, the disparity between observational and modeled distributions is not as great as at Hinton Street, but the modeled ethylene is still almost twice the observed distribution (however, almost all of the modeled and observed values are still < 1.5 ppb). The dotted lines on the first two panels of this set, visible on some earlier plots, but not as prominent as on these, represent modeled values that are paired with observations. For various reasons not all hours have observational data, but all hours have modeled concentrations. The dotted lines are plotted only for the modeled values which correspond to non-missing observations.

Denton and Eagle Mountain Lake lack observational data, but the cumulative distribution plots on the bottom row of Figure 5-16 show that the Reg2_MVS base case concentrations at both sites are nearly identical to the Reg2 concentrations.

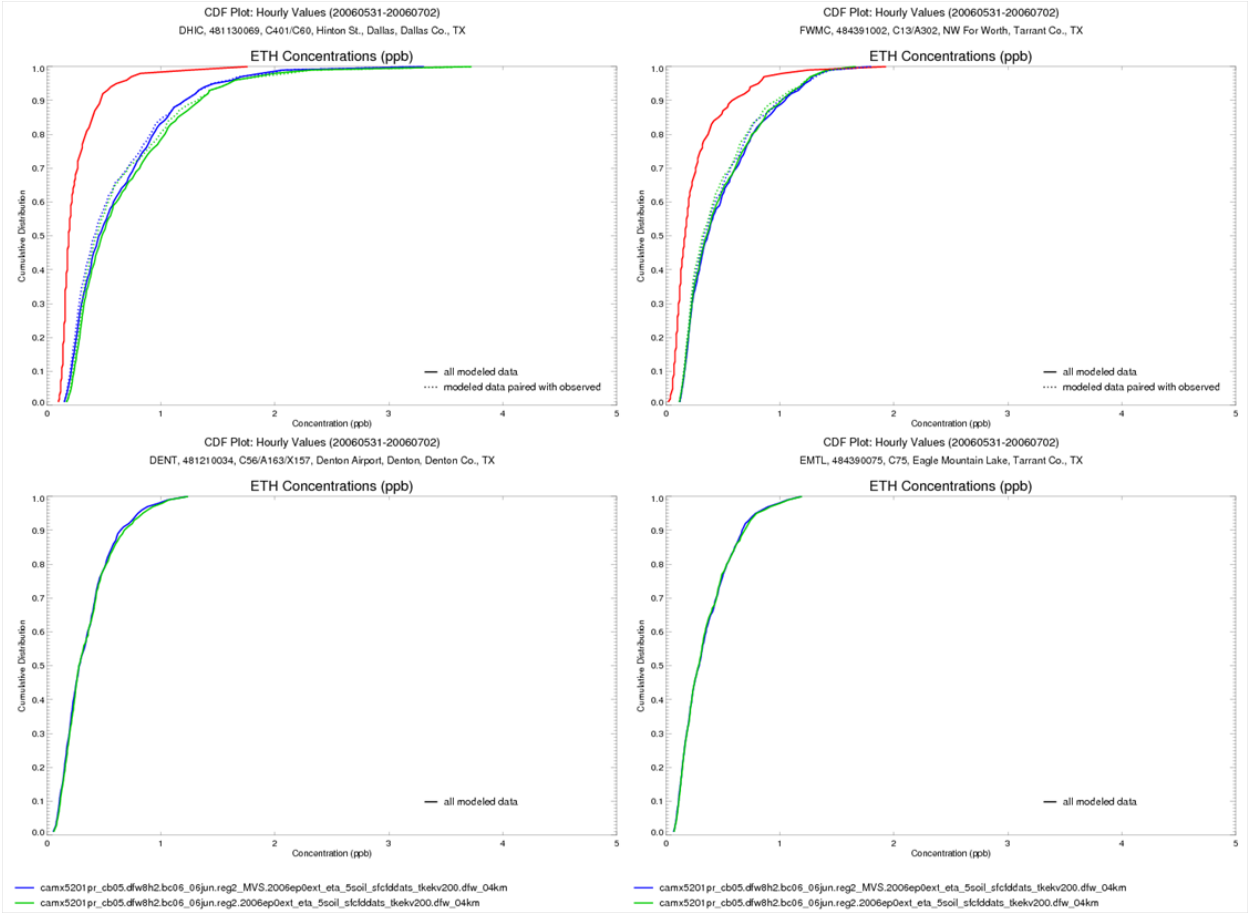

Figure 5-16: Cumulative Distribution Plots of Modeled and Observed Ethylene Concentrations at Hinton Street (DHIC) (upper left), Meacham Field (FWMC) (upper right), Denton (DENT) (lower left) and Eagle Mountain Lake (EMTL) (lower right)

Figure 5-17: *Cumulative Distribution Plots of Modeled and Observed OLE Concentrations at Hinton Street* (DHIC) (upper left), *Meacham Field* (FWMC) (upper right), *Denton (DENT*) (lower left) and *Eagle Mountain Lake (EMTL*) (lower right) shows cumulative distributions of the CB05 OLE species at these sites. The upper left-hand panel shows that at the lower end of the distribution, the modeled OLE concentrations at Hinton Street are smaller than observed, but this may be partially due to non-zero detection limits on the Auto-GC. Above around 0.2 ppb, the modeled distribution is higher than the observed distribution, but both distributions are mostly below 1.5 ppb.

At Meacham Field, the modeled distribution of OLE matches the observed distribution fairly well. Again concentrations are low, with most observed and modeled concentrations < 1.5 ppb. At both Denton and Eagle Mountain Lake the OLE concentrations from Reg2 and Reg2_MVS are very similar to one another.

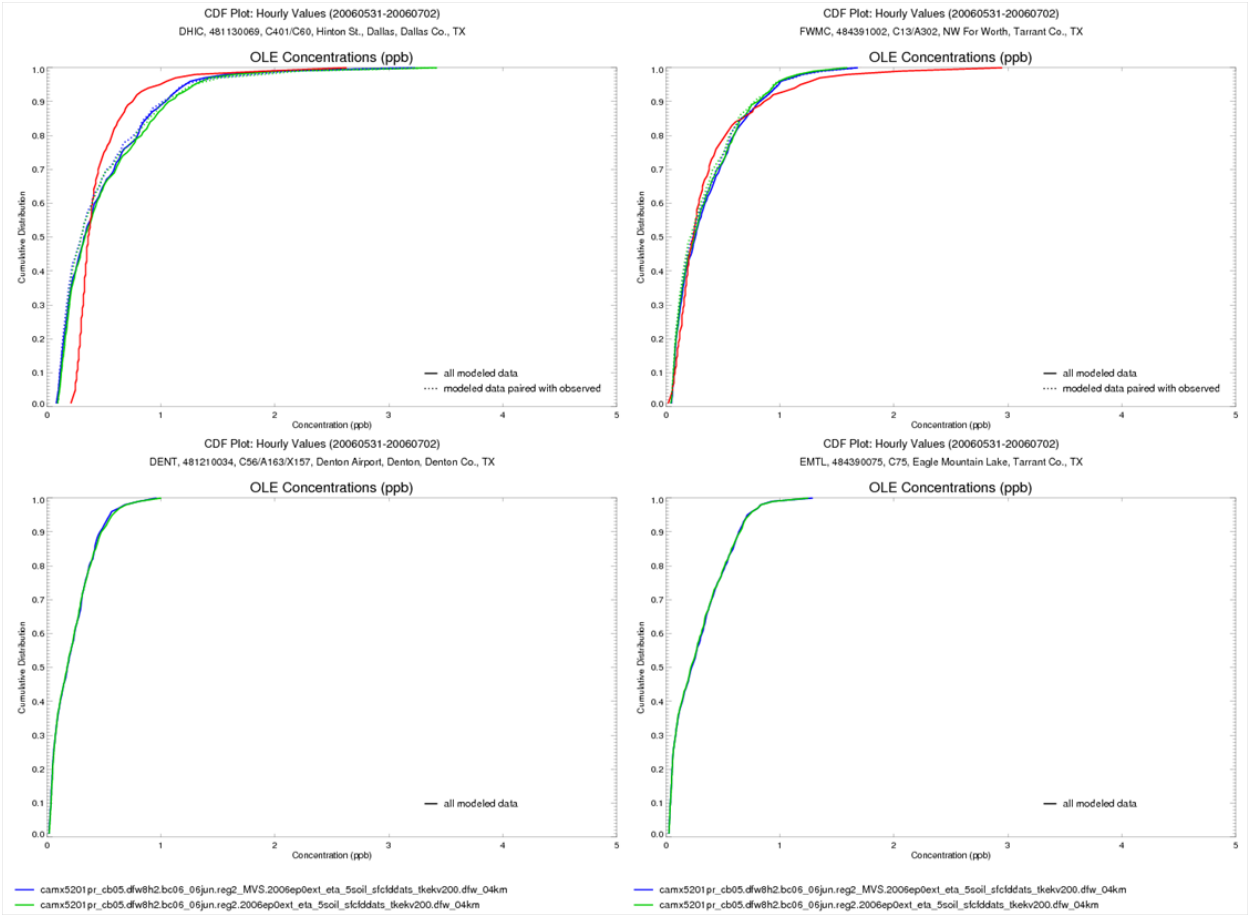

Figure 5-17: Cumulative Distribution Plots of Modeled and Observed OLE Concentrations at Hinton Street (DHIC) (upper left), Meacham Field (FWMC) (upper right), Denton (DENT) (lower left) and Eagle Mountain Lake (EMTL) (lower right)

The upper left-hand panel of Figure 5-18: *Cumulative Distribution Plots of Modeled and Observed Isoprene Concentrations at Hinton Street* (DHIC) (upper left), *Meacham Field* (FWMC) (upper right), *Denton (DENT*) (lower left) and *Eagle Mountain Lake (EMTL*) (lower right) shows that a third of the observed and modeled isoprene concentrations at Hinton Street are very small, less than 0.2 ppb. Beyond this point, the observed concentration distribution increases faster than the modeled distribution, with many more concentrations in the 0.5-1 ppb range than were modeled. At Meacham Field, the trend was reversed; the first third of the observed and modeled distributions are near zero, but beyond that point the modeled distribution increases much faster than the observed. However, both sets of concentrations are low, almost entirely < 1.0 ppb. At Denton and Eagle Mountain Lake, the distributions of Reg2 and Reg2_MVS concentrations are nearly identical.

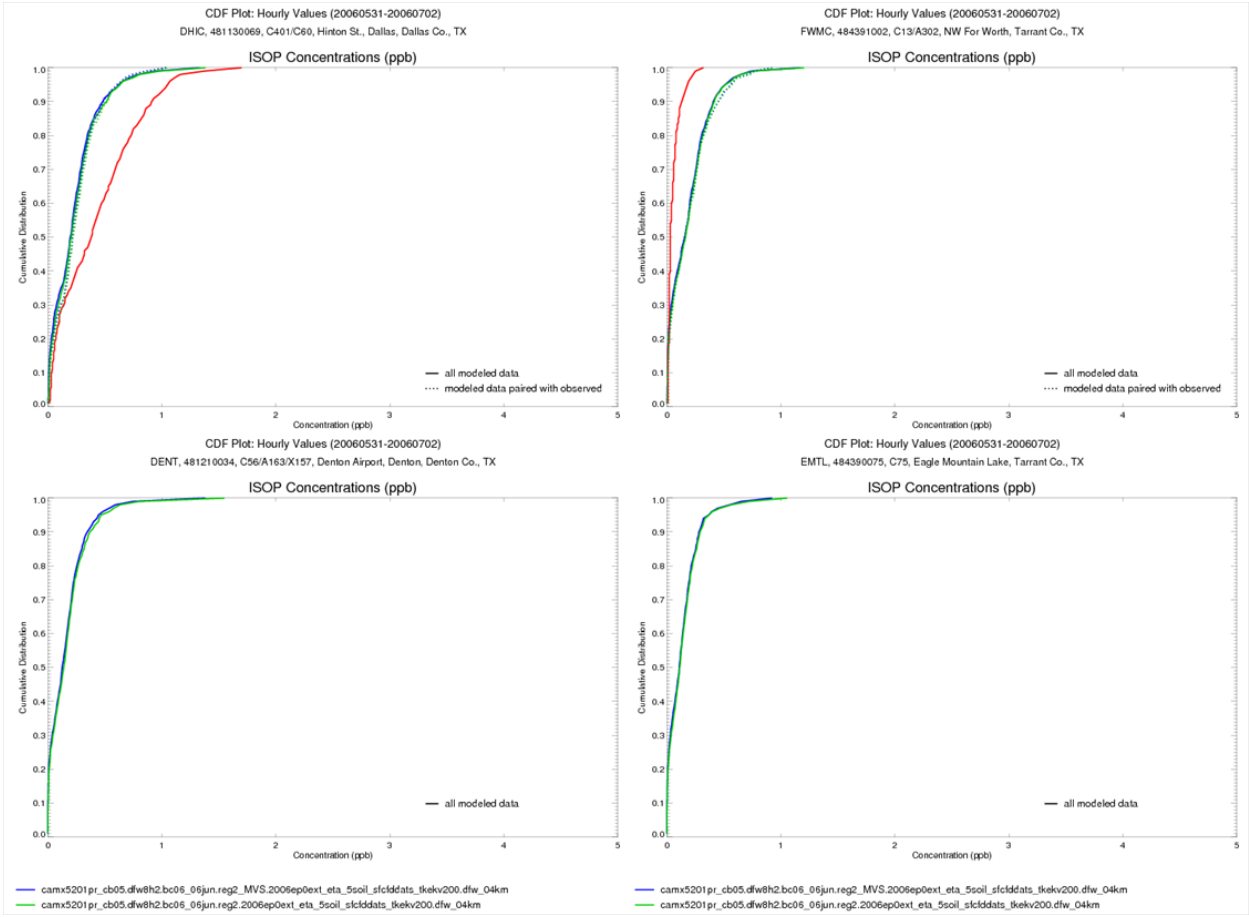

Figure 5-18: Cumulative Distribution Plots of Modeled and Observed Isoprene Concentrations at Hinton Street (DHIC) (upper left), Meacham Field (FWMC) (upper right), Denton (DENT) (lower left) and Eagle Mountain Lake (EMTL) (lower right)

5.2.3 Peak Ozone Tile Plot

Along with time series and cumulative density plots, the TCEQ employs several additional graphical analysis techniques, including scatter plots, QQ plots, hourly ozone animations, and customized graphics. One of the most intuitive graphics is a plot showing the daily peak ozone across the modeling domain. This plot is akin to the contour plots often used to display terrain elevations, and is a good tool for visually comparing the modeled peak ozone across the domain with observations. It is important to note that the plots below are not snapshots in time, but for each grid cell show the maximum value (in this case, peak daily eight-hour ozone) regardless of when it occurred during the day. Areas downwind of the urban core will generally have peaks that occur later in the day than upwind areas.

The following graphics depict modeled and measured daily peak eight-hour ozone concentrations for the four days with the highest measured ozone concentrations during the episode: June 9 (106.8 ppb at Eagle Mountain Lake), June 12 (101.8 ppb at Weatherford), June 14 (107.5 ppb at Eagle Mountain Lake), and June 30 (102.5 ppb at Denton). For comparison, both the Reg2 and Reg2_MVS base cases are displayed.

Figure 5-19: *Peak Daily Modeled and Observed Eight-Hour Peak Ozone Concentrations across the DFW Modeling Domain on June 9 and 12, 2006* displays the eight-hour peaks for June 9 and 12. On June 9, the model does a good job of locating the highest ozone concentrations, but overall modeled ozone concentrations are lower than monitored. Every site in the domain reported a peak eight-hour concentration of 70 ppb or higher, but both the Reg2 and Reg2_MVS base cases showed predicted values around 60 ppb for several of these sites. At the other end of the spectrum, the peak modeled concentrations were about 10 ppb lower than the observed maximum of 106.8 ppb. Reg2 MVS performed better than Reg2, with respective peaks of 97.2 ppb and 94.6 ppb, and the right-hand plot (Reg2_MVS) shows noticeably enhanced ozone concentrations across most of the 4 km domain compared with Reg2. The cause of the overall under-prediction of both base cases appears to be regional background levels that are too low, although other causes such as wind speed errors, poorly characterized vertical mixing, or emission inventory issues may play a role.

On June 12, the model replicated the observed eight-hour ozone peaks quite well, both spatially and in terms of magnitude. The modeled ozone plume is slightly displaced a few kilometers east of what is indicated by the monitors, but overall performance is very good. The modeled peak for Reg2 of 102.6 ppb closely replicated the observed maximum of 101.8 ppb on this day, while the modeled peak for Reg2_MVS is somewhat higher at 105.0 ppb. Since the modeled peak is taken across every grid cell in the domain and the observed peak is from only a limited number of monitoring sites, it is expected that the domain-wide peak simulated by a good-performing model will exceed the monitored peak.

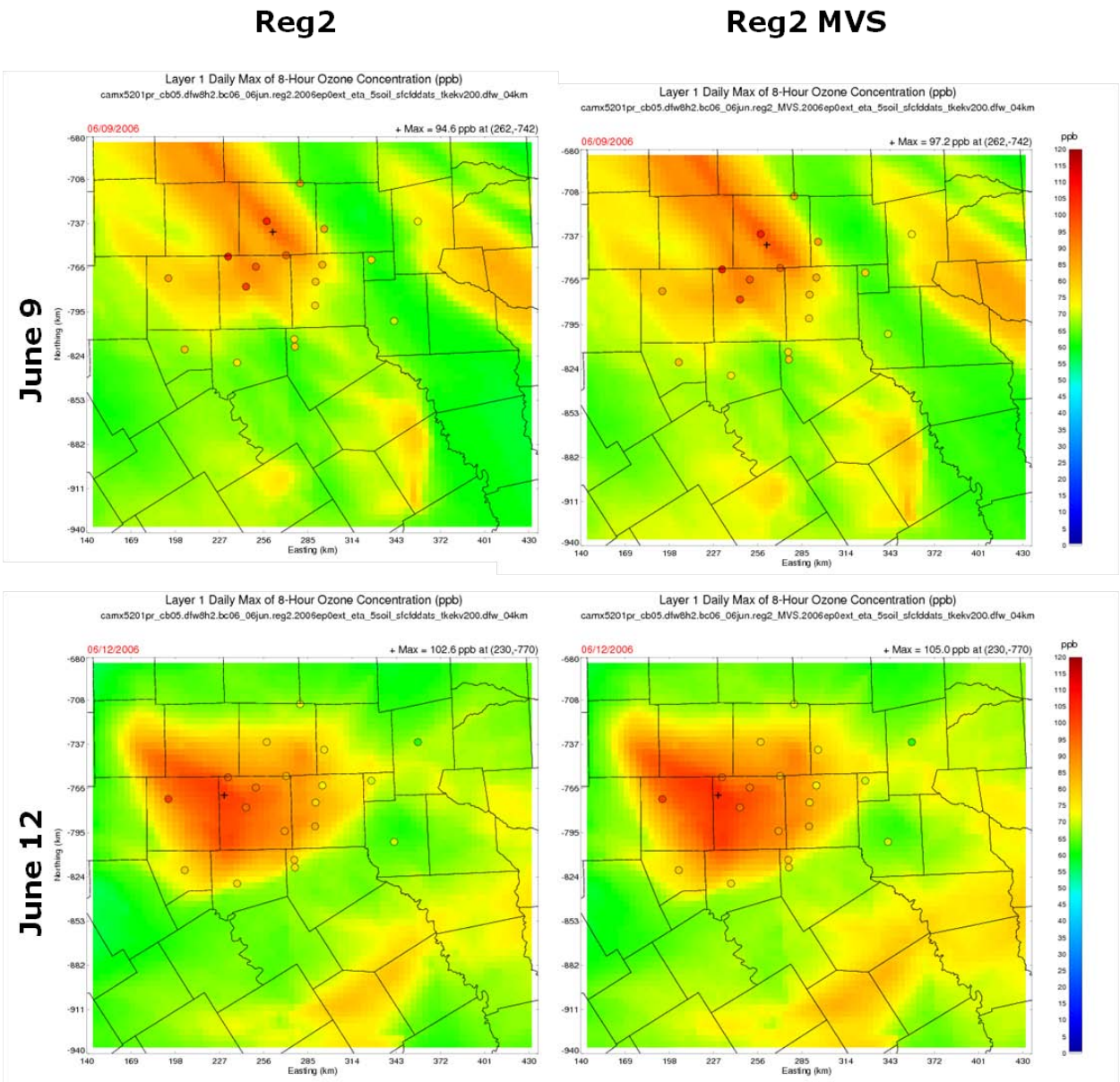

Figure 5-19: Peak Daily Modeled and Observed Eight-Hour Peak Ozone Concentrations across the DFW Modeling Domain on June 9 and 12, 2006

Figure 5-20: *Peak Daily Modeled and Observed Eight-Hour Peak Ozone Concentrations across the DFW Modeling Domain on June 14 and 30, 2006* displays the eight-hour peaks for June 14 and 30. On June 14, the model again does a good job of locating the highest ozone concentrations, but overall modeled ozone concentrations are lower than monitored. For both base cases, the modeled peaks are near the location of the observed peak concentration, Eagle Mountain Lake, but the modeled peaks are both more than 12 ppb lower than the measured peak of 107.5. The upwind modeled concentrations on this day were only slightly lower than observed (70 ppb observed versus 68 ppb for Reg2_MVS), but local ozone production appears to be too low. The Reg2_MVS base case again out-performs Reg2, with a modeled peak of 95.1 ppb versus 92.8 ppb.

Finally, on June 30 the model again does a very good job of locating the ozone peaks, but again under-predicts the maximum eight-hour ozone concentration by around 10 ppb. Background modeled values are once again too low for several sites (Kaufman was under-predicted by 7 ppb by Reg2_MVS), but the model under-predicted the peak at Midlothian by only 2 ppb. Again, the Reg2_MVS base case did a better job predicting the observed peak of 102.5 ppb than Reg2 (93.6 ppb versus 90.3 ppb). The main cause for the overall under-prediction again appears to be low simulated background values. A comparison of the lower two panels of Figure 5-20 shows a notable enhancement of peak 8-hour ozone in the Reg2_MVS case. Interestingly, the simulated peak in Reg2_MVS moved several grid cells downwind from the location in Reg2.

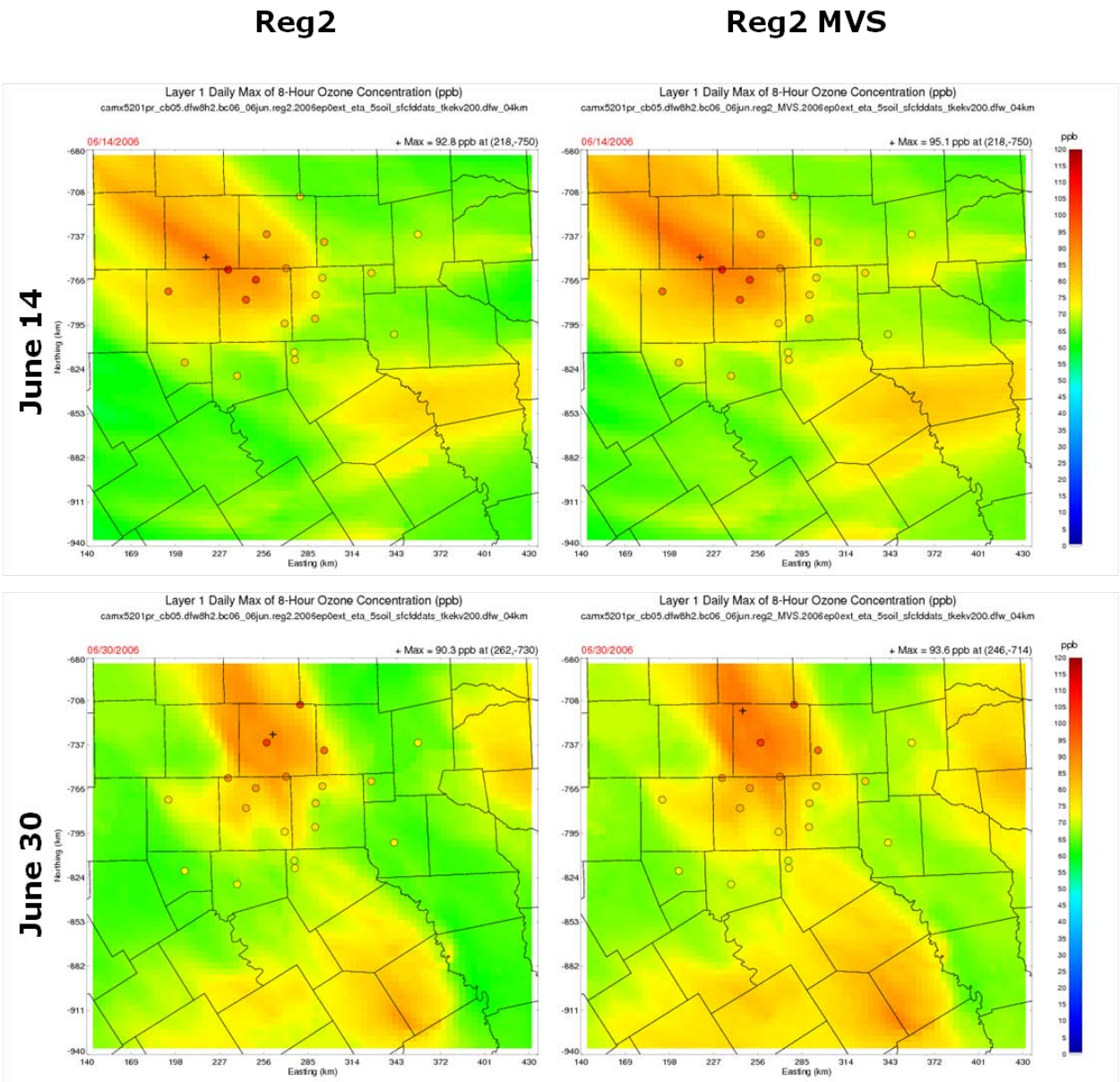

Figure 5-20: Peak Daily Modeled and Observed Eight-Hour Peak Ozone Concentrations across the DFW Modeling Domain on June 14 and 30, 2006

5.2.4 Summary

This section has presented three of the graphical analysis methods used to assess model performance in the DFW area, and has provided some insight into how the model behaves and why. The time series plots showed detailed comparisons of modeled and predicted ozone, NO_X, and hydrocarbon species and showed that overall the model follows the temporal distribution of ozone and precursor concentrations quite well. These plots also showed some discrepancies between modeled and observed precursor concentrations. The cumulative density plots compared the distribution of modeled values with the observed distribution and showed some issues with hydrocarbon concentrations at the two Auto-GC sites. These plots also highlighted the differences between Reg2 and Reg2_MVS NO_X concentrations. The peak ozone plots showed that the model overall replicated the placement of the high ozone concentrations very well, but tended to under-predict concentrations across the domain except on June 12. The overall patterns suggest that modeled background levels are too low, but that on at least one day local ozone production is too low. Overall, the Reg2_MVS base was seen to perform better than the Reg2 base case.

5.3 Rural Monitor Model Performance Evaluation

Most air quality monitoring is population-oriented as monitors are generally sited to measure the levels of pollutants that will be encountered by people in their everyday lives. Normally, little data useful for assessing background pollutant levels or for characterizing inter- or intra-state transport are collected. Without this information, it is impossible to evaluate how well the photochemical model simulates the regional component of urban ozone concentrations.

Because of limited rural monitoring data available in Texas, the TCEQ contracted with the University of Texas to deploy and maintain several additional monitors during much of 2005 and 2006 for TexAQS II. These, non-regulatory, special-purpose monitors were located near Texas' eastern and northern borders and in other rural areas of the state. Most monitors collected ozone data only, but some collected NO_X data. The model performance evaluation described in this document is based on time-series plots of modeled and measured ozone at a representative set of rural monitors, along with available NO_X. In addition to the special monitors deployed for TexAQS II, some routine monitors were included in the evaluation because of their relatively large distances from city centers (Figure 5-21: *TexAQS II Rural Monitoring Sites*). In these latter instances, pollutant concentrations usually represent background conditions, but sometimes observe urban plumes downwind from their sources.

All of the monitors, except for Palestine (PLTN), are within the 12 km CAMx domain. While finer scale modeling (4 km or less) is necessary to capture plumes and pollutant concentration gradients in the urban areas, the performance of the model at regional sites can be examined to evaluate incoming background air. Hourly minima, maxima, and spikes are not expected to be captured at a 12 km resolution.

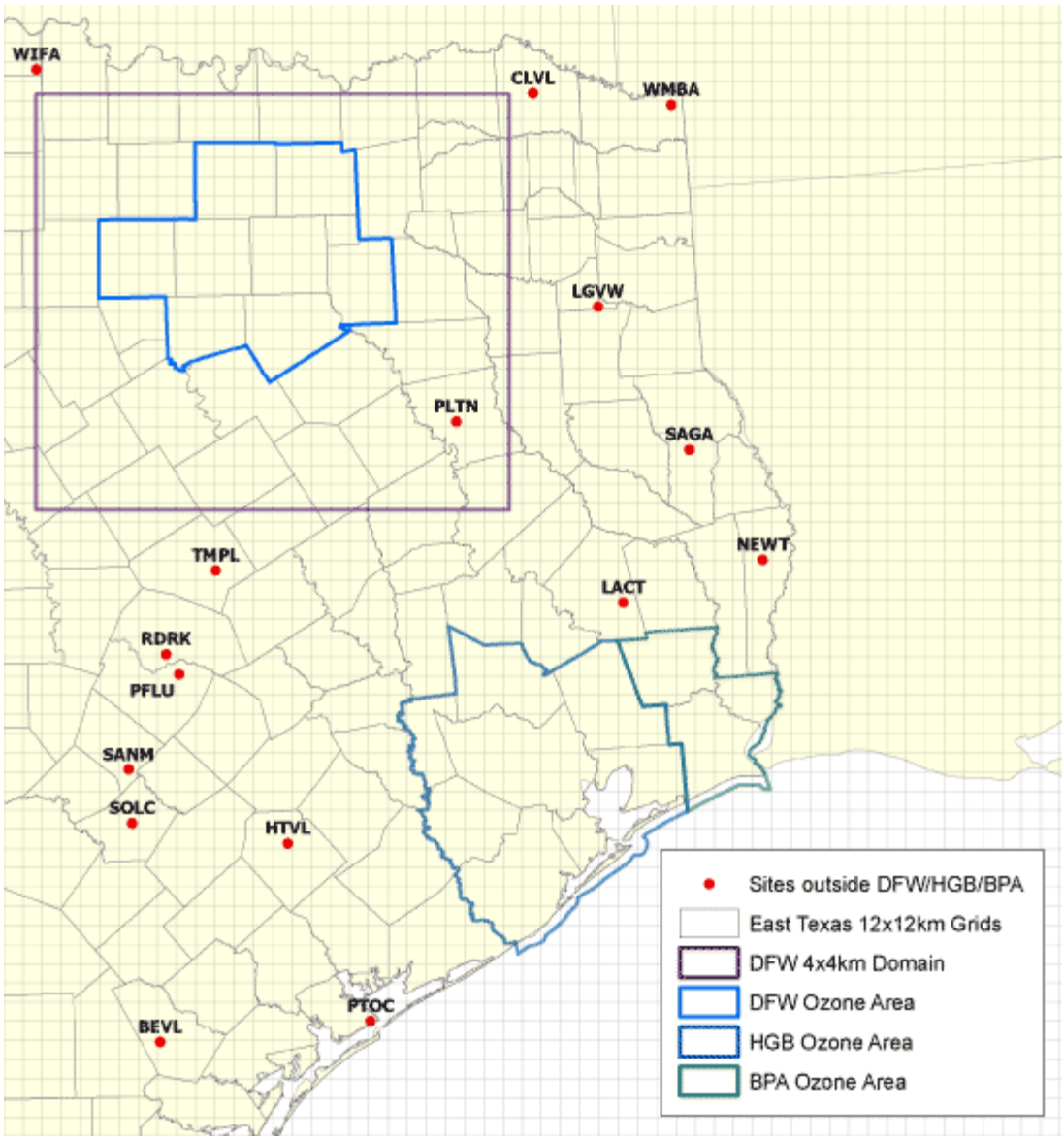

Figure 5-21: TexAQS II Rural Monitoring Sites

Table 5-3: Monitors in Eastern Texas used in Model Performance Assessment lists the monitors used in this assessment. Data from the CLVL, WMBA, LGVW, PLTN, SAGA, and TMPL monitors are of particular importance to the DFW area as their locations allow measurement of background concentrations during typical east to south flow on high eight-hour ozone days. Performance of the base case modeling at these monitors is shown and discussed below.

Table 5-3: Monitors in Eastern Texas used in Model Performance Assessment

Site Name	Description	TCEQ Region	Type	Jun 2006
CLVL	Clarksville C648, eastern TX-OK border	Region 5	TexAQS II	O3

WMBA	Wamba C645, Near Texarkana	Region 5	TexAQS II	O3
LGVW	Longview C19, Northeast Texas	Region 5	Regulatory	O3, NO_X
PLTN	Palestine C647, Central East Texas	Region 5	TexAQS II	O3
SAGA	San Augustine C646, Central TX-LA Border	Region 10	TexAQS II	O3, NO_X
TMPL	Temple C651, Central Texas	Region 9	TexAQS II	O3

At the Clarksville monitor (Figure 5-22: *Time Series of Hourly Ozone Concentrations at the Clarksville C648 Monitor*), the model follows the general diurnal pattern and trend of hourly ozone throughout the episode. The model under-predicts the highest concentrations and over-predicts the nighttime concentrations near the end of the episode.

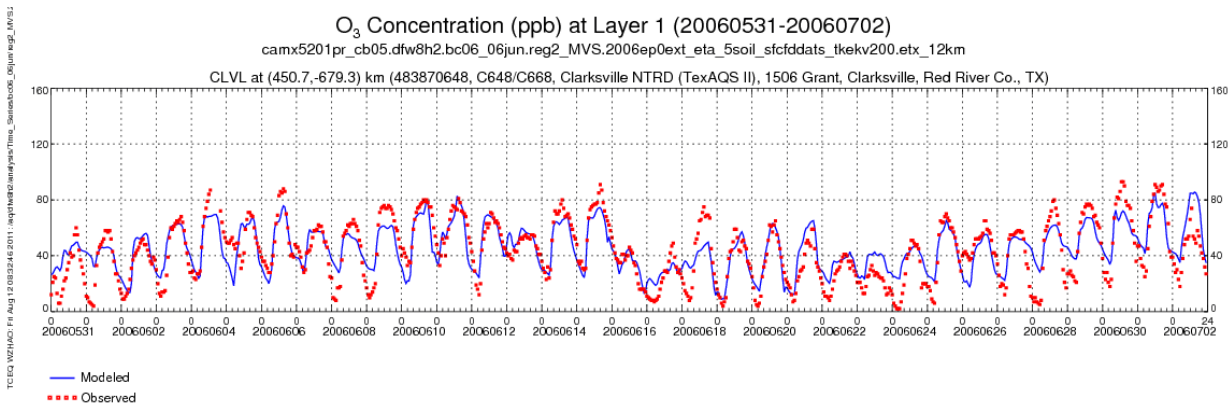

Figure 5-22: Time Series of Hourly Ozone Concentrations at the Clarksville C648 Monitor

At the Wamba monitor, the model had difficulty replicating the nighttime minima of hourly ozone. The model predicted the afternoon ozone peaks well, with limited under-prediction at the end of the episode. During the June 12-14 and June 26-27 time periods, conditions were favorable for transport from the northeast. While the nighttime performance could be improved, the daytime performance gives confidence that the model is simulating the observed ozone concentrations crossing the northeast Texas border.

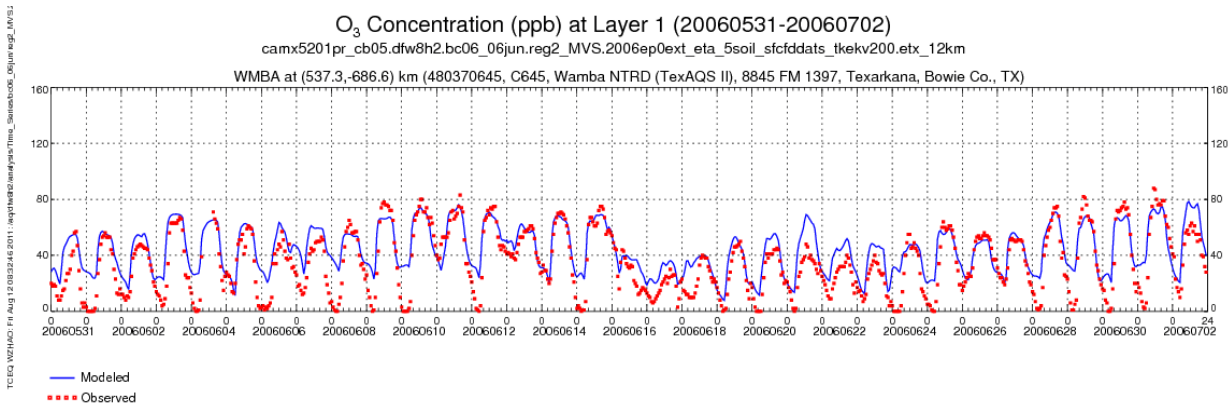

Figure 5-23: Time Series of Hourly Ozone Concentrations at the Wamba C645 Monitor

The Longview (LGVW) monitor is a TCEQ regulatory monitor in TCEQ Region 5. It is in the vicinity of the Longview urban area, a chemical manufacturing complex, and downwind of power plants. It is upwind of the DFW area during easterly wind conditions. Along with an ozone instrument, the LGVW site also measures NO_X. With some of the other northeast Texas sites, the model over-estimates the hourly ozone concentrations at night, especially during the later part of the episode (Figure 5-24: *Time Series of Hourly Ozone Concentrations at the Longview C19 Monitor*). The model replicates the afternoon ozone peaks well but misses the June 12 peak that may have been power plant-related as evidenced by elevated SO_2 concentrations (Environ, 2006).

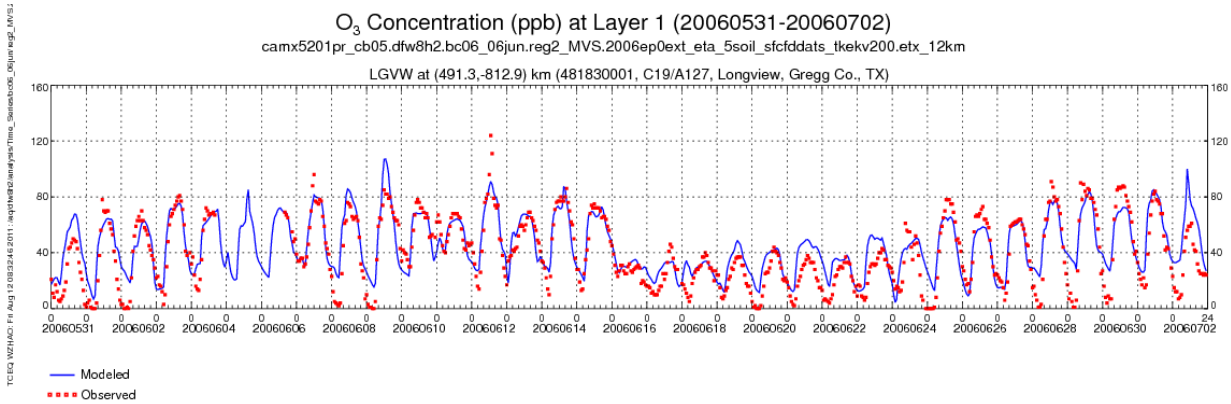

Figure 5-24: Time Series of Hourly Ozone Concentrations at the Longview C19 Monitor

For most of the period, NO_X was observed (and modeled) at less than 40 ppb (Figure 5-25: *Time Series of Hourly NOX Concentrations at the Longview C19 Monitor*). Only during the latter part of the episode did concentrations become elevated, mostly in the morning hours. NO_X concentrations on June 12 were not high compared to other days. An aged power plant plume as Environ suggests would agree with these observations (Environ, 2006). For most days, the model predicts the diurnal pattern, minima, and maxima well.

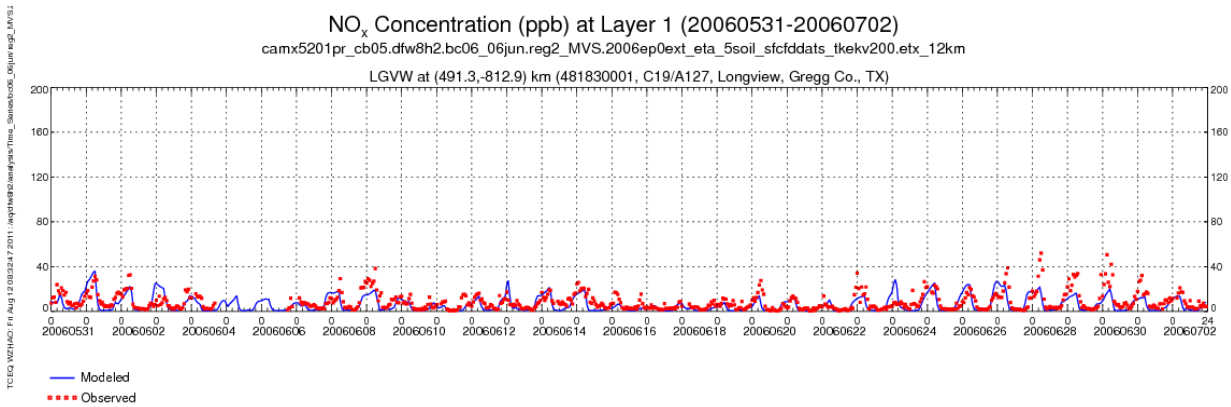

Figure 5-25: Time Series of Hourly NO_X Concentrations at the Longview C19 Monitor

At the Palestine monitor (Figure 5-26: *Time Series of Hourly Ozone Concentrations at the Palestine C647*), the model replicates the diurnal pattern of hourly ozone very well during the first part of the episode. After June 16, the overnight modeled concentrations poorly match the observed lows when strong southerly flow occurs. The cause of this is still being evaluated.

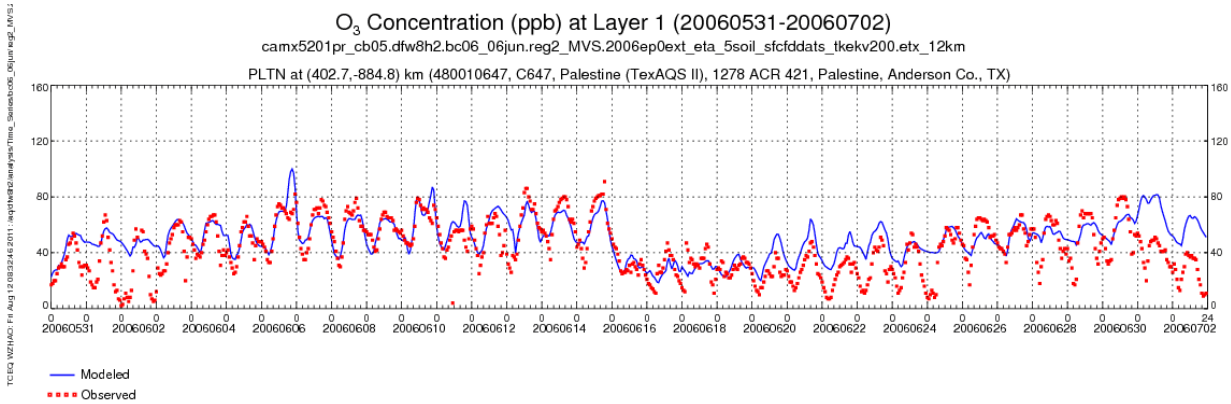

Figure 5-26: Time Series of Hourly Ozone Concentrations at the Palestine C647 Monitor

The model's hourly ozone response at the SAGA monitor (Figure 5-27: *Time Series of Hourly Ozone Concentrations at the Saga C646 Monitor*) is very similar to that at the Palestine monitor (Figure 5-26). A general over-prediction at night and in the morning exists after June 16 when southerly flow is constant but ozone concentrations are low. Observations at both monitors are similar indicating that they represent regional conditions in central-east Texas rather than a smaller local area. These results indicate that the model may over-predict ozone on the southeast side of DFW during southerly flow conditions.

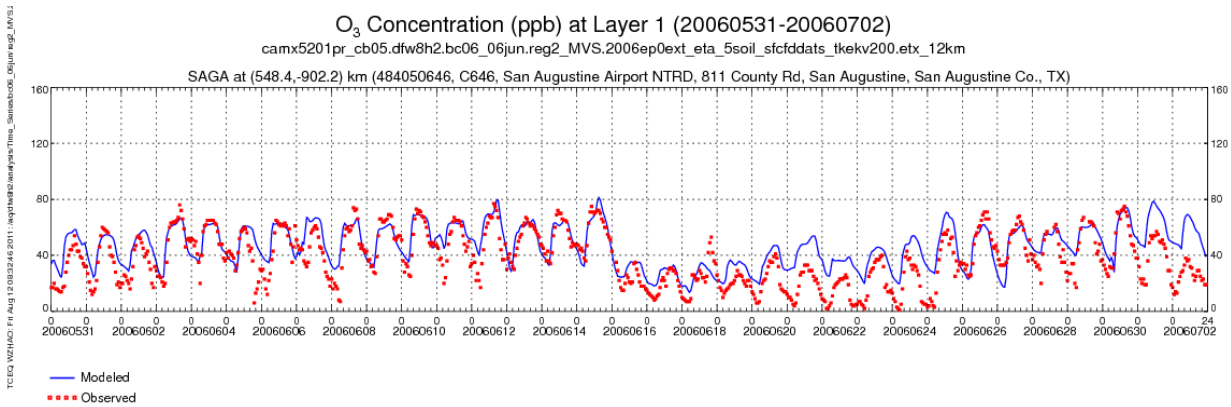

Figure 5-27: Time Series of Hourly Ozone Concentrations at the Saga C646 Monitor

The Temple monitor is located south of the DFW area near the IH-35 highway corridor. The hourly ozone predicted by CAMx matches the observations very well (Figure 5-28: *Time Series of Hourly Ozone Concentrations at the Temple C651 Monitor*). This gives confidence that the model represents conditions on the south side of DFW appropriately.

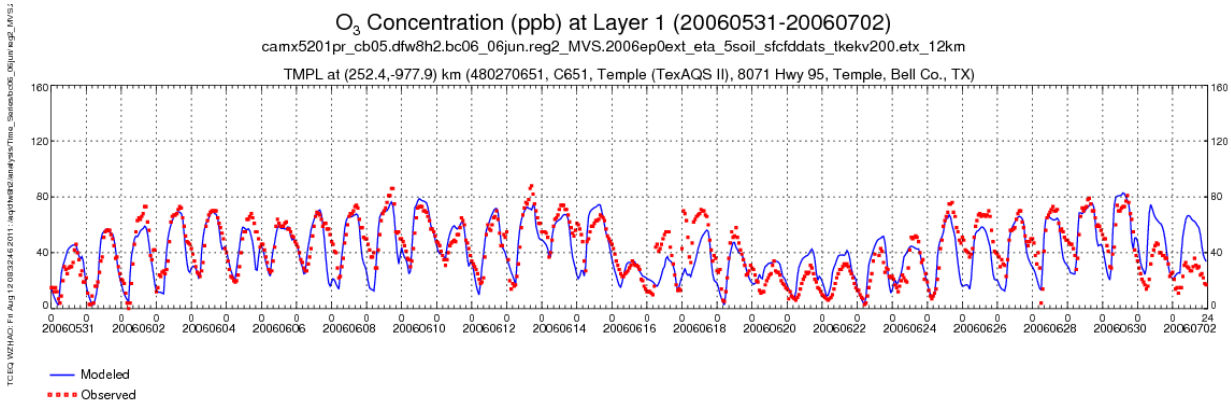

Figure 5-28: Time Series of Hourly Ozone Concentrations at the Temple C651 Monitor

Overall, the model predicts daytime ozone well throughout the episode at the rural monitors, but tends to carry too much ozone overnight, which may have some influence on the modeled concentrations in the DFW area. However, this assessment is based on a very small number of sites and may not represent overall rural model performance.

5.4 Ozone Sonde Model Performance Evaluation

Ozone sondes are instruments lofted by balloons that measure ozone concentrations as they ascend (and descend), and transmit the readings via radio signal to the researcher. In 2005 and 2006 prior to the start of the TexAQS II Intensive, a number of sondes were launched from Rice University, located about five kilometers southwest of downtown Houston. During the June 2006 episode, five sondes were launched from Rice University. One sonde was launched from Texas A&M University (TAMU) in College Station, Texas and one from Stephen F. Austin State University (SASU) in Nacogdoches, Texas (Figure 5-29: 2*006 Ozone Sonde Launch Locations*).

These launches were conducted as part of the Tropospheric Ozone Pollution Project (TOPP) operated by Dr. Gary Morris of Valparaiso (formerly of Rice) University.

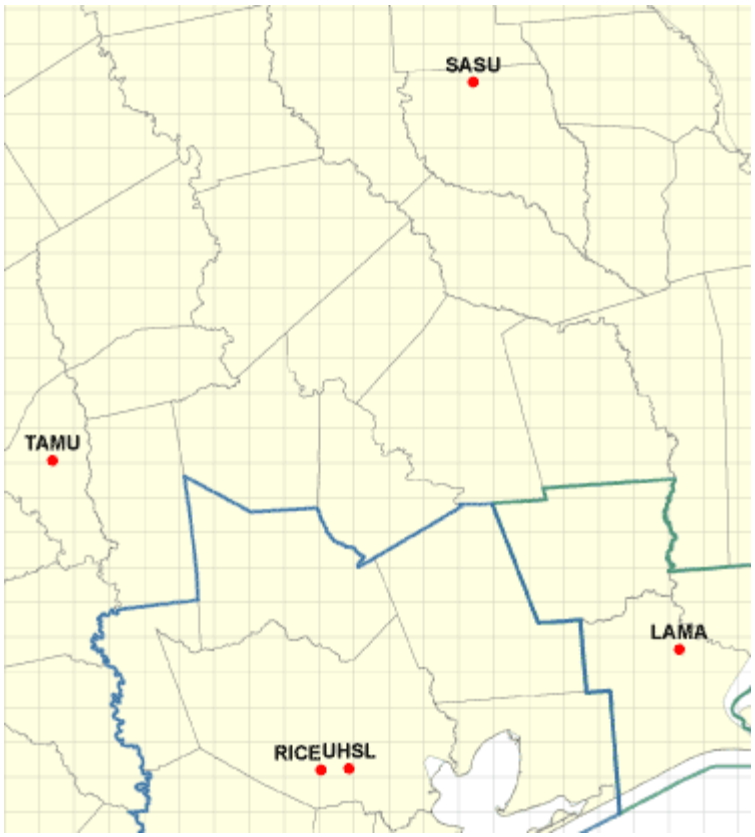

Figure 5-29: 2006 Ozone Sonde Launch Locations

Ozone concentrations reported by the sondes were compared to ozone concentrations modeled at the time and location of the measurement. Specifically, if the balloon reported an ozone concentration at location (x,y,z,t), we determined the specific grid cell that the balloon was in at that time was determined, and the modeled concentration used for comparison.

While the sondes reported the geographic coordinates of the measurements, the comparisons reported here assume that the balloons ascended vertically. This assumption is reasonable unless there were strong winds, since the balloon usually drifted no more than a couple of kilometers laterally within the first 2000 meters of rise. Beyond that point (i.e. above the PBL), ozone concentrations are not expected to show steep horizontal gradients, so the sonde measurements in that range should be generally representative of conditions over the launch location.

All of the launches occurred in the 12 km CAMx domain so the model may be unable to capture some of the finer scale features observed by the sondes, especially the Houston area's land-sea breeze. Often it is possible to diagnose the modeled and actual mixing depths based on ozone profiles. In many of the charts, it is possible to visually estimate both the modeled and observed mixing depths by looking for sharp inflection points in the ozone profiles. This analysis generally refrains from explicitly comparing modeled and measured mixing depths, but since the sondes also recorded temperature, humidity, and atmospheric pressure, it would be possible

to calculate independent estimates of observed mixing depth, which could reasonably be compared with the modeled mixing parameterization. The TCEQ hopes to make use of this information in future work.

Figure 5-30: *June 7, 2006 Ozone Sonde from Rice University* shows the observed ozone concentrations from June 7, 2006 in red up to 10000 m AGL, compared to modeled concentrations (blue) from the Rice University campus. On this day, the sonde recorded a well-mixed atmosphere with stable ozone concentrations of 60-65 ppb to about 2000 meters (2 km). Above 2 km, many levels of differing ozone concentrations were observed. The model, meanwhile, showed uniform concentrations of about 70 ppb up to around 2000 m, when its concentrations dropped to about 60 ppb and remained relatively constant to the top of the plot. In this case, the model over-predicted observed ozone concentrations by about 10-15 ppb through the boundary layer, but then generally under-predicted ozone concentrations up to 10 km.

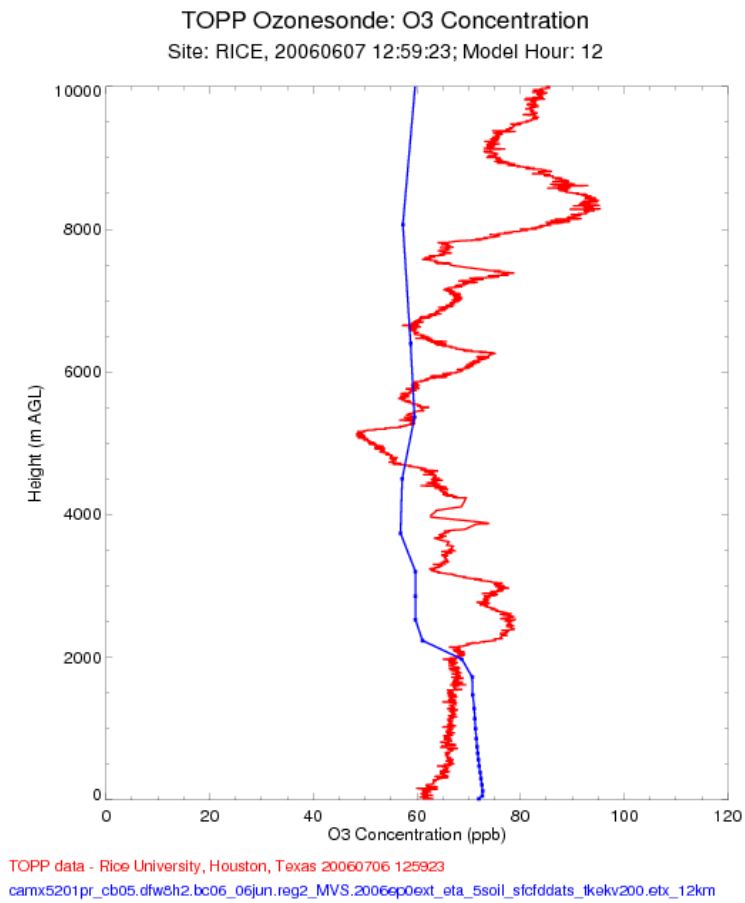

Figure 5-30: June 7, 2006 Ozone Sonde from Rice University

On June 14, 2006 an ozone sonde was launched from Rice University at 12:59 PM (Figure 5-31: *June 14, 2006 Ozone Sonde Rice University*). The sonde observed ozone concentrations in excess of 100 ppb at the surface, extending to almost 2km. The model (blue) estimated surface concentrations above 90 ppb and decreased thru 2 km. Many different layers were observed by

the sonde thru 9 km but the model predicted a more stable atmosphere with ozone concentrations below 60 ppb.

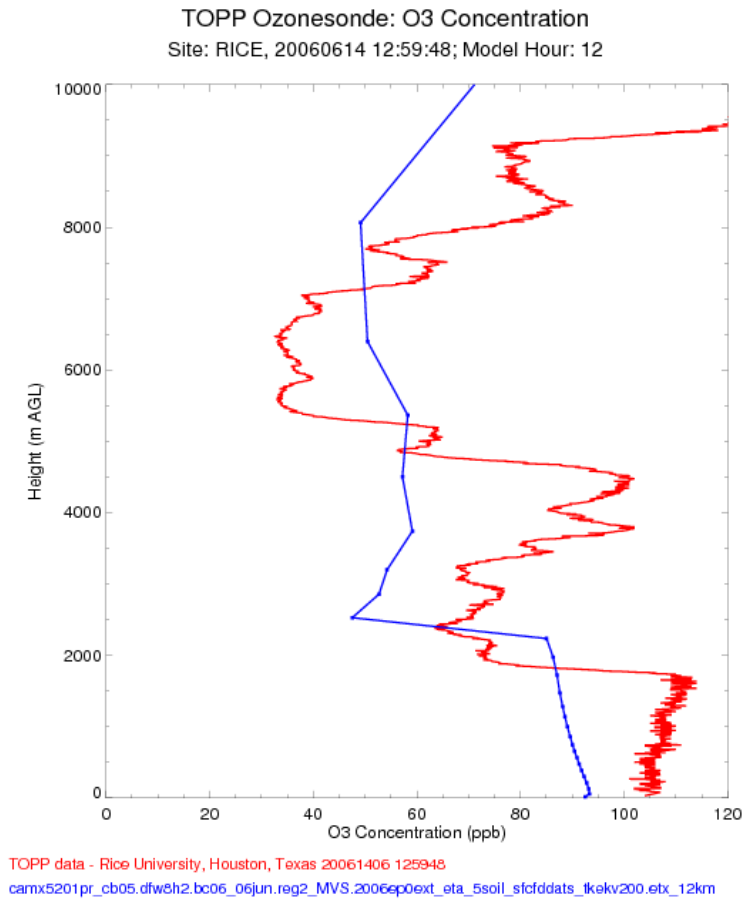

Figure 5-31: June 14, 2006 Ozone Sonde Rice University

On June 15, 2006 an ozone sonde was released from Texas A&M University near College Station, TX at 12:28 PM (Figure 5-32: *June 15, 2006 Ozone Sonde Texas A&M University*). Ozone concentrations were observed at 75 ppb through 3 km. The model predicted similar conditions though 5-10 ppb lower. Above 2 km, the model was 20-25 ppb lower than observed.

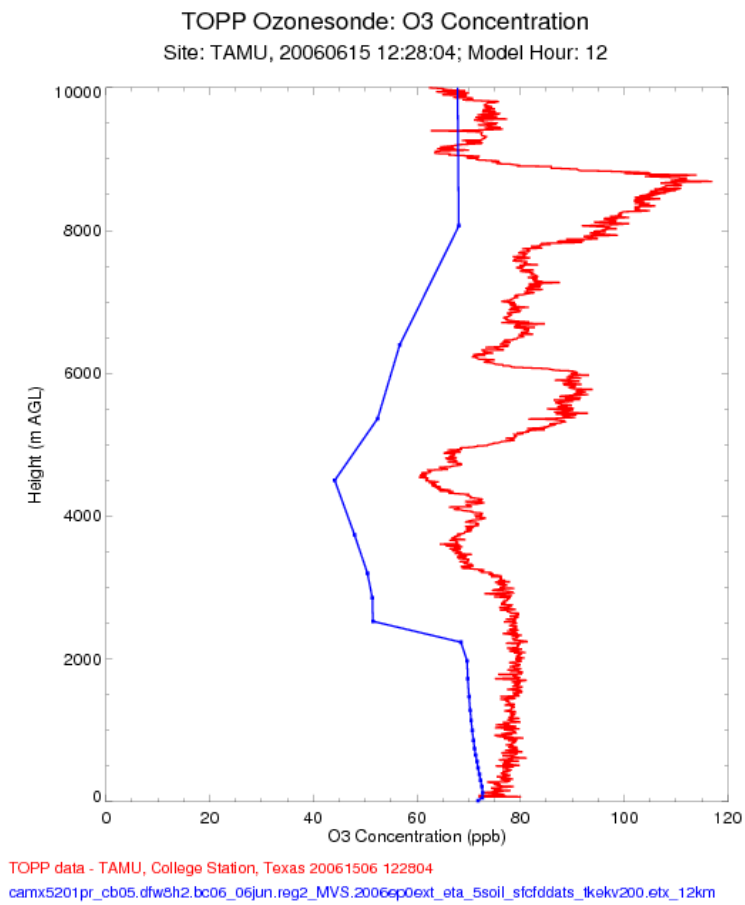

Figure 5-32: June 15, 2006 Ozone Sonde Texas A&M University

Figure 5-33: *June 21, 2006 Ozone Sonde Rice University* shows the ozone sonde launch on June 21, 2006 at 11:25 AM from Rice University. On this day, surface ozone was observed near 25 ppb and steadily increased throughout the 10 km of the record. The model predicted similar conditions but started with surface concentrations of 40 ppb.

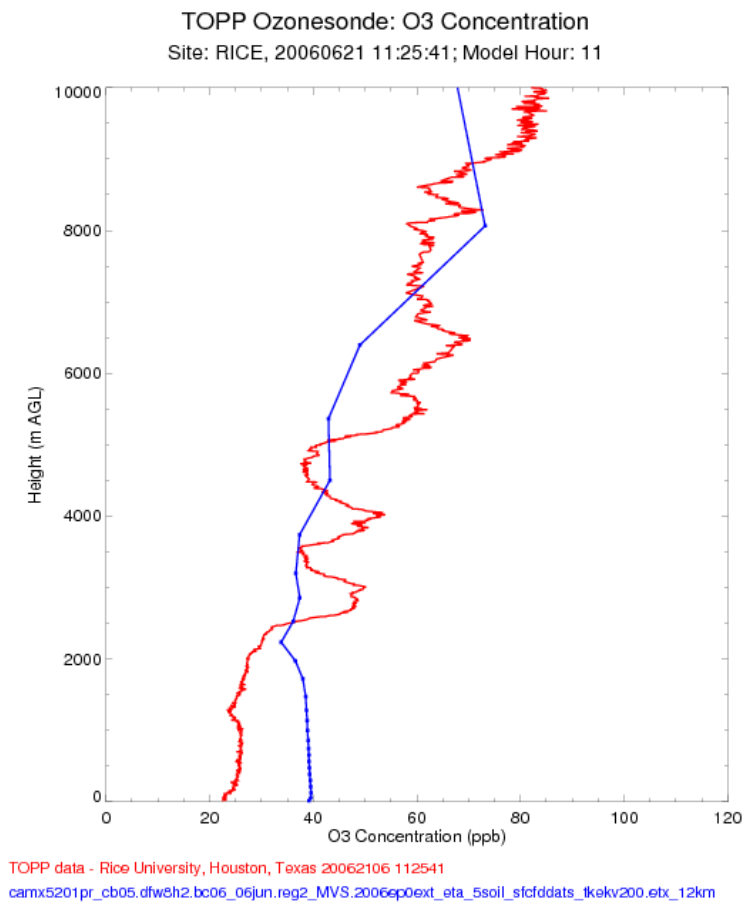

Figure 5-33: June 21, 2006 Ozone Sonde Rice University

Figure 5-34: *June 23, 2006 Ozone Sonde Stephen F. Austin State University* exhibits the ozone sonde launched from Stephen F. Austin State University in Nacogdoches, TX on June 23, 2006 at 12:08 PM. The model does a good job tracking the observed ozone concentrations, though over-predicts the surface concentrations and under-predicts above 2 km.

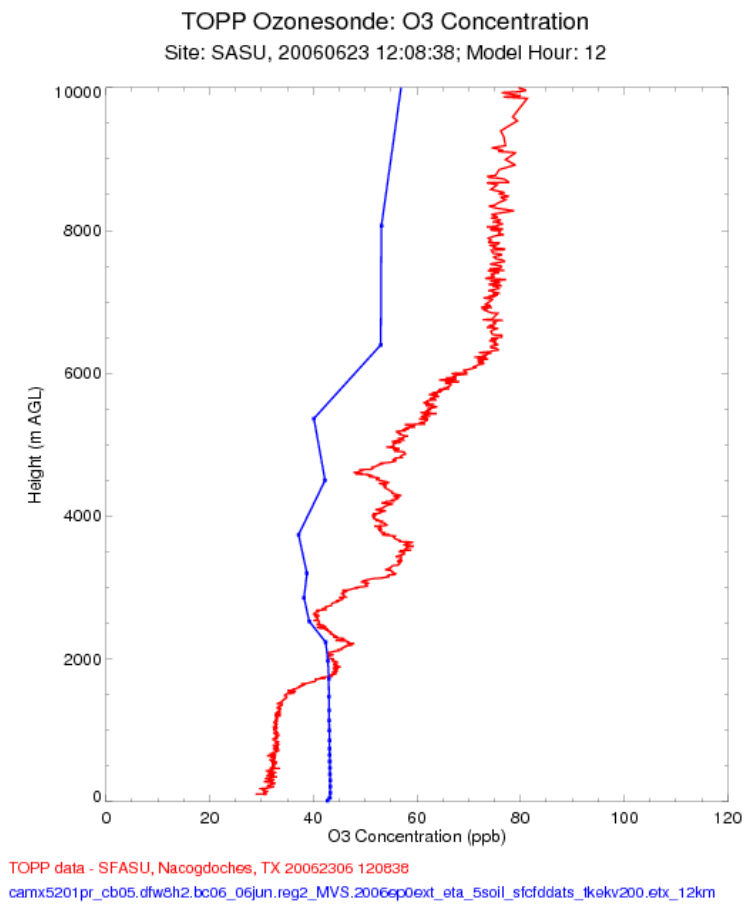

Figure 5-34: June 23, 2006 Ozone Sonde Stephen F. Austin State University

On June 27, 2006 at Rice University an ozone sonde was launched at 1:14 PM (Figure 5-35: *June 27, 2006 Ozone Sonde Rice University*). While the model replicates the reduction in ozone concentrations at 2 km, the model under-predicts the lower tropospheric concentrations by almost 10 ppb at the surface to 15 ppb below 2 km. The 12 km domain resolution for this launch site may be inhibiting the ozone formation where strong emission gradients may be occurring.

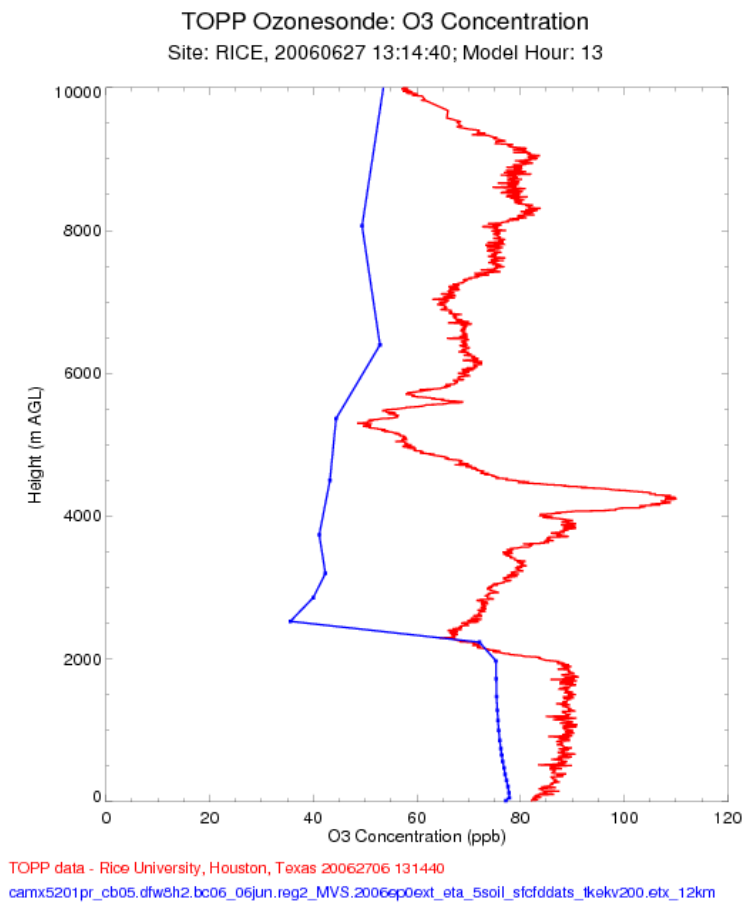

Figure 5-35: June 27, 2006 Ozone Sonde Rice University

Figure 5-36: *June 28, 2006 Ozone Sonde Rice University* shows the June 28, 2006 ozone sonde launch from Rice University at 1:00 PM. The model does a very good job of replicating the conditions over the entire recorded atmosphere. The surface concentrations were observed near 100 ppb with the model predictions approximately the same.

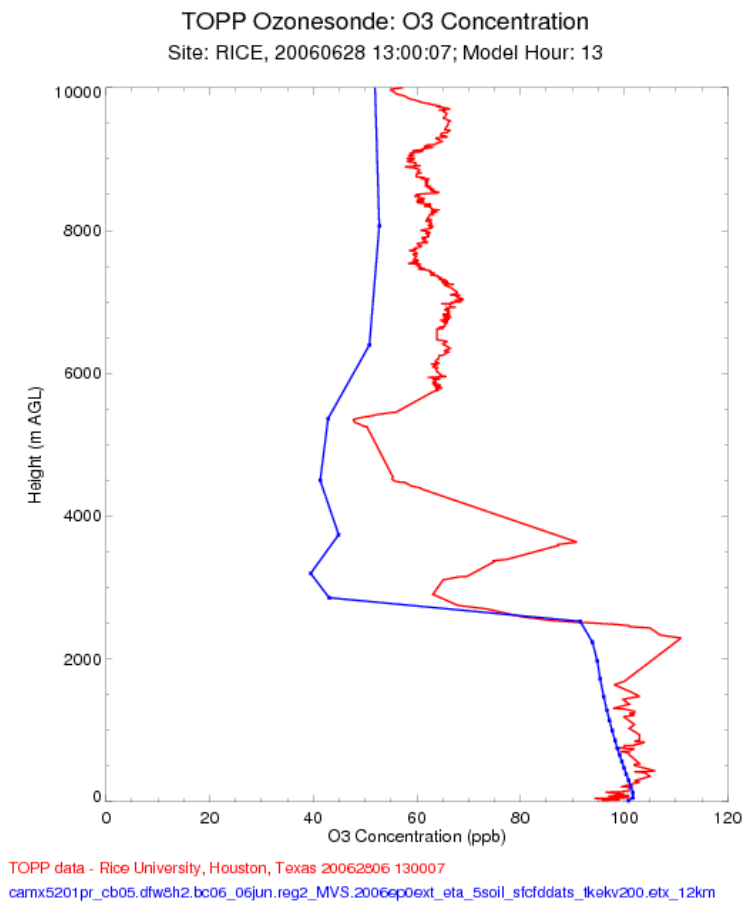

Figure 5-36: June 28, 2006 Ozone Sonde Rice University

5.4.1 Summary and Conclusions

The ozone sonde data has provided a unique and valuable means for assessing the model's performance. Besides simply allowing modeled concentrations to be compared with measurements aloft, the detailed profiles provide insight into how the model characterizes vertical mixing compared to the real atmosphere.

The most striking difference between observed and modeled vertical ozone profiles is the wide variability in ozone concentrations with altitude, observed on most days. The model, meanwhile, tends to vary much more slowly, which is not unexpected as it tends to organize wind flow and vertical motion.

No attempt was made to diagnose the actual mixing depth from meteorological data carried by the sondes (a topic for future research), but based on ozone profiles it is possible in many cases to approximate both modeled and actual mixing depths. In many cases the apparent observed and modeled mixing depths are close to one another.

As noted earlier, the TCEQ hopes to incorporate the sonde meteorological data into a more detailed analysis of vertical mixing. Additional plans for future work include tracking the sondes' paths through the model grid cells instead of assuming vertical ascent, and investigating the feasibility of using data collected as the instruments descended after balloon burst.

5.5 Diagnostic Evaluations

5.5.1 Sensitivity Analyses

5.5.1.1 Alternative Meteorological Configuration

The TCEQ conducted CAMx modeling using meteorological inputs from MM5 modeling with two different planetary boundary layer (PBL) schemes in the 4 km domain, ETA and MRF. The primary purpose for investigating different PBL schemes was to evaluate the effect on wind speeds, PBL heights, and vertical mixing. This section will examine the effects of the ETA and MRF PBL schemes on model performance. The ETA PBL was chosen for the final SIP modeling configuration.

The following four figures are scatter plots of modeled versus observed average wind direction and speed in the DFW area from the MM5 output. Each circle represents one hour of the June 2006 episode; red circles are daytime hours and blue are nighttime hours. The box in the upper left of each figure exhibits the percent of hours that fall within specified error benchmarks for all, day, or night hours. For wind speed a regression line is plotted to evaluate the correlation of the model versus observed.

Comparing the two plots and benchmarks for wind direction, both PBL schemes perform similarly. For wind direction errors less than 20 and 10 degrees, using MRF (Figure 5-38: Scatter plot of DFW area average wind direction with the MRF PBL scheme) appears to have a slight performance edge over the ETA PBL scheme (Figure 5-37: *Scatter plot of DFW area average wind direction with the ETA PBL scheme*), especially at night.

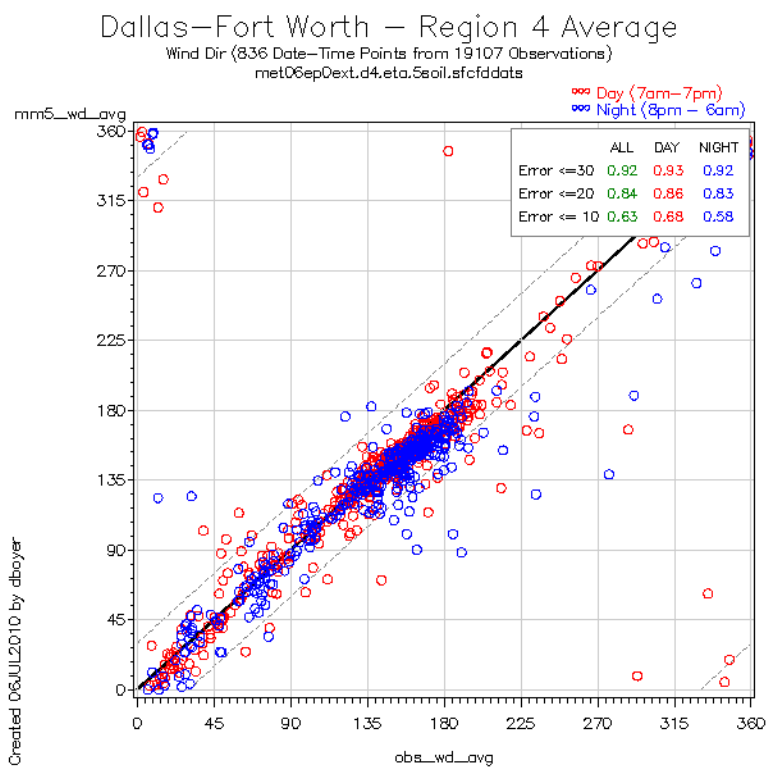

Figure 5-37: Scatter plot of DFW area average wind direction with the ETA PBL scheme

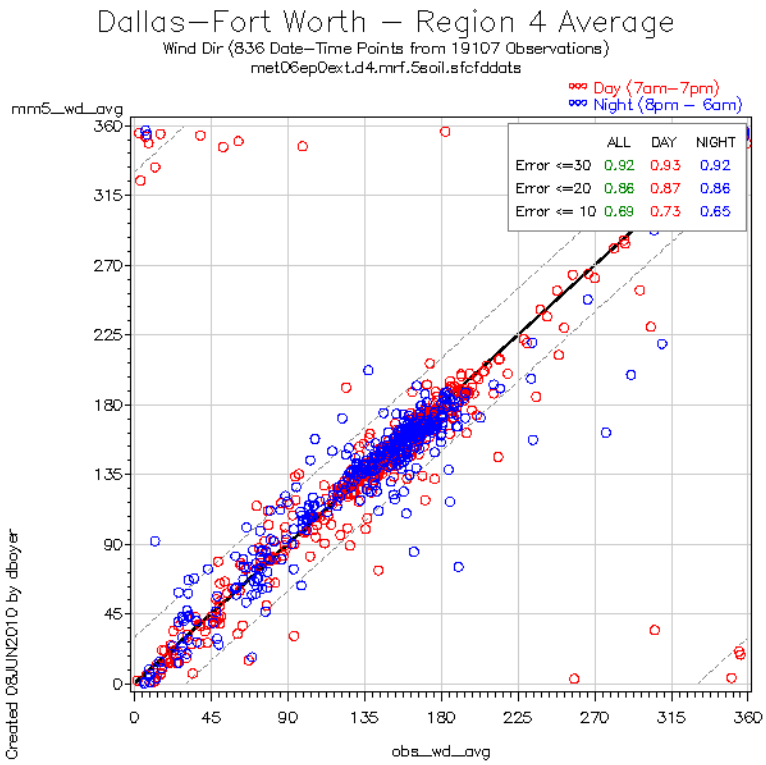

Figure 5-38: Scatter plot of DFW area average wind direction with the MRF PBL scheme

For wind speed, the ETA scheme (Figure 5-39: Scatter plot of DFW area average wind speed with the ETA PBL scheme) improves performance compared to the MRF scheme (Figure 5-40: *Scatter plot of DFW area average wind speed with the MRF PBL scheme*), especially at night. 85% of nighttime hours with the ETA scheme are within 1 m/s of the observations compared to 49% for the MRF scheme. Daytime hours have similar performance between schemes.

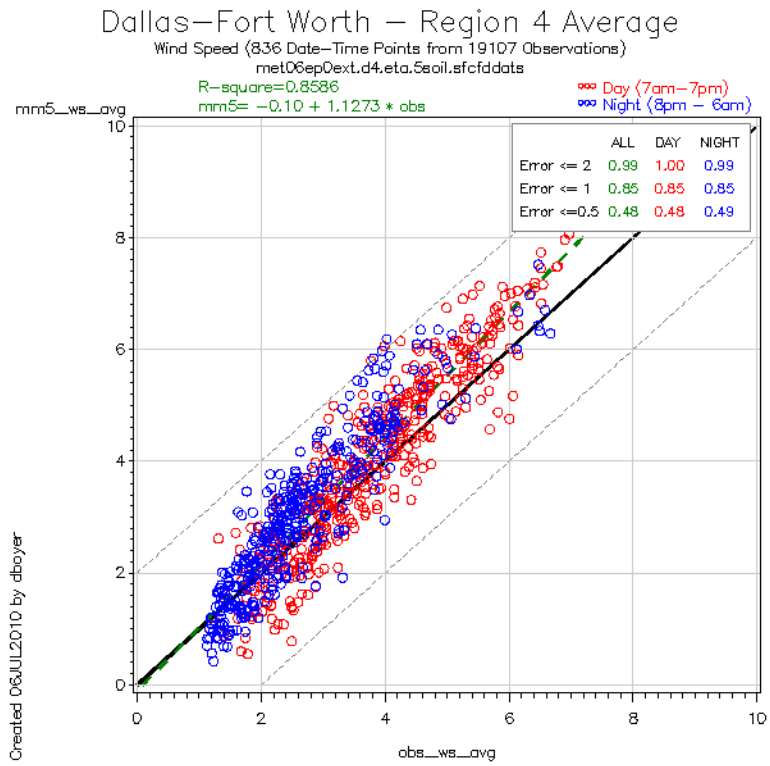

Figure 5-39: Scatter plot of DFW area average wind speed with the ETA PBL scheme

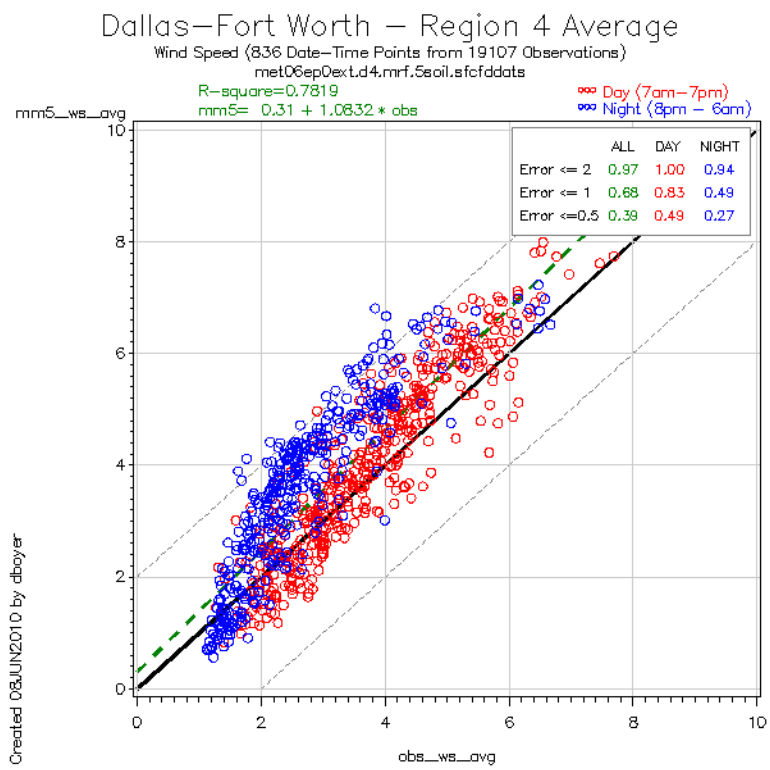

Figure 5-40: Scatter plot of DFW area average wind speed with the MRF PBL scheme

Comparing the time series of wind speed bias shows this difference as well (Figure 5-41: *Time Series of DFW Average Wind Speed Bias (m/s) for ETA PBL (top) and MRF PBL (bottom) scheme*). The top time series of Figure 5-41 exhibits the average wind speed bias for the model with the ETA PBL scheme compared to the DFW area observed average. The bottom time series shows the average wind speed bias for the MRF PBL scheme. The MRF time series is farther away from the zero line, indicating a higher wind speed bias (error). This occurs more often at night throughout the episode.

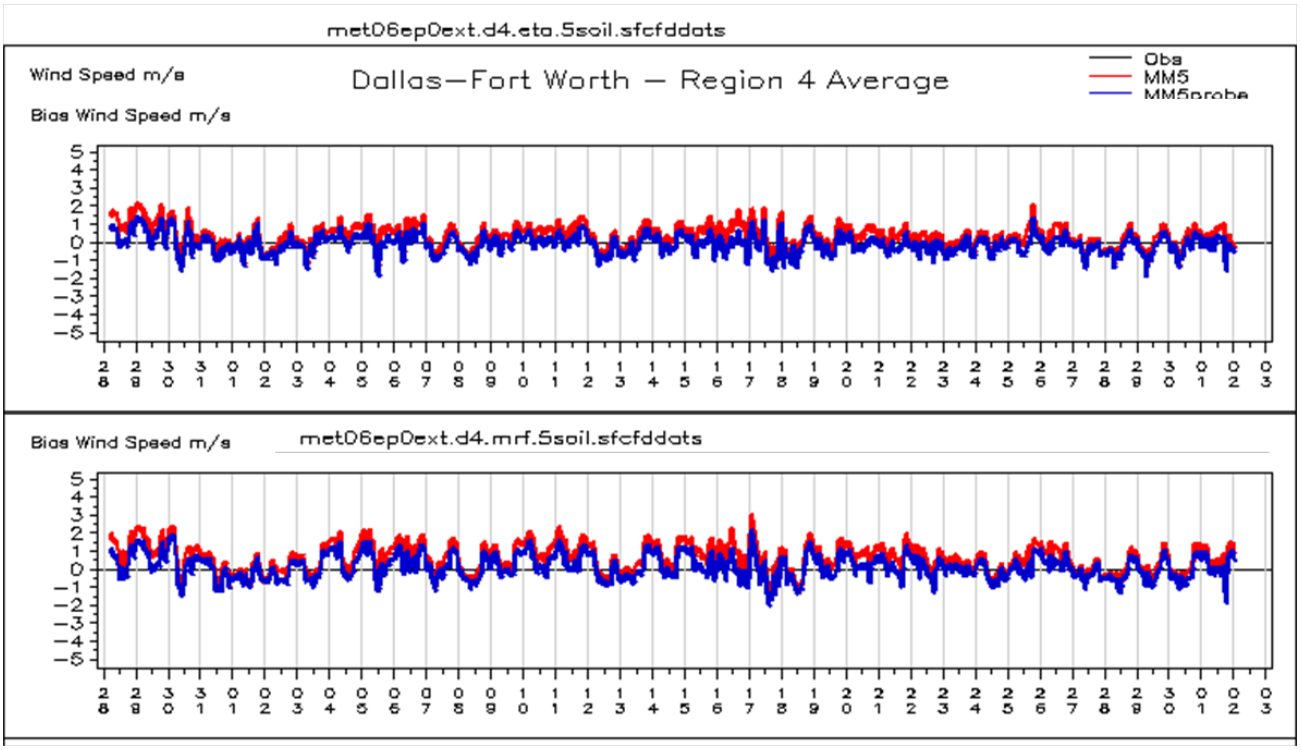

Figure 5-41: Time Series of DFW Average Wind Speed Bias (m/s) for ETA PBL (top) and MRF PBL (bottom) schemes

The following two figures show the upper air horizontal wind conditions at the Cleburne radar wind profiler for one episode day. Vertical winds (rising or descending air) are not shown. The model winds (CAMx input) are shown as blue vectors and the observed winds (profiler) are shown as red vectors. Each hour of the episode day is depicted on the x-axis. Winds from just above the surface to 3 km are illustrated by vectors pointing in the compass direction from which the wind is blowing. Also on these plots are the model (blue) and profiler (red) estimated planetary boundary layer (PBL) depths shown by horizontal lines between hours. The observed data is generally only available during daylight hours.

Because the two model runs used the same input and nudging data, the wind performance is similar. The PBL heights can differ by hundreds of meters though. On June 12, 2006 the PBL height at the Cleburne profiler peaked at 2 km from 2:00 – 4:00 CST. The ETA PBL run followed the morning rise of the PBL and slightly over-estimated the peak in the afternoon (Figure 5-42: *Time-height plot for June 12, 2006 with ETA PBL*). With MRF, the model produces a higher than observed mixing height too early in the morning and over-estimates the afternoon peak slightly (Figure 5-43: *Time-height plot for June 12, 2006 with MRF PBL*).

Based on Knoderer et al. (2008), the morning rise of the PBL may be more important to ozone production than the peak mixing depth.

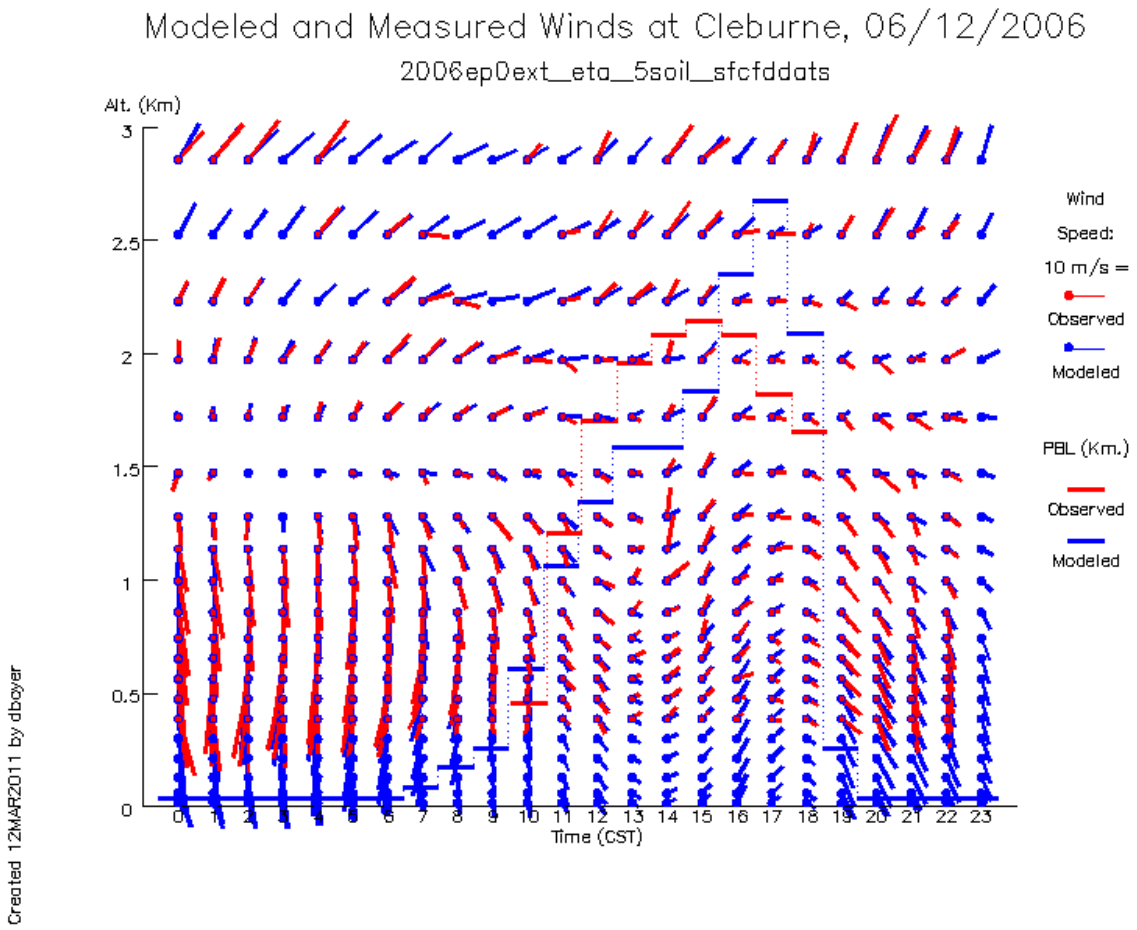

Figure 5-42: Time-height plot for June 12, 2006 with ETA PBL

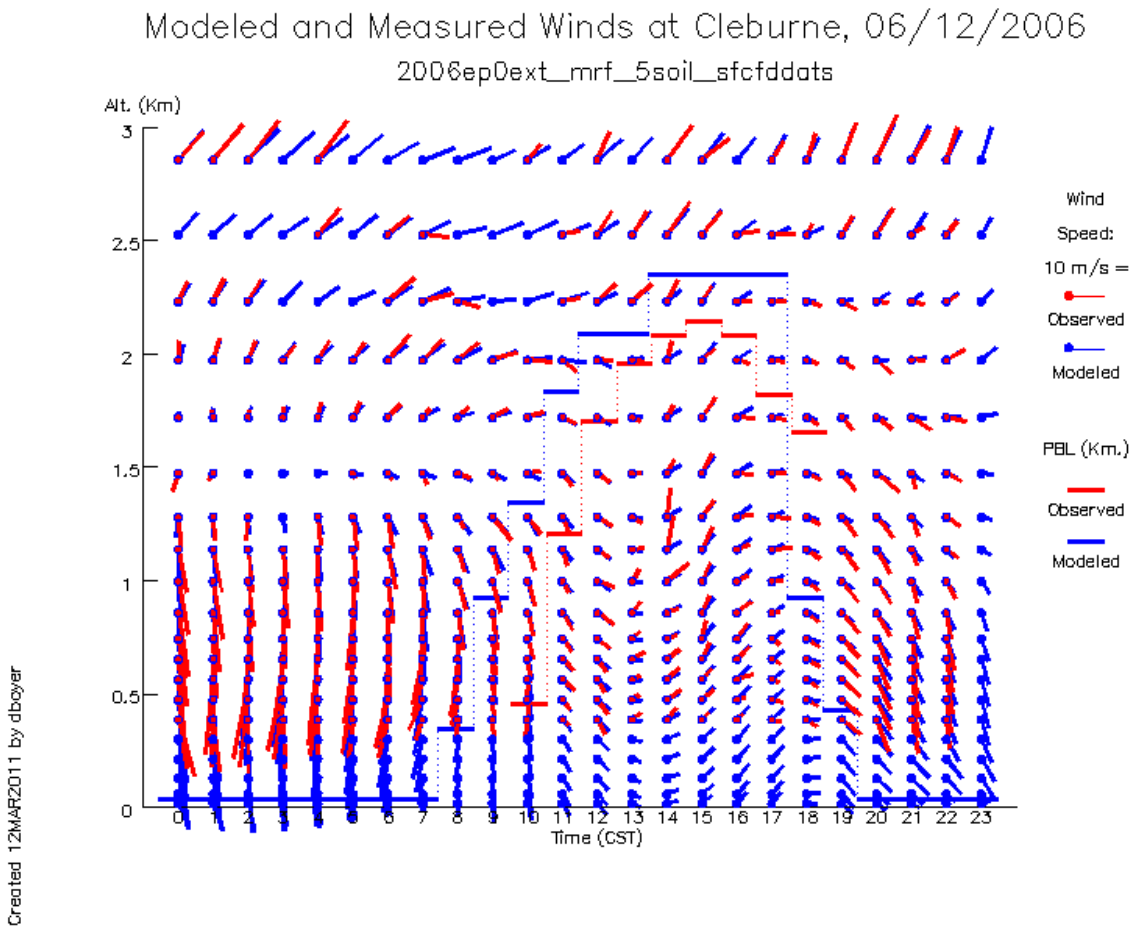

Figure 5-43: Time-height plot for June 12, 2006 with MRF PBL

These model responses were typical for the episode with the ETA PBL matching the morning rise better but the MRF PBL estimating higher mixing heights that more closely match the peak observations. Scatter plots of the model versus observed mixing heights corroborate those findings. With the ETA PBL scheme (Figure 5-44: Scatter plot of PBL heights with ETA PBL Scheme), the model matches the observations better at the lower PBL heights than the MRF scheme (Figure 5-45: *Scatter plot of PBL heights with MRF PBL Scheme*), which are observed during the morning rise and late afternoon fall. As stated before, the MRF scheme (Figure 5-45) produces deeper mixing heights and matches the higher values better than the ETA scheme (Figure 5-44).

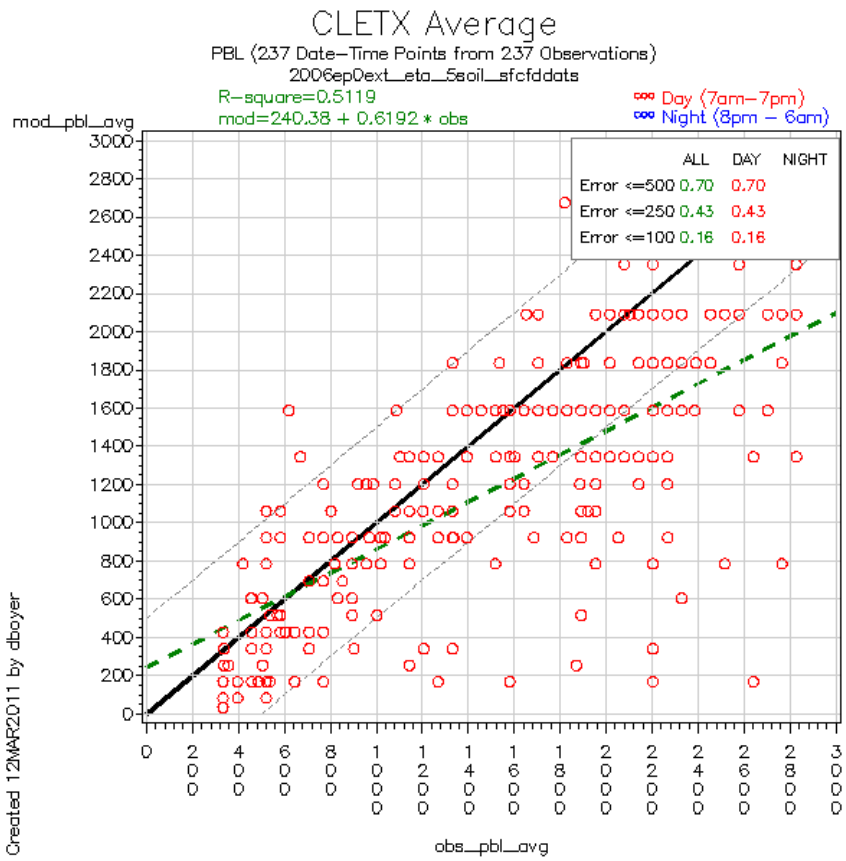

Figure 5-44: Scatter plot of PBL heights with ETA PBL Scheme

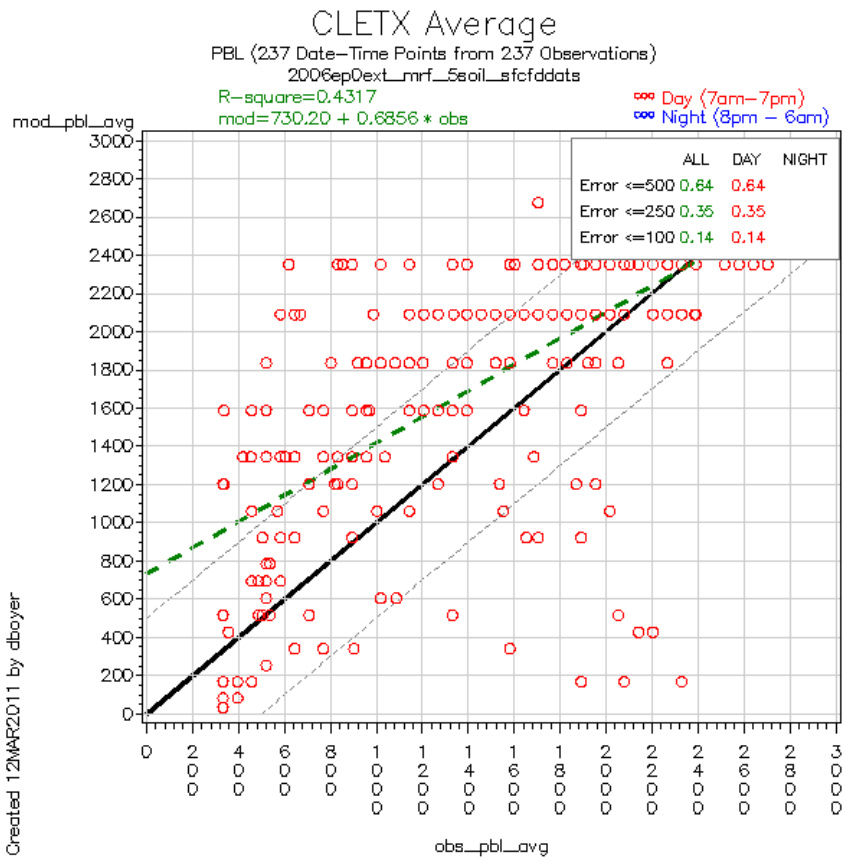

Figure 5-45: Scatter plot of PBL heights with MRF PBL Scheme

Figure 5-46: *Hourly Ozone Time Series at Denton, Eagle Mountain Lake, and Fort Worth NW* shows the CAMx model's hourly ozone response with the ETA PBL (blue) and MRF PBL (green) schemes at the Denton, Eagle Mountain Lake, and Fort Worth Northwest monitors. Throughout the episode, both model runs predict similar hourly ozone concentrations. In terms of daily peak ozone, the results are day dependent. On some days the ETA PBL produces peak ozone closer to the observations, on other days the MRF PBL performs better.

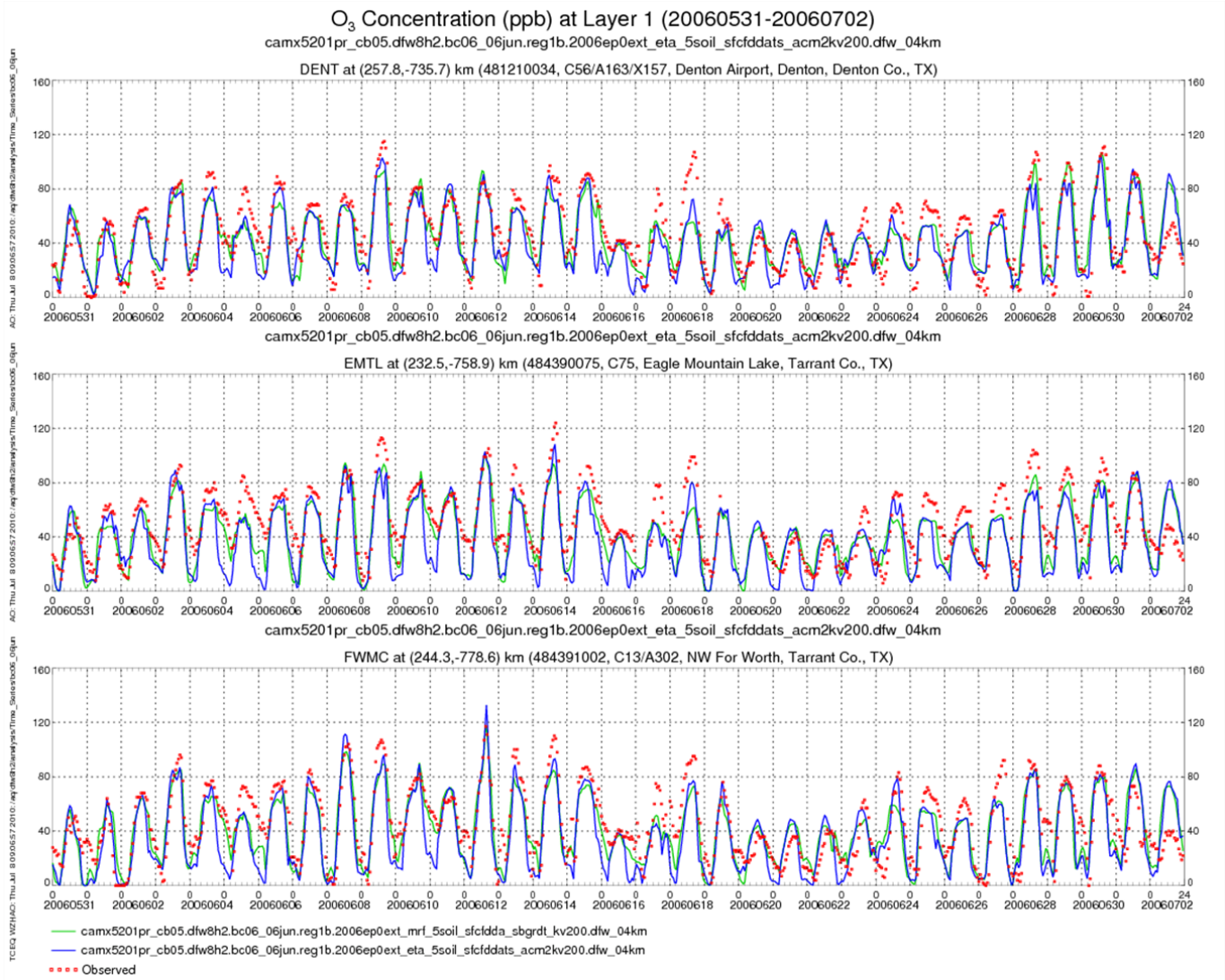

Figure 5-46: Hourly Ozone Time Series at Denton, Eagle Mountain Lake, and Fort Worth NW

Based on the analysis above, the ETA scheme does not appear to have a consistent effect on ozone concentrations but surface wind speed bias is reduced compared to using the MRF scheme, especially at night. Using the ETA scheme also aids in predicting the morning rise of the PBL, which may be more important for replicating peak eight-hour ozone formation than the afternoon PBL maximum.

5.5.1.2 Alternative Initial and Boundary Conditions

The TCEQ conducted CAMx modeling using episode-specific initial and boundary conditions derived from the application of the MOZART global air quality model. The TCEQ contracted with Environ to derive initial and boundary conditions using the MOZART version 4 global air quality model (noted as MOZART Run3). Compared to the original MOZART boundary conditions (Figure 5-47: *Original MOZART Boundary Conditions of Ozone (ppb)*), MOZART run3 (Figure 5-48: *MOZART Run3 Boundary Conditions of Ozone (ppb)*) had less ozone, especially on the northern and southern sides of the domain.

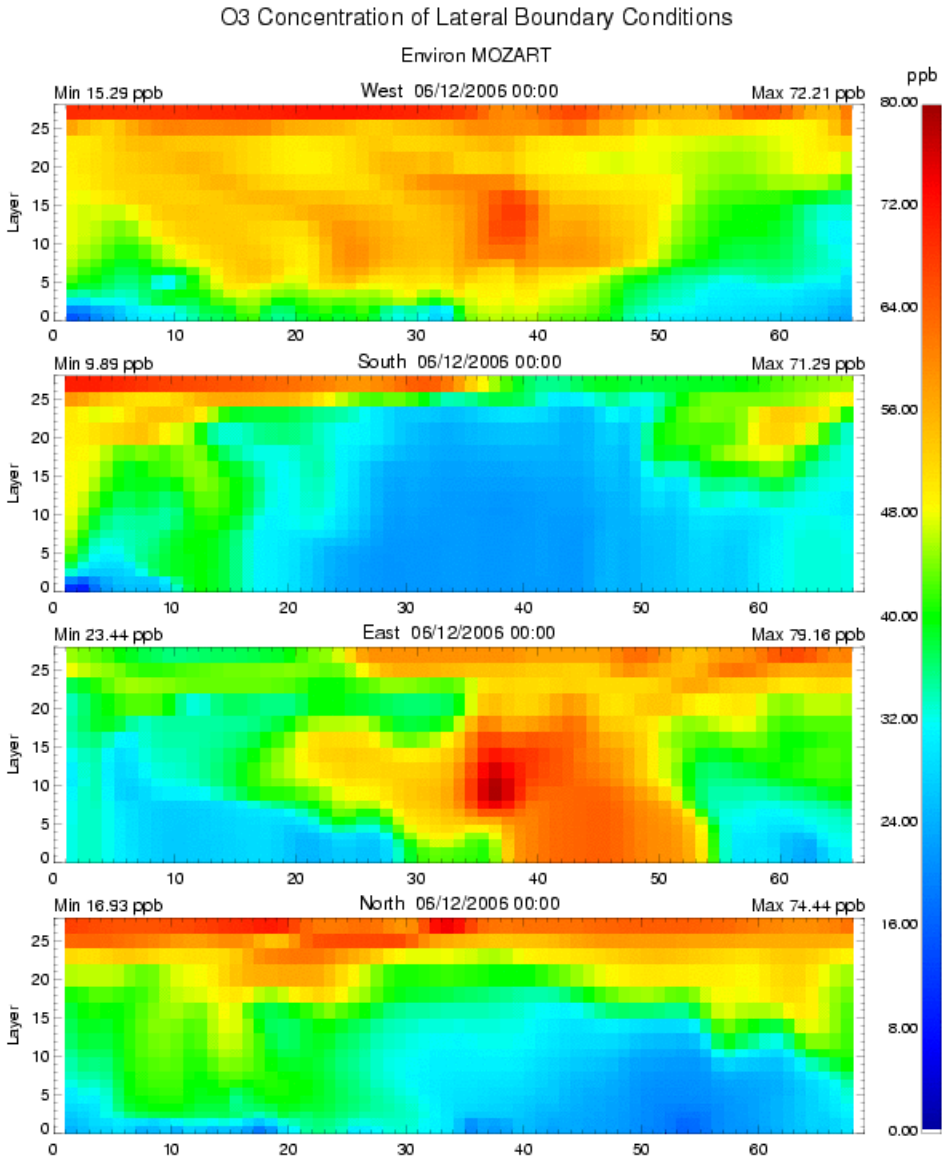

Figure 5-47: Original MOZART Boundary Conditions of Ozone (ppb) for June 12, 2006

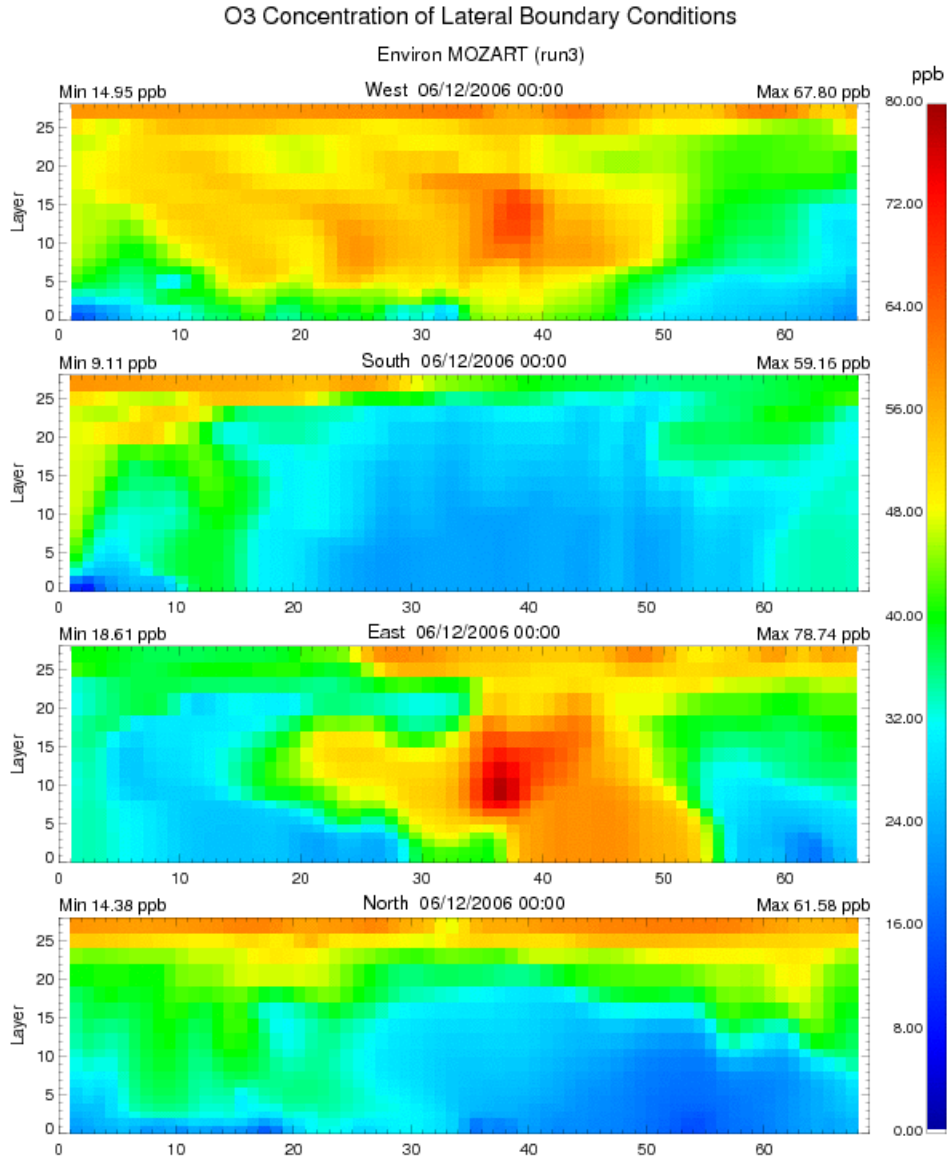

Figure 5-48: MOZART Run3 Boundary Conditions of Ozone (ppb) for June 12, 2006

The difference in MOZART boundary conditions did not change the modeled surface ozone values significantly. In general, the MOZART Run3 boundary conditions increased eight-hour ozone normalized bias and gross error throughout the episode as shown by Figure 5-49: *Soccer-style Plot of Hourly MNGE and MNB by Day for Boundary Condition Model Runs*. The green circles represent the MOZART Run3 conditions, which are slightly shifted towards the edges of the plot (greater error and bias) compared to the original MOZART conditions (red circles).

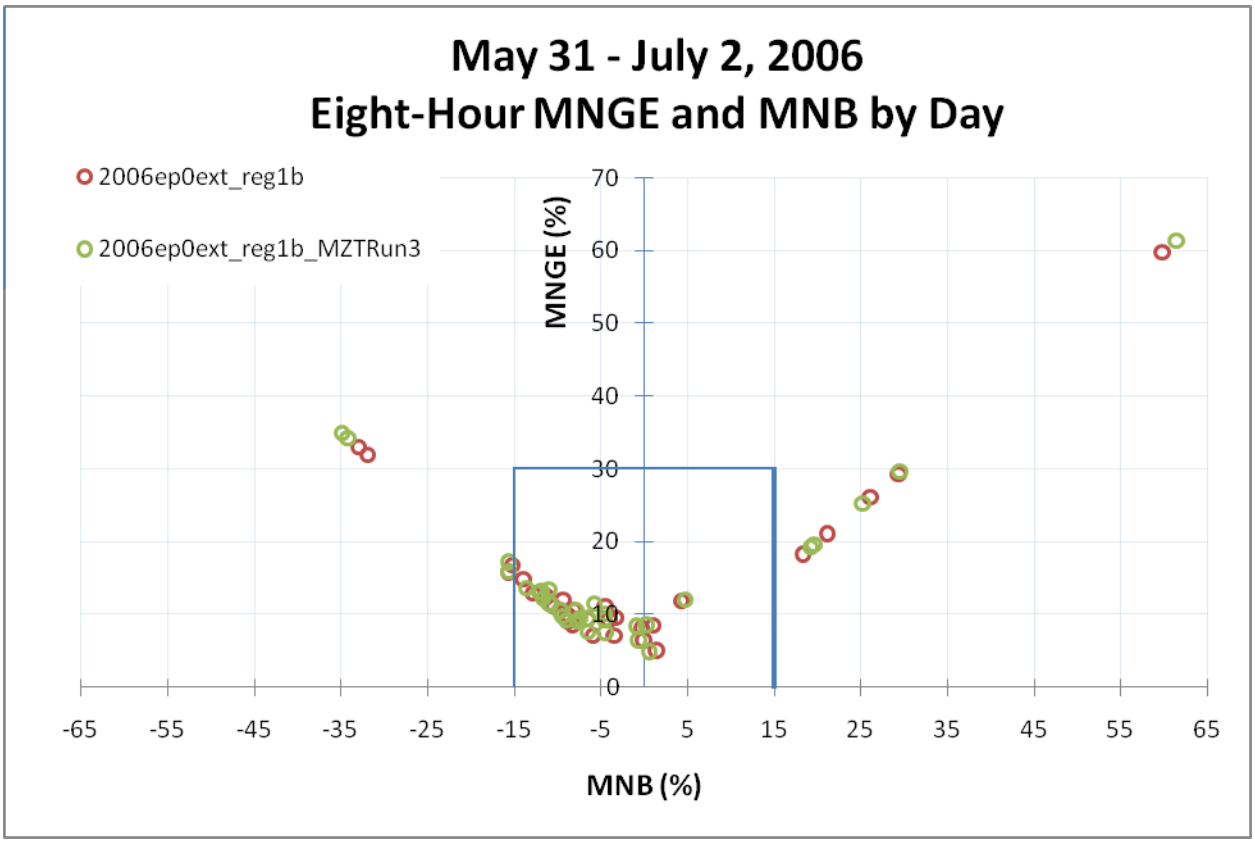

Figure 5-49: Soccer-style Plot of Hourly MNGE and MNB by Day for Boundary Condition Model Runs

Similar results by monitor are shown in Figure 5-50: *Soccer-style Plot of Hourly MNGE and MNB by Monitor for Boundary Condition Model Runs.*

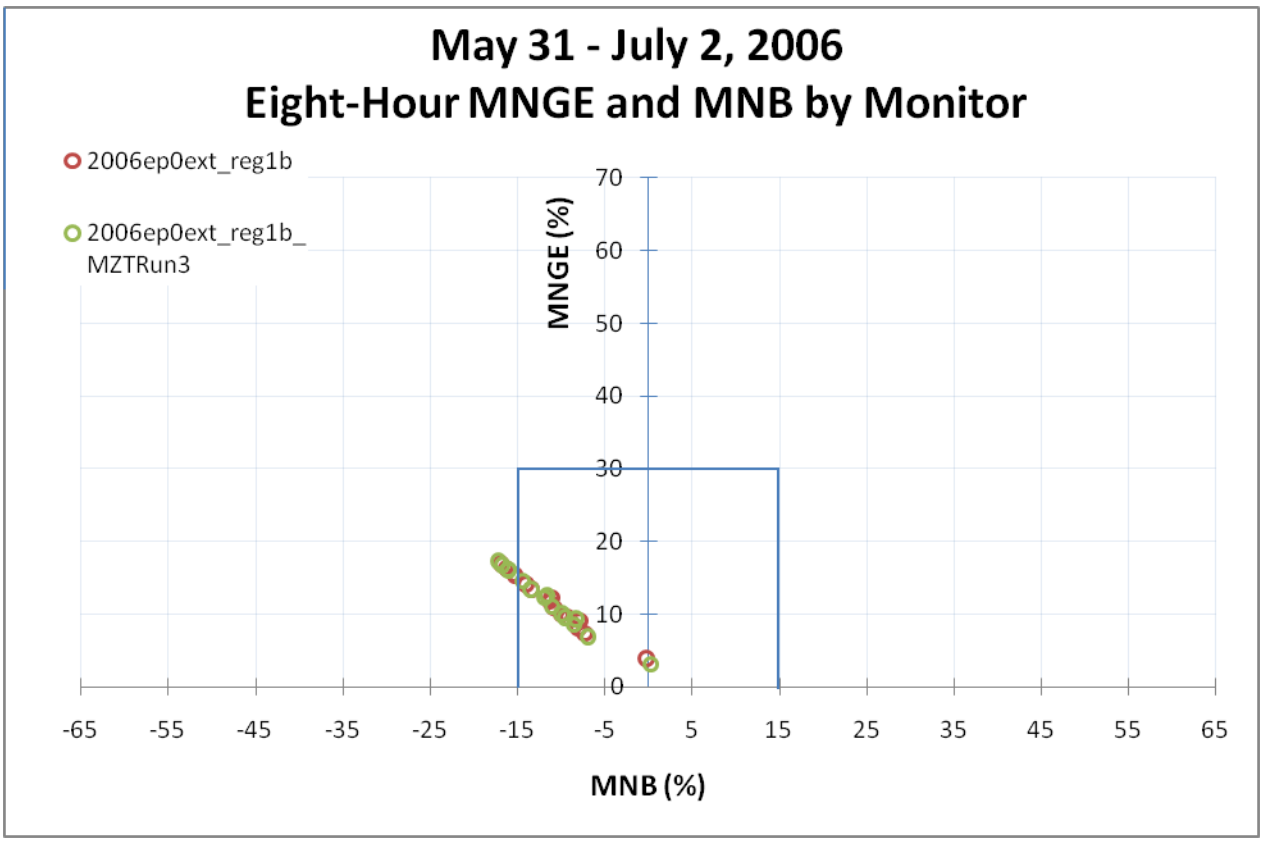

Figure 5-50: Soccer-style Plot of Hourly MNGE and MNB by Monitor for Boundary Condition Model Runs

The difference between model runs with the original and Run3 MOZART boundary conditions was slight but the Run3 conditions produced eight-hour results with greater error and bias statistics. The original MOZART conditions were chosen for the final SIP runs.

5.5.1.3 Alternative Modeling Emissions: Louisiana Haynesville Shale Drill Rig Emissions

The TCEQ conducted CAMx modeling using emissions modeling inputs with and without the estimated 2012 Louisiana Haynesville Shale drill rig emissions. The CAMx modeling iterations designated as cs01 and cs00 differ by these modeling inputs. As based on the 2002 NEI, the cs00 future year emissions for Louisiana had no onshore oil and gas drilling emissions. Because of the rapid oil and gas development within the Haynesville Shale in northeast Texas and northwest Louisiana since 2008 and the upwind location to DFW during easterly wind conditions, including these sources was a priority. Figure 5-51: Haynesville Shale Counties/Parishes (Environ, 2009) shows the location of the Haynesville Shale. The 2008 Texas oil and gas inventory used in these modeling runs already included activity in the Texas Haynesville Shale counties so only Louisiana sources were added (Environ, 2009). Forty-eight tpd of NO_X emissions were added in the Louisiana parishes (Figure 5-52: *2012 Louisiana Drill Rig NOX Emissions*). Just over 1 tpd of VOC emissions was added (not shown). For more on the development of this oil and gas inventory, see Section 1.4.3 of Appendix B.

Figure 5-51: Haynesville Shale Counties/Parishes (Environ, 2009)

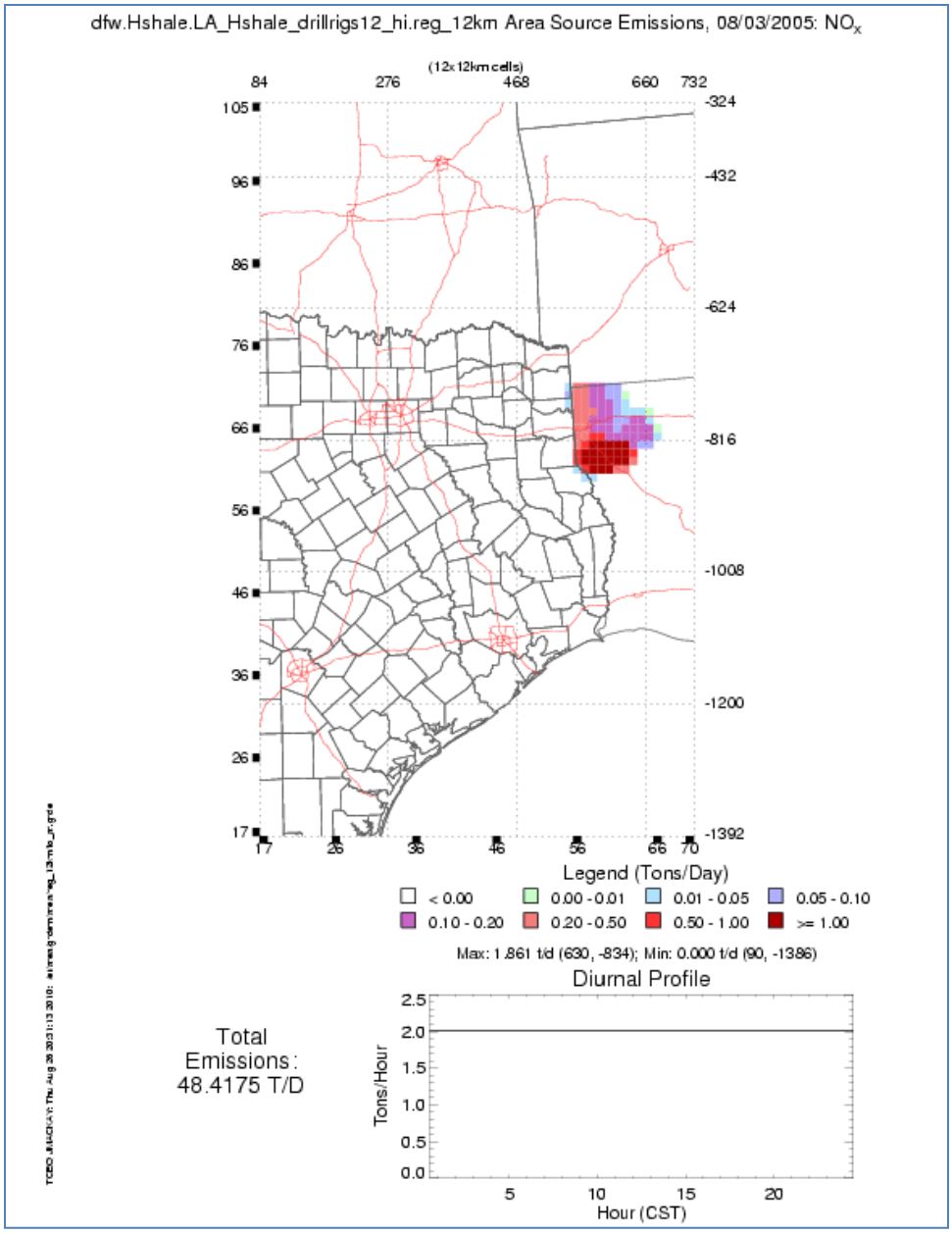

Figure 5-52: 2012 Louisiana Drill Rig NO_X Emissions

Compared to the base cs00 2010 run, the addition of the Louisiana drill rigs increased maximum daily eight-hour ozone on days with easterly winds. The figure below shows the difference in daily maximum eight-hour ozone concentrations for June 9, 2006 between the base cs00 inventory and the cs01 inventory with the Louisiana drill rigs (Figure 5-53: *June 9, 2006 Maximum Eight-Hour Impact of Louisiana Drill Rigs*). In the DFW nonattainment area, an increase of about 1-2 ppb in eight-hour modeled ozone occurred. Throughout the episode a 0-2 ppb increase was observed on days with appropriate wind directions (e.g. Figure 5-54: *June 13, 2006 Maximum Eight-Hour Impact of Louisiana Drill Rigs*). These results are similar to an Environ study conducted for the northeast Texas area (Environ, 2009).

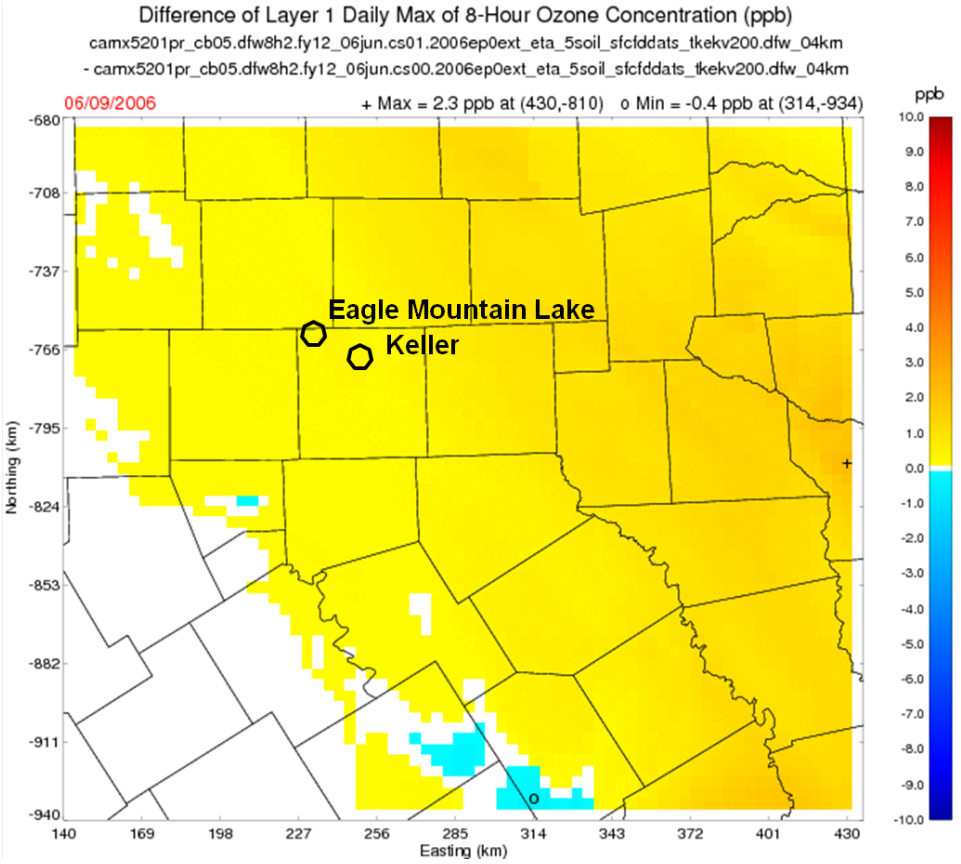

Figure 5-53: June 9, 2006 Maximum Eight-Hour Impact of Louisiana Drill Rigs

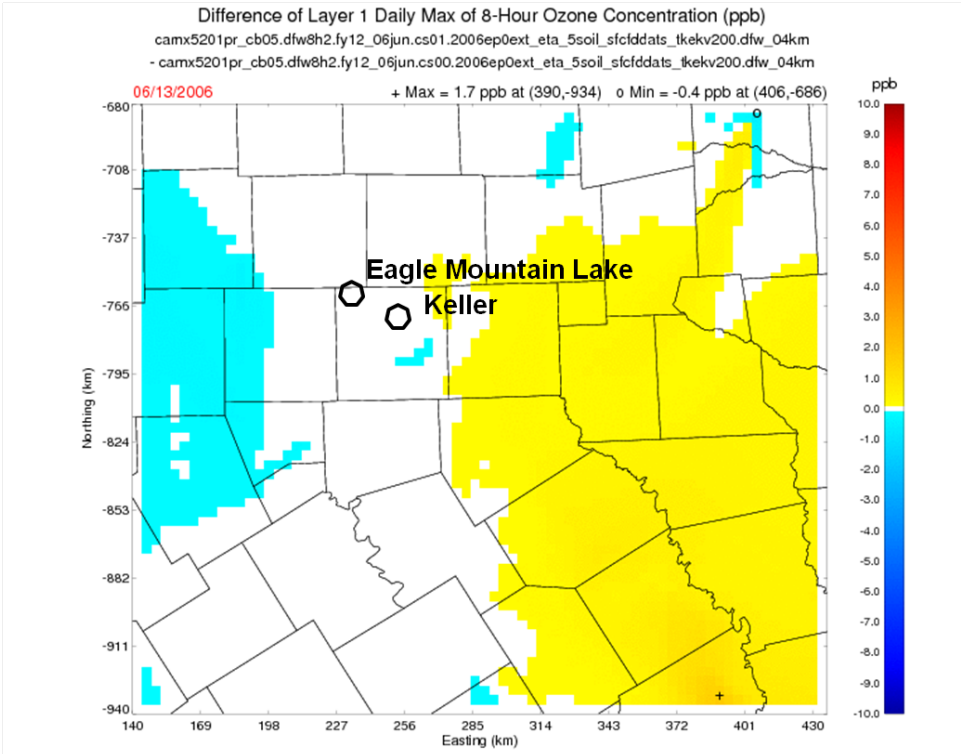

Figure 5-54: June 13, 2006 Maximum Eight-Hour Impact of Louisiana Drill Rigs

This emission change also affected the 2012 future design value as shown in Table 5-4: Future Design Value Change due to Louisiana Drill Rigs. At all but one monitor the future design value increased as indicated in the Diff column. The largest increase of 0.29 ppb is seen at the Greenville monitor, just east of the DFW nonattainment area (Figure 3-3: *DFW Area Monitors*) and closest to the Louisiana Haynesville Shale sources. While this analysis was conducted using a 2008 Texas oil and gas inventory during SIP development, the results indicated the importance of including this distant emission source. The Louisiana drill rigs were included in the final 2012 SIP modeling.

Table 5-4: Future Design Value Change due to Louisiana Drill Rigs

Monitor	2012 Future Design Value (cs00)	2012 Future Design Value (cs01)	Diff (ppb)
Denton	77.0	77.1	0.13
Eagle Mountain Lake	79.9	80.0	0.06
Keller	76.9	77.1	0.17
Grapevine Fairway	76.6	76.7	0.16
Fort Worth Northwest	75.8	75.9	0.10
Frisco	73.9	74.1	0.16
Parker County	74.5	74.6	0.09
Dallas North	70.6	70.8	0.24
Dallas Exec Airport	70.7	70.9	0.20
Cleburne	70.8	70.9	0.04
Arlington	70.5	70.6	0.06
Dallas Hinton	67.4	67.6	0.19
Pilot Point	67.2	67.4	0.22
Midlothian Tower	67.0	67.0	-0.03
Rockwall Heath	63.6	63.7	0.05
Midlothian OFW	62.4	62.5	0.08
Kaufman	61.4	61.6	0.18
Granbury	72.0	72.1	0.10
Greenville	60.1	60.4	0.29

5.5.1.4 Alternative Modeling Emissions: MOBILE6.2 On-road Emissions

The TCEQ conducted modeling with two different on-road mobile emission models, MOBILE6.2 and the Motor Vehicle Emission Simulator (MOVES) version 2010a. SIP development began with MOBILE6.2 prior to the EPA officially releasing the MOVES2010 model as a replacement to MOBILE6.2 for SIP applications on March 2, 2010 (EPA, 2011). A comparison of the NO_X and VOC emissions between the models for 2006 and 2012 is provided in *Table 5-5: MOBILE6.2 and MOVES2010a Summer Weekday On-Road NOX Emissions for the Nine-County DFW Area* and *Table 5-6: MOBILE6.2 and MOVES2010a Weekday On-Road VOC Emissions for the Nine-County DFW Area*. MOVES2010a estimates higher NO_X emissions in both years while the VOC emissions are similar.

Table 5-5: MOBILE6.2 and MOVES2010a Summer Weekday On-Road NOX Emissions for the Nine-County DFW Area

Calendar Year	MOBILE6.2 (tpd)	MOVES 2010a (tpd)	Difference (tpd)	Relative Change
2006	225.31	259.11	33.80	15%
2012	122.47	181.40	58.93	48%
Difference	-102.84	-77.71		
Change	-46%	-30%		

Table 5-6: MOBILE6.2 and MOVES2010a Weekday On-Road VOC Emissions for the Nine-County DFW Area

Calendar Year	MOBILE6.2 (tpd)	MOVES 2010a (tpd)	Difference (tpd)	Relative Change
2006	105.04	111.02	5.98	6%
2012	79.77	80.48	0.71	1%
Difference	-25.27	-30.54		
Change	-24%	-28%		

Modeled ozone levels in the base case with MOBILE6.2 were lower than ozone levels with MOVES as a result of the difference in mobile source NO_X emissions as shown in Figure 5-55: *Peak Monitored versus Modeled Eight-Hour Ozone Concentrations with MOBIE6.2 and MOVES2010a for May 31 through June* 15, 2006 and Figure 5-56: *Peak Monitored versus Modeled Eight-Hour Ozone Concentrations with MOBIE6.2 and MOVES2010a for June 16 through July* 2, 2006. The orange bars represent the observed peak concentrations, the green bars represent the base model run with MOBILE6.2 emissions, and the blue bars represent the modeled peak eight-hour ozone concentrations with MOVES2010a. The error bars on the daily peak observed eight-hour ozone concentrations represent the ± 20% Unpaired Peak Accuracy (UPA) range for comparison with the daily maximum modeled eight-hour ozone concentrations. Many of the eight-hour exceedance days were underestimated by the photochemical model with the MOBILE6.2 emissions. The use of MOVES2010a on-road mobile inventories improved performance on those eight-hour exceedance days (blue bars closer to the orange bars). Days that over-predicted the observed peak concentrations with MOBILE6.2 over-predicted slightly more with MOVES2010a emissions, indicating performance issues on these days were not related to mobile source NO_X emissions.

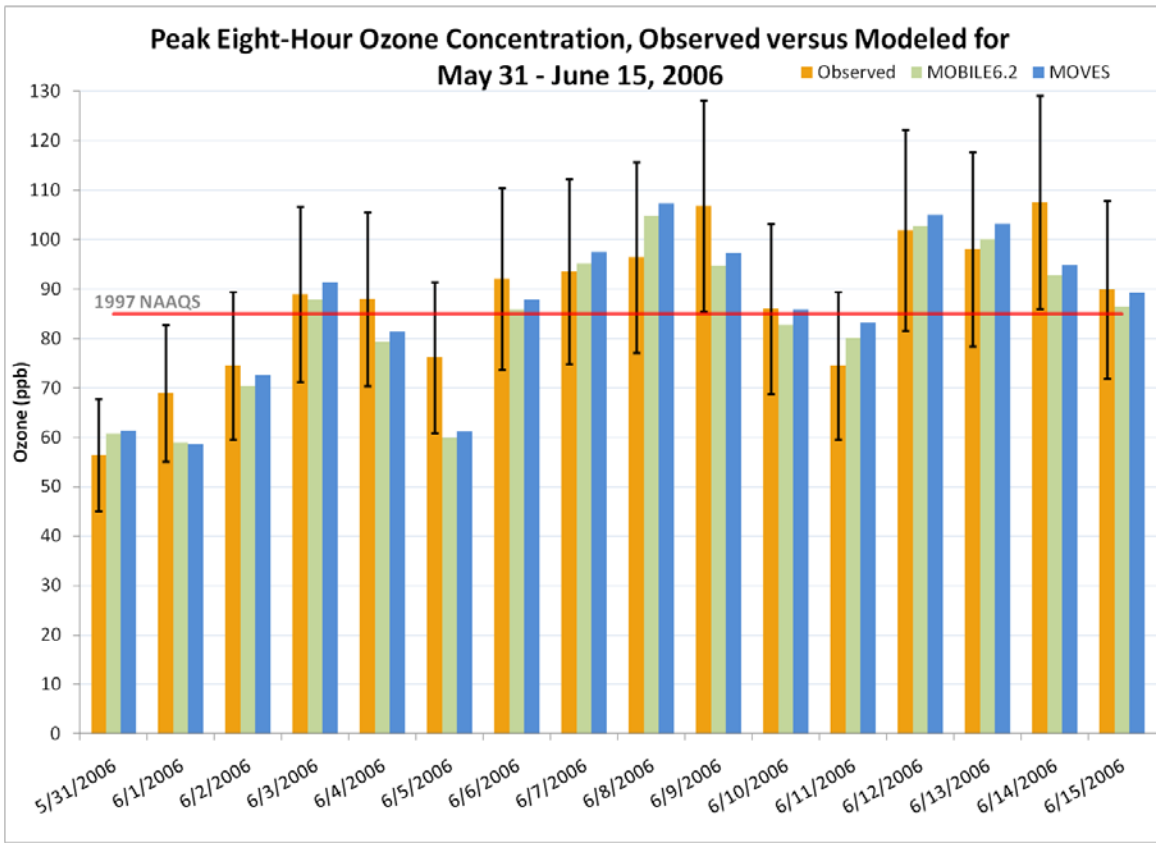

Figure 5-55: Peak Monitored versus Modeled Eight-Hour Ozone Concentrations with MOBIE6.2 and MOVES2010a for May 31 through June 15, 2006

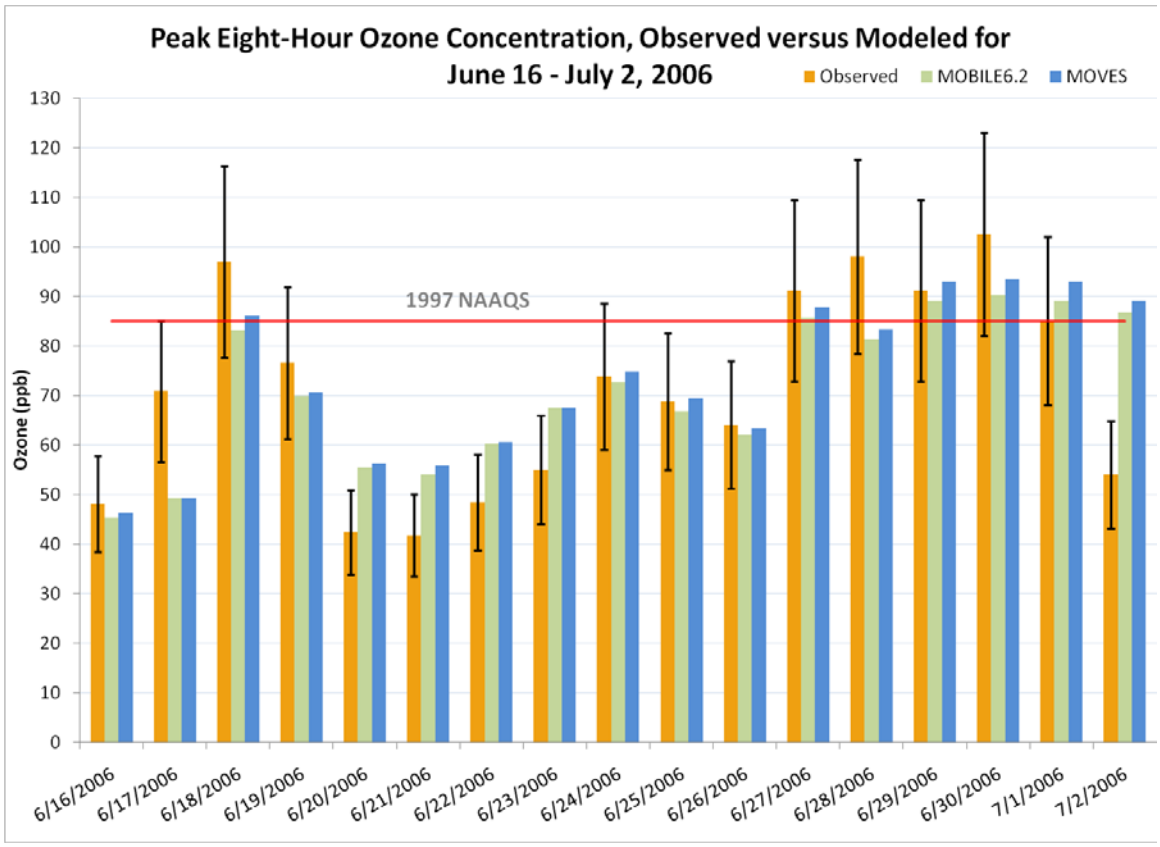

Figure 5-56: Peak Monitored versus Modeled Eight-Hour Ozone Concentrations with MOBIE6.2 and MOVES2010a for June 16 through July 2, 2006

The difference in model performance on eight-hour ozone exceedance day using MOBILE6.2 and MOVES2010a is also noted in the daily mean normalized bias (MNB) and mean normalized gross error (MNGE) statistics (Figure 5-57: *Daily MNB (top) and MNGE (bottom) Statistics for MOVES2010a and* MOBILE6.2 Photochemical Model Runs). The green bars representing the MOBILE6.2 run show more bias and error than theMOVES2010a run (blue bars) for the eight-hour ozone exceedance days (starred). The EPA's MNB and MNGE benchmarks are shown as red dashed bars (EPA, 2007). Two eight-hour ozone exceedance days (June 18 and July 1) do not comply with the EPA benchmarks with MOBILE6.2 or MOVES.

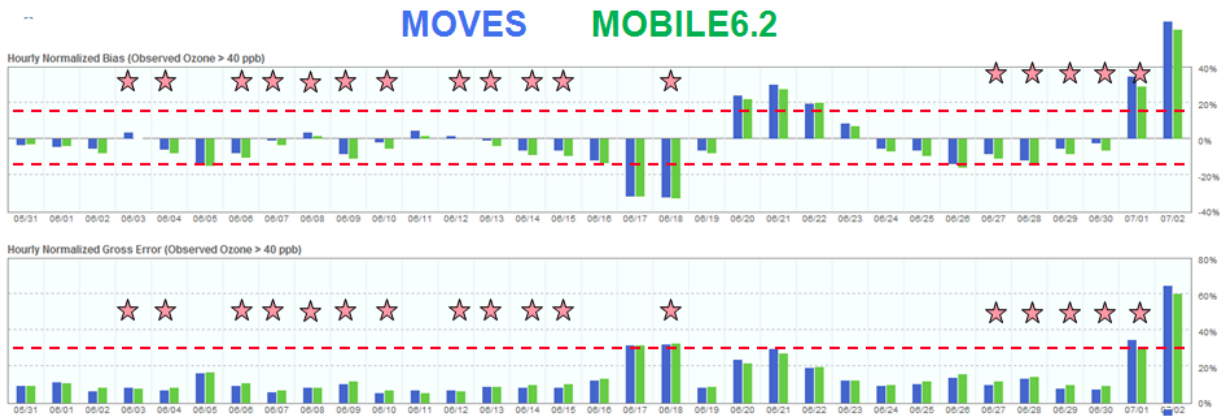

Figure 5-57: Daily MNB (top) and MNGE (bottom) Statistics for MOVES2010a and MOBILE6.2 Photochemical Model Runs

A monitor-by-monitor basis performance evaluation of the MNB and MNGE statistics is shown in Figure 5-58: *Soccer-Style Plot of Eight-Hour MNGE and MNB by Monitor with MOVES2010a and MOBILE6.2*. Each marked plotted is a monitor. The MOBILE6.2 run (green triangles) under predicts the eight-hour ozone concentrations as noted by the MNB (x-axis). While still under-predicting the eight-hour ozone concentrations, the MOVES2010a run (blue circles) has improved bias and gross error statistics. All monitors fall within the performance benchmarks using the MOVES2010a emissions while Eagle Mountain Lake's bias exceeds the -15% goal with MOBILE6.2.

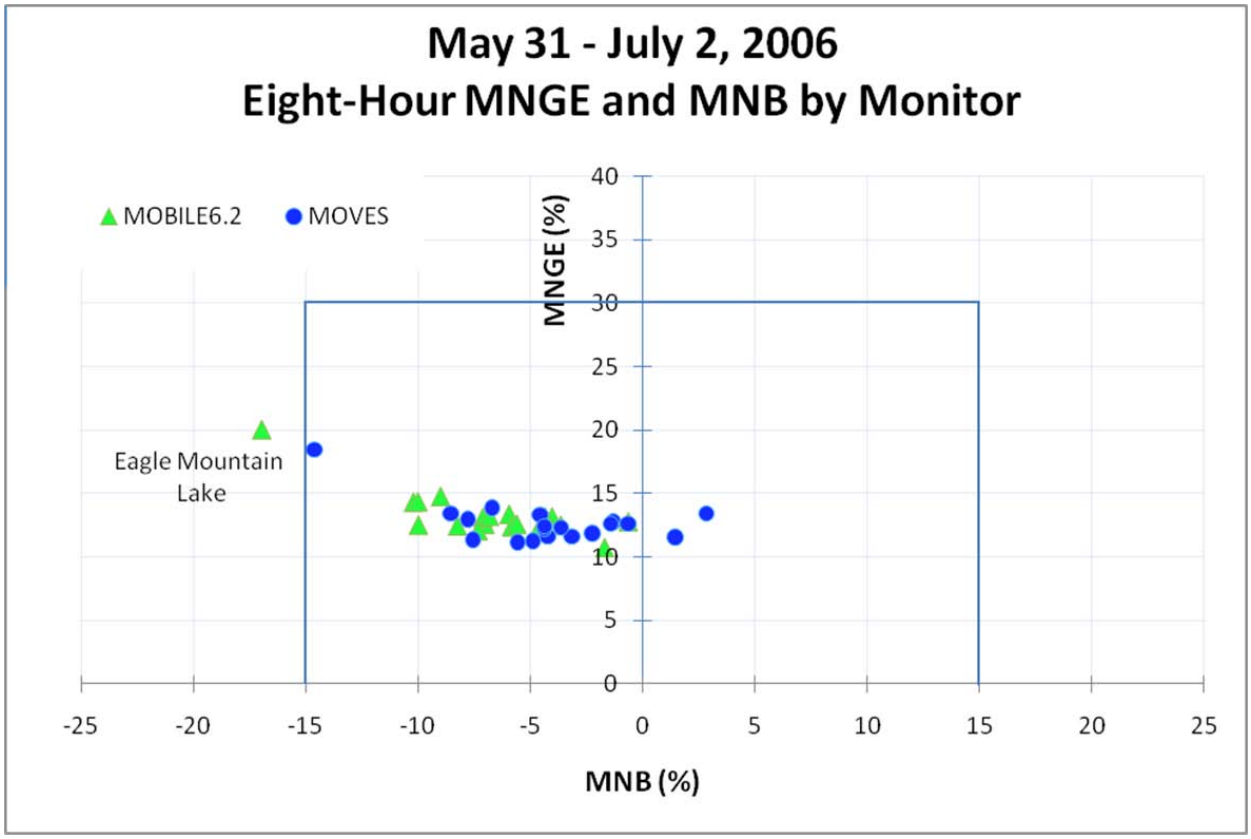

Figure 5-58: Soccer-Style Plot of Eight-Hour MNGE and MNB by Monitor with MOVES2010a and MOBILE6.2

The difference in mobile source NO_X emissions from MOBILE6.2 and MOVES2010a also impacted the future design values (DV_Fs). Compared to MOBILE6.2, the increase in mobile source emissions from MOVES2010a in the base and future resulted in higher future design values at all monitors as shown in Table 5-7: *2012 Future Design Values with MOBILE6.2 and MOVES2010a*. While all monitors are predicted to have a 2012 future design value less than 85 ppb with both models, using MOVES2010a increases the DV_Fs over one ppb at all but three DFW monitors.

Table 5-7: 2012 Future Design Values with MOBILE6.2 and MOVES2010a

Site	Monitor	2012 DV_F w/ MOBILE6.2 (ppb)	2012 DV_F w/ MOVES2010a (ppb)	DV_F Diff. (ppb)
DENT	Denton C56	75.37	77.03	1.66
EMTL	Eagle Mountain Lake C75	76.05	78.06	2.01
KELC	Keller C17	74.83	76.45	1.62
GRAP	Grapevine Fairway C70	74.67	76.17	1.50
FWMC	Fort Worth Northwest C13	73.78	75.36	1.58
FRIC	Frisco C31	72.93	74.45	1.52
WTFD	Weatherford Parker County C76	71.30	72.71	1.41
DALN	Dallas North C63	69.64	71.15	1.51
REDB	Dallas Exec Airport C402	69.40	70.58	1.18

Site	Monitor	2012 DV_F w/ MOBILE6.2 (ppb)	2012 DV_F w/ MOVES2010a (ppb)	DV_F Diff. (ppb)
CLEB	Cleburne C77	70.26	70.85	0.59
ARLA	Arlington C61	68.95	70.32	1.37
DHIC	Dallas Hinton C401	66.52	67.89	1.37
PIPT#	Pilot Point C1032#	65.97#	67.35#	1.38#
MDLT#	Midlothian Tower C94#	65.31#	66.63#	1.32#
RKWL	Rockwall Heath C69	62.47	63.27	0.80
MDLO#	Midlothian OFW C52#	61.09#	62.24#	1.15#
KAUF	Kaufman C71	59.27	60.42	1.15
GRAN*	Granbury C73*	68.18	69.66	1.48
GRVL*	Greenville C1006*	58.97	59.96	0.99

Pilot Point C1032, Midlothian Tower C94, and Midlothian OFW C52 did not measure enough data from 2004 through 2008 to calculate a complete baseline design value. A DV_B was calculated using all available data for the DV_Fs shown.

* Granbury C73 and Greenville C1006 are outside the 1997 eight-hour ozone NAAQS DFW nonattainment area.

Additional information on the difference between model runs using MOBILE6.2 or MOVES2010a on-road emissions can be found in Section 4.3.4: Episodic Model Performance Assessment.

5.5.1.5 Alternative Modeling Emissions: Cross State Air Pollution Rule Point Source (CSAPR) Emissions

The EPA's CSAPR reduces Electric Generating Unit (EGU) NO_X emissions from 27 states starting in 2012. This rule replaces the EPA's Clean Air Interstate Rule (CAIR). As Table 5-8: *CSAPR versus CAIR ARD NOX Emissions* shows, significant NO_X reductions are projected above the CAIR reductions in Texas, Texas' surrounding states (except Arkansas), and the rest of the eastern United States.

Table 5-8: CSAPR versus CAIR ARD NO_X Emissions

Area	2012 CSAPR NO_X (tpd)	2012 CAIR NO_X (tpd)	Difference (tpd)	Difference (%)
DFW	11.00	18.95	-7.95	-41.97%
Texas	331.32	401.41	-70.09	-17.46%
Arkansas	97.60	71.51	26.09	36.49%
Louisiana	87.15	106.08	-18.93	-17.85%
Oklahoma	138.95	247.44	-108.49	-43.84%
Other States	3680.83	4109.11	-428.28	-10.42%

A 2012 modeling sensitivity was completed using the CSAPR allocations for the entire country. In general, ozone concentrations in 2012 with CSAPR were lower than with CAIR. *Figure 5-59: June 29 Eight-Hour Ozone Max Difference Tile Plot Comparing CSAPR to CAIR* below shows the difference of the maximum eight-hour ozone concentrations on June 29 with the CSAPR versus the CAIR allocations. The blue colors represent ozone reductions while yellow through red represent ozone increases due to the CSAPR. Almost every grid cell had ozone reductions in

the 4 km DFW modeling domain on June 29 and similar results occurred for all days during the June 2006 episode.

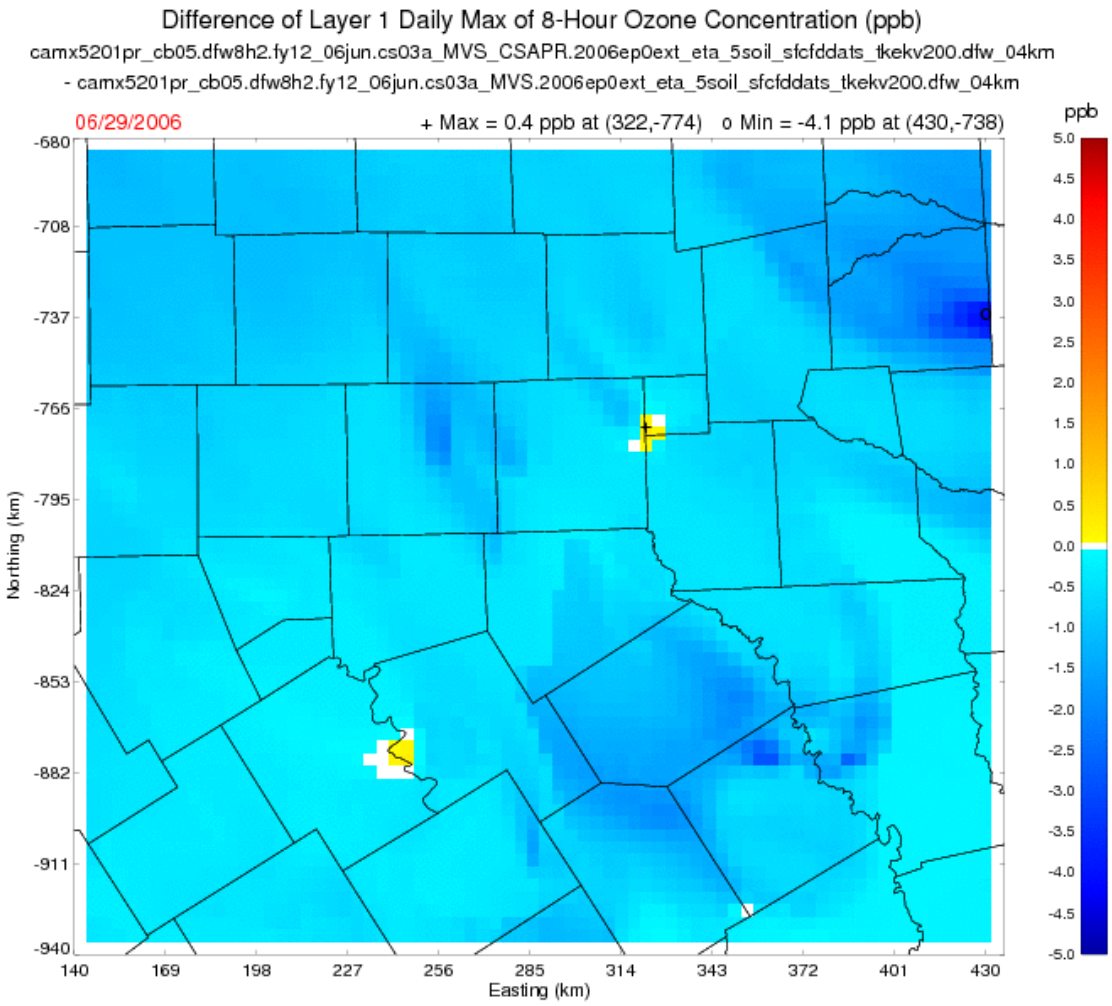

Figure 5-59: June 29 Eight-Hour Ozone Max Difference Tile Plot Comparing CSAPR to CAIR

By modeling the reduced NO_X emissions in DFW, Texas, and the eastern United States with the CSAPR instead of the CAIR allocations, the 2012 DFW ozone design values were also reduced. *Table 5-9: CSAPR versus CAIR 2012 Future Design Values* shows that every monitor's DV_F was reduced by modeling CSAPR compared to CAIR by at least 0.5 ppb.

Table 5-9: CSAPR versus CAIR 2012 Future Design Values

Monitor	2012 DVF w/ CAIR (ppb)	2012 DVF w/ CSAPR (ppb)	DVF Difference (ppb)
Denton C56	77.03	76.48	-0.55
Eagle Mountain Lake C75	78.06	77.12	-0.94
Keller C17	76.45	75.32	-1.13
Grapevine Fairway C70	76.17	75.55	-0.62

Monitor	2012 DVF w/ CAIR (ppb)	2012 DVF w/ CSAPR (ppb)	DVF Difference (ppb)
Fort Worth Northwest C13	75.36	74.29	-1.07
Frisco C31	74.45	73.82	-0.63
Weatherford Parker Co. C76	72.71	72.03	-0.68
Dallas North C63	71.15	70.55	-0.60
Dallas Exec Airport C402	70.58	69.80	-0.78
Cleburne C77	70.85	70.04	-0.81
Arlington C61	70.32	69.47	-0.85
Dallas Hinton C401	67.89	67.24	-0.65
Pilot Point C1032#	67.35#	66.73#	-0.62#
Midlothian Tower C94#	66.63#	65.92#	-0.71#
Rockwall Heath C69	63.27	62.74	-0.53
Midlothian OFW C52#	62.24#	61.57#	-0.67#
Kaufman C71	60.42	59.86	-0.56
Granbury C73*	69.66*	68.92*	-0.74*
Greenville C1006*	59.96*	59.23*	-0.73*

Pilot Point C1032, Midlothian Tower C94, and Midlothian OFW C52 did not measure enough data from 2004 through 2008 to calculate a complete baseline design value. A DV_B was calculated using all available data for the DV_Fs shown.

* Granbury C73 and Greenville C1006 are outside the 1997 eight-hour ozone NAAQS DFW nonattainment area.

The results of the CSAPR sensitivity complement the DFW SIP revision modeling with CAIR as both indicate the DFW area will attain the 1997 eight-hour ozone standard by June 2013. These results agree with the EPA's attainment assessment for DFW using their own modeling for the CSAPR rule (EPA, 2011).

5.5.2 Diagnostic Analyses

Diagnostic analyses were conducted to focus more specifically on the change in model-predicted ozone to changes in the ozone precursor emissions as compared to observed changes in ozone resulting from changes in emissions. The TCEQ conducted several diagnostic analyses, including retrospective modeling, observational modeling and source apportionment analysis.

5.5.2.1 Retrospective Modeling – 1999 Backcast

The purpose of this diagnostic analysis is to test the model in a forecast (in this case, backcast) mode, where the answer is known in advance. Retrospective modeling is usually difficult to implement in practice because of the need to create an inventory, but a 1999 inventory was already available. In this test, most of the 2006 baseline inventory was replaced with a base case inventory (a 1999 baseline inventory was preferred but not available) previously developed for the 1999 ozone episode used in prior SIP revisions. However, the episode day-specific biogenic emissions for the 2006 episode were not replaced, as is also the practice when modeling a future base emissions inventory. Similarly, the 2006 meteorology was used with the 1999 base case emissions as is the procedure when modeling with the future emissions. The 1999 and 2006 inventories used the MOBILE6.2 model for on-road emissions in this analysis as a 1999 MOVES-based on-road emission inventory was not developed.

Since the model predictions of a typical future design value is based on a DV_B, which is the average of three regulatory design values (EPA, 2007), the quantity forecast in this test is not a specific future year's design value but rather the average of three years. Thus, the regulatory design values for 1999, 2000, and 2001 were averaged in the same manner as the 2006 DV_B was calculated as the average of the 2006, 2007, and 2008 regulatory design values (Table 5-10: *1999 Baseline Design Values for Retrospective Analysis*). Only monitors that had at least one regulatory design value in both the 1999 through 2001 and the 2006 through 2008 periods were used. Many monitors have been added to the DFW area since 1999, which are noted by the missing 1999 baseline design values in Table 5-10.

Table 5-10: 1999 Baseline Design Values for Retrospective Analysis

Site	Monitor	1999 Baseline Design Value (ppb)
DENT	Denton C56	101.50
EMTL	Eagle Mountain Lake C75	-
KELC	Keller C17	96.33
GRAP	Grapevine Fairway C70	-
FWMC	Fort Worth Northwest C13	98.33
FRIC	Frisco C31	100.33
WTFD	Weatherford Parker County C76	-
DALN	Dallas North C63	93.00
REDB	Dallas Exec Airport C402	88.00
CLEB	Cleburne C77	-
ARLA	Arlington C61	-
DHIC	Dallas Hinton C401	92.00
PIPT	Pilot Point C1032	-
MDLT	Midlothian Tower C94	92.33
RKWL	Rockwall Heath C69	-
MDLO	Midlothian OFW C52	-
KAUF	Kaufman C71	-
GRAN	Granbury C73	-
GRVL	Greenville C1006	-

Once the model was run with the 1999 baseline emissions, RRFs were calculated. In a retrospective analysis, most of the RRFs are expected to be greater than 1 because ozone has decreased since the retrospective year. Table 5-11: *1999 Projected DVs Compared with Calculated DVs* shows the calculated RRFs and the respective projected 1999 design values.

Table 5-11: 1999 Projected DVs Compared with Calculated DVs

Site	Monitor	1999 Baseline Design Value (ppb)	1999 Modeled Average (ppb)	2006 to 1999 RRF	1999 Projected Design Value (ppb)
DENT	Denton C56	101.50	96.48	1.161	108.37
EMTL	Eagle Mountain Lake C75		96.56	1.141	106.53
KELC	Keller C17	96.33	97.59	1.147	104.42
GRAP	Grapevine Fairway C70		96.79	1.121	101.67
FWMC	Fort Worth Northwest C13	98.33	95.88	1.127	100.69
FRIC	Frisco C31	100.33	92.51	1.131	99.16
WTFD	Weatherford Parker County C76		89.11	1.127	98.78
DALN	Dallas North C63	93.00	89.53	1.128	95.91
REDB	Dallas Exec Airport C402	88.00	89.68	1.142	97.05
CLEB	Cleburne C77		87.75	1.137	96.65
ARLA	Arlington C61		93.31	1.126	93.86
DHIC	Dallas Hinton C401	92.00	89.01	1.127	92.04
PIPT	Pilot Point C1032		95.01	1.170	94.78
MDLT	Midlothian Tower C94	92.33	88.00	1.146	92.29
RKWL	Rockwall Heath C69		82.22	1.137	88.34
MDLO	Midlothian OFW C52		90.12	1.145	85.87
KAUF	Kaufman C71		81.56	1.184	88.45
GRAN	Granbury C73		88.45	1.130	93.80
GRVL	Greenville C1006		80.43	1.161	87.05

For five of the eight sites, the projections were within 3 ppb of the 1999 calculated baseline values. For the other three sites with 1999 DV_Bs, the model-projected 1999 DVs were higher than the calculated values, indicating that the model responded more to emission changes than the actual airshed for these sites. The overall modeled response was close to the actual airshed's response to 1999-2006 emission changes, though the model's response at a few of the monitors was stronger than the airshed.

5.5.2.2 Observational Modeling – Weekday/Weekend

Weekend emissions of NO_X in urban areas tend to be lower than weekday emissions because of fewer vehicle miles driven. The effect is most pronounced on weekend mornings, especially Sundays, since commuting is much lower than weekdays. Figure 5-60: *Comparison of modeled 6 AM NOX and VOC emissions for Wednesdays, Saturdays, and Sundays* shows a comparison of modeled 6 AM NO_X and VOC emissions for Wednesdays, Saturdays, and Sundays. Early morning emissions tend to be especially important in determining peak eight-hour ozone levels (McDonald, 2010), so the weekday-weekend differences should manifest themselves noticeably in the relative levels of weekday and weekend ozone concentrations. Because there are relatively few Saturdays, Sundays, and Wednesdays (chosen to represent typical weekdays) in the episode, the TCEQ employed a novel approach which allowed each day of the episode to be treated as a Saturday, Sunday, and Wednesday, providing a total of 33 of each day type. This approach is possible since meteorology is independent of day-of-week, so replacing the emissions of any episode day with Saturday (or Sunday or Wednesday) emissions creates an appropriate representation of that day. The modeling procedure involved a series of runs using the 2006

baseline, designed to ensure that each day-type was preceded by the appropriate predecessor day-type, i.e., each Sunday was modeled following a Saturday, each Saturday followed a Friday, and each Wednesday followed a Wednesday (baseline modeled Tuesday emissions are very similar to Wednesdays).

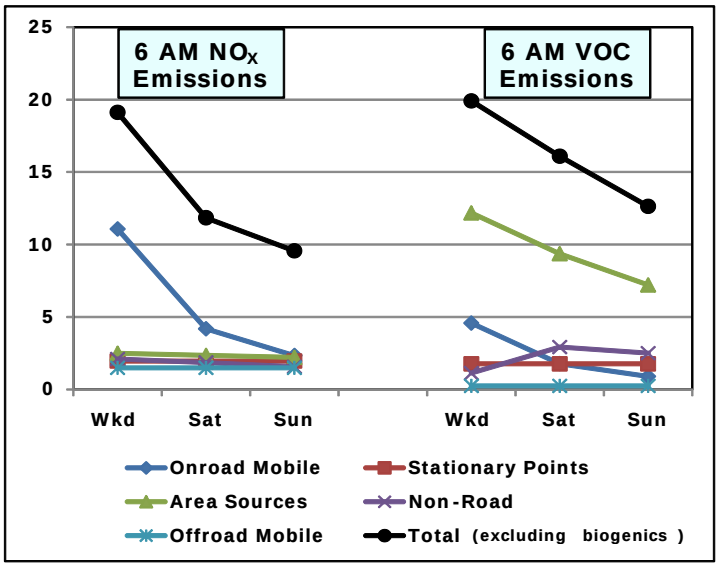

Figure 5-60: Comparison of modeled 6 AM NO_X and VOC emissions for Wednesdays, Saturdays, and Sundays

For comparison with the modeled emissions, median monitored 6:00 AM NO_X concentrations were calculated for every Wednesday, Saturday, and Sunday between May 15 through October 15 in the years 2005 through 2009, which gives around 125 observations for each type of day (less for some monitors because of missing data). Figure 5-61: *Mean Observed NOX Concentrations at DFW Monitors as a Percentage of Wednesday Mean Values, May 15 through October 15, 2005 through 2009* shows observed and modeled 6 AM NO_X concentrations at 11 sites in the DFW area. All sites show observed and modeled NO_X concentrations that decline monotonically from Wednesday through Saturday to Sunday, except for the Midlothian observations which show essentially no change from Saturday to Sunday. The modeled values have somewhat greater variability than their observed counterparts, with all sites showing declines between 30% and 70% from Wednesday to Sunday, while all the observed sites dropped by between 40% and 70%.

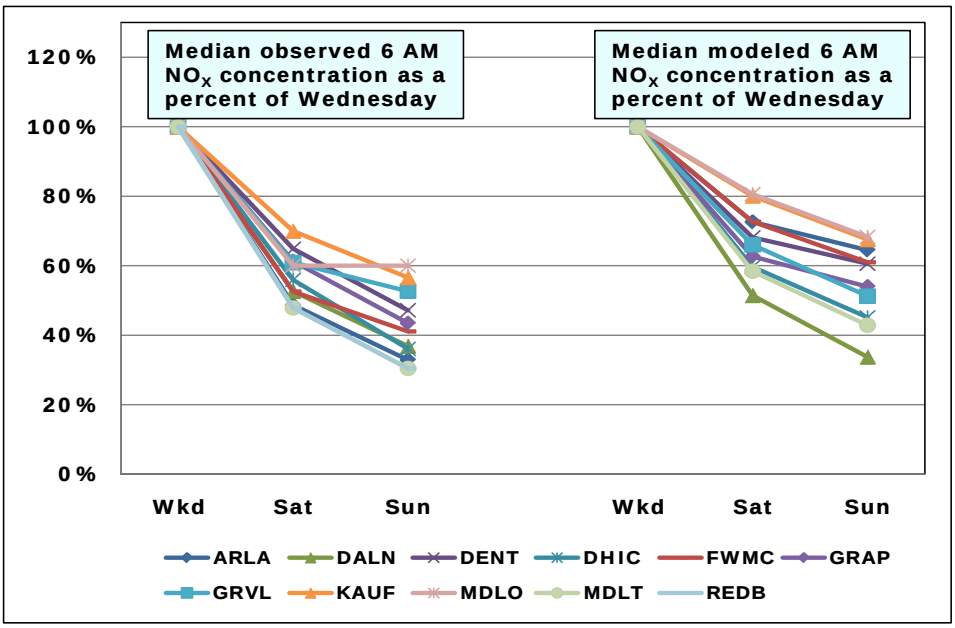

Figure 5-61: Mean Observed NO_X Concentrations at DFW Monitors as a Percentage of Wednesday Mean Values, May 15 through October 15, 2005 through 2009

Figure 5-62: *Observed and Modeled Daily Peak Eight-Hour Ozone Concentrations as a Percentage of Wednesdays* shows observed and modeled median daily peak eight-hour ozone concentrations as a percentage of Wednesdays for 19 DFW-area sites. The observed Saturday ozone concentrations (as a percent of Wednesday) are spread between a 10% increase and a 7% decrease, with more sites increasing than decreasing. Sunday concentrations ranged between a 2% increase and a 16% decrease from Wednesday, with all but three sites showing a decrease. The modeled values consistently decreased between 2% and 4% on Saturday and between 4% and 7% on Sunday (compared with Wednesday), and showed very little spread compared with the observations.

Part of the apparent discrepancy between the observed and modeled concentrations can be attributed to the comparison of observations from the entire ozone season with a modeled episode which was selected specifically to represent a period of especially high ozone concentrations. When the median observed concentrations are replaced with 90th percentile concentrations (representing high ozone days), the behavior of the observed and modeled concentrations is more consistent as seen in Figure 5-63: *Observed 90th Percentile and Median Modeled Daily Peak Eight-Hour Ozone Concentrations as a Percentage of Wednesdays*. The observed 90th percentile concentrations range between a 4% increase and an 11% decrease on Saturday (compared with Wednesday), while on Sunday, all sites decrease from Wednesday, between 2% and 18%. The model is successfully replicating the observed weekday-weekend trends, especially for the higher ozone days.

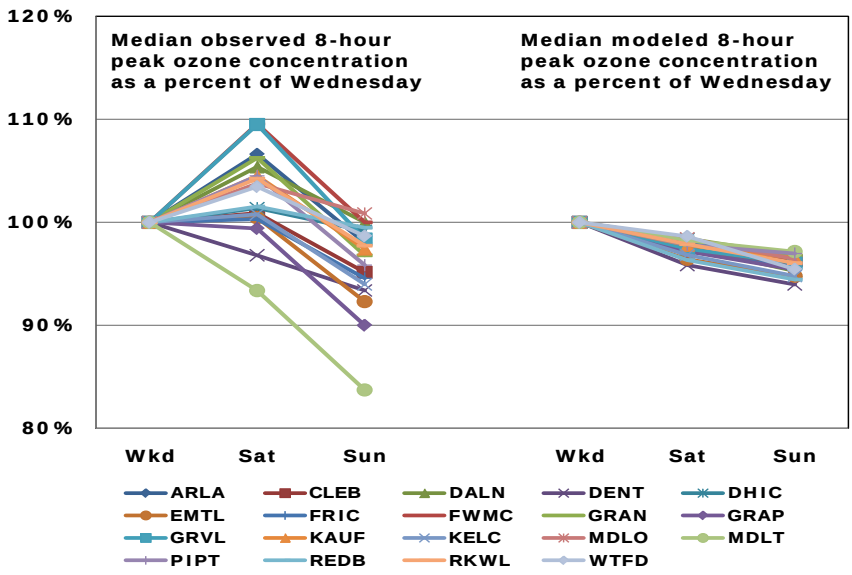

Figure 5-62: Observed and Modeled Daily Peak Eight-Hour Ozone Concentrations as a Percentage of Wednesdays

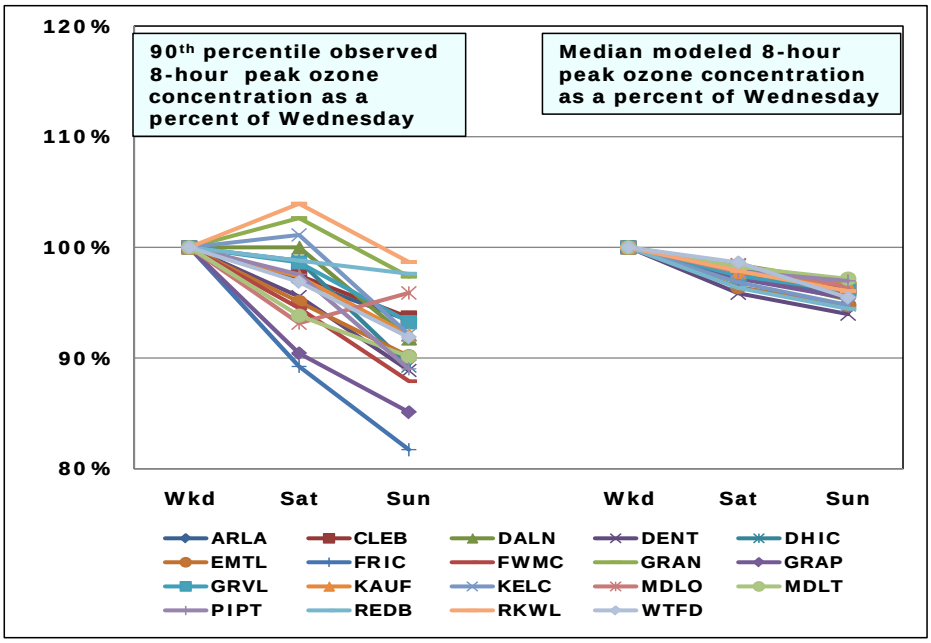

Figure 5-63: Observed 90th Percentile and Median Modeled Daily Peak Eight-Hour Ozone Concentrations as a Percentage of Wednesdays

Finally, the modeled concentrations exhibit very little site-to-site variability compared to the observations. This is because the modeling procedure applied Wednesday, Saturday, and Sunday emissions to exactly the same set of days. The day-to-day and site-to-site meteorological variability, which clearly affects the observed concentrations, is absent in the modeled concentrations. This modeling technique isolated the model response to weekday-weekend emission changes from the meteorological variability, allowing a clean assessment of the model's response to the emission variability.

5.5.2.3 Anthropogenic Precursor Culpability Assessment (APCA)

APCA keeps track of the origin of the NO_X and VOC precursors creating the ozone during the model run, which can then be apportioned to specific user-defined sources groups and regions. APCA recognizes that the biogenics source category is not controllable, unlike the ozone source apportionment tool (OSAT). Where OSAT would apportion ozone production to biogenic emissions, APCA reallocates that ozone production to the controllable or anthropogenic emissions that combined with the biogenic emissions to create ozone. Only ozone created from both biogenic NO_X and VOC precursors is apportioned to the biogenic emission source group by APCA.

5.5.2.3.1 APCA Set-up

The results of the June 2006 baseline (bl06_reg2) and 2012 future case (fy12_cs03) modeling runs were analyzed using APCA for the Eagle Mountain Lake (EMTL, CAMS 56) and Denton (DENT, CAMS 75) monitors. Figure 5-64: *APCA Emission Source Regions* exhibits the geographic regions used in the APCA analysis, and Table 5-12: *APCA Emission Source Categories* lists the emission categories and their respective abbreviations.

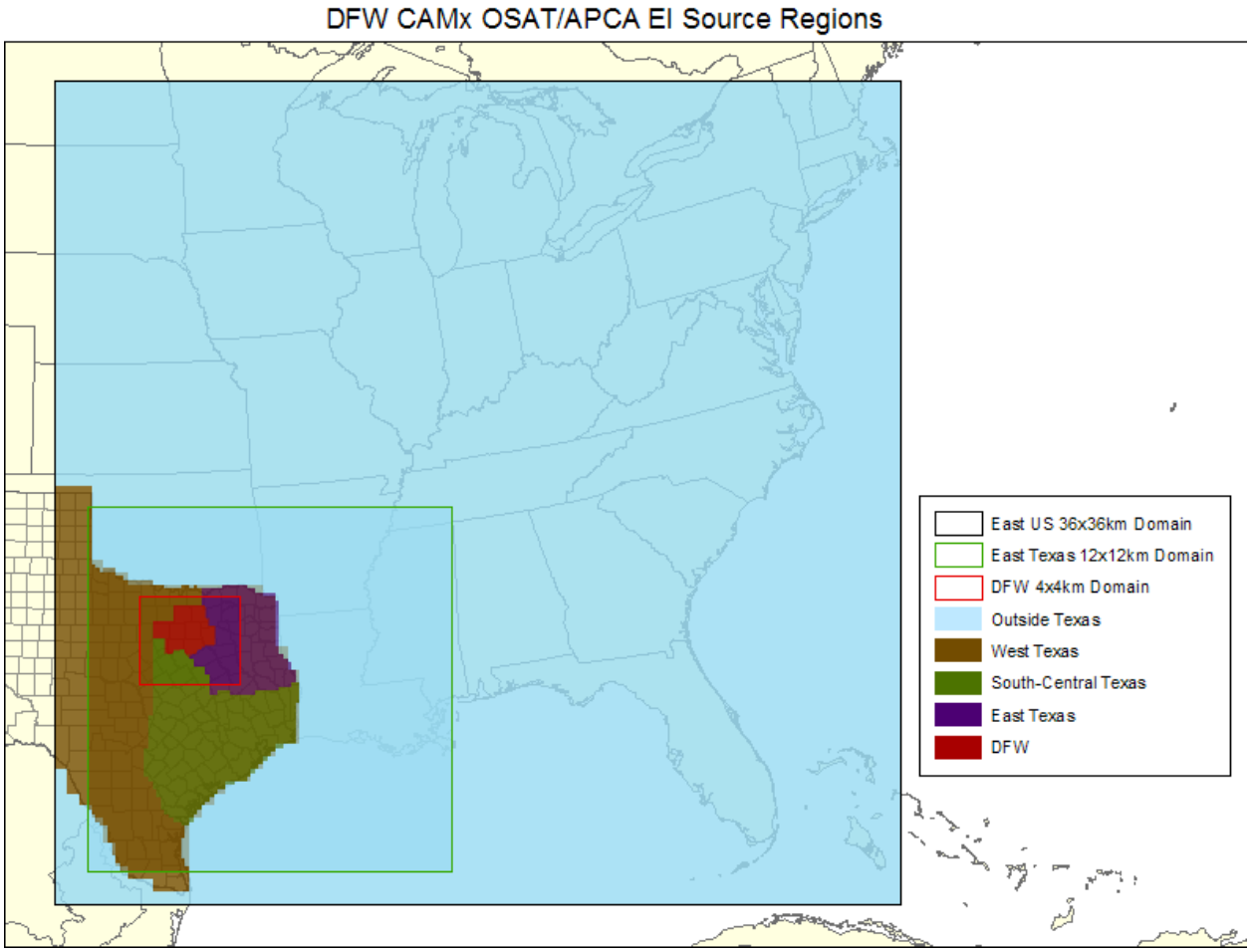

Figure 5-64: APCA Emission Source Regions

The EMTL and DENT monitors were selected for analysis because they have the highest projected 2012 future design values at 76.0 ppb and 75.4 ppb, respectively. In addition, several of the 2006 baseline modeled days, with high maximum daily eight-hour average concentrations

used in calculating the RRF, were common to both monitors. For this analysis, the daily eight-hour average ozone concentration for the period from 1000 hours to 1700 hours (CST) was used. This eight-hour period is typically the period of the maximum eight-hour average ozone concentration.

Of particular interest are the changes in the contribution to the maximum daily eight-hour average ozone concentration (i.e., culpability) between the 2006 baseline and 2012 future modeling from the emission source categories and regions. The source category and region contribution to the change in ozone can also be evaluated. These differences in the contribution to the maximum daily eight-hour average ozone concentration between 2006 and 2012 reflect the culpability of the various emission source categories and regions to the modeled reduction in the maximum daily eight-hour average ozone concentration.

Table 5-12: APCA Emission Source Categories

Figure Legend Abbreviation	Description of Source Group and Region
IC	Initial Conditions
TOPBC	Top Boundary Condition
WSTBC	West Boundary Condition
ESTBC	East Boundary Condition
STHBC	South Boundary Condition
NTHBC	North Boundary Condition
Biogenics	Biogenic emissions
EI Points	Elevated point source emissions
On-Road	On-road mobile sources
Non-Road	Non/Off-Road mobile sources
Area-nO&G	Area sources excluding oil and gas sources
O&G_All	Oil and Gas production and drilling sources
Other(low pts)	Other sources including low-level point sources

5.5.2.3.2 APCA Evaluation

Table 5-13: *Daily Maximum Eight-Hour Ozone (ppb) for Common Modeled Days at the EMTL and DENT monitors* lists the 2006 baseline (bl06reg2_MOVES) and 2012 future (fy12cs03_MOVES) maximum daily eight-hour ozone concentrations for the ten modeled days used in the calculation of the respective RRFs that were common to both the EMTL and DENT monitors.

Table 5-13: Daily Maximum Eight-Hour Ozone (ppb) for Common Modeled Days at the EMTL and DENT monitors

Date	EMTL 2006	EMTL 2012	DENT 2006	DENT 2012
June 9, 2006	86.91	76.36	93.25	79.40
June 12, 2006	97.17	86.91	79.75	71.52
June 14, 2006	90.94	76.34	79.48	65.87
June 15, 2006	76.14	61.13	85.09	66.97
June 30, 2006	80.56	63.24	90.08	72.49
July 1, 2006	85.18	67.48	88.21	68.48

Figure 5-65: *APCA 2006 and 2012 for DENT June 9* and Figure 5-66: *APCA 2006 and 2012 for EMTL June 9* show the APCA contributions to the average eight-hour ozone concentration (1000 to 1700 hours CST and 1100 to 1800 hours CST, respectively) for the 2006 baseline (left-hand side) and 2012 future year (right-hand side) modeling. Noteworthy in both of these figures is the contribution to the eight-hour average ozone concentration from the west and north boundary conditions (i.e., WSTBC and NTHBC), which combined is greater than 15 ppb. Also notable is the contribution to the eight-hour ozone concentration from the oil and gas emission source category (O&G_All) from the DFW source region at the EMTL monitor, while the O&G_All source category from the DFW source region contributes less at the DENT monitor. Notable at the DENT monitor is the large contribution to the eight-hour average ozone concentration from the on-road mobile source category (On-Road) in the DFW source region (i.e., approximately 25 ppb in 2006 and 20 ppb in 2012).

2006 and 2012 APCA DENT (CAMS 56) June 9

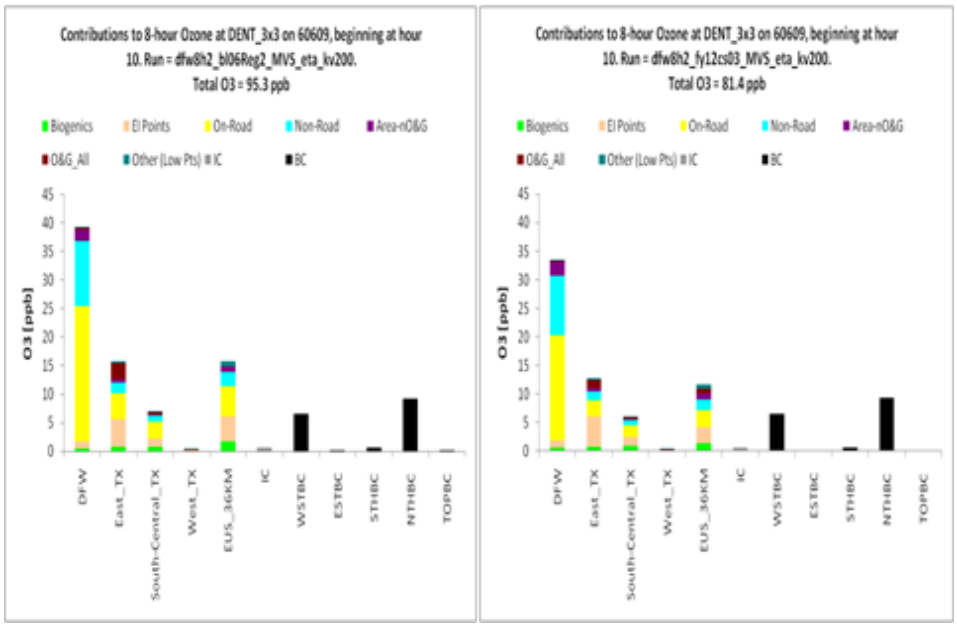

Figure 5-65: APCA 2006 and 2012 for DENT June 9

2006 and 2012 APCA EMTL (CAMS 75) June 9

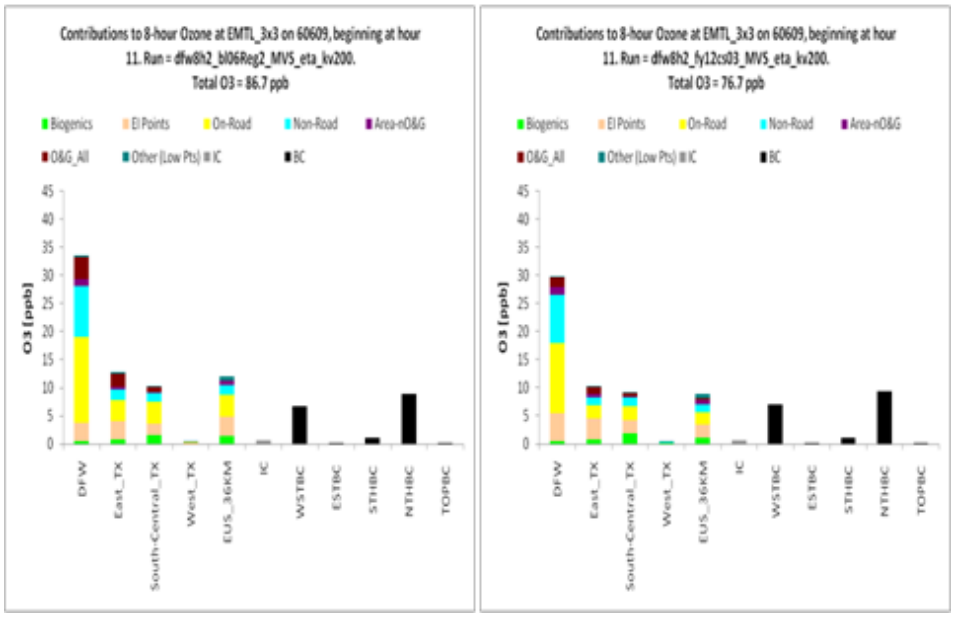

Figure 5-66: APCA 2006 and 2012 for EMTL June 9

Figure 5-67: *APCA Difference between 2006 and 2012 at DENT and EMTL June 9* shows the difference in the APCA contributions from non IC and BC source categories and regions to the reduction in the eight-hour average ozone (1000 to 1700 hours CST and 1100 to 1800 hours CST, respectively) between the 2006 baseline and 2012 future year modeling on June 9, for the DENT (left-hand side) and EMTL (right-hand side) monitors. For both of these monitors the modeling projects an eight-hour ozone concentration reduction of more than 10 ppb (i.e., 14.09 ppb for DENT and 10.60 ppb for EMTL). At both of these monitors, eight-hour average ozone concentration reductions from source categories in the DFW source region provide the majority of the eight-hour average ozone concentration reduction, especially the On-Road category, but also the O&G_All category at EMTL. At EMTL, there is a projected increase in the eight-hour average ozone concentration in the DFW source region contributed from the El Points source category, which is almost equal to the reduction from the O&G_All category. This projected increase is likely due to modeling 2012 with the CAIR NO_X emission allocations for electrical generating utilities (EGUs), which are larger than the 2006 reported EGU NO_X emissions. A slight increase in eight-hour ozone contributed was estimated from the O&G_All source category from the non Texas source region (EUS_36KM).

2006 to 2012 8-Hour Ozone Reduction DENT and EMTL by Source Category and Source Region for June 9

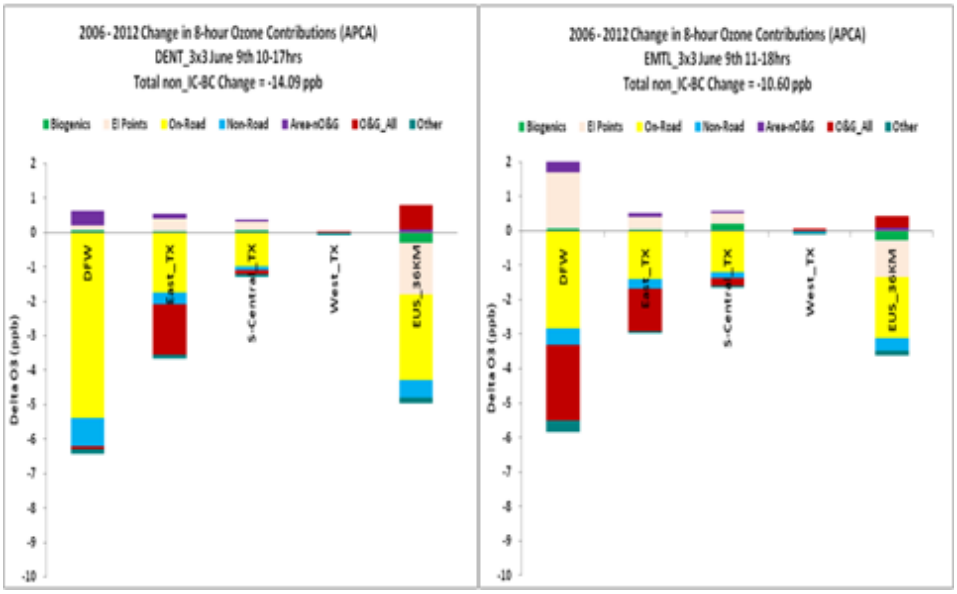

Figure 5-67: APCA Difference between 2006 and 2012 at DENT and EMTL June 9

June 12 was also a day used in the RRF calculation for both the DENT and EMTL monitors. Figure 5-68: APCA 2006 and 2012 for DENT June 12 and Figure 5-69: APCA 2006 and 2012 for EMTL June 12 show the APCA contributions to the eight-hour average ozone concentration (1100 to 1800 hours CST and 1200 to 1900 hours CST, respectively) for both the 2006 baseline (left-hand side) and 2012 future year (right-hand side) modeling. Noteworthy in both of these figures is the contribution to the eight-hour average ozone concentration from the west, south and north boundary conditions (i.e., WSTBC, STHBC and NTHBC), which combined is almost 20 ppb. Also noteworthy and distinctly different from June 9 is the relatively minimal contribution to the eight-hour average ozone concentration from all source categories in the East Texas (East_Tx) source region. This feature is consistent in both the 2006 baseline and 2012 future modeling results, as well at both the EMTL and DENT monitors.

2006 and 2012 APCA DENT (CAMS 56) June 12

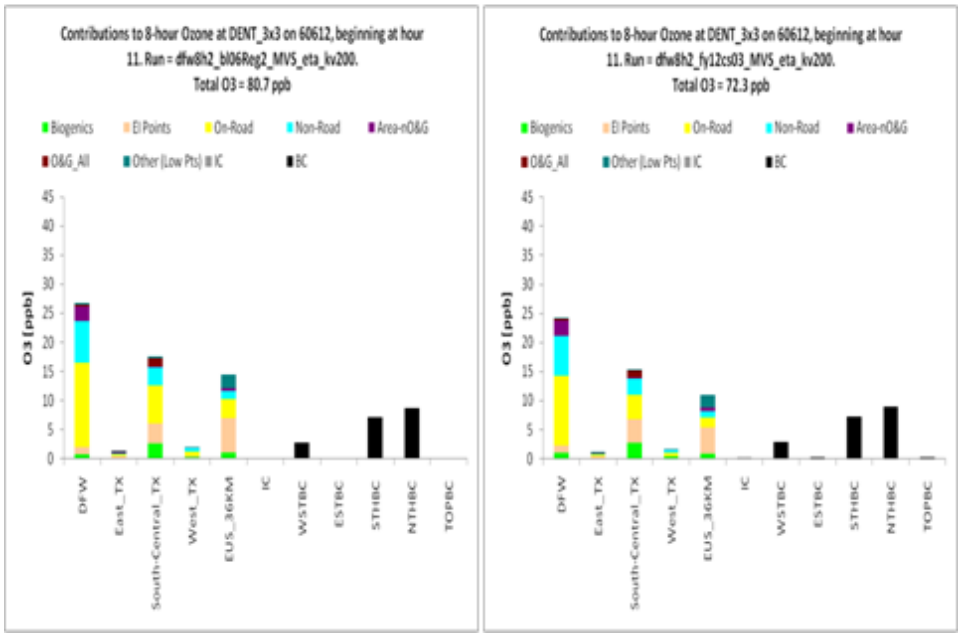

Figure 5-68: APCA 2006 and 2012 for DENT June 12

2006 and 2012 APCA EMTL (CAMS 75) June 12

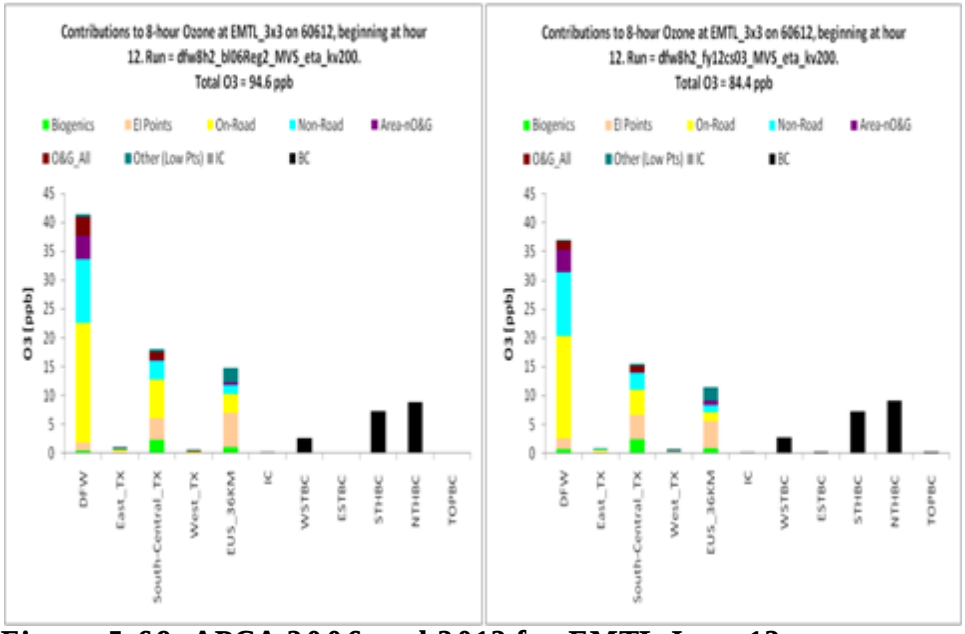

Figure 5-69: APCA 2006 and 2012 for EMTL June 12

Figure 5-70: *APCA Difference between 2006 and 2012 at DENT and EMTL June 12* shows the difference in the APCA contributions from non IC and BC source categories and regions to the eight-hour average ozone (1100 to 1800 hours CST and 1200 to 1900 hours CST, respectively) between the 2006 baseline and 2012 future year modeling on June 12 for the DENT (left-hand side) and EMTL (right-hand side) monitors. For both these monitors the modeling projects an

eight-hour average ozone concentration reduction of approximately 10 ppb (i.e., 8.97 ppb for DENT and 10.49 ppb for EMTL). Notable on this particular episode day at EMTL is the reduction from the O&G_All source category in the DFW region. Similar to June 9, there is a projected increase in the eight-hour average ozone concentration contributed from the El Points source category from the South-Central Texas (S-Central_TX) region at both DENT and EMTL, and more so from the DFW region at EMTL which is likely due to the 2006 reported EGU NO_X emissions in Texas being less than the 2012 CAIR NO_X emission allocations.

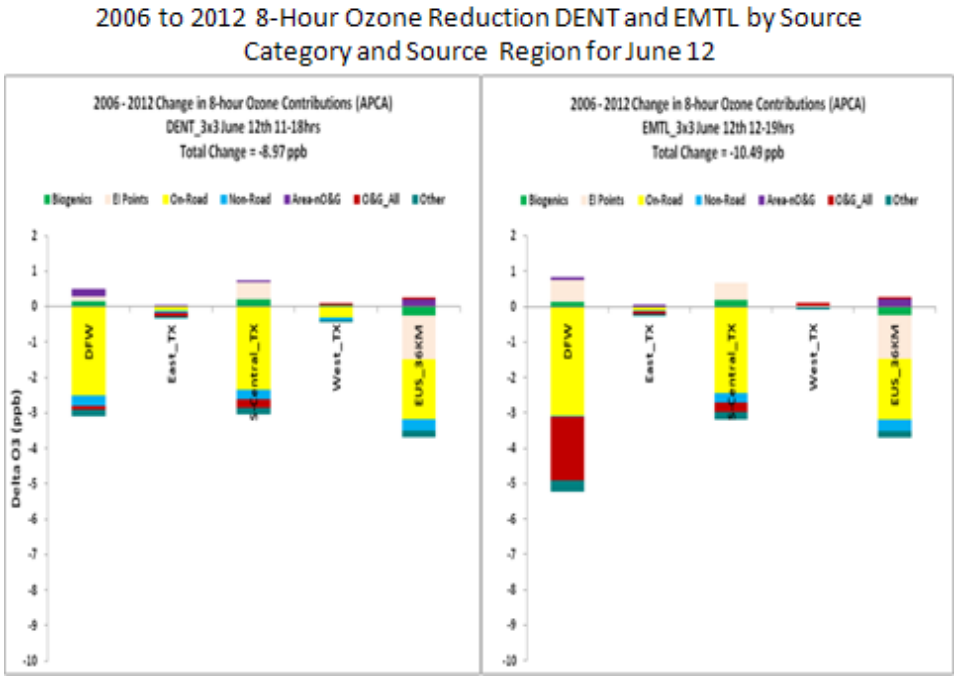

Figure 5-70: APCA Difference between 2006 and 2012 at DENT and EMTL June 12

June 14 was also a day used in the RRF calculation for both the DENT and EMTL monitors. Figure 5-71: APCA 2006 and 2012 for DENT June 14 and Figure 5-72: APCA 2006 and 2012 for EMTL June 14 show the APCA contributions to the eight-hour average ozone concentration (1000 to 1700 hours CST at both monitors) for both the 2006 baseline (left-hand side) and 2012 future year (right-hand side) modeling. Somewhat similar to June 9, the contribution to the eight-hour average ozone from the WSTBC and NTHBC is noteworthy, especially from the NTHBC (approximately 20 ppb) at both the DENT and EMTL monitors. Also noteworthy and distinctly different from June 9 and June 12 is the minimal contributions to the eight-hour average ozone concentration from all source categories in the Texas non DFW source regions. This feature is prominent at both monitors in the 2006 baseline and 2012 future modeling results.

2006 and 2012 APCA DENT (CAMS 56) June 14

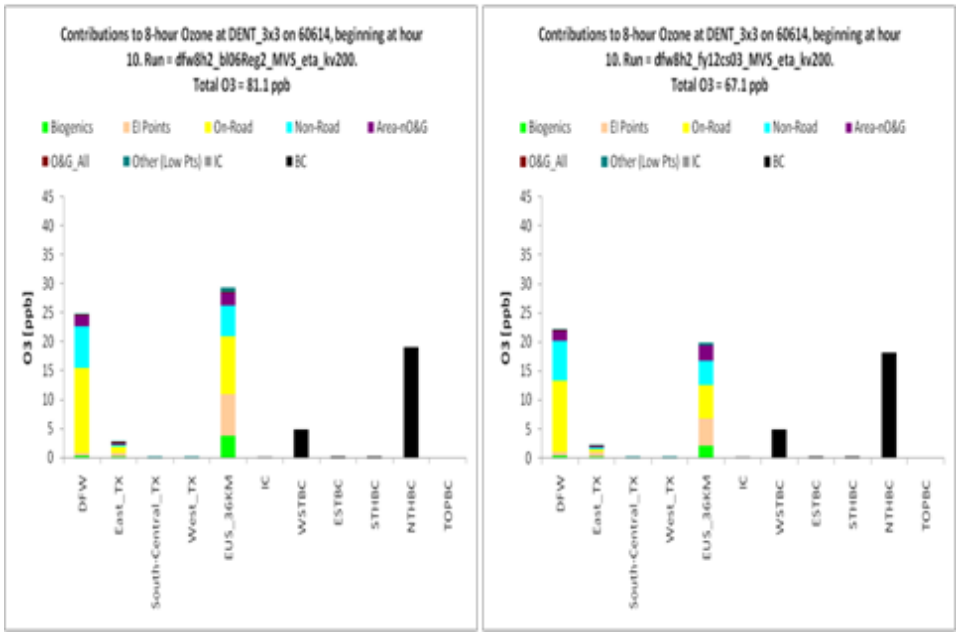

Figure 5-71: APCA 2006 and 2012 for DENT June 14

2006 and 2012 APCA EMTL (CAMS 75) June 14

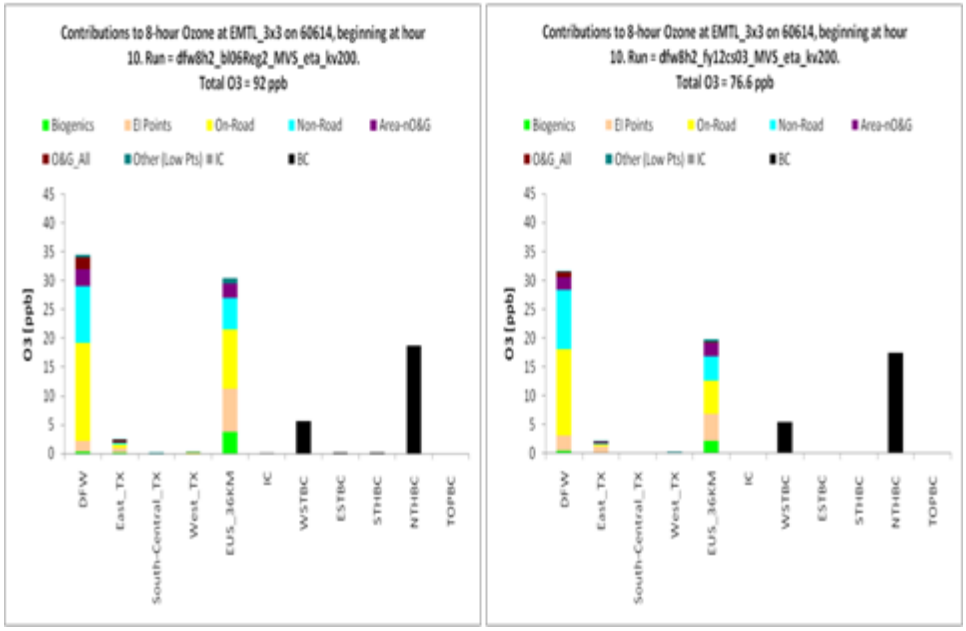

Figure 5-72: APCA 2006 and 2012 for EMTL June 14

Figure 5-73: *APCA Difference between 2006 and 2012 at DENT and EMTL June 14* shows the difference in the APCA contributions from non IC and BC source categories and regions to the eight-hour average ozone (1000 to 1700 hours CST) between the 2006 baseline and 2012 future year modeling on June 14 for the DENT (left-hand side) and EMTL (right-hand side) monitors. For both these monitors the modeling projects an eight-hour average ozone concentration

reduction of more than 10 ppb (i.e., 12.90 ppb for DENT and 14.08 ppb for EMTL). On this particular episode day, approximately 10 ppb of the net reduction in the eight-hour average ozone concentration at both the DENT and EMTL monitors is associated with source categories in the EUS_36KM source region.

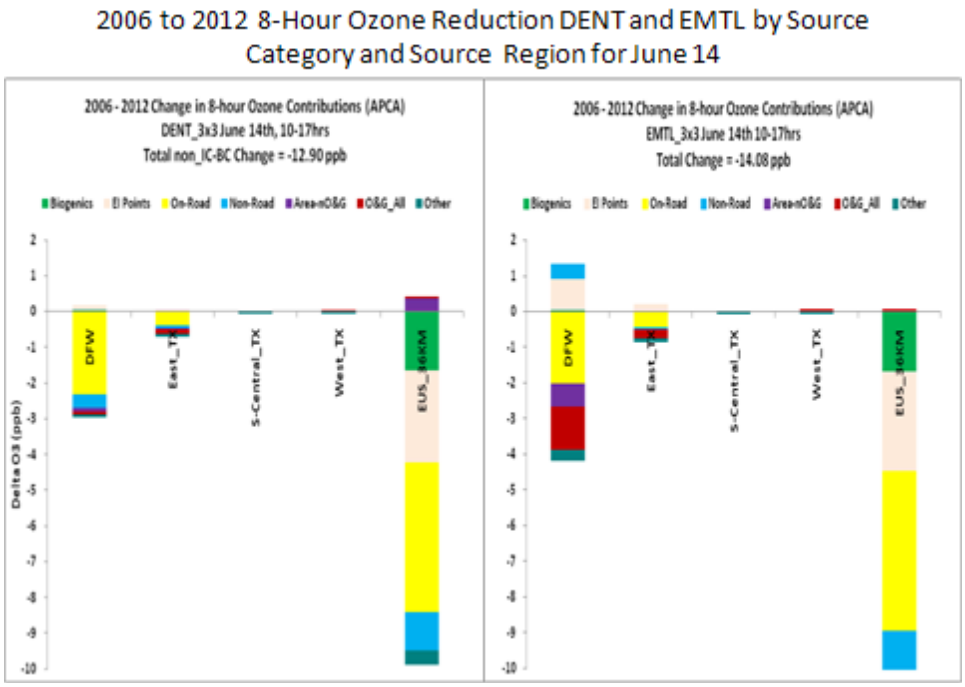

Figure 5-73: APCA Difference between 2006 and 2012 at DENT and EMTL June 14

June 15 was also a day used in the RRF calculation for both the EMTL and DENT monitors. Figure 5-74: APCA 2006 and 2012 for DENT June 15 and Figure 5-75: APCA 2006 and 2012 for EMTL June 15 show the APCA contributions to the eight-hour average ozone concentration (1000 to 1700 hours CST and 0900 to 1600 hours CST, respectively) for both the 2006 baseline (left-hand side) and 2012 future year (right-hand side) modeling. Similar to June 9, the combined contribution to the eight-hour average ozone from the WSTBC and NTHBC is noteworthy, being greater than 15 ppb at both the DENT and EMTL monitors. Also noteworthy and somewhat similar to June 14 is the relatively large contribution to the eight-hour average ozone concentration from all source categories, especially El Points and On-Road, in the non Texas (EUS_36KM) source region. This feature is prominent in both the 2006 baseline and 2012 future modeling results at both the DENT and EMTL monitors. A contrasting feature between the DENT and EMTL monitors is the contribution to the eight-hour average ozone concentration from all source categories in the East_TX region, being minimal at the EMTL monitor in both the 2006 baseline and 2012 future modeling results.

2006 and 2012 APCA DENT (CAMS 56) June 15

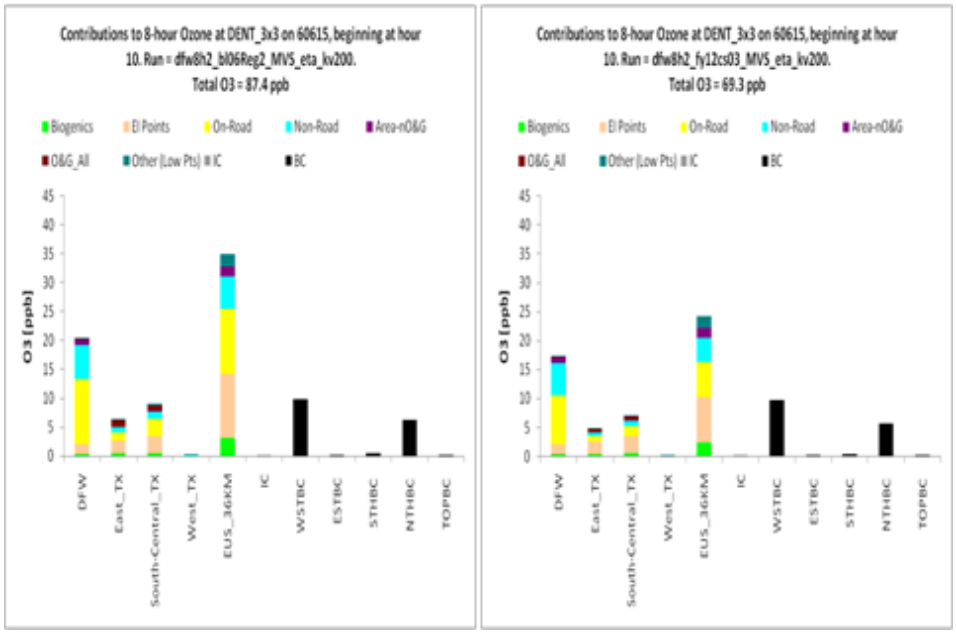

Figure 5-74: APCA 2006 and 2012 for DENT June 15

2006 and 2012 APCA EMTL (CAMS 75) June 15

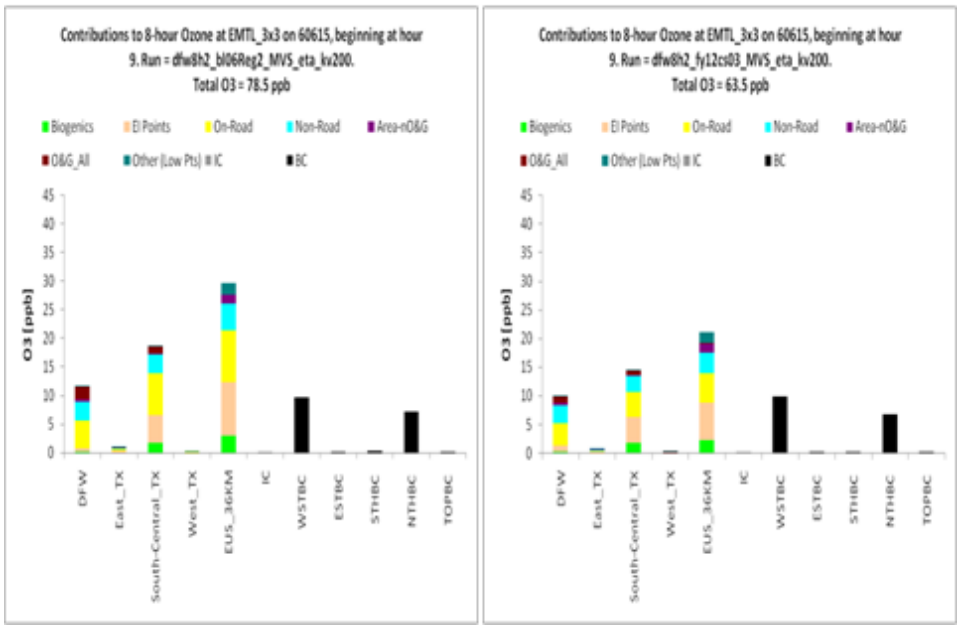

Figure 5-75: APCA 2006 and 2012 for EMTL June 15

Figure 5-76: *APCA Difference between 2006 and 2012 at DENT and EMTL June 15* shows the difference in the APCA contributions from non IC and BC source categories and regions to the eight-hour average ozone (1000 to 1700 hours CST and 0900 to 1600 hours CST, respectively) between the 2006 baseline and 2012 future year modeling on June 15 for the DENT (left-hand side) and EMTL (right-hand side) monitors. Somewhat similar to June 14, the modeling results

for June 15 indicate that at least half of the net reduction in the eight-hour average ozone concentration at both the DENT (17.59 ppb) and EMTL (14.85 ppb) monitors is associated with source categories in the EUS_36KM source region. In addition, the reduction in the eight-hour average ozone concentration from all the source categories in the DFW source region is no greater than the reduction from all source categories in the other regions of Texas at both the DENT and EMTL monitors.

2006 to 2012 8-Hour Ozone Reduction DENT and EMTL by Source Category and Source Region for June 15

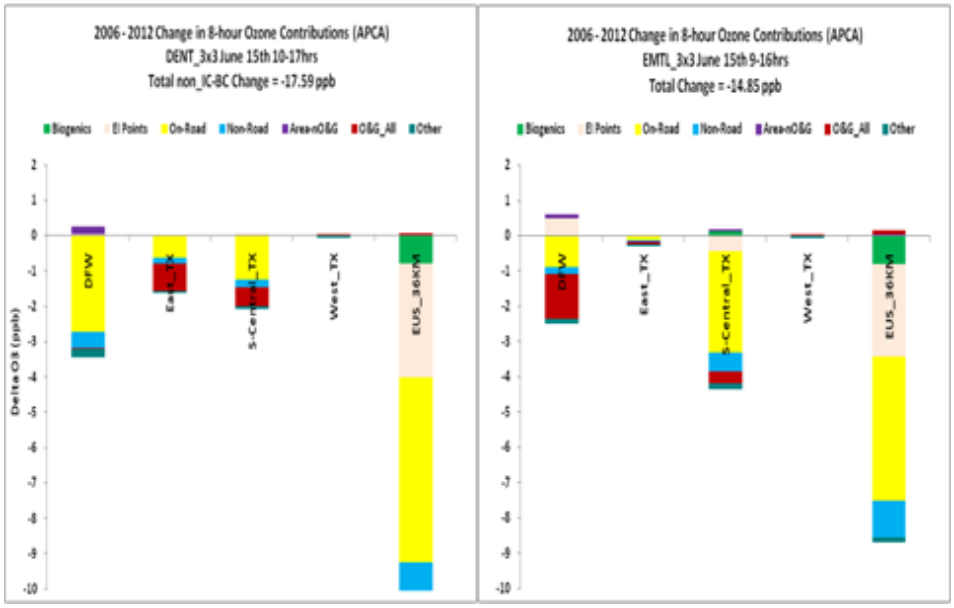

Figure 5-76: APCA Difference between 2006 and 2012 at DENT and EMTL June 15

June 30 was another day used in the RRF calculation for both the DENT and EMTL monitors. Figure 5-77: *APCA 2006 and 2012 for DENT June 30* and Figure 5-78: *APCA 2006 and 2012 for EMTL June 30* show the APCA contributions to the eight-hour average ozone concentration (1000 to 1700 hours CST at both monitors) for both the 2006 baseline (left-hand side) and 2012 future year (right-hand side) modeling. Somewhat similar to June 14 and June 15, the contribution to the eight-hour average ozone from the boundaries (approximately 10 ppb) is predominantly from the NTHBC and WSTBC at both the DENT and EMTL monitors. Also somewhat similar to June 14 and June 15, there is a notable contribution from all sources in the EUS_36KM source region, which is approximately equal to the contribution from the non DFW Texas regions (i.e., sum of East_TX, South-Centrl_TX and WEST_TX) at both monitors.

2006 and 2012 APCA DENT (CAMS 56) June 30

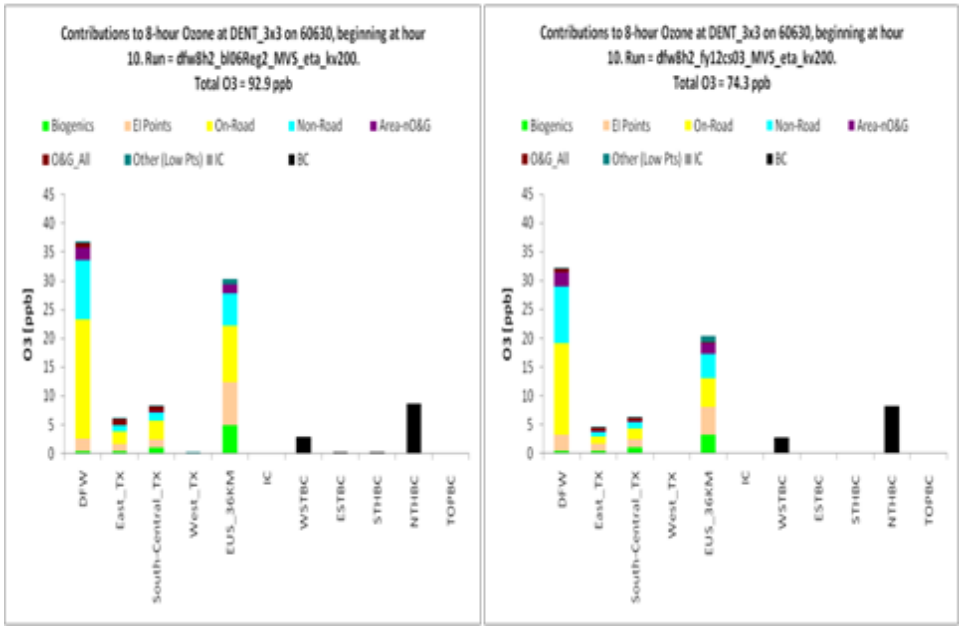

Figure 5-77: APCA 2006 and 2012 for DENT June 30

2006 and 2012 APCA EMTL (CAMS 75) June 30

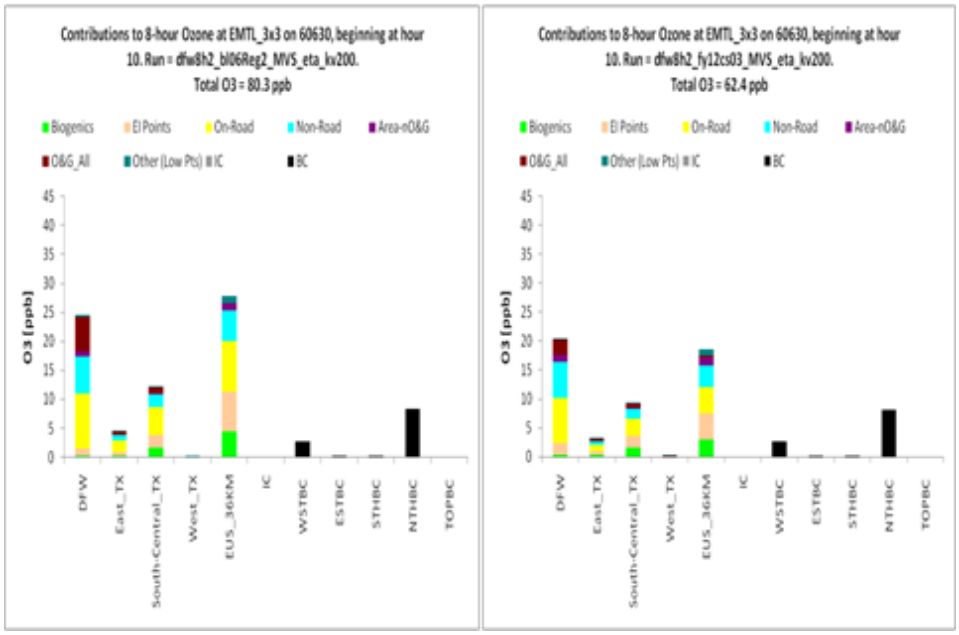

Figure 5-78: APCA 2006 and 2012 for EMTL June 30

Figure 5-79: *APCA Difference between 2006 and 2012 at DENT and EMTL June 30* shows the difference in the APCA contributions from non IC and BC source categories and regions to the eight-hour average ozone (1000 to 1700 hours CST at both monitors) between the 2006 baseline and 2012 future year modeling on June 30 for the DENT (left-hand side) and EMTL (right-hand side) monitors. For both of these monitors the modeling projects a net eight-hour average

ozone concentration reduction of more than 15 ppb (i.e., 18.27 ppb for DENT and 17.56 ppb for EMTL). At both of these monitors, the reductions in the eight-hour average ozone concentration associated with source categories in the EUS_36KM source region are approximately twice as larger than the reductions in the eight-hour average ozone concentration associated with source categories in the DFW source region. In addition, a slight increase in the eight-hour average ozone concentration associated with El Points in the DFW source region is evident at both the DENT and EMTL monitors. As indicated previously, this is likely due to modeling 2012 with the CAIR NO_X emission allocations for EGUs, which are larger than the reported 2006 EGU NO_X emissions.

Similar to the previously discussed days, at the DENT monitor, the On-Road source category in the DFW source region is associated with the largest reduction in the eight-hour average ozone concentration. However, at the EMTL monitor, on this day, the O&G_All source category in the DFW source region is the major source of reductions in the eight-hour average ozone concentration. At both monitors, the El Points and On-Road source categories in the EUS_36KM source region are associated with the largest reductions in the eight-hour average ozone concentration.

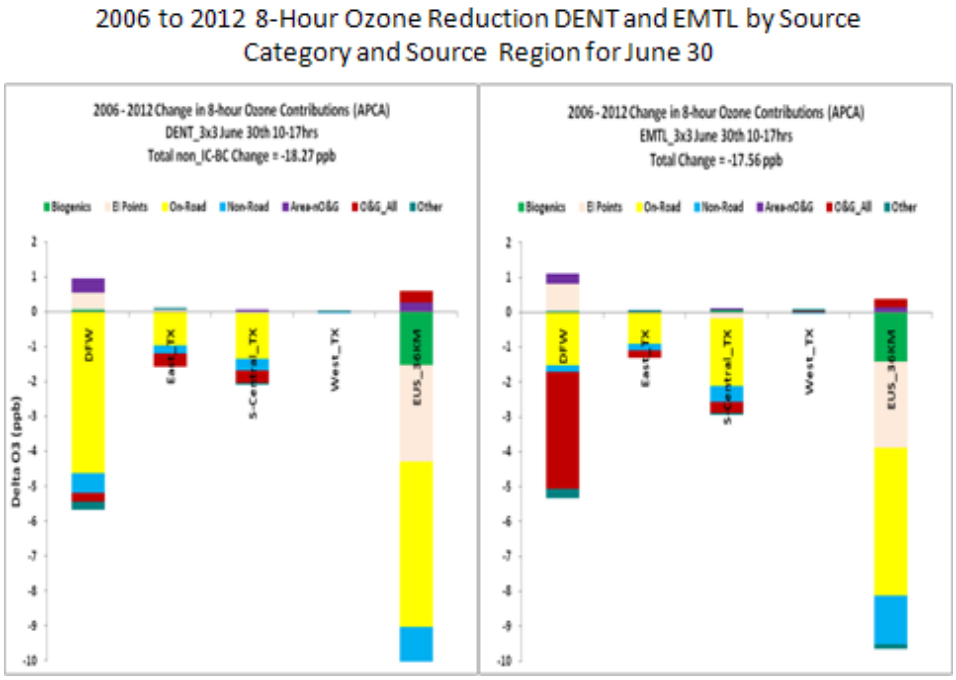

Figure 5-79: APCA Difference between 2006 and 2012 at DENT and EMTL June 30

July 1 was another day used in the RRF calculation for both the DENT and EMTL monitors. Figure 5-80: *APCA 2006 and 2012 for DENT July 1* and Figure 5-81: *APCA 2006 and 2012 for EMTL July 1* show the APCA contributions to the eight-hour average ozone concentration (1000 to 1800 hours CST at both monitors) for both the 2006 baseline (left-hand side) and 2012 future year (right-hand side) modeling.

Somewhat distinct from the previous days, the contribution to the eight-hour average ozone from the WSTBC and NTHBC is less than 10 ppb at both monitors. Also somewhat distinct from the previous days is the larger contribution to the eight-hour average ozone concentration from all source categories in the EUS_36KM source region, than either the DFW or the South-

Central_TX source regions at both the EMTL and DENT monitors for 2006 and 2012. Similar to June 12 is the minimal contribution to the eight-hour average ozone concentration from both the East and West Texas source regions, and the noteworthy contribution to the eight-hour average ozone concentration from all source categories from the South-Central_TX source region at both the EMTL and DENT monitors.

2006 and 2012 APCA DENT (CAMS 56) July 1

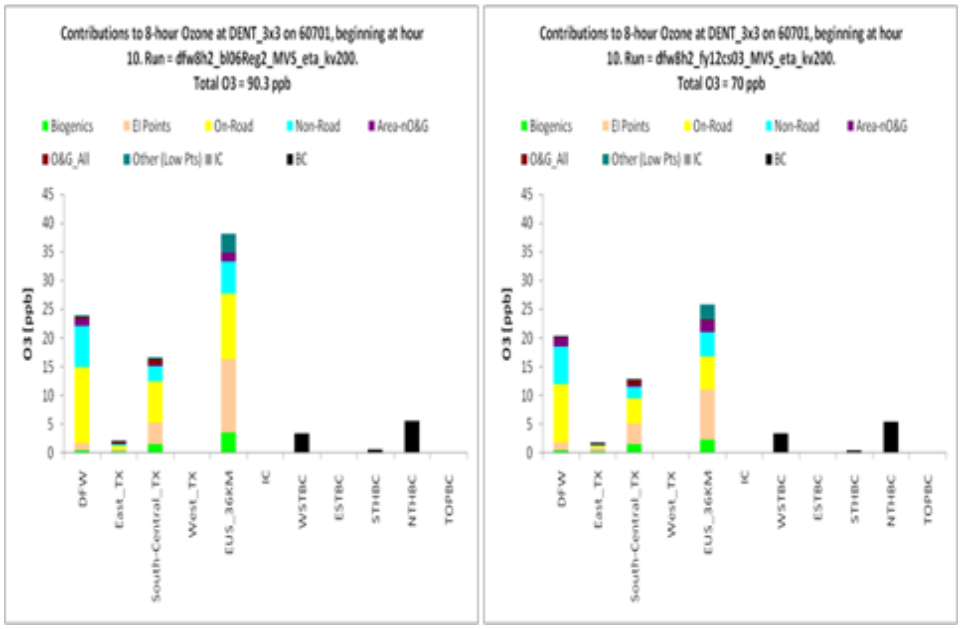

Figure 5-80: APCA 2006 and 2012 for DENT July 1

2006 and 2012 APCA EMTL (CAMS 75) July 1

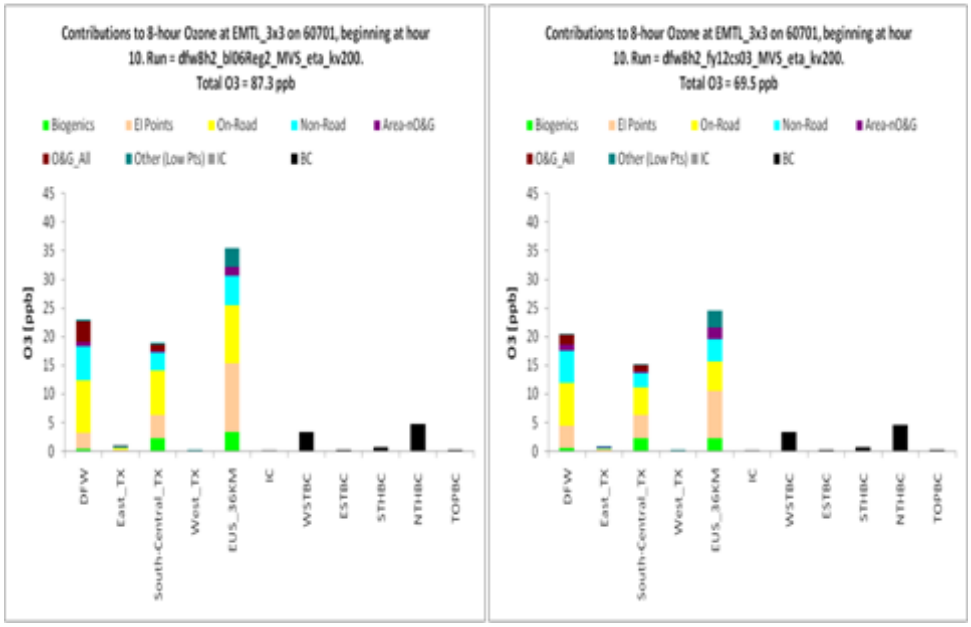

Figure 5-81: APCA 2006 and 2012 for EMTL July 1

Figure 5-82: *APCA Difference between 2006 and 2012 at DENT and EMTL July 1* shows the difference in the APCA contributions from non IC and BC source categories and regions to the eight-hour average ozone (1000 to 1700 hours CST at both monitors) between the 2006 baseline and 2012 future year modeling on July 1 for the DENT (left-hand side) and EMTL (right-hand side) monitors. For both of these monitors the modeling projects a net eight-hour average ozone concentration reduction of more than 15 ppb (i.e., 19.91 ppb for DENT and 17.68 ppb for EMTL).

At both monitors, the reductions in the eight-hour average ozone concentration associated with source categories in the EUS_36KM source region are slightly more than twice as large as the reductions in the eight-hour average ozone concentration associated with source categories in the DFW source region. Also similar to June 30, the reductions in the eight-hour average ozone concentration associated with source categories, especially El Points and On-Road, in the EUS_36KM source region account for approximately half the net reduction in the eight-hour average ozone concentration at both monitors. In addition, at both monitors, the reduction in the eight-hour average ozone concentration associated with source categories, particularly On-Road, in the South-Central_TX source region is approximately the same as the reduction in the eight-hour average ozone concentration associated with source categories in the DFW source region.

Notable and similar to the previous days at the EMTL monitor is the increase in the eight-hour average ozone concentration associated with El Points (slightly more than 1 ppb) in the DFW source region, which is likely due to modeling 2012 with the CAIR NO_X emission allocations for EGUs larger than the reported 2006 EGU NO_X emissions.

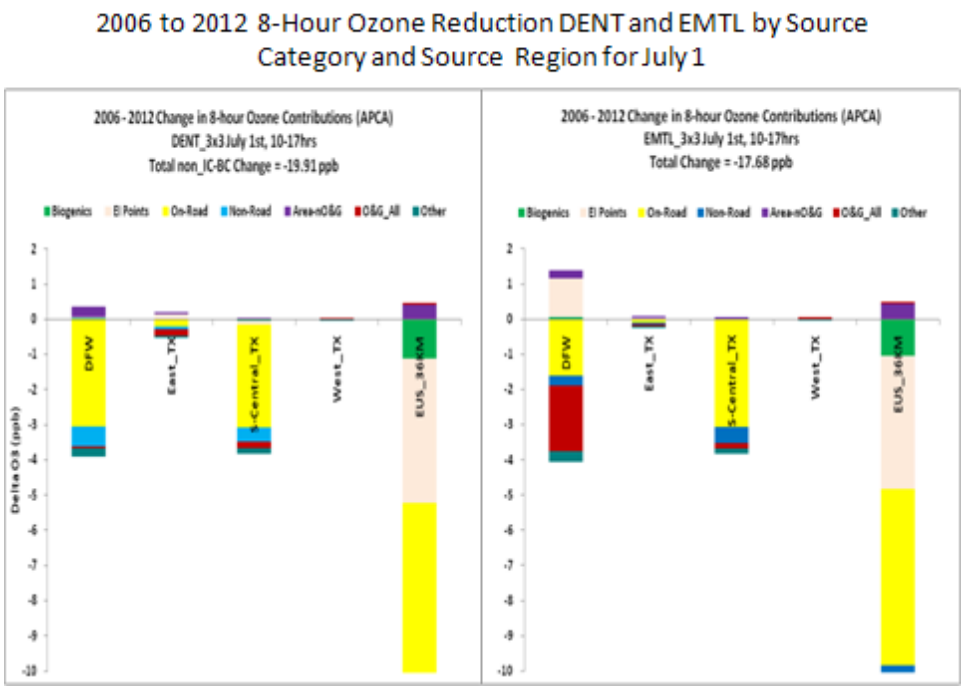

Figure 5-82: APCA Difference between 2006 and 2012 at DENT and EMTL July 1

APCA Findings and Implications

- Typically, the combined WSTBC and NTHBC contribute approximately 15 ppb to the maximum daily average eight-hour ozone concentration at the EMTL and DENT monitors.

- On days with high ozone at both the EMTL and DENT monitors the contribution from all source categories in the DFW source region is generally half the maximum daily average eight-hour ozone concentration.

- On some high ozone days at the EMTL and DENT monitors, the contribution to the maximum daily average eight-hour ozone concentration from all source categories in the EUS_36KM source region is at least as much or more than the contribution from all source categories in the DFW source region.

- The contribution to the maximum daily average eight-hour ozone concentration from the O&G_All source category in the DFW source region is more prevalent at EMTL than DENT on high ozone days occurring at both monitors.

- On high ozone days, the component of the total reduction in the maximum daily average eight-hour ozone concentration from 2006 to 2012, from all source categories in the EUS_36KM source region is generally greater than or equal to the component of the total reduction in the maximum daily average eight-hour ozone concentration from 2006 to 2012, from all source categories in the DFW source region.

- The modeled decrease in the design values for the EMTL and DENT monitors from 2006 to 2012 is at least as dependent on ozone reduction outside of Texas as it is on ozone reductions within Texas.

5.5.2.4 Chemical Process Analysis

Process analysis is a valuable modeling tool that allows modelers to analyze the internal workings of the model in detail. In a standard photochemical grid modeling run, the output of the model is composed of concentration fields for different chemicals such as ozone and nitrogen dioxide. In a process analysis modeling run, the rates of chemical production and destruction are preserved as well as the concentrations, so that it is easier to trace the pathway by which ozone is formed.

In previous modeling projects, the TCEQ has used process analysis to examine radical budgets, in an effort to determine why simulated ozone concentrations were not as high as observed in Houston industrial plumes. Process analysis has also been used to evaluate relative rates of VOC-sensitive and NO_X-sensitive ozone formation, VOC reactivity and OH radical loss rates, and the role of photolysis on ozone formation rates (TCEQ Houston Attainment SIP, 2010).

For this DFW modeling project, process analysis was primarily used to evaluate the relative roles of local ozone production and regional background ozone, and to examine the sensitivity of ozone formation in DFW to VOC and NO_X concentrations.

5.5.2.4.1 Description of ozone episode days

Process analysis was performed for seven of the high ozone days included in the DFW SIP modeling episode: June 9, June 12, June 14, June 15, June 18, June 28, and July 1, 2006. Before examining the process analysis runs, it is useful to briefly review what happened on those days, and how well the model has simulated the high ozone.

The wind flow within the DFW area has been characterized by back trajectories calculated from wind measurements at the different monitoring sites. Figure 5-83: *Observed and Modeled Back Trajectories for June 9, 2006 in DFW* shows twelve-hour back trajectories based on observations (red) and modeling of the wind fields (blue) for June 9, 2006, in DFW; *Figure 5-84: Observed and Modeled Back Trajectories for DFW Episode Days* shows similar graphs for June 12, 14, 15, 18, 28, and July 1, the rest of the episode days that were examined with process analysis. From these graphs, one can observe the strength of the wind flow, direction of the flow, variation in the speed and direction of the winds, and the areas likely to influence the ozone concentrations at the end point of the back trajectory. In addition, one can compare the simulated wind field to the observed wind field. Based upon the figure, there are four days with winds blowing steadily from the southeast quadrant for the full twelve-hour period: June 9, June 14, June 15, and July 1. For these days, it is relatively easy to determine which monitoring sites are upwind and downwind of the urban area, and therefore it is possible to estimate regional background ozone and local ozone production. For three of the days studied, however, the winds are much more variable in direction and speed during the twelve hours, as shown by the back trajectories: June 12, June 18, and June 28. For two days, June 12 and 18, there is a reversal in the direction of the wind flow. In Houston, where flow reversals occur relatively often, this type of wind pattern is closely associated with strong ozone gradients and high ozone. For June 28, the wind flow changes direction during the day, but no flow reversal occurs.

Model performance of the winds on these seven days is relatively good, but the model performs better on days with steady, relatively brisk winds than on days with light winds and large changes in wind direction. Since the DFW urban area lacks a significant number and concentrated area of large point sources, the relatively small discrepancies observed in modeled and observed winds are unlikely to affect ozone model performance dramatically.

Five-minute ozone concentrations at all monitoring sites in DFW provide a quick representation of ozone behavior during each high ozone day. Figure 5-85: *Five-Minute Observed Ozone Concentrations for all DFW Monitoring Sites, June 9, 2006* presents time series of five-minute average ozone concentrations for June 9; Figure 5-86: *Five-Minute Observed Ozone Concentrations for All DFW Monitoring Sites During Six Episode Days* presents the time series for the other six episode days.

Four days show similar patterns in the ozone time series: June 9, 14, 28, and July 1. These four days show a distinction between upwind and downwind monitoring sites. The upwind sites have lower, steady concentrations all day long; the downwind sites gradually diverge from the other sites as the ozone forms downwind of the urban core during the day, peaking in the late afternoon. For these days, it is simple to estimate regional background ozone and local ozone contribution, because the simple flow-through conditions allow it. For one day, June 15, the flow pattern indicates that flow-through conditions exist, but the five-minute ozone data for this day are somewhat different. It appears that there is little or no local contribution of ozone to the concentrations measured in the DFW area on June 15, because most of the monitors have very similar ozone concentrations, i.e., between 70-85 ppb, and these concentrations persist all day. Winds on this day are notably stronger than any other day, implying that the lower concentrations may be due to strong dilution of the local ozone contribution. Further explanation is provided in the process analysis discussion below.

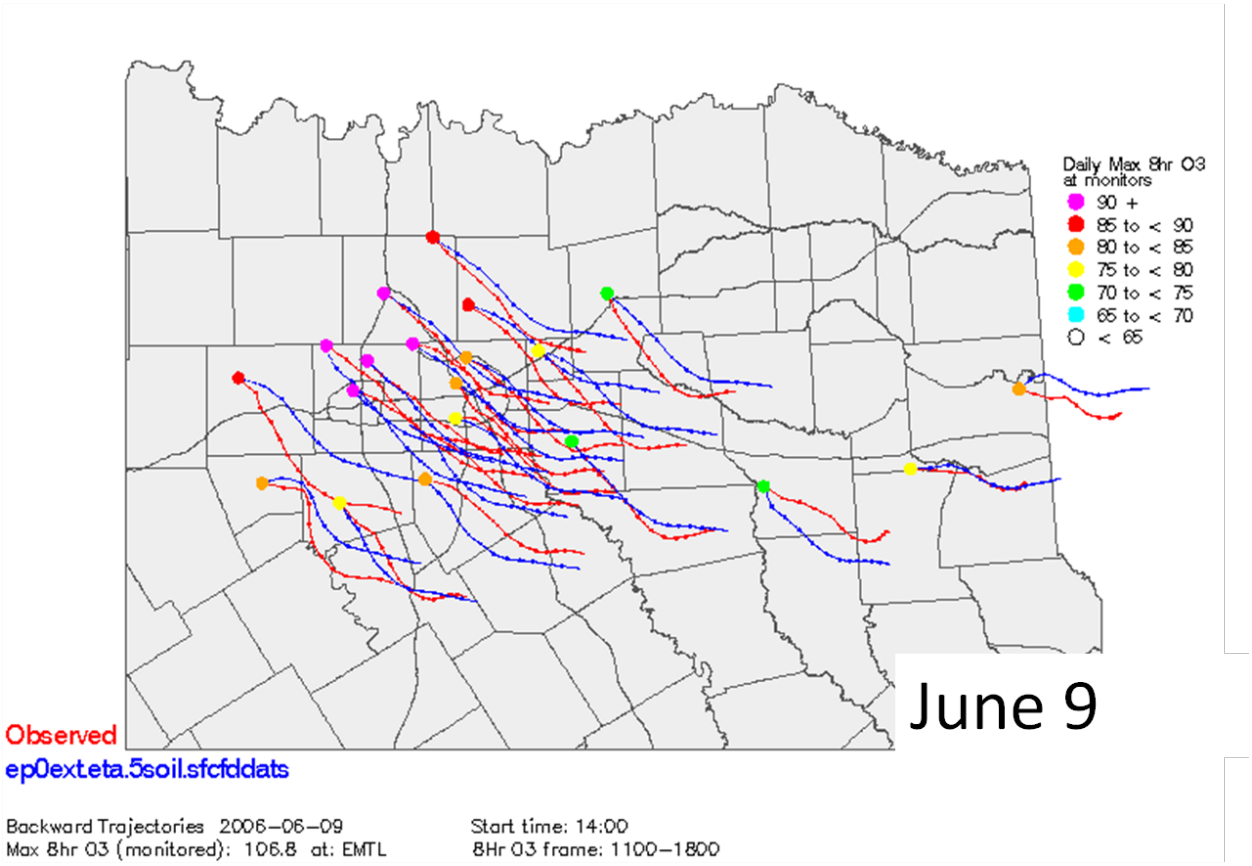

Figure 5-83: Observed and Modeled Back Trajectories for June 9, 2006 in DFW

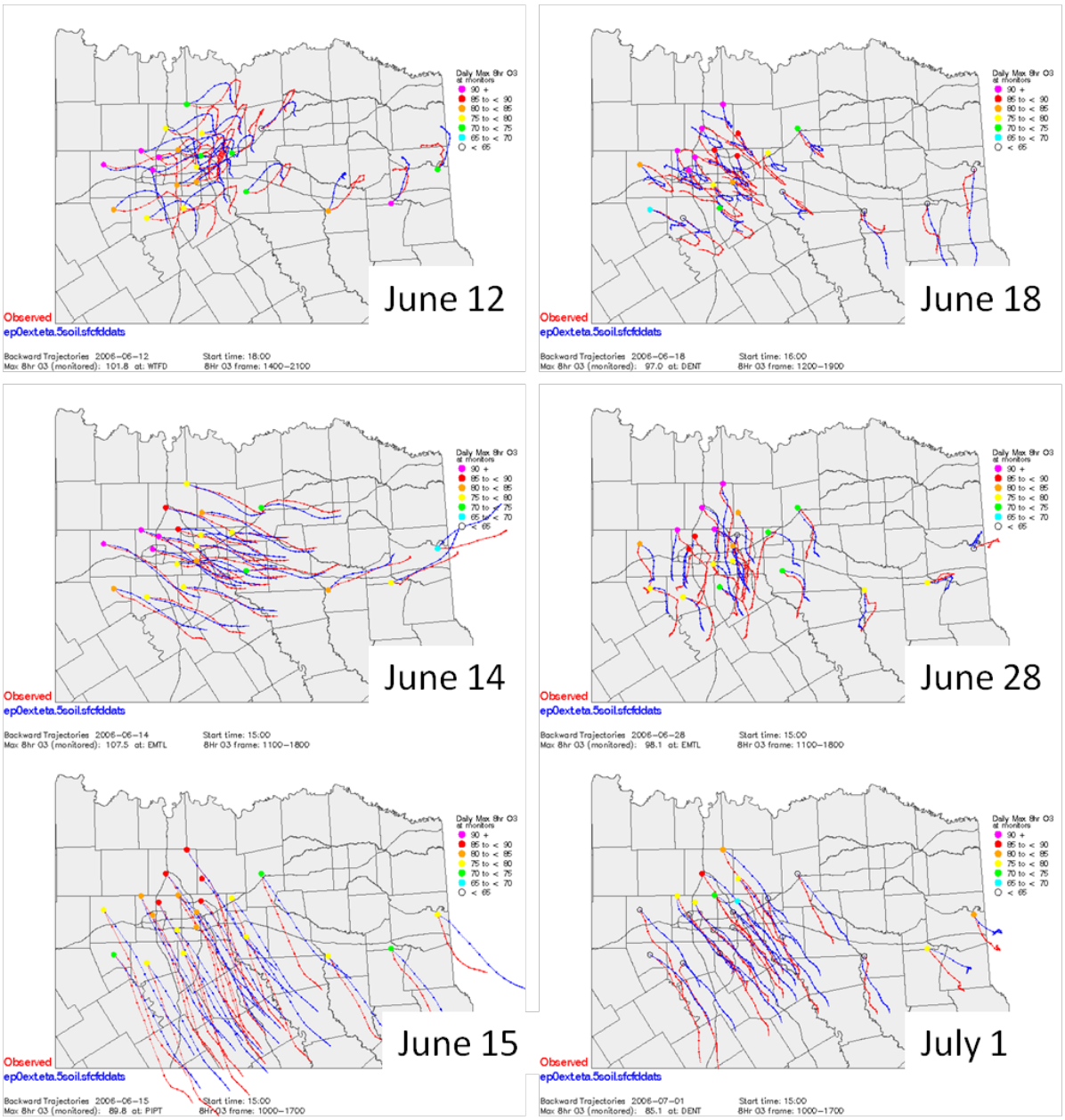

Figure 5-84: Observed and Modeled Back Trajectories for DFW Episode Days

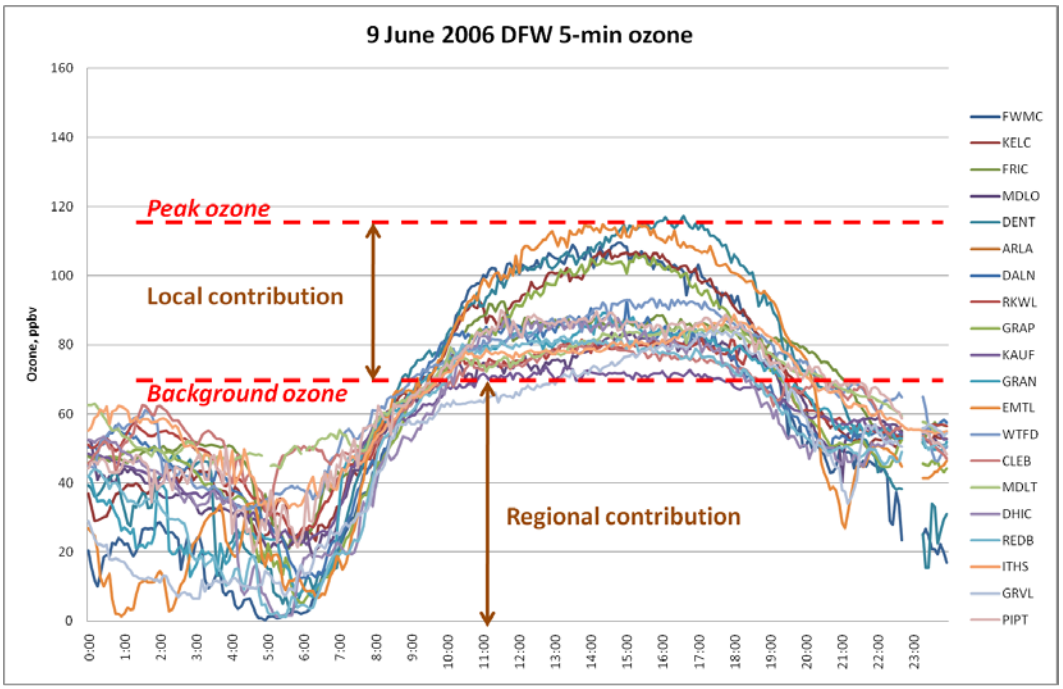

Figure 5-85: Five-Minute Observed Ozone Concentrations for all DFW Monitoring Sites, June 9, 2006

Ozone data from the upwind sites are along the lower edge of the daytime data, near the line labeled "Background ozone." Data from the downwind sites are near the upper edge of the daytime data, near the line labeled "Peak ozone." For this particular day, there is a distinct gap between the upwind and downwind ozone data from about 11:00 to 18:00 CST. The regional contribution is larger than the local contribution.

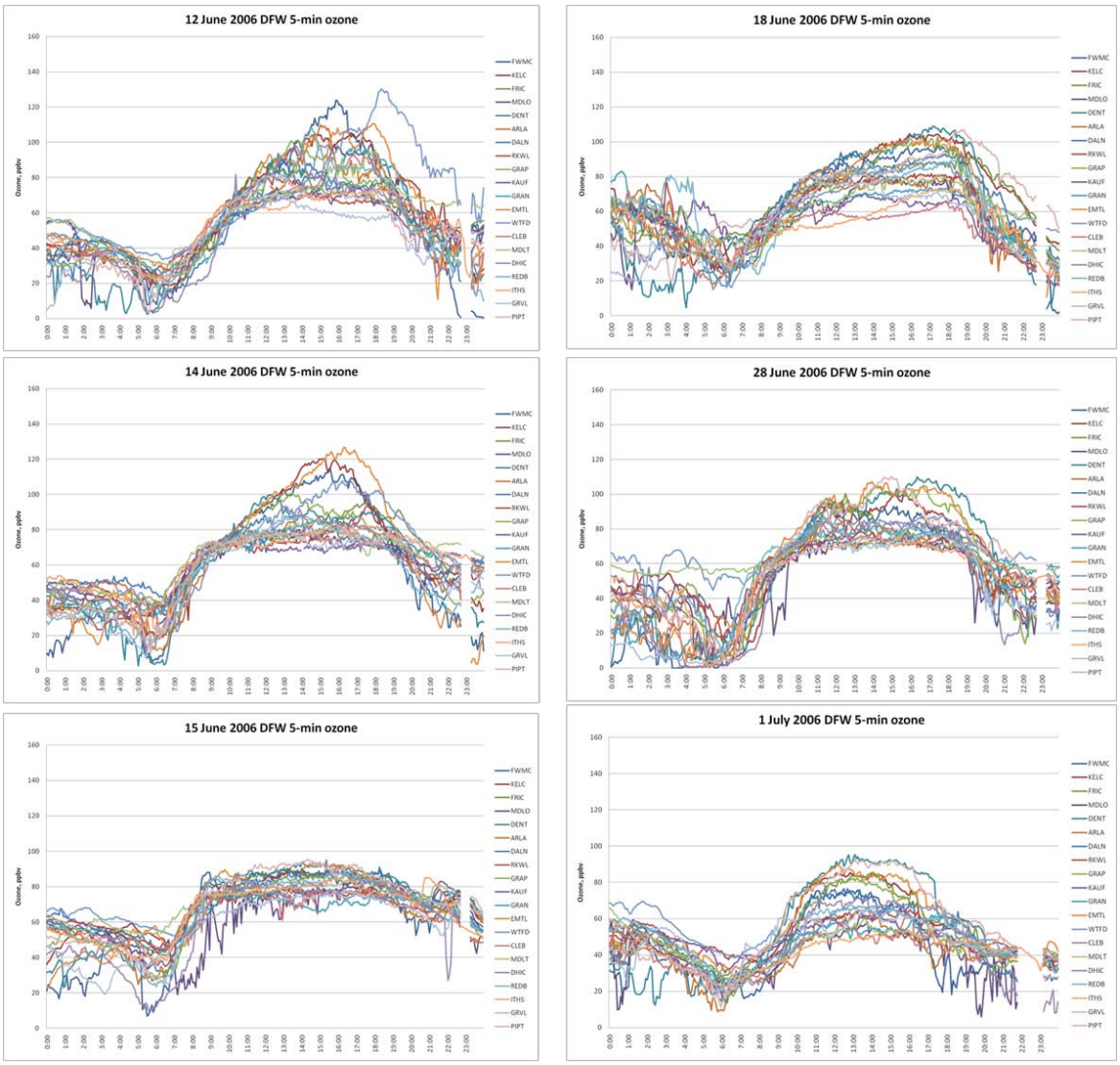

Figure 5-86: Five-Minute Observed Ozone Concentrations for All DFW Monitoring Sites During Six Episode Days

Figure 5-87: *Daily Peak Modeled Eight-Hour Ozone Concentrations for DFW Domain, June 9, 2006* and Figure 5-88: *Daily Peak Modeled Eight-Hour Ozone Concentrations for DFW Domain for Six Episode Days in 2006* illustrate the model performance on the process analysis days. Figure 5-87 shows peak modeled eight-hour ozone concentrations for the DFW modeling domain for June 9; Figure 5-88 shows analogous tileplots for the other six episode days. The observed eight-hour concentrations at each monitor are depicted by circles. The ozone concentrations are color-coded in the same manner for both the modeled ozone field and the monitors. Model performance can be seen easily by comparing the color of the modeled ozone field surrounding each monitor to the color of the monitor. These fields show that days with steady wind flow and days with flow reversals or light winds can be distinguished relatively well by ozone concentrations. The steady flow days show prominent ozone plumes extending downwind of the urban centers and large power plants in the domain. The flow reversal days show a pool of ozone in the urban area that is not being transported out of the city.

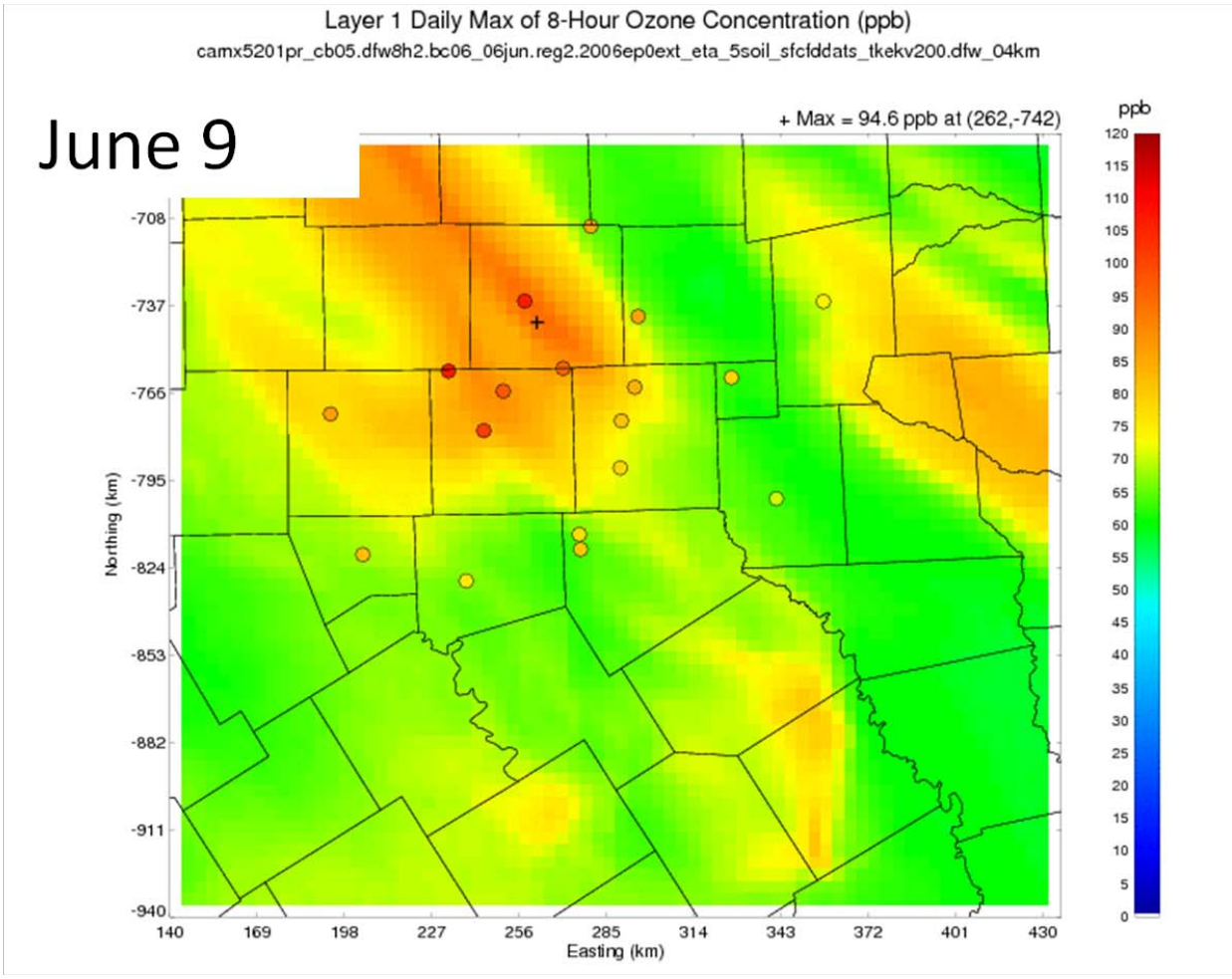

Figure 5-87: Daily Peak Modeled Eight-Hour Ozone Concentrations for DFW Domain, June 9, 2006

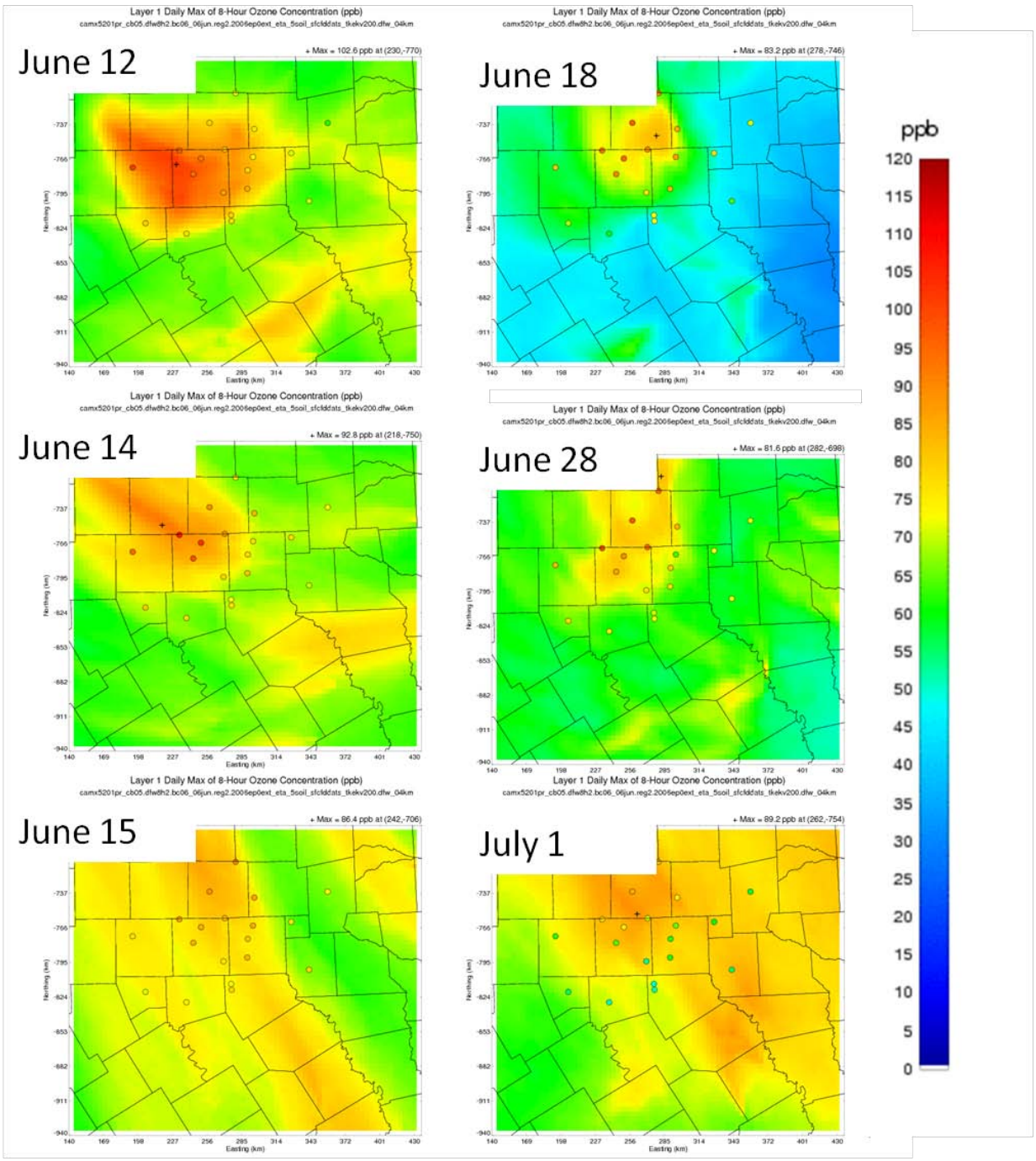

Figure 5-88: Daily Peak Modeled Eight-Hour Ozone Concentrations for DFW Domain for Six Episode Days in 2006

5.5.2.4.2 Process analysis of ozone episode days

Chemical process analysis of photochemical modeling provides information on how the model arrives at the final concentrations of ozone and ozone precursors. By keeping track of the rates of many important reactions, the process analysis algorithms provide detailed information about ozone production rates, rates of VOC oxidation and transformation, radical formation, propagation, and termination rates, photolysis rates, and other reactions that indicate in detail

the factors influencing model performance. This process analysis of DFW modeling focuses upon radical chemistry, local ozone formation, and the sensitivity of ozone formation to VOC and NO_X concentrations.

Ozone production upwind, downwind, and in the urban core

The critical reaction for forming and accumulating high ozone concentrations in a city is the oxidation of VOCs by the OH radical. After the OH radical attacks an organic compound, a peroxy radical is created, which can then react with NO to form NO_2. NO_2 then photolyzes, splitting off an oxygen atom, which reacts with molecular oxygen (O_2) in the atmosphere, creating ozone (O_3). During this ozone formation process, radicals can undergo additional reactions that depend strongly upon whether there is an abundance of VOCs or NO_X. These radical termination reactions can leave relatively stable residual products in the atmosphere. By examining the rates at which the residual products are created, or by measuring the residuals directly, one can determine whether the environment in which ozone is being formed is more sensitive to VOC or NO_X concentrations. The Chemical Process Analysis algorithm included in CAMx tags the ozone formation according to whether it is VOC-sensitive or NO_X-sensitive, and these ozone formation parameters can help determine which control strategies are likely to be most effective.

Another parameter of interest is O_X production, where O_X is approximately equal to $O_3 + NO_2$. When O_3 reacts with NO (the titration reaction), it forms NO_2. Since NO_2 can photolyze quickly to reform ozone, O_X is conserved during titration even though ozone decreases. Ozone titration often occurs in an area with high NO emissions, especially from motor vehicles. An air mass can have high O_X production in the presence of high NO emissions; when the air mass is transported out of the zone of high NO emissions, ozone can form rapidly from the NO_2 that has accumulated. Therefore, examining O_X concentrations and production rates is a way to keep track of potential ozone.

Figure 5-89: *Hourly Ozone Production at Selected DFW Sites During Seven Episode Days in 2006* shows hourly ozone formation time series for three monitoring sites in the DFW area for all seven days examined with process analysis. The ozone production presented is gross ozone production, rather than net ozone production, i.e., it does not account for dry deposition of ozone, or chemical destruction of ozone. For that reason, it represents the upper limit of contributions to peak ozone concentrations. The Kaufman site (top) is usually upwind of DFW. The Hinton site (middle) is an urban core site; the Keller site (bottom) is a downwind site, and consistently has observed a high design value (86 ppb in 2010, the highest in DFW). All sites in the DFW area have VOC-limited ozone production in early morning, shifting to NO_X-limited production after a few hours. Urban core and downwind sites have a slightly longer period of VOC-limited ozone production than upwind sites, with greater ozone production rates. Upwind sites have low ozone production. The Hinton site has high O_3 production, with VOC-limited O_3 production peaking at greater than 10 ppb per hour on five of seven days. Ozone formed in the urban core can be observed at the downwind sites. High production at urban core sites leads to high concentrations downwind. However, in DFW, even the downwind sites have active ozone production, at rates comparable to urban core sites. The high rate of ozone production at the downwind sites suggests that the ozone concentrations observed at these sites near the edge of the DFW monitoring network may not be observing the peak ozone concentrations in north central Texas. Other sites not shown in Figure 5-89 have similar behavior to these three, e.g., Greenville and Rockwall are upwind sites, and Denton, Fort Worth Northwest, and Eagle Mountain Lake are downwind sites, and ozone production at all upwind and downwind sites behaves in a similar way.

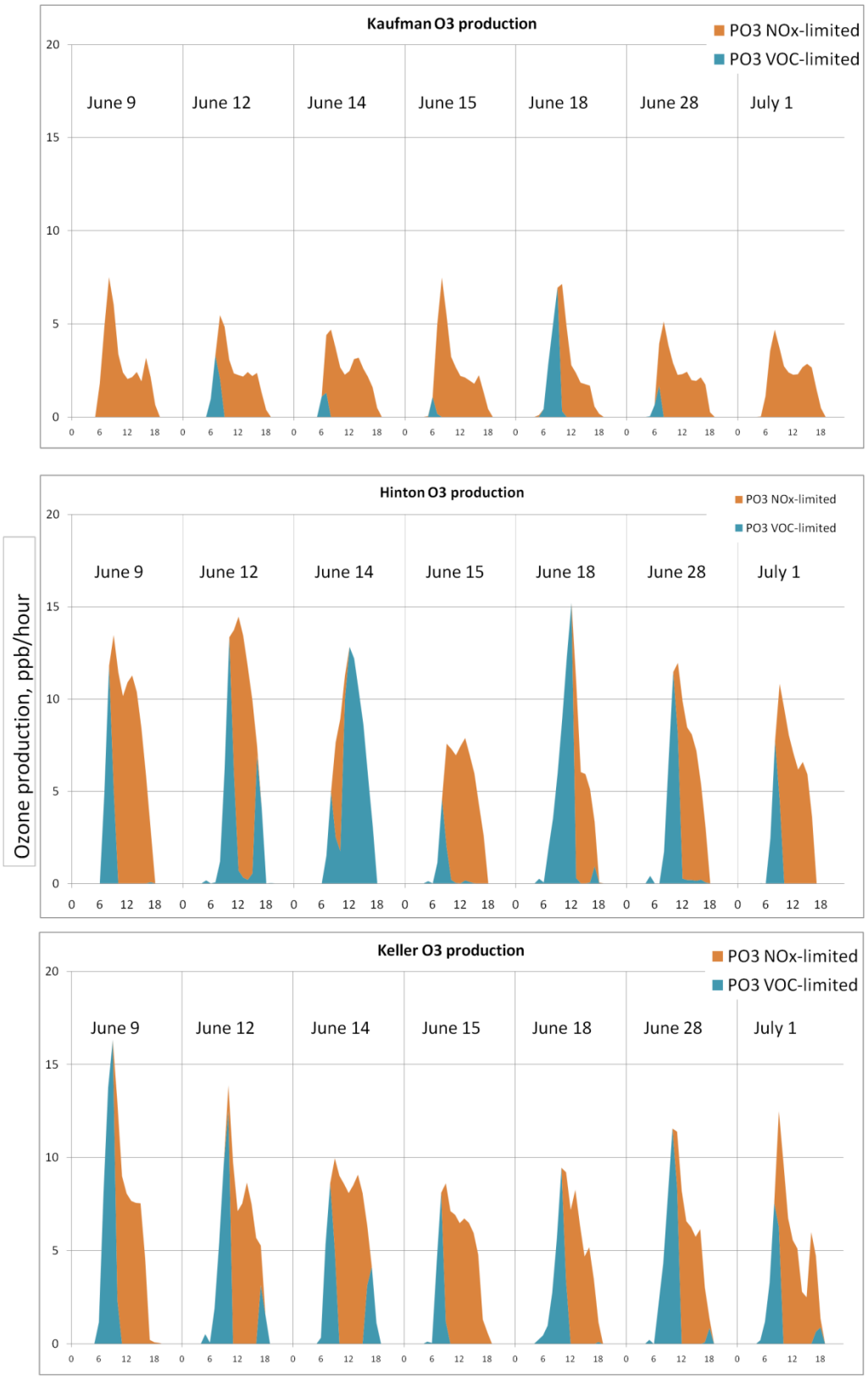

Figure 5-89: Hourly Ozone Production at Selected DFW Sites During Seven Episode Days in 2006

Local ozone production vs. regional background ozone

The DFW Conceptual Model analyses indicate that the regional background ozone contributes substantially to ozone exceedances in the DFW area. Studies by Nielsen-Gammon et al. (2005) and NOAA scientists have shown that the regional background ozone experienced by the DFW area tends to be higher on average than in southeast Texas. Regional-scale transport studies have shown that transport patterns associated with high regional background ozone are also associated with ozone exceedances in DFW (Chan and Vet, 2009; Sullivan, 2010).

The TCEQ used a simple upwind-downwind technique for estimating the contributions of regional background ozone and locally-produced ozone for Texas cities. Four of the episode days studied with process analysis have been analyzed to estimate local and regional ozone (Table 5-14: *Regional Background Ozone and Net Locally Produced Ozone, Estimated from Observations and Modeling*). Modeled regional background ozone was estimated by examining the peak modeled eight-hour ozone concentrations at the monitoring sites used at the TCEQ Significant Events web page (TCEQ, 2010) to estimate observed background concentrations.

Table 5-14: Regional Background Ozone and Net Locally Produced Ozone, Estimated from Observations and Modeling

DFW episode date	Observed / Modeled Peak 8-hour ozone (ppb)	Observed / Modeled Range of regional background ozone (ppb)	Observed / Modeled Range of net locally-produced ozone (ppb)
June 9	106 / 95	70-80 / 63-69	26-36 / 16-22
June 12	101 / 103	62-70 / 64-75	31-39 / 28-39
June 14	107 / 93	70-77 / 66-70	30-37 / 23-27
June 15	89 / 86	75-79 / 66-74	10-14 / 12-20

Observed data are from TCEQ Significant Events web page (TCEQ, 2010). Modeled data are from the bc06_06jun.reg2 modeling run. For modeled estimates of background ozone, sites identified as observed background sites were used.

Estimates of net local ozone production, based upon upwind-downwind analyses, account for no more than a third of the peak ozone observed in DFW on these four days. These estimates are generally consistent with the findings of the TCEQ DFW Conceptual Model, Nielsen-Gammon et al. (2005), and Kemball-Cook et al. (2010).

The model estimates for regional background are virtually identical for each day. For June 9, 14 and 15, modeled regional background ozone is lower than observed. For June 9 and 14, peak eight-hour ozone is also biased low, by more than 10 ppb. But for June 12 and June 15, peak ozone is within 3 ppb of the observed maxima. For June 9 and 14, the low bias in regional background may explain the low bias in peak ozone. The net amount of locally contributed ozone was estimated well by the modeling for June 12 and June 15, with June 12 indicating much higher local net production than June 15 in both the observations and the modeling.

The upwind-downwind technique is an indirect method of estimating net ozone production. Process analysis can be used to directly calculate local ozone production from modeling results. Figure 5-90: *Total Modeled Ozone Production for June 9, 12, 14, and 15, 2006 in DFW* shows total ozone production on June 9, 12, 14, and 15. The figure presents the sum of VOC-sensitive and NO_X-sensitive ozone production, averaged through the planetary boundary layer in each grid cell for each hour, and then summed for each grid cell over the entire day. The resulting field shows the location and intensity of ozone formation (in ppb) for each day in the DFW

domain. The amount of ozone formed in each grid cell is color-coded, with the lighter colors indicating less ozone formation, and the darker colors indicating more ozone formation.

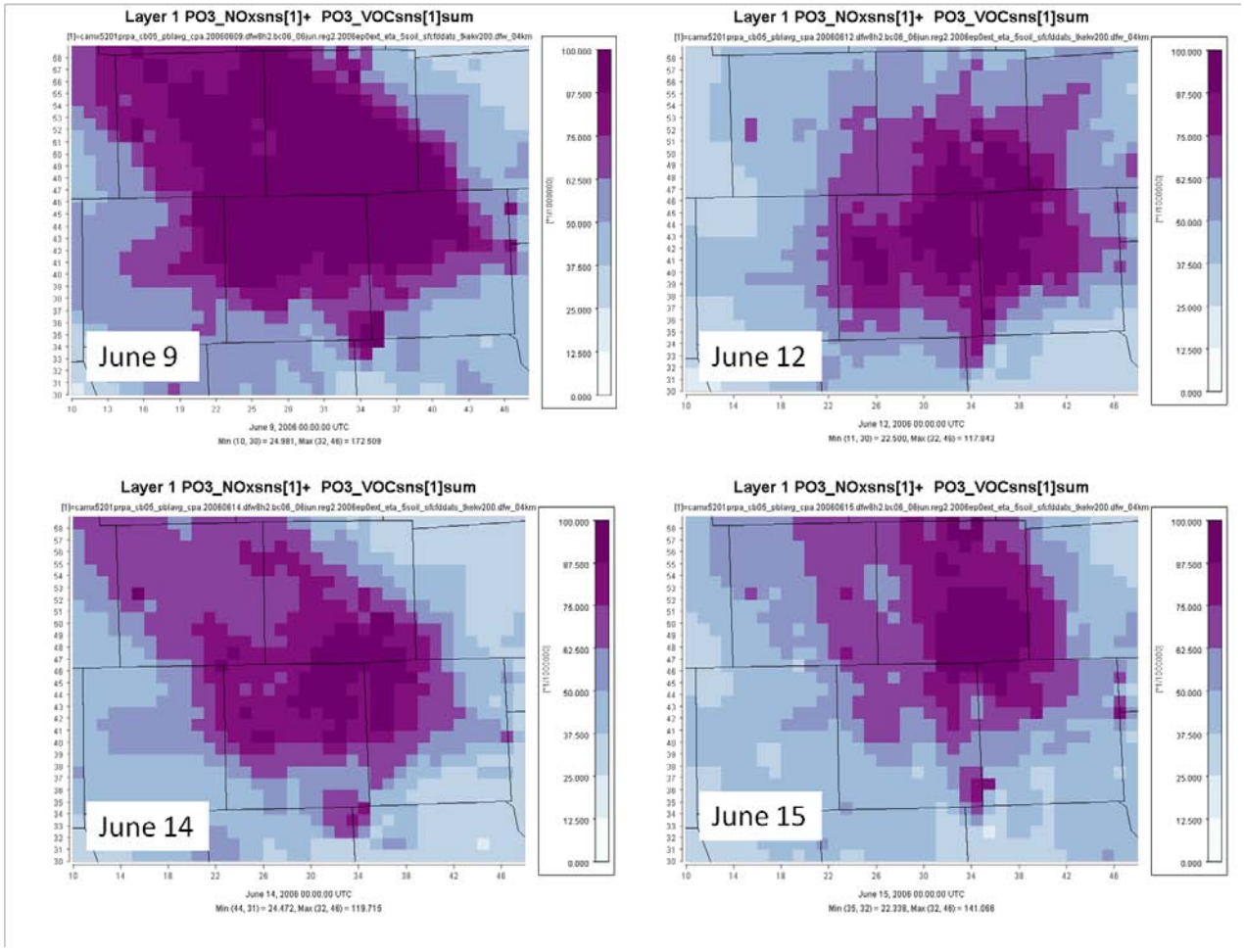

Figure 5-90: Total Modeled Ozone Production for June 9, 12, 14, and 15, 2006 in DFW

Table 5-15: *Total Ozone Production Index for Modeling of Selected DFW Episode Days* quantifies the differences in ozone production rate. The ozone production index is calculated by summing 24-hour ozone production (in ppb) in every grid cell within the subset of the DFW domain shown in Figure 5-90, for each day analyzed. The highest modeled rate of ozone production was for June 9; the other three days had lower rates, but were similar to each other. June 12 and 14 had much higher peak ozone concentrations than June 15, but the ozone production rates were within 3%. June 9 had the highest ozone production rate, but had peak concentrations lower than June 12. From these calculations, one can conclude that the peak ozone depends on additional factors besides local ozone production.

Table 5-15: Total Ozone Production Index for Modeling of Selected DFW Episode Days

Date	Total O_3 production index	Peak modeled one-hour O_3 concentration, ppb	Peak modeled eight-hour O_3 concentration, ppb
June 9	78,607	101	95
June 12	62,932	131	103
June 14	62,908	108	93
June 15	60,609	93	86

One factor that appears to be affecting how total ozone production translates to peak ozone concentrations is wind speed. June 15 had observed peak eight-hour ozone 18 ppb lower than June 14, but the amount of total ozone production was comparable. As Figure 5-84 shows, winds on June 15 were notably higher than winds on June 14. Likewise, June 12 had higher modeled ozone concentrations than the other three days, but its local ozone formation was similar in magnitude to June 14 and 15. Again, Figure 5-91 shows that winds on June 12 were lighter than winds on June 14 and 15, and underwent a flow reversal, which kept locally produced ozone in the DFW area, rather than transporting ozone away. These findings suggest that the wind speed plays a major role in ozone accumulation. Although June 15 had high local ozone production, the high winds on that day transported the ozone out of the nonattainment area. June 12 had low winds, so that the ozone produced locally was able to accumulate locally. It was not necessary for ozone production to be particularly high on that day in order to accumulate enough ozone to exceed the standard.

Other factors that can determine the importance of locally-produced ozone include chemical destruction, dry deposition, and PBL depth. The factors that combine to determine the fate of locally-produced ozone vary from day to day in DFW, suggesting that meteorological factors are very important.

For the days with strong transport, ozone formation extends a considerable distance downwind of the urban core. This is consistent with monitoring data, which show that the peak eight-hour ozone concentrations on high ozone days often occur at the edge of the DFW monitoring network. If ozone production still actively occurs at the edge of the network, or even further downwind, the peak ozone on some episode days may occur outside of the DFW monitoring network.

TCEQ transport analyses are presented in Figure 5-91: *Wind Flow and One-Hour Ozone on Four Selected High Ozone Days in June 2006 in DFW*; the streamlines represent transport from midnight to the hour of the ozone concentrations shown at each monitoring site. For June 9, 14, and 15, the far downwind sites with high one-hour ozone concentrations are circled in red. For June 12, areas just outside DFW indicative of regional background concentrations are circled in red. Figure 5-91 shows that on June 9, 14, and 15, high ozone spreads from DFW north into Oklahoma, but on the flow reversal day of June 12, ozone is confined to the DFW area. On June 15, peak one-hour ozone observed downwind of DFW occurs at the Oklahoma border (101 ppb). The peak one-hour ozone observed downwind of DFW within the DFW monitoring network on June 15 ranged from 87 to 93 ppb at sites along the north and west edges of the monitoring network.

These data indicate that DFW emissions can be transported far downwind of the metropolitan area on days when transport winds are suitable. On days with light winds and/or flow reversals, DFW emissions remain in the local area, and boost ozone concentrations. Recent studies

downwind of Houston (Senff et al., 2010; Luria et al., 2008) show that Houston's emissions behave in a similar manner in the eastern half of Texas.

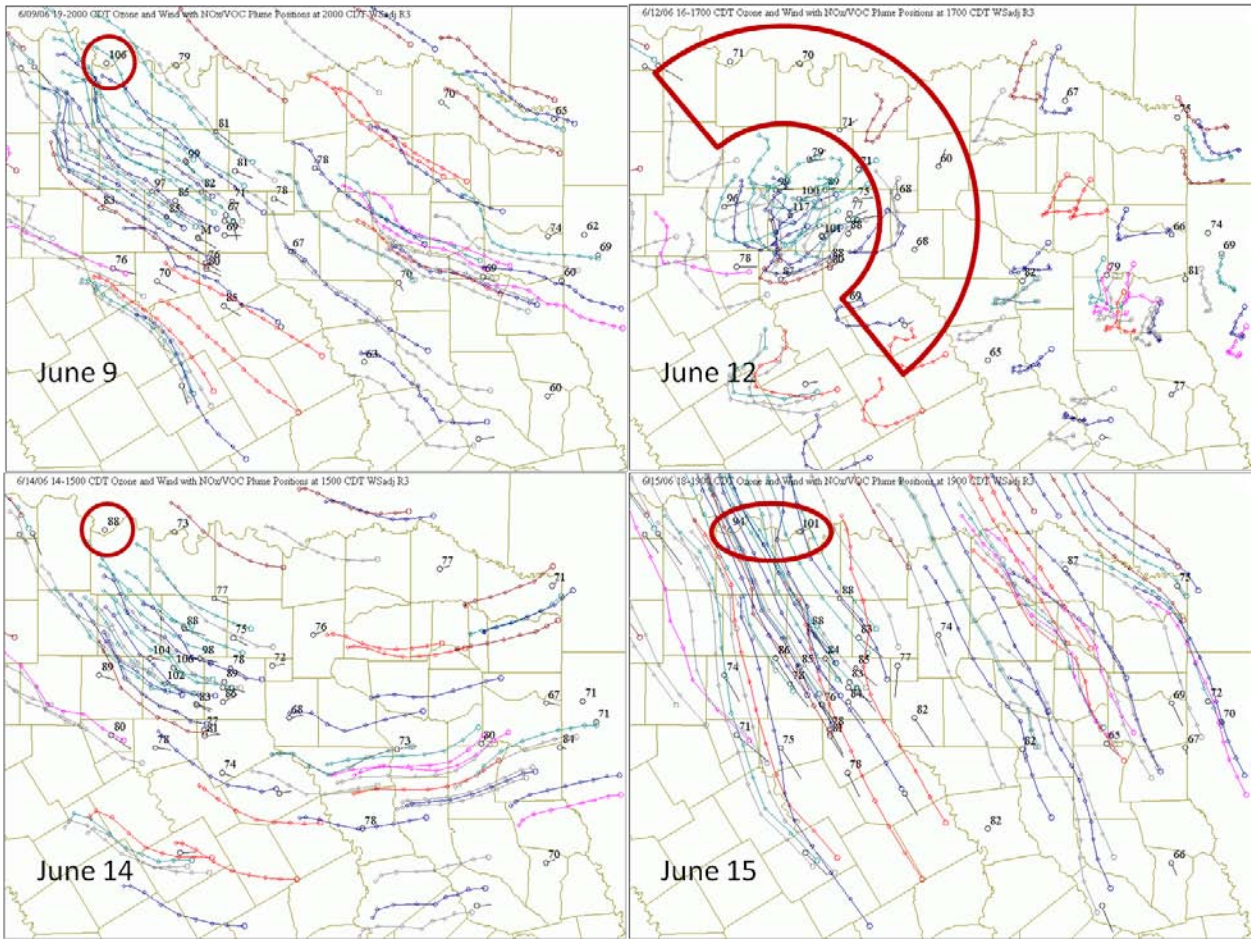

Figure 5-91: Wind Flow and One-Hour Ozone on Four Selected High Ozone Days in June 2006 in DFW

VOC-sensitive ozone production and NO_X-sensitive ozone production in DFW

Process analysis tracks ozone formation concurrently with the ratio between production of hydrogen peroxide and the production of nitric acid (Environ, 2010). This ratio has been shown to be the best indicator of the sensitivity of ozone formation to NO_X and VOC. Hydrogen peroxide is a by-product of NO_X-sensitive conditions. H_2O_2 forms when two HO_2 radicals react with each other; in the presence of NO, HO_2 will react with NO to form NO_2 + OH. The presence of substantial amounts of H_2O_2 indicates that little NO is present, and therefore, ozone formation occurring at the same time is limited by the amount of NO_X present. By contrast, nitric acid (HNO_3) is a product of OH+NO_2. The presence of substantial quantities of HNO_3 indicates that there is an abundance of NO_X, because OH will quickly react with VOCs if they are present. Sillman et al. (1995) and Tonnesen and Dennis (2000) found that the dividing point between NO_X-sensitivity and VOC-sensitivity occurs at a ratio of approximately $P(H_2O_2)/P(HNO_3) = 0.35$, which has been used by Environ to track VOC- and NO_X-sensitive ozone production.

Figure 5-92: *VOC and NOX Sensitivity in Ozone Production on Four Episode Days in DFW* shows the rates of total ozone production, NO_X-sensitive ozone production, and VOC-sensitive ozone production in DFW for four episode days. In each case, NO_X-sensitive conditions occur over a broad area of the domain. VOC-sensitive conditions occur in the urban core, in the urban plume for a short time downwind, and in the plumes of large power plants—all of these areas are rich in NO_X.

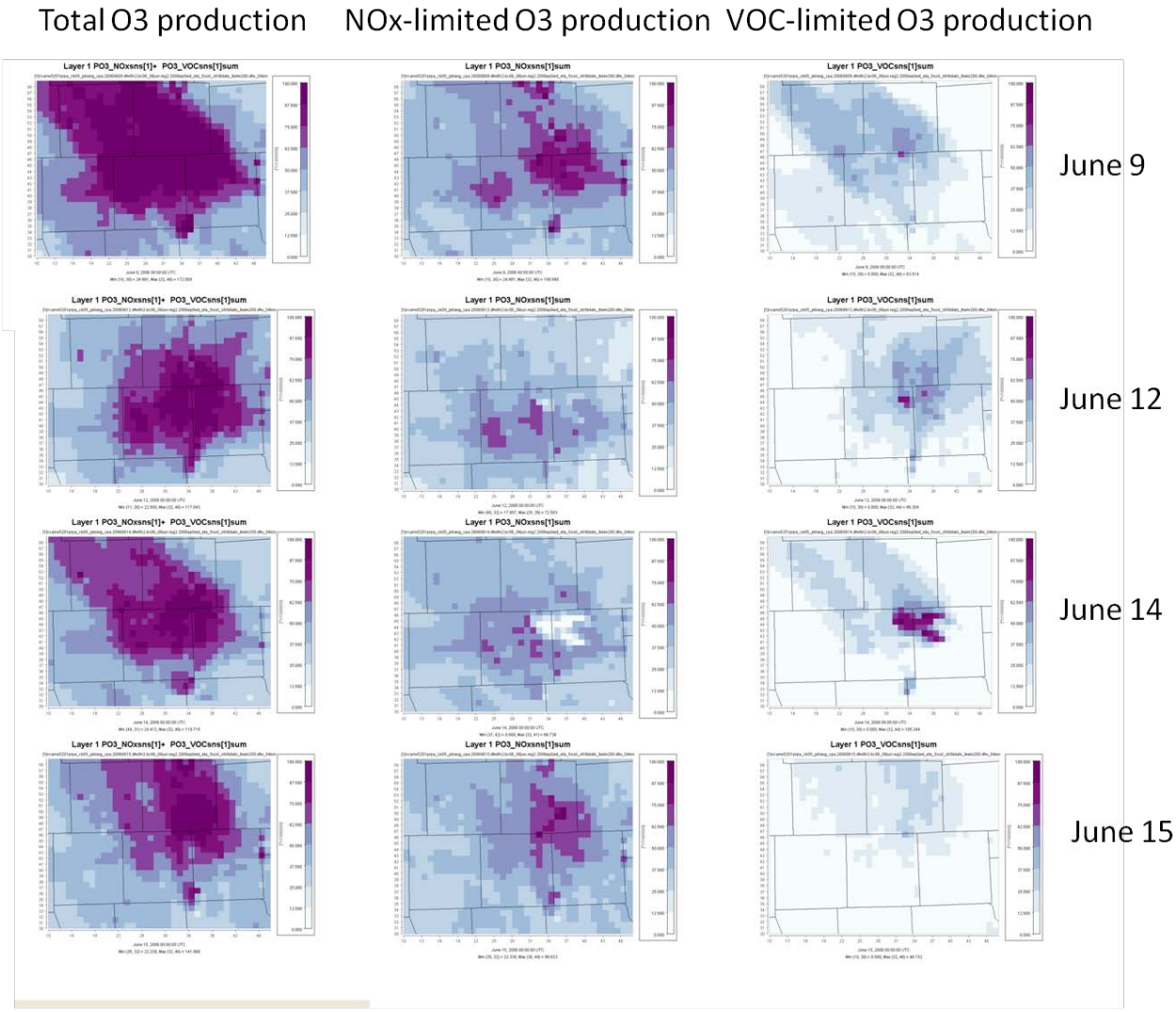

Figure 5-92: VOC and NO_X Sensitivity in Ozone Production on Four Episode Days in DFW

The VOC-sensitive regime occurs at most sites during rush hour, when NO_X emissions are at their highest and the PBL is relatively shallow, allowing NO_X emissions to accumulate, and NO_X concentrations to reach their peak. As the PBL deepens with solar heating, and the rush hour subsides, NO_X concentrations decrease rapidly, changing the ozone formation regime from VOC-limited to NO_X-limited. The urban core has more VOC-limited ozone formation than the other sites, because NO_X is abundant. The upwind sites have virtually no VOC-limited ozone formation, because at these locations the NO_X concentrations are low all day long.

Table 5-16: *Ozone Production in VOC and NOX-Sensitive Ozone Production for DFW* quantifies the differences in ozone production rates in NO_X- and VOC-sensitive ozone production regimes in DFW. For the high ozone days included in these analyses, the NO_X-sensitive ozone production is 2 to 5 times larger than the VOC-sensitive ozone production every day.

Table 5-16: Ozone Production in VOC and NO_X-Sensitive Ozone Production for DFW

Date	Total O_3 production index	NO_X-sensitive O_3 production index	VOC-sensitive O_3 production index
9-Jun-06	78,607	55,507	23,100
12-Jun-06	62,932	42,278	20,655
14-Jun-06	62,908	46,043	16,865
15-Jun-06	60,609	49,724	10,885
18-Jun-06	57,079	35,248	21,831
28-Jun-06	56,171	34,180	21,992
1-Jul-06	59,345	46,130	13,215

Conclusions

- DFW peak ozone is strongly affected by regional background ozone concentrations; high regional background ozone can greatly increase the likelihood of ozone exceedances in DFW.

- Local ozone production in DFW can be vigorous, exceeding 100 ppb per day over much of the metropolitan area. The fate of locally-produced ozone, and whether it contributes to high local concentrations or high ozone far downwind, depends (at least in part) on wind speed and transport conditions. Other factors that can determine the importance of locally-produced ozone include chemical destruction, dry deposition, and PBL depth. The factors that determine the fate of locally-produced ozone vary from day to day in DFW, suggesting that meteorological factors are very important.

- On all DFW episode days studied, NO_X-limited ozone formation was greater than VOC-limited ozone formation, by factors ranging from two to five times. VOC-sensitive ozone formation is most important in the DFW urban core, and in the vicinity of power plants, which emit large quantities of NO_X. Both VOC-sensitive and NO_X-sensitive ozone formation occur throughout the DFW area each day, with VOC-sensitive formation occurring in the morning, and NO_X-sensitive formation occurring in the afternoon.

6 BASELINE (2006) AND FUTURE CASE (2012) MODELING

6.1 Baseline Modeling

The TCEQ used 2006 as the baseline year for conducting the attainment modeling. Two features of the baseline year are used. First, the baseline year identifies the three consecutive years with design values (DVs) that include the fourth high of the baseline year. These three DVs are averaged to calculate the DV_B, as previously illustrated in Figure 1-1, for each of the regulatory monitors. Second, the baseline year is used to develop the typical ozone-season-day (OSD) modeling emissions as shown in Table 6-1: *Summary of 2006 Baseline Anthropogenic Modeling Emissions for DFW*.

Table 6-1: Summary of 2006 Baseline Anthropogenic Modeling Emissions for DFW

Category	2006 NO_X tpd	2006 VOC tpd
On-Road Mobile (MOVES)	259	111
Non-Road (excl. Oil & Gas Drilling)	85	60
Off-Road	40	7
Points	51	41
Area (excl. Oil & Gas)	16	213
Oil & Gas Production	50	72
Oil & Gas Drilling	18	1
DFW Total	**519**	**505**

The baseline modeling results are used to calculate the denominator of the RRF (RRF_D) for each of the regulatory monitors. The RRF_D is calculated as the average of the modeled daily maximum eight-hour ozone concentrations above 84 ppb within the 3 x 3 grid cell array about the monitor (Figure 6-1: *Near Monitoring Site Grid Cell Array Size*).

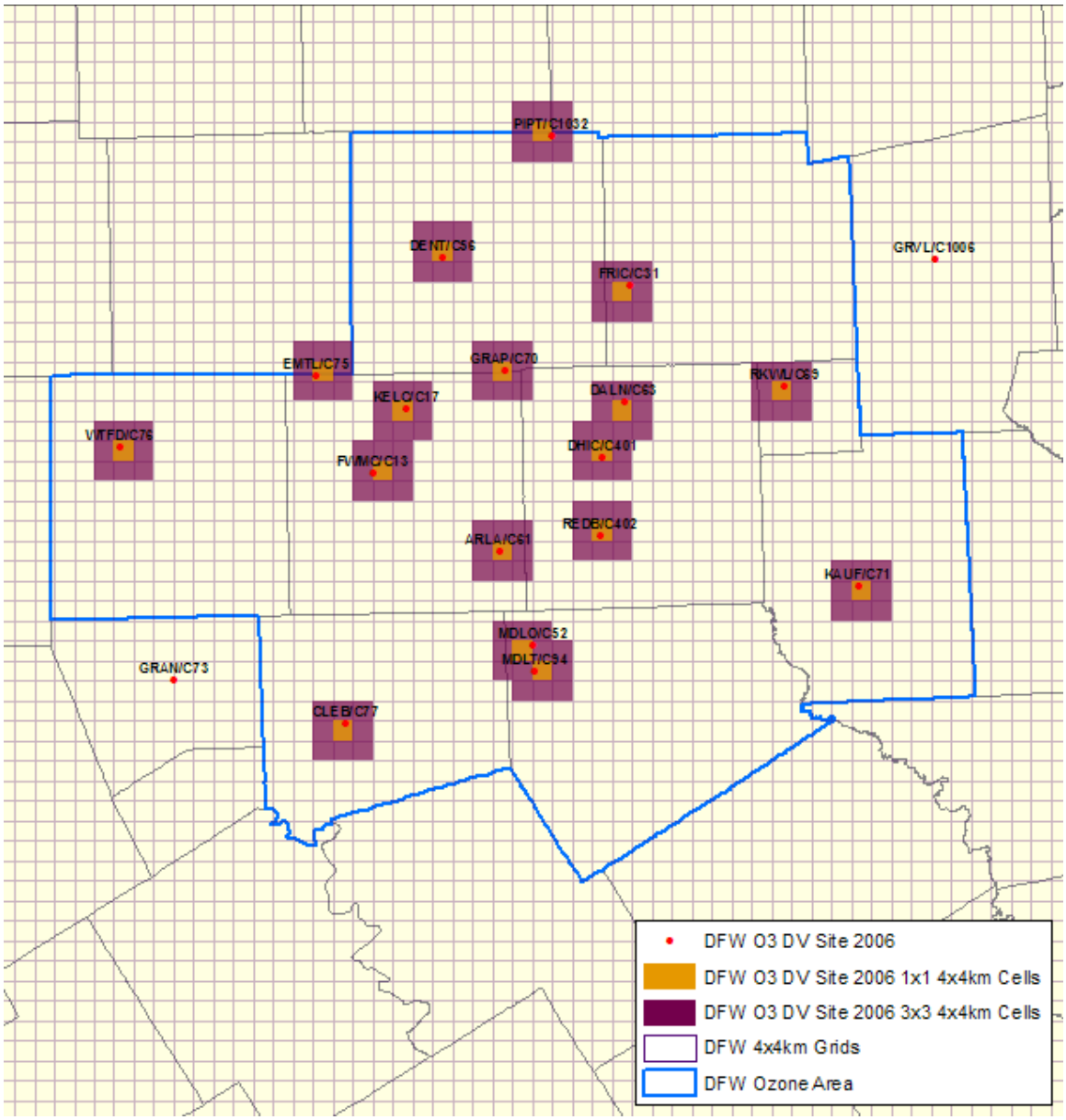

Figure 6-1: Near Monitoring Site Grid Cell Array Size

Per the EPA's modeling guidance, if there are fewer than 10 days with 2006 baseline modeled concentrations greater than 84 ppb, then days with modeled concentrations greater than or equal to 70 ppb can be used in the average. Table 6-2: *2006 DVB, RRFD, and Number of Baseline Modeled Days Averaged* summarizes the DV_B and the RRF_D for the DFW monitors. Three monitors in the DFW area did not have ten modeled days above 70 ppb. These monitors are not located where the highest area ozone concentrations are typically observed.

Table 6-2: 2006 DVB, RRF_D, and Number of Baseline Modeled Days Averaged

Site	Monitor	2006 DV_B (ppb)*	RRF_D (ppb)	Modeled Days
DENT	Denton C56	93.33	87.16	10
EMTL	Eagle Mountain Lake C75	93.33	86.95	10
KELC	Keller C17	91.00	88.33	10
GRAP	Grapevine Fairway C70	90.67	88.26	10
FWMC	Fort Worth Northwest C13	89.33	88.02	10
FRIC	Frisco C31	87.67	83.34	10
WTFD	Weatherford Parker County C76	87.67	81.45	10
DALN	Dallas North C63	85.00	81.00	10
REDB	Dallas Exec Airport C402	85.00	80.49	10
CLEB	Cleburne C77	85.00	80.39	9
ARLA	Arlington C61	83.33	85.01	10
DHIC	Dallas Hinton C401	81.67	81.02	10
PIPT†	Pilot Point C1032†	81.00†	84.23	10
MDLT†	Midlothian Tower C94†	80.50†	79.49	10
RKWL	Rockwall Heath C69	77.67	74.55	10
MDLO†	Midlothian OFW C52†	75.00†	81.17	10
KAUF	Kaufman C71	74.67	75.02	7
GRAN#	Granbury C73#	83.00	80.38	10
GRVL#	Greenville C1006#	75.00	73.54	9

* DV_B values 85 ppb or greater are shown in red.
† PIPT, MDLT, and MDLO did not measure enough data from 2004 through 2008 to calculate a complete DV_B. The DV_B shown uses all available data.
# Granbury C73 and Greenville C1006 are outside the 1997 eight-hour ozone NAAQS DFW nonattainment area.

6.2 Future Baseline Modeling

Similar to the 2006 baseline modeling, the 2012 modeling was conducted for each of the episode days using the projected 2012 ozone season day emissions. The 2012 anthropogenic modeling emissions for the DFW 9-county area are shown in Table 6-3: *Summary of 2012 Future Base Anthropogenic Modeling Emissions for DFW*.

Table 6-3: Summary of 2012 Future Base Anthropogenic Modeling Emissions for DFW

Category	2012 NO_X tpd	2012 VOC tpd
On-Road Mobile (MOVES)	181	80
Non-Road (excl. Oil & Gas Drilling)	64	43
Off-Road	37	6
Points	51	39
Area (excl. Oil & Gas)	18	240
Oil & Gas Production	10	113
Oil & Gas Drilling	9	1
DFW Total	**370**	**522**

Figure 6-2: *2006 Baseline and 2012 Future Base Anthropogenic NOX and VOC Modeling Emissions for DFW* exhibits a comparison between 2006 and 2012 modeling emissions. From 2006 to 2012, NO_X emissions decrease from the mobile and oil and gas production sources. VOC emissions slightly increase due to oil and gas production and area sources.

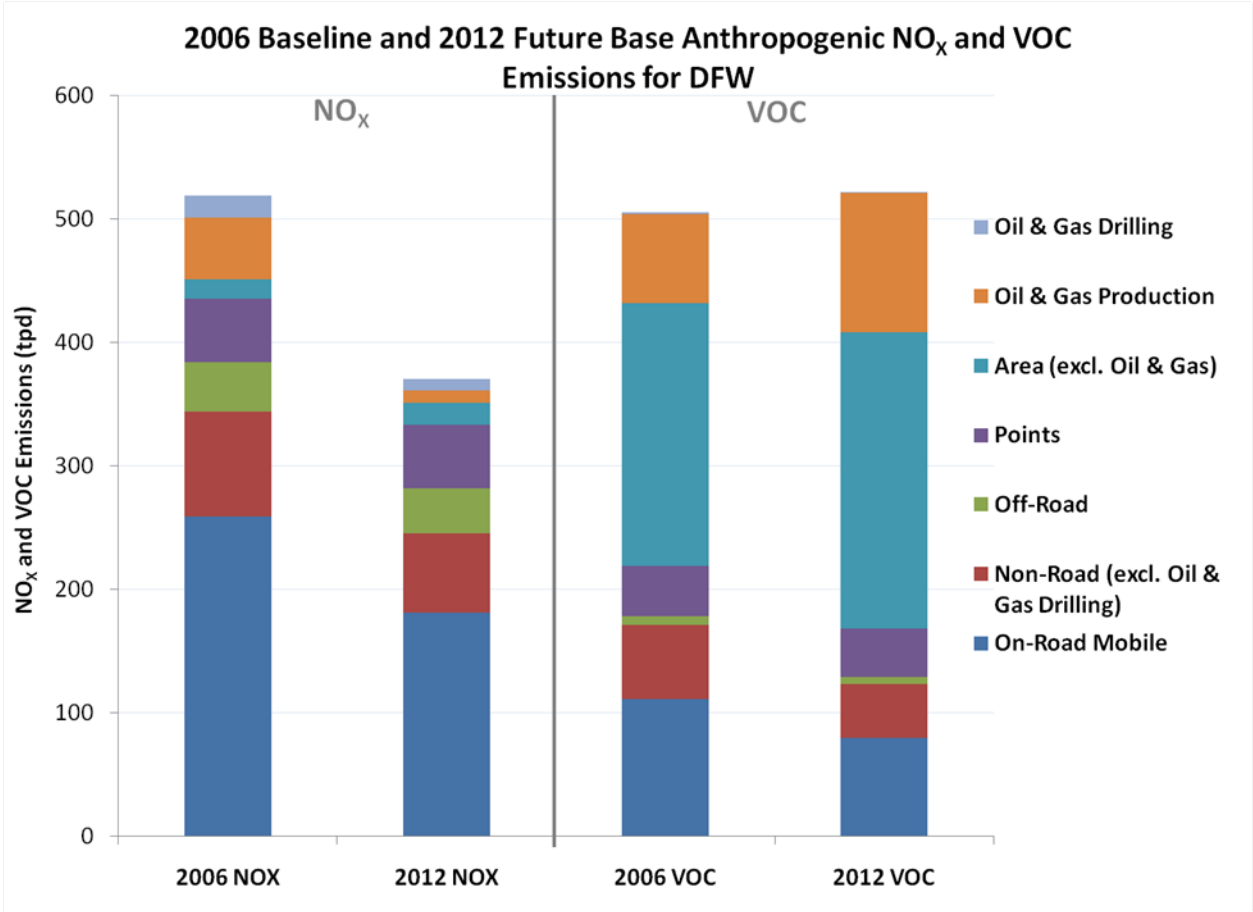

Figure 6-2: 2006 Baseline and 2012 Future Base Anthropogenic NO_X and VOC Modeling Emissions for DFW

Using the same days as used in the 2006 baseline modeling to calculate the RRF_D, an RRF numerator (RRF_N) was calculated as the average of the of the 2012 modeled maximum daily eight-hour ozone concentrations within the 3 x 3 grid cell array about each monitor (Figure 6-1). The RRF at each monitor was calculated as the ratio RRF_N / RRF_D, and the 2012 future design value (DV_F) at each monitor was estimated as per EPA's modeling guidance, by the multiplying the 2006 DV_B by the RRF. Table 6-4: *Summary of the RRF and 2012 Future Design Values* summarizes the 2006 DV_B, RRF and 2012 DV_F at each of the regulatory monitors.

Table 6-4: Summary of the RRF and 2012 Future Design Values

Site	Monitor	2006 DV_B (ppb)*	RRF	2012 DV_F (ppb)*
DENT	Denton C56	93.33	0.825	77.03
EMTL	Eagle Mountain Lake C75	93.33	0.836	78.06
KELC	Keller C17	91.00	0.840	76.45

Site	Monitor	2006 DV_B (ppb)*	RRF	2012 DV_F (ppb)*
GRAP	Grapevine Fairway C70	90.67	0.840	76.17
FWMC	Fort Worth Northwest C13	89.33	0.844	75.36
FRIC	Frisco C31	87.67	0.849	74.45
WTFD	Weatherford Parker County C76	87.67	0.829	72.71
DALN	Dallas North C63	85.00	0.837	71.15
REDB	Dallas Exec Airport C402	85.00	0.830	70.58
CLEB	Cleburne C77	85.00	0.834	70.85
ARLA	Arlington C61	83.33	0.844	70.32
DHIC	Dallas Hinton C401	81.67	0.831	67.89
PIPT†	Pilot Point C1032†	81.00†	0.831†	67.35†
MDLT†	Midlothian Tower C94†	80.50†	0.828†	66.63†
RKWL	Rockwall Heath C69	77.67	0.815	63.27
MDLO†	Midlothian OFW C52†	75.00†	0.830†	62.24†
KAUF	Kaufman C71	74.67	0.809	60.42
GRAN#	Granbury C73#	83.00	0.839	69.66
GRVL#	Greenville C1006#	75.00	0.799	59.96

* DV_B values 85 ppb or greater are shown in red.
† PIPT, MDLT, and MDLO did not measure enough data from 2004 through 2008 to calculate a complete DV_B. The DV_B shown uses all available data, which was used to calculate the RRF and DV_F.
# Granbury C73 and Greenville C1006 are outside the 1997 eight-hour ozone NAAQS DFW nonattainment area.

The 2012 baseline attainment modeling projects zero regulatory monitors to have DV_Fs greater than 84 ppb.

6.2.1 Alternative Future Design Value Calculations

The attainment test applied above was based on the EPA's guidance (EPA, 2007), which was documented in the modeling protocol supplied to the EPA. However, the calculation of RRFs using different methods may provide information about the sensitivity of the model.

6.2.1.1 Minimum Threshold Analysis:

The EPA's guidance suggests calculating the RRF using at least 10 days when the baseline modeled peak eight-hour ozone concentration is 85 ppb or greater. Zero monitors during June 2006 episode observed 10 days at or above 85 ppb. If there are not 10 days above the 85 ppb threshold, the EPA's modeling guidance suggests lowering the threshold until 10 days are reached at the monitors. The minimum threshold in the proposed DFW Attainment Demonstration SIP revision was dropped to 70 ppb so almost all DFW monitors would have 10 modeled days for the RRF calculation, in accordance with the EPA's modeling guidance.

Table 6-5: *Minimum Threshold Analysis* exhibits the change in 2012 RRFs, future design values (DV_Fs), and the number of applicable days using different minimum thresholds in the attainment test calculation (shown in parentheses in the table header). By raising the minimum threshold from 70 ppb, as was used in the proposed DFW Attainment Demonstration SIP revision, the applicable days drop below the EPA-suggested 10 for many additional monitors. While the calculation then uses days that modeled higher baseline ozone concentrations, the calculation becomes less statistically robust. The maximum DV_F increases by one ppb to 79 ppb

at Eagle Mountain Lake (EMTL) by raising the minimum threshold to 85 ppb, though only 6 days are included in the calculation. DV_Fs at other sites, including Denton (DENT), decrease by raising the minimum threshold.

Table 6-5: Minimum Threshold Analysis

Site	2006 DVB	RRF (70 ppb)	DVF (70 ppb)	# Days (70 ppb)	RRF (75 ppb)	DVF (75 ppb)	# Days (75 ppb)	RRF (80 ppb)	DVF (80 ppb)	# Days (80 ppb)	RRF (85 ppb)	DVF (85 ppb)	# Days (85 ppb)
DENT	93.33	0.825	77.03	10	0.825	77.03	10	0.825	77.03	10	0.809	75.55	6
EMTL	93.33	0.836	78.06	10	0.836	78.06	10	0.839	78.30	7	0.847	79.03	6
KELC	91.00	0.840	76.45	10	0.840	76.45	10	0.842	76.59	9	0.846	76.94	7
GRAP	90.67	0.840	76.17	10	0.840	76.17	10	0.840	76.17	10	0.832	75.46	7
FWMC	89.33	0.844	75.36	10	0.844	75.36	10	0.849	75.83	9	0.858	76.64	6
FRIC	87.67	0.849	74.45	10	0.849	74.45	10	0.841	73.70	7	0.805	70.57	2
WTFD	87.67	0.829	72.71	10	0.830	72.74	8	0.857	75.15	3	0.863	75.66	2
DALN	85.00	0.837	71.15	10	0.837	71.15	10	0.828	70.35	7	0.834	70.87	2
REDB	85.00	0.830	70.58	10	0.837	71.15	9	0.821	69.78	4	0.860	73.08	2
CLEB	85.00	0.834	70.85	9	0.842	71.57	7	0.858	72.90	3	0.879	74.69	2
ARLA	83.33	0.844	70.32	10	0.844	70.32	10	0.861	71.79	6	0.878	73.20	5
DHIC	81.67	0.831	67.89	10	0.831	67.89	10	0.843	68.87	5	0.901	73.57	1
PIPT[#]	81.00	0.831	67.35	10	0.830	67.25	9	0.823	66.66	8	0.812	65.78	4
MDLT[#]	80.50	0.828	66.63	10	0.828	66.68	8	0.876	70.55	3	0.841	67.68	1
RKWL	77.67	0.815	63.27	10	0.823	63.96	4	0.750	58.24	1	0.750	58.24	1
MDLO[#]	75.00	0.830	62.24	10	0.833	62.45	9	0.878	65.83	4	0.878	65.83	4
KAUF	74.67	0.809	60.42	7	0.786	58.69	2	0.765	57.10	1	0.765	57.10	1
GRAN*	83.00	0.839	69.66	10	0.851	70.63	6	0.870	72.19	4	0.881	73.14	2
GRVL*	75.00	0.799	59.96	9	0.794	59.58	3	0.741	55.56	1			0

[#] PIPT, MDLT, and MDLO did not measure enough data from 2004 through 2008 to calculate a complete DV_B. A DV_B was calculated using all available data for the RRF and DV_F shown.

* Granbury C73 and Greenville C1006 are outside the 1997 eight-hour ozone NAAQS DFW nonattainment area.

6.2.1.2 Daily RRF Analysis:

The EPA's guidance states to calculate the RRF by dividing the averaged future case concentrations by the averaged baseline concentrations over the same modeled days using the minimum threshold discussed above. An alternative calculation can be made by dividing the future by the baseline for each day and then averaging the resulting daily RRFs. Table 6-6: *June 2 through 14 Daily RRFs* and Table 6-7: *June 15 through July 1 Daily RRFs* below show the daily RRFs at each monitor throughout the episode (June 16 and 21 through 23 not shown or included in RRF calculation due to low observed ozone concentrations). Using the same days above 70 ppb as in the proposed DFW Attainment Demonstration SIP revision, the DVFs are very similar.

In general the highest daily RRFs occurred on low ozone days with strong winds and/or cloudy conditions. The highest mean daily RRFs occurred on June 17 and 18 (0.975 and 0.938 respectively), which featured a slow-moving front that the meteorological model had difficulty replicating.

June 15 (0.787), June 30 (0.775) and July 1 (0.771) had the lowest mean daily RRFs. June 15 was a high ozone day on the north side of the urban areas at six sites with south-southeast winds. June 30 was a high ozone day with Denton and Pilot Point measuring eight-hour exceedances over 100 ppb due to clear skies and slow south-southeast winds. On July 1 Denton was the only monitor to observe an exceedance at 85 ppb on a somewhat cloudy day with south to southeast winds. The photochemical modeling replicated June 15 and June 30 very well but over-predicted on July 1 due to the simulation of clear skies.

Table 6-6: June 2 through 14 Daily RRFs

Site	6/2	6/3	6/4	6/5	6/6	6/7	6/8	6/9	6/10	6/11	6/12	6/13	6/14
DENT	0.839	0.810	0.909	0.950	0.845	0.856	0.842	0.852	0.851	0.835	0.896	0.781	0.829
EMTL	0.839	0.825	0.900	0.949	0.827	0.850	0.842	0.878	0.834	0.858	0.893	0.819	0.841
KELC	0.837	0.838	0.905	0.934	0.846	0.869	0.875	0.874	0.840	0.854	0.896	0.816	0.840
GRAP	0.838	0.809	0.912	0.947	0.864	0.873	0.853	0.853	0.852	0.843	0.908	0.805	0.837
FWMC	0.821	0.846	0.904	0.935	0.850	0.886	0.875	0.887	0.837	0.858	0.898	0.833	0.839
FRIC	0.836	0.818	0.890	0.953	0.873	0.864	0.842	0.849	0.848	0.820	0.898	0.776	0.800
WTFD	0.838	0.834	0.906	0.906	0.867	0.847	0.841	0.862	0.818	0.857	0.885	0.839	0.843
DALN	0.850	0.814	0.900	0.962	0.864	0.874	0.850	0.862	0.851	0.825	0.898	0.812	0.826
REDB	0.857	0.812	0.898	0.929	0.851	0.893	0.853	0.859	0.839	0.829	0.887	0.834	0.808
CLEB	0.842	0.813	0.895	0.909	0.858	0.900	0.856	0.856	0.808	0.847	0.890	0.858	0.806
ARLA	0.848	0.839	0.906	0.920	0.865	0.892	0.869	0.860	0.831	0.848	0.893	0.844	0.811
DHIC	0.854	0.820	0.900	0.956	0.866	0.885	0.862	0.863	0.846	0.822	0.901	0.832	0.835
PIPT#	0.844	0.800	0.894	0.947	0.866	0.862	0.837	0.844	0.852	0.824	0.884	0.768	0.785
MDLT#	0.854	0.875	0.890	0.913	0.850	0.889	0.833	0.851	0.816	0.824	0.884	0.841	0.796
RKWL	0.851	0.815	0.879	0.930	0.819	0.863	0.836	0.835	0.846	0.829	0.887	0.783	0.790
MDLO#	0.853	0.854	0.891	0.913	0.850	0.884	0.839	0.854	0.815	0.835	0.886	0.841	0.800
KAUF	0.824	0.768	0.860	0.917	0.810	0.851	0.811	0.839	0.834	0.830	0.883	0.778	0.783
GRAN*	0.808	0.837	0.906	0.899	0.867	0.902	0.862	0.869	0.811	0.860	0.879	0.835	0.787
GRVL*	0.838	0.766	0.867	0.877	0.825	0.862	0.835	0.821	0.849	0.831	0.875	0.786	0.799
Mean	0.841	0.821	0.896	0.929	0.851	0.874	0.848	0.856	0.836	0.838	0.891	0.815	0.813

PIPT, MDLT, and MDLO did not measure enough data from 2004 through 2008 to calculate a complete DV_B. A DV_B was calculated using all available data for the RRF and DV_F shown.

* Granbury C73 and Greenville C1006 are outside the 1997 eight-hour ozone NAAQS DFW nonattainment area

Table 6-7: June 15 through July 1 Daily RRFs

Site	6/15	6/17	6/18	6/19	6/20	6/24	6/25	6/26	6/27	6/28	6/29	6/30	7/1	Mean RRF	DVF
DENT	0.789	0.990	0.938	0.906	0.929	0.903	0.892	0.882	0.853	0.862	0.822	0.805	0.778	0.826	77.09
EMTL	0.804	0.978	0.950	0.932	0.954	0.884	0.901	0.900	0.913	0.851	0.798	0.787	0.794	0.835	77.93
KELC	0.787	0.989	0.963	0.952	0.936	0.896	0.868	0.869	0.887	0.867	0.825	0.805	0.780	0.839	76.32
GRAP	0.788	0.993	0.940	0.930	0.927	0.912	0.880	0.879	0.869	0.866	0.831	0.805	0.782	0.841	76.22
FWMC	0.790	0.999	0.968	0.961	0.951	0.917	0.863	0.882	0.913	0.868	0.812	0.785	0.793	0.841	75.15
FRIC	0.793	0.991	0.928	0.884	0.916	0.911	0.882	0.884	0.882	0.890	0.830	0.814	0.780	0.850	74.54
WTFD	0.813	0.972	0.905	0.920	0.894	0.894	0.900	0.884	0.840	0.860	0.797	0.762	0.777	0.827	72.53
DALN	0.787	1.002	0.949	0.920	0.919	0.926	0.869	0.899	0.928	0.882	0.835	0.797	0.768	0.837	71.17
REDB	0.793	0.982	0.938	0.914	0.905	0.923	0.866	0.903	0.922	0.837	0.803	0.764	0.763	0.830	70.52
CLEB	0.794	0.954	0.899	0.938	0.918	0.914	0.858	0.880	0.938	0.822	0.798	0.756	0.772	0.831	70.60
ARLA	0.783	0.952	0.962	0.938	0.913	0.918	0.872	0.900	0.897	0.846	0.807	0.784	0.770	0.842	70.19
DHIC	0.783	1.004	0.965	0.935	0.917	0.926	0.870	0.896	0.946	0.865	0.827	0.792	0.773	0.831	67.84
PIPT#	0.787	0.971	0.925	0.863	0.912	0.867	0.889	0.890	0.874	0.872	0.825	0.790	0.772	0.833	67.44
MDLT#	0.781	0.946	0.918	0.906	0.906	0.932	0.868	0.895	0.905	0.820	0.797	0.745	0.748	0.826	66.49
RKWL	0.779	0.980	0.943	0.863	0.911	0.918	0.867	0.881	0.873	0.837	0.821	0.757	0.750	0.815	63.30
MDLO#	0.780	0.945	0.979	0.882	0.906	0.921	0.865	0.897	0.904	0.834	0.803	0.754	0.766	0.827	62.03
KAUF	0.812	0.945	0.944	0.861	0.906	0.905	0.849	0.875	0.867	0.812	0.798	0.732	0.765	0.811	60.52
GRAN*	0.805	0.951	0.899	0.929	0.926	0.890	0.877	0.892	0.883	0.841	0.801	0.769	0.783	0.837	69.47
GRVL*	0.709	0.980	0.918	0.841	0.922	0.891	0.875	0.881	0.858	0.799	0.813	0.717	0.741	0.800	60.02
Mean	0.787	0.975	0.938	0.909	0.919	0.908	0.874	0.888	0.892	0.849	0.813	0.775	0.771	0.830	69.97

PIPT, MDLT, and MDLO did not measure enough data from 2004 through 2008 to calculate a complete DV_B. A DV_B was calculated using all available data for the RRF and DV_F shown.

* Granbury C73 and Greenville C1006 are outside the 1997 eight-hour ozone NAAQS DFW nonattainment area.

6.2.1.3 Grid Cell Array Size Analysis:

The grid cell array size is chosen as an area around a monitor to be spatially representative of that site. For the RRF calculation the maximum concentration in the grid cell array around a monitor from the baseline and future case modeling is used, which may not be at the cell where the monitor is located. The EPA guidance states that this method is beneficial for many reasons, including that the model may displace the peak around a monitor. For the proposed DFW Attainment Demonstration SIP revision a 3x3 grid cell array was chosen. As Figure 6-3: *Grid Cell Array Size Around DFW Monitors* shows, a 5x5 or 7x7 grid cell array causes overlap among many DFW monitors. This contradicts the idea that the grid cell array should be representative of a specific monitoring site. Nevertheless, the RRFs and DV_Fs for the 5x5 and 7x7 grid cell arrays are presented in Table 6-3: *Summary of 2012 Future Base Anthropogenic Modeling Emissions for DFW*. The maximum DV_F is reduced less than one ppb with a 5x5 array. With a 7x7 array the maximum DVF is almost identical to the 3x3 array, though it has moved from Eagle Mountain Lake (EMTL) to Denton (DENT).

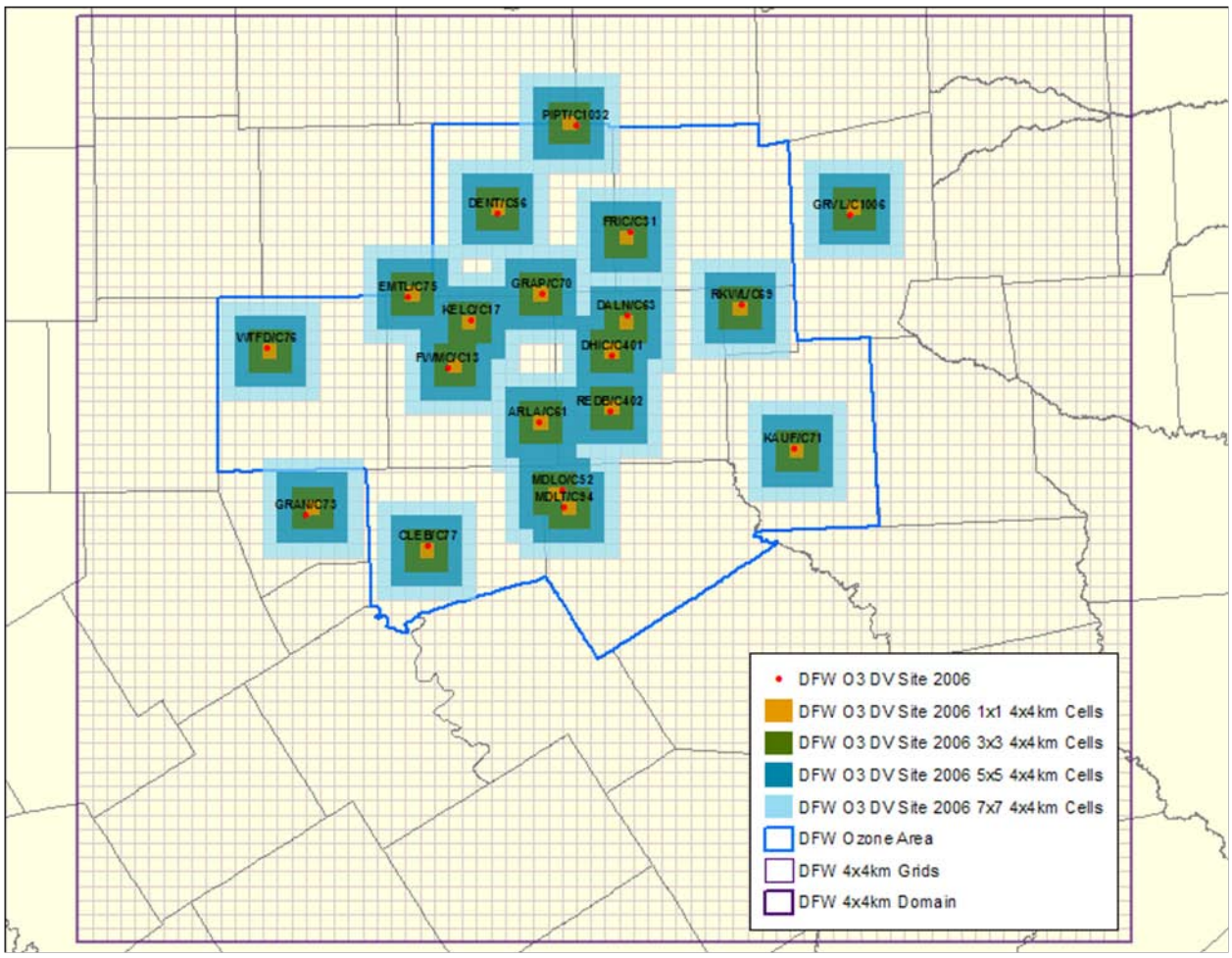

Figure 6-3: Grid Cell Array Size Around DFW Monitors

Table 6-8: RRFs and DVFs using 3x3, 5x5, and 7x7 Grid Cell Arrays

Site	RRF (3x3)	DVF (3x3)	RRF (5x5)	DVF (5x5)	RRF (7x7)	DVF (7x7)
Area Max	0.849	78.06	0.844	77.68	0.855	78.11
DENT	0.825	77.03	0.828	77.32	0.837	78.11
EMTL	0.836	78.06	0.832	77.68	0.835	77.97
KELC	0.840	76.45	0.840	76.46	0.841	76.52
GRAP	0.840	76.17	0.843	76.43	0.842	76.35
FWMC	0.844	75.36	0.843	75.33	0.844	75.42
FRIC	0.849	74.45	0.842	73.85	0.840	73.64
WTFD	0.829	72.71	0.830	72.77	0.833	73.05
DALN	0.837	71.15	0.840	71.39	0.839	71.33
REDB	0.830	70.58	0.834	70.90	0.835	70.95
CLEB	0.834	70.85	0.841	71.49	0.849	72.15
ARLA	0.844	70.32	0.844	70.33	0.855	71.23
DHIC	0.831	67.89	0.834	68.13	0.833	68.00
PIPT#	0.831	67.35	0.832	67.36	0.833	67.44
MDLT#	0.828	66.63	0.829	66.71	0.833	67.04
RKWL	0.815	63.27	0.815	63.34	0.819	63.61
MDLO#	0.830	62.24	0.833	62.48	0.841	63.05
KAUF	0.809	60.42	0.811	60.56	0.807	60.25
GRAN*	0.839	69.66	0.838	69.57	0.840	69.71
GRVL*	0.799	59.96	0.800	59.97	0.801	60.05

PIPT, MDLT, and MDLO did not measure enough data from 2004 through 2008 to calculate a complete DV_B. A DV_B was calculated using all available data for the RRFs and DV_Fs shown.

* Granbury C73 and Greenville C1006 are outside the 1997 eight-hour ozone NAAQS DFW nonattainment area

6.2.2 Unmonitored Area Analysis

The EPA guidance (EPA, 2007) recommends that areas not near monitoring locations (unmonitored areas) be subjected to an unmonitored area (UMA) analysis to demonstrate that these areas are expected to reach attainment by the area's attainment year, in this case 2012. The standard attainment test is applied only at monitor locations, and the UMA analysis is intended to identify any areas not near a monitoring location that are at risk of not meeting the attainment date. Recently, the EPA provided software that can be used to conduct UMA analyses, but has not specifically recommended using its software (called the Modeled Attainment Test Software (MATS)) in EPA guidance, instead stating that "States will be able to use the EPA-provided software or are free to develop alternative techniques that may be appropriate for their areas or situations."

Delays in the release of MATS prompted the TCEQ to develop its own technique for performing unmonitored area analyses, called the Texas Attainment Test for Unmonitored areas (TATU). While both procedures incorporate modeled predictions into a spatial interpolation procedure, TATU is integrated into the TCEQ's model Linux-based post-processing stream, while MATS requires that modeled concentrations be exported to a Windows-based platform. Additionally, MATS requires input in latitude and longitude for monitor coordinates, while the TCEQ's procedures work directly with the Lambert Conformal Projection (LCP) monitoring coordinates used in the photochemical modeling applications. Finally, MATS uses the Voronoi Neighbor Averaging (VNA) technique for spatial interpolation, while TATU relies on the more familiar

kriging geospatial interpolation technique. For these reasons, TCEQ chose to use TATU for the UMA analysis. More information about TATU is provided in Appendix C: Photochemical Modeling for the HGB Attainment Demonstration SIP Revision for the 1997 Eight-Hour Ozone Standard, Attachment 2.

Figure 6-4: *Spatially Interpolated 2006 Baseline (left) and 2012 Future Case (right) Design Values for the DFW Area* shows two color contour maps of ozone concentrations produced by TATU, one for the 2006 baseline (left) and one for the 2012 future case (right). The figure shows the extent and magnitude of the expected improvements in ozone design values, with zero grid cells at or above 84 ppb in the future case plot. The maximum design value in the domain is predicted at 81.8 ppb.

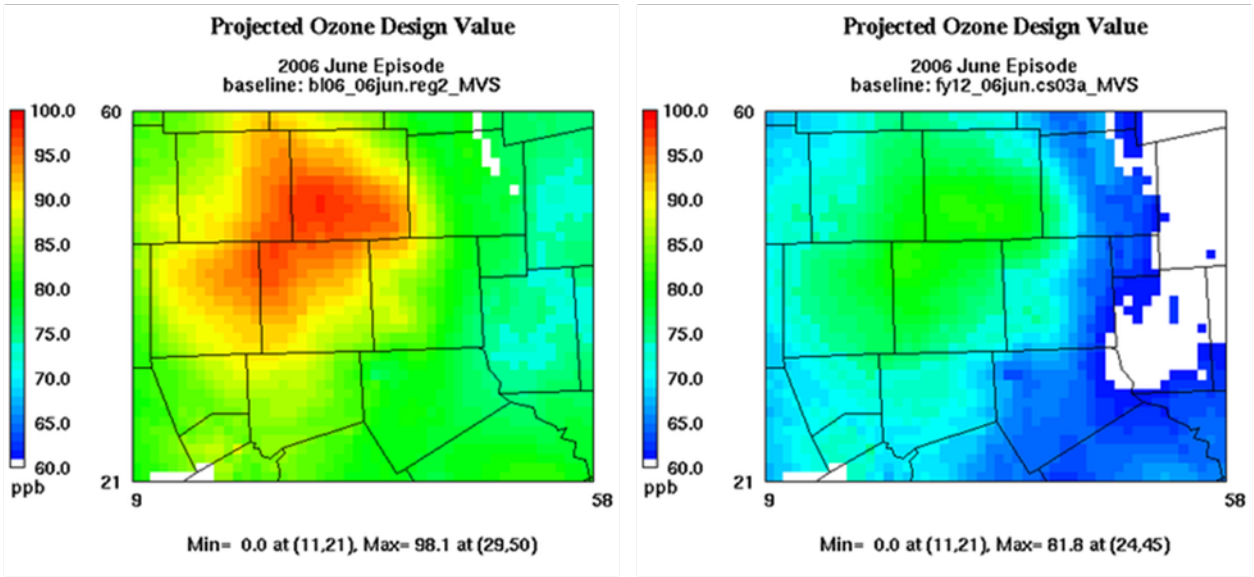

Figure 6-4: Spatially Interpolated 2006 Baseline (left) and 2012 Future Case (right) Design Values for the DFW Area

In conclusion, all grid cells within the 4 km domain are projected to attain the NAAQS in 2012 using the TATU unmonitored area analysis. It is predicted that there will not be a population exposed to design value exceedance conditions.

6.2.3 Ozone Metrics

Table 6-9: *Changes in the Area and Population Affected by an Eight-Hour Ozone Design Value Greater than or Equal to 85 ppb in Response to Growth and Controls* shows how the area affected by high ozone is expected to shrink in response to the emission changes projected to occur between 2006 and 2012. Peak ozone drops by 17% and the area with an estimated ozone design value greater than the 84 ppb standard shrinks by 100%. The 2012 population living in the DFW nine-county area is projected to be residing in attainment of the 1997 eight-hour ozone standard. The population data is from the 2000 Census and has not been grown to reflect changes in population in those areas in 2006 or 2012. Also, the numbers reflect areas where people reside, i.e., their home addresses, not necessarily where they might be during the hours of highest ozone during the ozone season. However, the decrease in the area with high ozone suggests that ozone decreases are likely to benefit many residents of the DFW area.

Table 6-9: Changes in the Area and Population Affected by an Eight-Hour Ozone Design Value Greater than or Equal to 85 ppb in Response to Growth and Controls

Run name	Peak Ozone (ppb)	Area with design value >84 ppb, km^2	2000 population in area with design value >84 ppb
2006 baseline (reg2_MVS)	98	2632	3590819
2012 future year (cs03a_MVS)	81	0	0
Percentage decrease from 2006 to 2012	17%	100%	100%

7 MODELING ARCHIVE AND REFERENCES

7.1 Modeling Archive

The TCEQ has archived all modeling documentation and modeling input/output files generated as part of the DFW SIP modeling analysis. Interested parties can contact the TCEQ for information regarding data access or project documentation. Most modeling files and performance evaluation products may be found on TCEQ's modeling ftp site.

7.2 Modeling References

Castineira and Edgar, 2006. Computational Fluid Dynamics for simulation of steam-assisted and air-assisted flare combustion systems, Energy & Fuels, 2006, 20, 1044-1056.

Chan and Vet, 2009. Background ozone over Canada and the United States. *Atmos. Chem. Phys. Discuss.*, 9: 21111-21164, http://www.atmos-chem-phys-discuss.net/9/21111/2009/.

Emery, C., E. Tai, and G. Yarwood, 2001. Enhanced Meteorological Modeling and Performance Evaluation for Two Texas Ozone Episodes, Final Report to the Texas Natural Resource Conservation Commission under TNRCC Umbrella Contract No. 582-0-31984, Environ International Corporation, Novato, CA.

Environ, 2006. Longview Ozone on June 12, 2006, Presentation to the NETAC Technical Committee, http://etcog.sitestreet.com/UserFiles/File/NETAC/pdf/reports/air%20quality/Longview_ozone_onJune%2012_a1.pdf.

Environ, 2007. User's Guide Emissions Processor, Version 3, Environ International Corporation, Novato, CA.

Environ, 2008. Description from MM5CAMx README file contained in mm5camx.21feb08.tar.gz archive, http://www.camx.com/files/mm5camx.21feb08.tar.gz, Environ Holdings, Inc.

Environ, 2008b. Boundary Conditions and Fire Emissions Modeling, Final Report to the Texas Commission on Environmental Quality, Contract No. 582-7-84005-FY08-06, Environ International Corporation, Novato, CA.

Environ, 2009. *Development of Emissions Inventories for Natural Gas Exploration and Production Activity in the Haynesville Shale*, Draft Report to the Northeast Texas Air Care, http://www.netac.org/UserFiles/File/NETAC/9_29_09/Enclosure_2b.pdf, August 31, 2009.

Environ, 2010. ENVIRON – Downloads, http://www.camx.com/down/camx.php, Environ Holdings, Inc.

EPA, 2007. Guidance on the Use of Models and Other Analyses for Demonstrating Attainment of Air Quality Goals for Ozone, PM2.5, and Regional Haze, http://www.epa.gov/scram001/guidance/guide/final-03-pm-rh-guidance.pdf.

EPA, 2011. Spreadsheet of CSAPR Ozone and PM2.5 Design Values, http://www.epa.gov/airtransport/pdfs/CSAPR_Ozone%20and%20PM2.5_Design%20Values.xls.

Feldman, M.S., T. Howard, E. McDonald-Buller, G. Mullins, D.T. Allen, A. Webb, Y. Kimura, 2007. Applications of Satellite Remote Sensing Data for Estimating Dry Deposition in Eastern Texas. Atmospheric Environment, Volume 41, Issue 35, November 2007, pages 7562-7576.

Grell, G., J. Dudhia, and D. Stauffer, 1994. A description of the Fifth Generation Penn State/NCAR Mesoscale Model (MM5), Tech. Rep. NCAR/TN-398+STR, National Center of Atmospheric Research (NCAR) Tech Note.

H-GAC 2006, HGAC 2035 Regional Growth Forecast, http://www.h-gac.com/community/socioeconomic/documents/2035_regional_growth_forecast.pdf, August 2006.

Kemball-Cook, S., D. Parrish, T. Ryerson, U. Nopmongcol, J. Johnson, E. Tai, and G. Yarwood, 2009. Contributions of regional transport and local sources to ozone exceedances in Houston and Dallas: Comparison of results from a photochemical grid model to aircraft and surface measurements, *J. Geophys. Res.*, 114, D00F02, doi:10.1029/2008JD010248.

Kinnee et al., 1997. United States Land Use Inventory for Estimating Biogenic Ozone Precursor Emissions. Ecological Applications 7(1): 46-58.

Knoderer, C. A., S. A. Bratek, C. P. MacDonald, 2008. Spatial and Temporal Characteristics of Winds and Mixing During TexAQS-II, Final Report to Texas A&M University for Texas Commission on Environmental Quality Proposal under Grant Activity 582-5-64593-FY08-20, Sonoma Technology Inc, Petaluma, CA, April 2008.

Luria, M., R. Valente, S. Bairai, W. Parkhurst, R. Tanner, (2008), Airborne study of ozone formation over Dallas, Texas. *Atmos. Environ*. 42: 6951-6958, doi: 10.1016/j.atmosenv.2008.04.057.

MacDonald, Nicole and Hakami, A, 2010. Temporal Source Apportionment of Policy-Relevant Air Quality Metrics, Presented at the 9th CMAS Conference Oct. 11-13, 2010, Chapel, Hill, N.C.

Mao, J., Ren, X., Chen, S., Brune, W.H., Chen, Z., Martinez, M., Harder, H., Lefer, B., Rappenglück, B., Flynn, J., Leuchner, M., 2009. Atmospheric oxidation capacity in the summer of Houston 2006: comparison with summer measurement in other metropolitan studies. *Atmospheric Environment*, doi:10.1016/j.atmosenv.2009.01.013.

NCAR, 2005. MM5 Online Tutorial Home Pages, http://www.mmm.ucar.edu/mm5/On-Line-Tutorial/teachyourself.html, National Center for Atmospheric Research, Boulder, Colorado.

NCEP, 2009. GCIP NCEP Eta Model Output, CISL RDA: ds609.2 Home Page, http://dss.ucar.edu/datasets/ds609.2/, National Center for Environmental Prediction.

Nielsen-Gammon, J., J. Tobin, and A. McNeel, 2005. *A Conceptual Model for Eight-Hour Ozone Exceedances in Houston, Texas, Part I: Background Ozone Levels in Eastern Texas*. Research report, supported by HARC, TERC, and TCEQ, HARC project H012.2004.8HRA, January 29, 2005.

Popescu, Sorin C., Jared Stukey, Mark Karnauch, Jeremiah Bowling, Xuesong Zhang, William Booth, and Nian-Wei Ku, 2008. The New Central Texas Land Use Land Cover Classification Project, Final Report to the Texas Commission on Environmental Quality (TCEQ), Contract No. 582-5-64593-FY08-23, Texas A & M University, College Station, Texas.

Robinson, R., T. Gardiner, and B. Lipscombe, 2008. Measurements of VOC emissions from petrochemical industry sites in the Houston area using Differential Absorption Lidar (DIAL) during summer 2007, Draft. Submitted to Russell Nettles, TCEQ, by Rod Robinson, Tom Gardiner, and Bob Lipscombe of the National Physical Laboratory, Teddington, Middlesex UK TW11 0LW, February 8, 2008, pp. 86.

Senff, C. J., R. J. Alvarez II, R. M. Hardesty, R. M. Banta, and A. O. Langford (2010), Airborne lidar measurements of ozone flux downwind of Houston and Dallas, *J. Geophys. Res.*, 115, D20307, doi:10.1029/2009JD013689.

Smith, Jim and Estes, M, 2010. Dynamic Model Performance Evaluation Using Weekday-Weekend and Retrospective Analysis, Presented at the 9th CMAS Conference Oct. 11-13, 2010, Chapel, Hill, N.C.

Starcrest, 2000. Houston-Galveston Area Vessel Emissions Inventory, Starcrest Consulting Group, Houston, Texas.

Sullivan, 2009. *Effects of Meteorology on Pollutant Trends*, Final Report to TCEQ, Grant 582-5-86245-FY08-01, March 16, 2009, 163 pgs.

TCEQ, 2007. Revisions to the State Implementation Plan (SIP) for the Control of Ozone Air Pollution, Dallas-Fort Worth Eight-Hour Ozone Nonattainment Area Attainment Demonstration, Texas Commission on Environmental Quality (TCEQ), Austin, Texas.

TCEQ, 2009. Texas Commission on Environmental Quality (TCEQ) Air Modeling and Data Analysis (AMDA) Section file transfer protocol (FTP) site, ftp://ftp.tceq.state.tx.us/.

TCEQ, 2010. Texas Commission on Environmental Quality (TCEQ) 2006 Significant Air Pollution Events web site, http://www.tceq.texas.gov/airquality/monops/sigevents06.html.

Wiedinmyer et al., 2001. A Land Use Database and Examples of Biogenic Isoprene Emission Estimates for the State of Texas, USA. Atmospheric Enviro